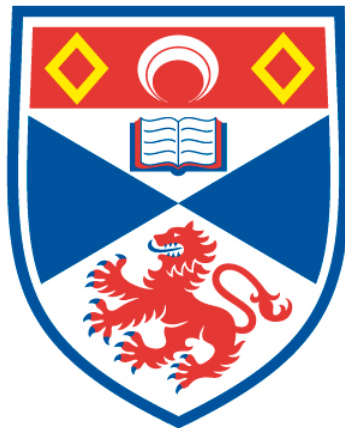


ZEBRAFISH AS A MODEL TO STUDY GENES ASSOCIATED WITH NEURODEVELOPMENTAL DISORDERS

Monika Gostić

A Thesis Submitted for the Degree of PhD
at the
University of St Andrews



2018

Full metadata for this thesis is available in
St Andrews Research Repository
at:

<http://research-repository.st-andrews.ac.uk/>

Identifiers to use to cite or link to this thesis:

DOI: <https://doi.org/10.17630/sta/10023-16446>

<http://hdl.handle.net/10023/16446>

This item is protected by original copyright

This item is licensed under a
Creative Commons License

<https://creativecommons.org/licenses/by-nc-nd/4.0>

Zebrafish as a model to study genes associated with neurodevelopmental disorders

Monika Gostić



**University of
St Andrews**

This thesis is submitted in partial fulfilment for the degree of

Doctor of Philosophy (PhD)

at the University of St Andrews

September 2018

Abstract

Dyslexia is a neurodevelopmental disorder that affects between 5% and 12% of school-aged children. Individuals with dyslexia have difficulties in learning to read despite normal IQ levels and adequate socio-economical and educational opportunities. Dyslexia has a strong genetic component, but only a few candidate genes have been characterized to date. The *KIAA0319* gene is a strong dyslexia candidate found to be associated with dyslexia in independent studies. The *KIAA0319* genetic variants associated with dyslexia reside in a regulatory region. Studies in rat suggested that this gene is required for neuronal migration during early cortex formation. The *KIAA0319-like* (*KIAA0319L*) is a *KIAA0319* homolog in structure and has recently been shown to play a role in dyslexia. I used zebrafish as a model organism both to study the effects of non-coding variants and to characterise *kiaa0319* gene function. I used Gateway Tol2 technology to study the role of regulatory sequences. While these experiments led to inconclusive results, they highlighted some of the challenges but also the feasibility of using zebrafish as model organism to study genetic associations. In parallel, I studied the *kiaa0319* function with knockout and knockdown experiments. Additionally, I conducted a detailed gene expression analysis with different *in situ* hybridisation protocols showing *kiaa0319* ubiquitous expression in the whole embryo before 12 hours post fertilisation, with later specification to the eyes, brain, otic vesicle and notochord. Additionally, I have tested for the expression of *kiaa0319l* and showed similar expression pattern to the *kiaa0319*, but with significantly lower expression of *kiaa0319l* in zebrafish notochord. My data show, for the first time, that *kiaa0319* has stage-specific expression in the brain and notochord during zebrafish early development, suggesting *kiaa0319* specific role in the development of these structures. These results are in line with recent mouse studies. With this project I support the idea of *kiaa0319* role being extended beyond the brain function and propose a role for *kiaa0319* in the visual system and in the notochord.

Declarations

Candidate's declaration

I, Monika Gostic, do hereby certify that this thesis, submitted for the degree of PhD, which is approximately 30000 words in length, has been written by me, and that it is the record of work carried out by me, or principally by myself in collaboration with others as acknowledged, and that it has not been submitted in any previous application for any degree.

I was admitted as a research student at the University of St Andrews in September 2013.

I confirm that no funding was received for this work.

Date

Signature of candidate

Supervisor's declaration

I hereby certify that the candidate has fulfilled the conditions of the Resolution and Regulations appropriate for the degree of PhD in the University of St Andrews and that the candidate is qualified to submit this thesis in application for that degree.

Date

Signature of supervisor

Permission for publication

In submitting this thesis to the University of St Andrews we understand that we are giving permission for it to be made available for use in accordance with the regulations of the University Library for the time being in force, subject to any copyright vested in the work not being affected thereby. We also understand, unless exempt by an award of an embargo as requested below, that the title and the abstract will be published, and that a copy of the work may be made and supplied to any bona fide library or research worker, that this thesis will be electronically accessible for personal or research use and that the library has the right to migrate this thesis into new electronic forms as required to ensure continued access to the thesis.

I, Monika Gostic, confirm that my thesis does not contain any third-party material that requires copyright clearance.

The following is an agreed request by candidate and supervisor regarding the publication of this thesis:

Printed copy

Embargo on all of print copy for a period of 3 years on the following ground(s):

- Publication would preclude future publication

Supporting statement for printed embargo request

We have a publication prepared to publish and further work planned which is based on the finding from my thesis

Electronic copy

Embargo on all of electronic copy for a period of 3 years on the following ground(s):

- Publication would preclude future publication

Supporting statement for electronic embargo request

We have a publication prepared to submit and further work in line, which is based on my thesis. If the thesis comes out first, we risk others publishing our ideas first

Title and Abstract

- I agree to the title and abstract being published.

Date

Signature of candidate

Date

Signature of supervisor

Underpinning Research Data or Digital Outputs

Candidate's declaration

I, Monika Gostic, understand that by declaring that I have original research data or digital outputs, I should make every effort in meeting the University's and research funders' requirements on the deposit and sharing of research data or research digital outputs.

Date

Signature of candidate

Permission for publication of underpinning research data or digital outputs

We understand that for any original research data or digital outputs which are deposited, we are giving permission for them to be made available for use in accordance with the requirements of the University and research funders, for the time being in force.

We also understand that the title and the description will be published, and that the underpinning research data or digital outputs will be electronically accessible for use in accordance with the license specified at the point of deposit, unless exempt by award of an embargo as requested below.

The following is an agreed request by candidate and supervisor regarding the publication of underpinning research data or digital outputs:

No embargo on underpinning research data or digital outputs.

Date

Signature of candidate

Date

Signature of supervisor

Acknowledgements

This thesis is a sum of hard work, dedication and brilliant people in my life.

Firstly, I would like to thank my supervisor, Dr Silvia Paracchini who was my guide, my support and my friend throughout the process. Her patience, the eye for details and a passion for the project have provided me with the opportunity to learn and grow as a person as well as a scientist.

I would also like to thank my secondary supervisor Prof Keith Sillar for his invaluable support and contribution to our discussions and ideas. Additionally, I would like to thank Dr Javier Tello for helping me with technical aspects of my project and guiding me towards new methodologies.

Special thanks goes to Dr Carl Tucker, Zebrafish Facility manager at the University of Edinburgh, who has guided me throughout the entire zebrafish part of this project. He has provided me with technical support as well as insightful ideas and comments, helping me expand my field of knowledge and try new methods.

My thanks go to Dr Patrick Blader and his lab in CBI Toulouse for providing me with the opportunity to learn about zebrafish specific techniques. They were always there for me to answer my questions and have helped me with a great deal of data collection and analysis.

My work has constantly been supported by my fantastic colleagues Dr Rebeca Diaz, Dr Rob Shore and Angela Marinelli. With their broad knowledge in various techniques and weekly discussions, I have been able to learn and advance as a scientist.

My sincere gratitude goes to Rebecca Hornyak and her family. She has been the bright light in my darkest day and my greatest cheerleader throughout the entire process. She has enabled me to work and write by taking care of my daughter and providing me with motivation and support with no end. I will also be forever grateful to the Pearson family, who have stood by my side and have been family when I need one the most. My deepest thanks goes to Jen Bre, a valued friend who has been there for me despite her numerous responsibilities.

I would like to thank my friend Nina Ostir for being a wonderful Godmother to my daughter and a terrific friend whenever I have needed her. My thanks also goes to Dan Oblak and his wife for providing me with endless encouragement.

Table of Contents

1	Introduction	17
1.1	Dyslexia	17
1.1.1	Dyslexia theories	18
1.1.2	Laterality and dyslexia	19
1.2	Dyslexia Genetics	27
1.2.1	DYX1C1	27
1.2.2	DCDC2	28
1.2.3	ROBO1	29
1.2.4	KIAA0319	29
1.2.5	KIAA0319-like	32
1.3	Functional characterisation of <i>KIAA0319</i> in model organisms	34
1.3.1	Zebrafish as a model to study neurodevelopmental disorders	35
1.3.2	Tools to study disorders in zebrafish	37
1.4	Summary and aims	45
2	Kiaa0319 expression in zebrafish embryo development	46
2.1	Summary	46
2.2	Methods	47
2.2.1	Genomic mapping of zebrafish <i>kiaa0319</i> and <i>kiaa0319l</i>	47
2.2.2	Quantitative Real time PCR	48
2.2.3	Whole-mount <i>in situ</i> hybridization (WISH) on zebrafish embryos	52
2.2.4	Fluorescence In situ Hybridisation (FISH)	58
2.2.5	RNAScope	60
2.2.6	Imaging and Image reconstruction	63

2.3	Results	65
2.3.1	Zebrafish <i>kiaa0319</i> and <i>kiaa0319l</i> throughout development	65
2.3.2	Quantification of <i>kiaa0319</i> expression levels	68
2.3.3	<i>kiaa0319</i> WISH and FISH probe design	69
2.3.4	<i>kiaa0319</i> FISH protocol	71
2.3.5	<i>kiaa0319</i> RNAScope protocol	73
2.3.6	<i>kiaa0319</i> is asymmetrically expressed at specific developmental stages	80
2.3.7	<i>kiaa0319</i> -like	81
2.4	Concluding remarks	85
3	Kiaa0319 function in zebrafish	87
3.1	Abstract	87
3.2	Material and Methods	88
3.2.1	Morpholino experiments	88
3.2.2	CRISPR genome editing protocol	92
3.3	Results	99
3.3.1	Morpholino knock down of zebrafish <i>kiaa0319</i>	99
3.3.2	CRISPR/Cas9 knock-out of zebrafish <i>kiaa0319</i>	109
3.4	Concluding remarks	111
4	Human regulatory sequence characterisation in zebrafish using Gateway Tol2 Protocol	113
4.1	Abstract	113
4.2	Methods	114
4.2.1	The human KIAA0319 promoter	114
4.2.2	<i>PCSK6</i>	120
4.3	Results	126

4.3.2	Concluding remarks	134
5	Discussion	136
5.1	<i>Kiaa0319</i> and <i>Kiaa0319</i> -like expression pattern throughout zebrafish development	137
5.2	<i>Kiaa0319</i> function in zebrafish development	138
5.3	Testing for human regulatory sequences using zebrafish as a model organism	140
5.4	Summary	142
6	Appendices	179
6.1	Appendix A	179
6.1.1	Appendix A1 Enzyme catalogue	179
6.1.2	Appendix A2 Buffers and solutions	180
6.1.3	Appendix A3 Catalogue of Cells used in experiments	182
6.1.4	Appendix A4 catalogue of Kits used in experiments	183
6.1.5	Appendix A5 Plasmids	184
6.1.6	Appendix A6 Primer catalogue	185
6.2	Appendix B	186
6.2.1	Appendix B1 A standard PCR reaction using Phusion DNA Polymerase	187
6.3	Appendix C	188
6.3.1	Appendix C1 Primer catalogue	188
6.3.2	Appendix C2 Screenshot of zfin.org database on <i>kiaa0319</i> and <i>kiaa0319l</i>	189
6.3.3	Appendix C3 RT-qPCR standard curve	190
6.4	Appendix D	191
6.4.1	Appendix D1 RNAScope	191
6.4.2	Appendix D2 RNAScope Amp4 dye combination	192

6.4.3	Appendix D3 RNAScope probe design <i>kiaa0319l</i>	192
6.4.4	Appendix D4 RNAScope probe design <i>myod</i>	193
6.4.5	Appendix D5 RNAScope probe design <i>kiaa0319</i>	193
6.5	Appendix E	194
6.5.1	Appendix E1 <i>kiaa0319</i> human promoter	195
6.5.2	Appendix E2 Positive control HUMAN	196
6.5.3	Appendix E3 Positive control ZEBRAFISH	197
6.5.4	Appendix E4 Negative control	198
6.5.5	Appendix E5 Catalogue of multisite recombination plasmids	199
6.6	Appendix F	212
6.6.1	Appendix F1	212
6.6.2	Appendix F2	213
6.6.3	Appendix F3 <i>kiaa0319</i> Knock down – Morpholino	214
6.6.4	Appendix F4 Sequence alignment of Kiaa0319 protein and Kiaa0319-like protein against the peptide sequences of the chosen antibodies.	216
6.7	Appendix G	218
7	References	143
8	PUBLICATION	219

Table of Tables

Table 1.1 Three major criteria contributing to the heterogeneity of GWAS outcomes	26
Table 1.2 An overview of a few recent studies, using non-conserved sequences in a Tol2 assay.....	43
Table 2.1 Duration of Proteinase K treatment according to zebrafish developmental stage	56
Table 2.2 Duration of Pretreat 3 and PFA treatment according to zebrafish developmental stage	62
Table 3.1 Morpholino sequences for translational blocking (TB) and splice junction (SJ) targeting MOs.	89
Table 3.2 List of antibodies used for western blot analysis	91
Table 3.3 Titration of splice junction (SJ) MOs.....	100
Table 3.4 Titration of translational blocking (TB1 and TB2) MOs	102
Table 4.1 Duration of Proteinase K treatment relative to zebrafish developmental stage	125
Table 7.1 List of enzymes with reference numbers and the company	179
Table 7.2 List of buffers and solutions.....	180
Table 7.3 List of competent cells use for transformations	182
Table 7.4 List of kits with reference number and the company	183
Table 7.5 List of plasmids used in the Gateway Tol2 cloning protocol.....	184
Table 7.6 List of primers used in this thesis.....	185
Table 7.7 PCR mastermix for obtaining PCSK6 promoter sequence	187
Table 7.8 List of primers used in kiaa0319 isoform analysis.....	188
Table 7.9 RNAScope probes with their name and Ensembl accession number.....	191
Table 7.10 RNAScope dye combination in Amp4 channels A, B and C.....	192
Table 7.11 List of att recombination site sequences	194
Table 7.12 The components and the volume needed for the multisite recombination creating a pDest-Cherry-kiaa0319 destination vector.....	195
Table 7.13 The components and the volume needed for the multisite recombination creating a pDest-Cherry-hUBI destination vector	196
Table 7.14 The components and the volume needed for the multisite recombination creating a pDest-Cherry-zfUBI destination vector	197
Table 7.15 The components and the volume needed for the multisite recombination creating a pDest-Cherry-MCS destination vector	198
Table 7.16 The list of primers used to create oligo duplexes for gRNA.....	212
Table 7.17 List of primers for PCR genotyping of CRISPR/Cas9 injected embryos	213
Table 7.18 The survival rate and the number of embryos exhibiting phenotype of embryos injected with TB1 MOs, TB2 MOs and a coinjection of both MOs at a 100µM concentration.....	215

Table of Figures

Figure 1.1 Left hemisphere brain activation pattern in non-impaired readers compared to dyslexic readers.....	21
Figure 1.2 PCSK6 intronic promoter sequence with rs11855415 variant.....	25
Figure 1.3 KIAA0319 promoter sequence with the rs9461045 variant	31
Figure 1.4 <i>KIAA0319</i> and <i>KIAA0319L</i> expression profile in human tissues	33
Figure 1.5 Morpholino oligonucleotides.....	38
Figure 1.6 The Tol2 system	42
Figure 2.1 <i>In situ</i> Hybridisation procedure	55
Figure 2.2 Comparison of three <i>in situ</i> Hybridisation protocols used in this study	57
Figure 2.3 RNAScope probe design.....	61
Figure 2.4 A schematic representation of zebrafish <i>kiaa0319</i> and <i>kiaa0319l</i> genes	65
Figure 2.5 Zebrafish <i>kiaa0319</i> throughout embryo development.....	66
Figure 2.6 Primer design strategy for <i>kiaa0319</i> isoform screening	67
Figure 2.7 The expression levels of zebrafish <i>kiaa0319</i> throughout embryonic development	68
Figure 2.8 Agarose gels of transcribed WISH and FISH riboprobes.....	69
Figure 2.9 The expression of <i>kiaa0319</i> in early embryonic development	70
Figure 2.10 Fluorescence <i>in situ</i> hybridisation (FISH).....	72
Figure 2.11 The 5dpf embryos labelled with triple negative and the positive control for RNAScope protocol	73
Figure 2.12 Confocal images of <i>kiaa0319</i> expression in three developmental stages.....	74
Figure 2.13 <i>kiaa0319</i> and <i>kiaa0319-like</i> signal in zebrafish eye and otic vesicle.	76
Figure 2.14 Lightsheet microscopy and 3D reconstruction of 5dpf zebrafish control embryos.....	77
Figure 2.15 Lightsheet microscopy and 3D reconstruction of <i>kiaa0319</i> expression in three zebrafish developmental stages.....	78
Figure 2.16 Confocal images of RNAScope on <i>gfap:GFP Oligo2:dsRed</i> transgenic zebrafish.....	79
Figure 2.17 The asymmetric expression of <i>kiaa0319</i> in 28hpf zebrafish embryo	80
Figure 2.18 The RQ results of left vs right zebrafish eyes in three developmental stages	81
Figure 2.19 <i>Kiaa0319l</i> expression profile throughout embryonic development.....	82
Figure 2.20 <i>kiaa0319</i> expression profile of three developmental stages	83
Figure 2.21 The RQ results of left vs right zebrafish eyes in three developmental stages	84
Figure 3.1 USCS representation of morpholino locations on zebrafish <i>kiaa0319</i>	89
Figure 3.2 <i>kiaa0319</i> qPCR fragment	92
Figure 3.3 The CRISPR Cas9 protocol	94
Figure 3.4 Splice Junction MO knock down in 1 dpf vs 4dpf zebrafish embryos	101
Figure 3.5 Translation blocking MOs at 1 dpf and 4 dpf.....	104
Figure 3.6 Zebrafish MO – injected embryos exhibiting phenotype	105
Figure 3.7 The zebrafish embryos injected with 250µM TB morpholino oligonucleotides	106

Figure 3.8 Western blot analysis of Kiaa0319	107
Figure 3.9 Comparison of commercial vs custom made anti-KIAA0319 antibody at 24hpf and 48hpf zebrafish	108
Figure 3.10 gRNA oligo duplex sequencing results	109
Figure 3.11 Genotyping results for CRISPR/Cas9 genome editing	110
Figure 4.1 Gateway Multisite Recombination	118
Figure 4.2 <i>KIAA0319</i> and control Gateway destination vectors	127
Figure 4.3 A reverse transcription PCR of 4dpf zebrafish embryos injected with different Tol2 constructs	128
Figure 4.4 Bright field and fluorescence images of 4dpf zebrafish embryos injected with different pDestTol2pACryGFP Destination vectors	130
Figure 4.5 Gateway destination vectors used in PCSK6 analysis	131
Figure 4.6 Agarose gel image of RT PCR products for PCSK6 and the controls	132
Figure 4.7 Bright field and fluorescence images of Zebrafish injected with different pminTol-R4-R2 Destination vectors	133
Figure 6.1 A zebrafish <i>kiaa0319</i> cDNA sequence in pCR™-Blunt II-TOPO® vector ..	186
Figure 6.2 <i>kiaa0319</i> and <i>kiaa0319l</i> information as in zfin.org database	189
Figure 6.3 Standard curve using <i>kiaa0319</i> primers 518 and 519	190
Figure 6.4 <i>kiaa0319l</i> cDNA sequence	192
Figure 6.5 <i>myod</i> cDNA sequence	193
Figure 6.6 <i>kiaa0319</i> cDNA sequence	193
Figure 6.7 A pME-cherry vector	199
Figure 6.8 A p5E-MCS vector	200
Figure 6.9 A p3E-mcs 1 vector	201
Figure 6.10 A pDestTol2pACryGFP vector	202
Figure 6.11 A <i>kiaa03919</i> -promoter pDestTol2pACryGFP destination vector	203
Figure 6.12 An empty p5E-MCS pDestTol2pACryGFP destination vector	204
Figure 6.13 A zebrafish ubiquitous promoter in destination vector	205
Figure 6.14 A human ubiquitous promoter in destination vector	206
Figure 6.15 A pminTol2R4-R2 vector	207
Figure 6.16 A p5E-MCS-PSK6 vector	208
Figure 6.17 A PCSK6 promoter pminTol2R4-R2 vector	209
Figure 6.18 A zebrafish ubiquitous promoter in pminTol2R4-R2 destination vector ...	210
Figure 6.19 An empty p5E-MCS pMinTolR4R2 destination vector	211
Figure 6.20 The location of morpholino sequences in zebrafish <i>kiaa0319</i> gene	215
Figure 6.21 Pairwise sequence alignment for R7, 70 and Abcam anti-KIAA0319 antibody	217
Figure 6.22 Zebrafish developmental stages as per Kimmel et al (1995)	218

Abbreviations

°C	degree Celsius
µg	microgram
Ab	antibody
ADHD	attention-deficit hyperactivity disorder
Amp/Cam	ampicillin and chloramphenicol antibiotic resistance
BLAT	blast-like alignment tool
bp	base pairs
BSA	bovine serum albumin
cDNA	complementary DNA
CAT	chloramphenicol acetyltransferase
CamR	chloramphenicol antibiotic resistance
C _t	cycle at threshold
DNA	deoxyribonucleic acid
dpf	days post fertilisation
EGFP	enhanced green fluorescent protein
Fig	Figure
fMRI	functional magnetic resonance imaging
g	gravity acceleration

GFP	green fluorescent protein
GWAS	genome wide association study
h	hours
hpf	hours post fertilisation
HRP	horse radish peroxidase
IF	immunofluorescence
IQ	intelligence quotient
Kan	kanamycin antibiotic resistance
KO	knockout
LB	Lysogeny broth
MEPS	multi egg production system
min	minute(s)
ml	millilitre
NEB	New England Biolabs
nt	nucleotide
O/N	overnight
ORF	open reading frame
PBS	phosphate-buffered saline
PBT	Phosphate-buffered saline with 0.1% Tween 20
PCR	polymerase chain reaction

PKD	polycystic kidney disease
Poly-A	polyadenylate tail
qRT-PCR	quantitative reverse transcriptase polymerase chain reaction
RD	Reading disorder
RNA	ribonucleic acid
RNase	ribonuclease
ROI	region of interest
rpm	revolutions per minute
s	seconds
SNP(s)	single nucleotide polymorphism(s)
TSS	transcription start site
UTR	untranslated region
WIK	zebrafish wild type line
WT	wild type zebrafish
MeOH	methanol
UTR	untranslated region

1 Introduction

1.1 Dyslexia

Dyslexia, or reading disability (RD), has had various definitions through time [Hulme and Snowling, 2009]. The current accepted version defines RD as a neurobiological disability in which an individual's ability to accurately and/or fluently recognise words, spell and decode is significantly affected [Pennington and Bishop, 2009]. For meeting a dyslexia diagnosis individuals need to have difficulties in learning to read despite adequate educational opportunities, no brain damage, no other obvious neurological impairments or sensory deficits and no other syndromes [Pennington and Bishop, 2009].

Dyslexia affects between 5 and 12 percent of school-aged children [Peterson and Pennington, 2015] and is the most commonly studied learning disability [Shaywitz, 2003]. Dyslexia is highly correlated with phonological deficits in school-age children [Fletcher et al., 1994] as well as in adolescents [Shaywitz et al., 1999]. Although it is defined as a developmental disorder, functional difficulties persist throughout adulthood [Ramus et al., 2003; Shaywitz et al., 2003; Frauenheim, 1978]. Dyslexia often coexists with language impairment [Moats, 1994; Lindamood, 1994], deficits in mathematical abilities [Fletcher and Loveland, 1986], and/or attention disorder (Shankweiler, et al., 1995; B.A. Shaywitz, Fletcher, & S.E. Shaywitz, 1994).

1.1.1 Dyslexia theories

There are three most supported theories as to why and how to explain the pathophysiology of dyslexia:

1) *The phonological theory:*

Dyslexia is a consequence of inaccurate processing of the information in the brain due to deficits in phoneme awareness. An extensive line of research was reviewed by Schulte-Körne and Bruder (2010), highlighting the results in support of this theory [Schulte-Körne and Bruder, 2010].

2) *The cerebellar theory:*

The malfunction of the cerebellum leads to fine motor control and balance problems [Nicolson and Fawcett, 1990], inadequate information processing speed [Nicolson and Fawcett, 1994] and visual and auditory deficits [J and C, 2002; Stein, 2001b; Boets et al., 2008]. Cerebellum controls the majority of functions, which are dysfunctional in individuals with dyslexia (reviewed in Stoodley and Stein 2011).

3) *The Magnocellular theory:*

The magnocellular theory of dyslexia focuses on the changes in visual and auditory processing. The magnocells are large cells located in the retina and throughout the ventral lateral geniculate nucleus (LGN) and possibly other structures involved in visual processing [Livingstone et al., 1991]. The psychophysical and post-mortem data were first to suggest that dyslexia is a consequence of the abnormal function and appearance of magnocells [Livingstone et al., 1991; Lovegrove et al., 1980]. The magnocellular layer of dyslexic post-mortem brain seems to be disorganised and the cells are smaller in size, potentially influencing the processivity of the visual

information [Livingstone et al., 1991]. Taking up the idea, more studies have focused on the visual processing deficits, repetitively proposing impairment of the visual and auditory systems to be the underlying reason for dyslexia phenotype [Bosse et al., 2007; Bosse and Valdois, 2003; Stein, 2001a]. Ray et al (2005) showed that reading abilities in impaired population increased significantly when the visual input was stimulated with the addition of a yellow filter [Ray et al., 2005]. Despite the amount of research attributing to magnocellular/sensory theory of dyslexia origin, there are still challenges to be addressed before a conclusion is made (discussed in Goswami 2015).

1.1.2 Laterality and dyslexia

The human brain exhibits structural and functional asymmetries. Structural brain asymmetries can be detected already *in utero* and continue to change as the child grows older [Dubois et al., 2009; Kasprian et al., 2011; Habas et al., 2012; Kivilevitch et al., 2010; Zhang et al., 2011]. Functional asymmetries have been reported as early as in the 19th century, when Broca and Wernicke observed impaired language abilities as a consequence of brain trauma [Broca, 1861; Wernicke, 1874]. Asymmetries in brain regions underlying language are phylogenetically conserved and strongly heritable [Thompson et al., 2001; Toga and Thompson, 2003]. The lateralisation of language abilities can be observed already in infants and followed up throughout childhood. As the recurring theme in the dyslexia research is a reduced language lateralization [Illingworth and Bishop, 2009] and cerebral lateralization [Sun et al., 2010; de Guibert et al., 2011; Badcock et al., 2012], there has been a lot of research dedicated to understanding the correlation between these traits.

The first mention of dyslexia dates back to 1891, when Dejerine (1891) noticed the importance of the left posterior brain region in reading [Dejerine, 1891]. Following Dejerine, many scientists have worked on unravelling the morphological changes in the brain and their link to dyslexia [Damasio and Damasio, 1983; Friedman et al., 1993; Geschwind, 1965]. With the increase of novel techniques, investigations of the post-mortem brain [Galaburda et al., 1985] and its morphometry [Brown et al., 2001; Eliez et al., 2000; Filipek, 1996] and magnetic resonance imaging (MRI) [Eliez et al., 2000], differences in specific regions between dyslexic and non-impaired readers have been confirmed. Functional MRI (fMRI) studies have mainly focused on three brain areas (Figure 1.1) whose activity levels are altered in readers with dyslexia [Kronbichler et al., 2006; Brambati et al., 2006; Shaywitz et al., 2002]. The parietotemporal region (Figure 1.1 red), the inferior frontal gyrus (IFG; Broca's area) (Figure 1.1 blue) and the occipitotemporal region (Figure 1.1 green) are all found in the left brain hemisphere and are responsible for rapid word recognition [Cohen et al., 2000; Cohen and Dehaene, 2004; Dehaene et al., 2005; Vinckier et al., 2007; Price and Devlin, 2011]. These areas show under- or over-activation while performing reading tasks in dyslexic readers compared to non-impaired participants [Shaywitz et al., 2002; Richlan et al., 2011; Price and Mechelli, 2005; Shaywitz and Shaywitz, 2005; Richlan, 2012]. Furthermore, functional brain imaging in adult dyslexic readers has showed the left posterior brain region fails to function properly while reading [Simos et al., 2000; Salmelin et al., 1996; Rumsey et al., 1997, 1992; Horwitz et al., 1998; Helenius et al., 1991; Brunswick et al., 1999; Shaywitz, 1998; Paulesu et al., 2001]. In other words, non-impaired reader's language lateralization is dominant on the left hemisphere [Knecht, 2000], whilst in the dyslexic population, the language centre seems to be more bilateral [Finn et al., 2014]. However, the research is difficult to interpret due to the heterogeneity of data collection and analyses. A review of more than 50 imaging studies indicates that in a dyslexic brain, there is a specific lack of activation of the left occipito-temporal cortex (Figure 1.1 green), which is involved in reading and reading-like behaviours [Paulesu et al., 2014].

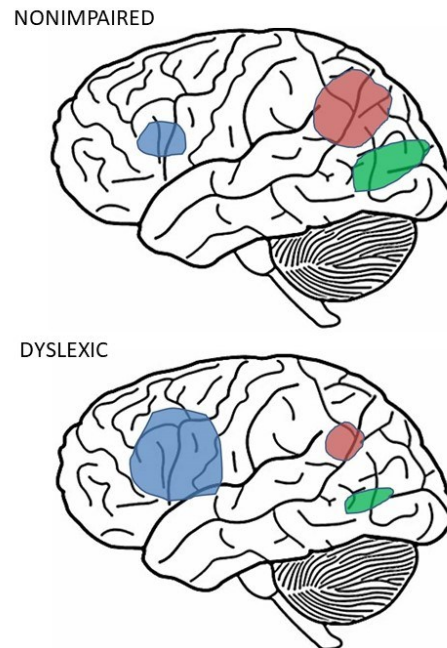


Figure 1.1 Left hemisphere brain activation pattern in non-impaired readers compared to dyslexic readers

Nonimpaired readers show activation in Broca's area (blue), parieto-temporal region (red) and the occipito-temporal region (green). The brain activation of parieto-temporal region (red) and the occipito-temporal region (green) in dyslexia is under-activated during performance of phonological tasks whilst Broca's area (blue) overcompensates for the loss of function [Shaywitz and Shaywitz, 2004]. Image adapted from Shaywitz, 2003.

1.1.2.1 Handedness and brain laterality

Handedness is considered as the most obvious of human lateralised behaviours, which can be observed as early as at 10 weeks of gestation [Hepper et al., 1998]. The right-left hand bias is seen across all cultures with right hand being dominant in more than 75% of tested subjects [McManus, 1991; Raymond et al., 1996; McKeever, 2000]. Left handedness has historically been connected to a variety of disorders, predisposing that left handers deviate from the “normal” right handed population (reviewed in Hepper 2013). However, new evidence indicate that left handers and severe right handers represent the two ends of the normal distribution of handedness across population [Gutwinski et al., 2011].

Handedness is weakly correlated to language dominance lateralisation. The brain of right handed individuals is exhibiting language dominance on the left in 96% of cases, whereas in the left handed population, the language centre lies on the left hemisphere only in 73% of individuals [Knecht, 2000]. Asymmetries in the language-related centres and motor cortex are also correlated with handedness [Amunts et al., 1996; Dassonville et al., 1997; Hervé et al., 2006]. Hemispheric structural differences are thought to play a role in functional variation (Reviewed in Hepper 2013). It is believed that the behavioural lateralisation (the preferred movement of the right hand) led to functional lateralisation, thus development of language [Morillon et al., 2010; Phan and Vicario, 2010]. Indeed, the left-handed subjects tend to have more diverse language lateralisation than the right-handers, which in part supports the afore-mentioned theory [Sommer et al., 2002].

1.1.2.2 Handedness and dyslexia

A study of more than 25000 families with twins revealed that handedness is genetically controlled in only about a quarter of a variance (~25%) [Medland et al., 2009]. Handedness is thought to be a polygenic trait, controlled by a large number of genetic factors [McManus et al., 2013]. However, there are only a few suggested handedness candidate genes to date. Francks *et al* (2007) have conducted a meta-analysis of 20 genome-wide linkage studies and shown that handedness is significantly linked to *LRRTM1* in a schizophrenic population [Francks et al., 2007]. The study was replicated in an independent German cohort, supporting the linkage between *LRRTM1* and schizophrenia [Ludwig et al., 2009]. *LRRTM1* (Leucine-rich repeat transmembrane neuronal 1) is expressed in thalamus and cerebral cortex of the forebrain and is likely to be involved in human brain asymmetry [Francks et al., 2007; Ludwig et al., 2009].

Furthermore, Scerri et al (2011) found two intronic associations through genome-wide association study (GWAS) between relative hand skill and the *PCSK6* gene in dyslexic population [Scerri et al., 2011a]. Scerri *et al* (2011) performed a meta-analysis of three samples selected for dyslexia, using a PegQ measure derived from a pegboard test. The pegboard test measures relative hand skill (right vs left) and returns a normal distribution of degree of handedness rather than a handedness type [Scerri et al., 2011a]. The carriers of minor alleles of either of the highly associated SNPs (rs9806256 or rs11855415) are significantly more skilled with their right hand compared to their left hand [Scerri et al., 2011a]. The association with rs11855415 was replicated in two independent cohorts of individuals with dyslexia, while the minor allele of the same SNP indicated lower right-handed bias in the general population [Scerri et al., 2011a].

PCSK6 (proprotein convertase subtilisin/kexin type 6) or *PACE4* promotes *NODAL* maturation [Constam and Robertson, 1999]. *NODAL* is the earliest conserved gene involved in setting up asymmetries in the vertebrates [Levin, 2005]. *NODAL* and *NODAL*-related genes are members of transforming growth factor beta (TGF- β) superfamily. The genes in *NODAL* pathway are well studied for their functions during embryo development [Morokuma et al., 2002]. *NODAL* members can potentially inhibit the Bone morphogenetic proteins (BMPs) and Wingless-related integration site (Wnt) ligands [Onuma et al., 2005], thus affecting the body axis patterning. In mouse, human and chick there is only a single *Nodal* gene, while in frogs (encoded by six *xNr* genes) and zebrafish (*cyclops*, *squint* and *southpaw*) there are several [Schier, 2003]. The *NODAL* ligands act as morphogens, activating responses in a dose-dependent manner [Ashe and Briscoe, 2006]. When it comes to neural development, *NODAL* plays a dual role in generating patterning of neural tissue, leading to maintenance and patterning of neural tissue [Shen, 2007]. The evolutionary conservation and the versatile functioning of *NODAL* and *NODAL*-related genes in LR patterning and neural development suggest *NODAL* being an important factor in the vertebrate development.

Additionally, members of *Nodal* family in zebrafish regulate the asymmetry of the brain development. The leftwards expression activates the asymmetry of the pineal gland complex, thus affecting the development of firstly left and then right habenulae [Liang et al., 2000; Concha et al., 2000, 2003, Gamse et al., 2002, 2003]. The pineal complex consists of a centrally positioned pineal organ (zebrafish epiphysis) and the left parapineal anlage. Next to them there are dorsal habenulae, which vary in size and gene expression. In the absence of *Nodal* leftward activity, the epithalamus develops asymmetries and the fish lateralised behaviour, “handedness”, becomes randomised [Concha et al., 2000].

The associations of handedness with *PCSK6* (but not *LRRTM1*) have further been confirmed in two independent studies, making *PCSK6* a more reliable handedness candidate [Arning et al., 2013; Brandler et al., 2013a]. Arning *et al* (2013) used the general population Edinburgh handedness inventory as a sample to test for the associations of handedness with *LRRTM1* and *PCSK6* [Arning et al., 2013]. Rather than testing for functional handedness distribution, they have analysed the degree of handedness using laterality quotient calculated based on the self-reported handedness questioner. The resulting significantly associated variant rs10523972 is an intronic 33bp variable-number tandem repeat (VNTR) with a long (9) or short (6) repetition being the most frequently observed [Arning et al., 2013]. Furthermore, Brandler *et al* (2013) replicated the handedness phenotype from Scerri *et al* (2011) study using the general population, however, they were driven by different associations, independent from *PCSK6*. Additionally, they have coupled the GWAS data with the gene-set enrichment analysis (GSEA) and the mouse phenotype data and showed the identified genes in dyslexic population are all involved in body left-right asymmetry [Brandler et al., 2013b]. They hypothesise the same mechanisms involved in establishing body laterality might be involved in determining behavioural laterality (handedness) and cerebral development [Brandler et al., 2013b].

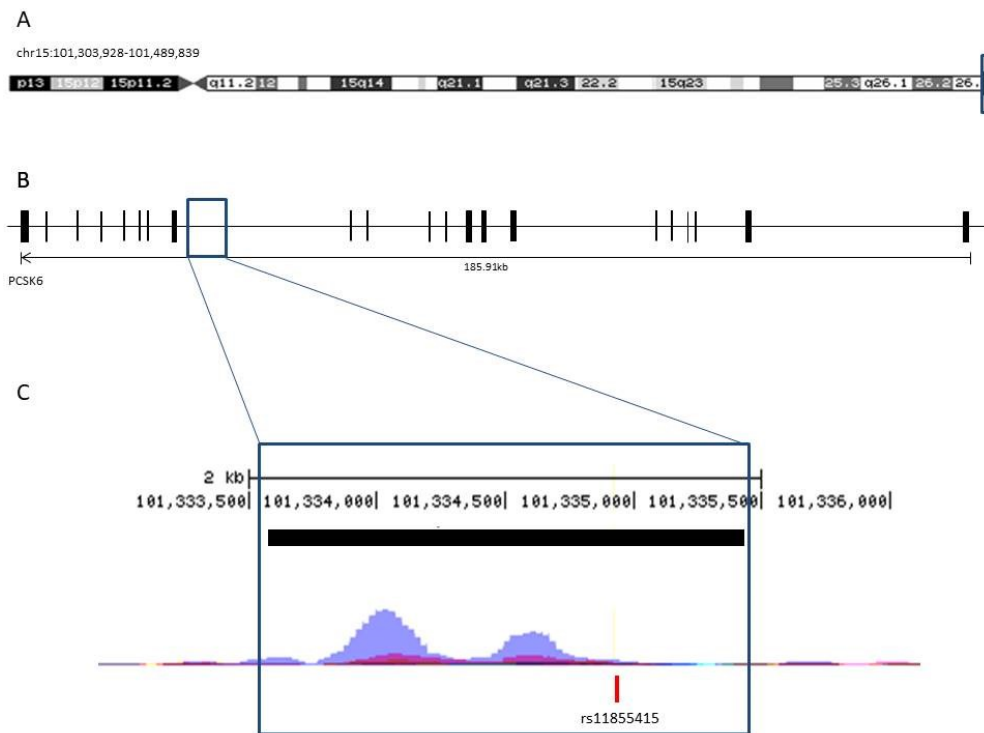


Figure 1.2 PCSK6 intronic promoter sequence with rs11855415 variant

A) Human Chromosome 15. Blue box represents *PCSK6*. B) Full *PCSK6* gene with 21 exons spanning 185,911 kb in antisense direction (black arrow). Blue box represents intronic promoter region C) Promoter sequence spanning 1806 bp (black thick line in blue box) across *PCSK6* intron 13. Red line represents rs11855415 SNP associated with relative hand skill in dyslexic population [Brandler et al., 2013a]. The blue and red peaks represent DNase I hypersensitivity clusters.

Recently, Shore *et al.* (2016) performed a functional study showing one of the top picks for *PCSK6* association with handedness, rs11855415 (Figure 1.2), has an effect on the nuclear factor binding site [Shore et al., 2016]. They used the Electrophoretic Mobility Shift Assays (EMSA) in multiple cell lines, confirming the minor allele (A) of rs11855415 variant promotes the binding of transcriptional factors, whereas the major allele (T) does not [Shore et al., 2016]. The association is located near the recently characterised intronic promoter which regulates the transcription of long non-coding RNA (lncRNA) and a shorter *PCSK6* isoform [Shore et al., 2016].

The association with handedness, the novel function and a proximity of the rs11855415 SNP, make the *PCSK6* regulatory region an attractive candidate to study, however, a model is needed that would allow for more complex study of the regulatory function in a time and tissue specific manner. The known function of *PCSK6* makes it an interesting candidate for handedness, as same biology of structural asymmetries is implicated in behavioural asymmetries.

Despite the selection of associations described above, there have been several studies, finding no associations between handedness and dyslexia [Bishop, 2013]. The GWAS are being discussed between scientists as a low power approach due to the impaired reproducibility of the results [McCarthy et al., 2008; Bishop, 2013]. A precaution is advised when analysing the outcomes of such studies. Here (Table 1.1) are some of the major reasons causing controversial results of GWA studies:

Table 1.1 Three major criteria contributing to the heterogeneity of GWAS outcomes

Criterion	Description
Sample size	Recommended sample size is 1000-1.000.000, however, each study is using a vastly different number of participants which attributes to inconsistent outcomes. Additionally, gathering high power sample size for complex traits can be time- and money-consuming, leading to further complications when designing the study [Newbury et al., 2014; Brandler and Paracchini, 2013; McCarthy et al., 2008]
Approach	Population-based (all the phenotypes represented in the population) or binary (case-control) qualitative GWA studies, quantitative GWA studies... Various approaches yield different outcomes [Newbury et al., 2014]
Phenotype definition	Defining the critical cut-off point of dyslexia phenotype. Phenotype has been defined differently in different studies, which affects the population selections and consequently, the outcomes of the GWAS [Newbury et al., 2014]

1.2 Dyslexia Genetics

Dyslexia is highly heritable (up to 70%) and results from the interactions between complex genetic and environmental risk factors [Fisher et al., 2002; Francks et al., 2002; DeFries et al., 1987]. Dyslexia candidate genes have been mapped on nine putative dyslexia loci: DYX1–DYX9 (reviewed in Schumacher et al. 2006; Paracchini et al. 2016). The most robust dyslexia candidate genes are *DYX1C1* on chromosome 15 [Taipale et al., 2003; Scerri et al., 2004; Wigg et al., 2004], *KIAA0319* [Francks et al., 2004; Cope et al., 2005; Harold et al., 2006; Luciano et al., 2007; Paracchini et al., 2008] and *DCDC2* [Meng et al., 2005; Schumacher et al., 2007] on chromosome 6, *KIAA0319-LIKE* on chromosome 1 [Couto et al., 2008] and *ROBO1* on chromosome 3 [Hannula-Jouppi et al., 2005].

1.2.1 DYX1C1

The first candidate gene for dyslexia was dyslexia susceptibility 1 candidate 1 (*DYX1C1*), discovered through linkage studies and mapped to the chromosome 15 using fluorescence *in situ* hybridisation [Rabin et al., 1993; Smith et al., 1983; Nopola-Hemmi et al., 2000]. *DYX1C1* has been shown to be involved in altered neuronal migration based on the only post-mortem anatomical study of dyslexic brain conducted to date [Galaburda et al., 1985]. More recent studies reported *DYX1C1* variant associations with deficits in the short-term memory [Dahdouh et al., 2009], verbal short-term memory [Marino et al., 2007] and non-word reading [Bates et al., 2010]. Molecular and cellular analyses of *DYX1C1* have pointed out *DYX1C1* involvement in neuronal migration in the developing cortex [Rosen et al., 2007; Wang et al., 2006] and cilia biology [Hoh et al., 2012; Ivliev et al., 2012a; Tarkar et al., 2013a]. RNAi knock down study in rats has again pointed towards the impaired migration of the neurons [Wang et al., 2006]. Furthermore, a knock down of *Dyx1c1* in rats resulted in defects in sound processing and spatial learning as well as in impaired development of the neocortex and hippocampus [Rosen et al., 2007;

Threlkeld et al., 2007]. Functional studies on zebrafish *dyx1c1* mutants report asymmetry phenotypes such as body curvature, hydrocephalus and kidney cysts [Chandrasekar et al., 2013]. Hydrocephalus and *situs inversus*, a complete reversal of body inner organs have also been reported in mouse *Dyx1c1* mutants [Tarkar et al., 2013b].

Despite the *DYX1C1* involvement in neuronal migration shown by the knock down studies, Rendall *et al* (2017) failed to reproduce the phenotype in homozygous knockout mice. They observed no significant differences in the cortex or in the cortical lamination patterning of the forebrain of the knockout mice in comparison to the controls [Rendall et al., 2017]. Further behavioural studies on the mice with disrupted function of *Dyx1c1* indicated the knockout animals have impaired memory performance [Rendall et al., 2017].

1.2.2 DCDC2

DCDC2 (doublecortin-domain-containing-2) is a member of a doublecortin (DCX) family and contains a doublecortin homology domain. DCX family members have been involved with abnormal neuronal migration leading to disruption of the cortex layering [des Portes et al., 1998]. Indeed, RNAi studies indicate *DCDC2* down regulation leads to alteration in neuronal migration in the brain regions related to reading [Meng et al., 2005]. The *DCDC2* harbours several variants associated with multiple reading traits [Meng et al., 2005] and dyslexia [Schumacher et al., 2006]. Furthermore, *DCDC2* localises to the microtubules of the mitotic spindle and the ciliary axoneme, suggesting its role in cilia biology [Grati et al., 2015; Schueler et al., 2015b; Massinen et al., 2011a]. Ciliary phenotypes have also been shown through a knockdown study of *dcdc2* in zebrafish (Schueler et al., 2015). Additional research on ciliopathy patients revealed the involvement of *DCDC2* mutations with cystic kidney disease, retina malformation [Schueler et al., 2015b] and deafness [Grati et al., 2015].

1.2.3 ROBO1

ROBO1 was found through translocation fine mapping, where an individual with dyslexia had a translocation breakpoint in the first intron of the *ROBO1* [Hannula-Jouppi et al., 2005]. Further gene expression study in lymphocytes resulted in lowered or absent *ROBO1* transcription, which led to believe dyslexia is caused by the reduction of *ROBO1* expression [Hannula-Jouppi et al., 2005]. *ROBO1* is a transmembrane protein, expressed in the brain cortex and has found to be involved in neuronal axon guidance [Kidd et al., 1999, 1998; Seeger et al., 1993; Hannula-Jouppi et al., 2005] and neuronal migration [Pini, 1993; Wong et al., 2002; Wu et al., 1999; Zhu et al., 1999; Skaper, 2012]. When one of the two active copies is inactive or mutated, the axonal guidance becomes impaired, which might lead to dyslexia [Hannula-Jouppi et al., 2005].

1.2.4 KIAA0319

KIAA0319 is one of the strongest dyslexia candidates due to the rising amount of association studies (reviewed below). The gene codes for a transmembrane protein with five PKD (Polycystic Kidney Disease) domains [Velayos-Baeza et al., 2008]. The presence of PKD domains suggests the involvement of the gene in the cilia biology. The genes containing PKD domains mostly play a role in human ciliopathies, diseases caused by cilia malfunctioning [Hildebrandt et al., 2011a]. In humans, *KIAA0319* is shown to have a specific spatial-temporal expression pattern in foetal brain [Paracchini et al., 2006a] and strong expression in adult human brain (Figure 1.2 A). The shRNA studies showed rat *Kiaa0319* involvement with impaired neuronal migration [Paracchini et al., 2006b]. However, a recent study of *Kiaa0319* knock out mice found no effects of *Kiaa0319* on neuronal migration [Martinez-Garay et al., 2017].

1.2.4.1 *KIAA0319* associations with dyslexia phenotype

Several studies have associated *KIAA0319* variants with reading-related traits. In 2004, Francks *et al.* performed an association analysis in three independent samples and showed a 77kb quantitative trait loci (QTLs) containing genes *TTRAP*, *KIAA0319* and *THEM2* to be associated with dyslexia [Francks *et al.*, 2004]. A further evidence in *KIAA0319* involvement in dyslexia emerged in 2005 when Cope *et al.* identified two additional SNPs associated with dyslexia [Cope *et al.*, 2005]. Harold *et al.* (2006) tested additional *KIAA0319* SNPs and found nine variations associated with dyslexia clustered around the first exon, suggesting that *KIAA0319* function could be affected by the mutations in the putative regulatory region [Harold *et al.*, 2006]. Luciano *et al.* (2007) replicated the significant association of variants within the *KIAA0319* (as shown by Cope *et al.* 2005) and *TTRAP* genes [Luciano *et al.*, 2007]. Furthermore, Couto *et al.* (2010) identified several putative regulatory regions near the associated markers within the *KIAA0319* and *DCDC2* genes, proposing the variation within regulatory regions as a likely cause of dyslexia-related traits [Couto *et al.*, 2010]. The associations located in the regulatory region were also described by Scerri *et al.* (2011), however these markers are not associated with dyslexia per se, but rather with reading and spelling skills in general [Scerri *et al.*, 2011b]. Additionally, the *KIAA0319/TTRAP/THEM2* locus has been associated with the reduction of brain left-hemisphere asymmetry during reading [Pinel *et al.*, 2012].

Despite the reproduced associations within *KIAA0319*, *TTRAP* and *THEM2* locus [Francks *et al.*, 2004], the *in situ* hybridisation indicated that risk haplotypes only reduce the expression of *KIAA0319*, while *TTRAP* and *THEM2* expression levels remain unaffected [Paracchini *et al.*, 2006a]. Similar trend was observed through the RNAi study in rats, where only the shRNA constructs against *Kiaa0319* led to the impaired neuronal migration and impaired neocortex formation [Paracchini *et al.*, 2006a]. Furthermore, upon identifying the association rs9461045 in the vicinity of *KIAA0319* transcription start site, Dennis *et al.* (2009) conducted a detailed analysis of *KIAA0319* promoter region (Figure 1.3) [Dennis *et al.*, 2009]. They have

characterised a minimal promoter (Figure 1.3 C) and shown that rs9461045 creates a nuclear protein-binding site, promoting the expression of the *KIAA0319* in both, neuronal and non-neuronal cell lines [Dennis et al., 2009].

Similarly to afore-mentioned *PCSK6* intronic regulatory region, containing the variant rs11855415 [Shore et al., 2016], *KIAA0319* promoter presents an interesting candidate region to study the spatiotemporal activity throughout early development. Studying regulatory sequence activity in cell lines provides us only with a limited information of temporal activity, therefore a new model is required to acquire the spatial distribution of the promoter activity as well.

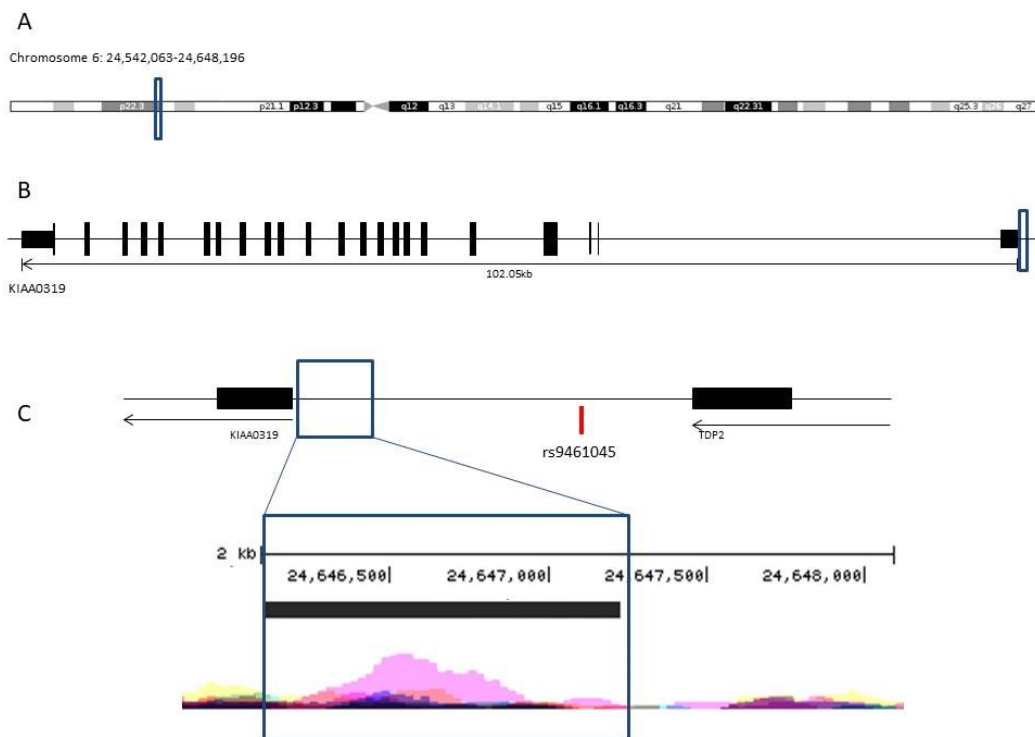


Figure 1.3 KIAA0319 promoter sequence with the rs9461045 variant

A) Human Chromosome 6. Blue box represents KIAA0319. B) Full KIAA0319 gene with 21 exons spanning 102.05kb in antisense direction (black arrow). Blue box represents adjusted KIAA0319 promoter region C) Adjusted promoter sequence spanning 1128bp (black thick line in blue box) across KIAA0319 promoter region. Red line represents rs9461045 variant associated with reading-measures and shown to have a functional effect [Dennis et al., 2009].

1.2.5 KIAA0319-like

An additional dyslexia candidate gene has been proposed, *KIAA0319-like* (*KIAA0319L*) [Couto et al., 2008]. *KIAA0319L* is expressed in the brain cortical neurons, hippocampus, olfactory bulb and other regions (Figure 1.4 B, Poon et al. 2011a). The protein sequence homology with *KIAA0319* is 61% similar. The *KIAA0319L* has been associated with dyslexia phenotypes, such as deficits in spelling and phonemic awareness [Couto et al., 2008]. The presence of PKD domains, interaction with Nogo receptor 1 and its positional homology with the *KIAA0319* gene suggest *KIAA0319L* potential involvement in neuronal migration [Couto et al., 2008; Poon et al., 2011b]. Subsequent study of *Kiaa0319l* function in mice confirmed its role in establishing the correct neuronal migration pattern in embryos [Platt et al., 2013]. However, a recently established *Kiaa0319l* knock out mouse line showed no impaired neuronal migration [Guidi et al., 2017]. Guidi *et al* (2017) also created a double knock out line *Kiaa0319/Kiaa0319l*, where again they could not observe any differences in neuronal migration. When moving towards behavioural studies, they have observed a specific role of *Kiaa0319l* in the auditory processing of the homozygous and double mutants [Guidi et al., 2017].

1.3 Functional characterisation of *KIAA0319* in model organisms

Functional studies conducted in model organisms show inconsistent results for the function of *KIAA0319*. Paracchini *et al* (2006) conducted an *in utero* RNAi knock down in rat, showing a significant reduction in the neuronal migration distance in the rat neurocortex and the impaired morphology of neurons when the *Kiaa0319* is knocked down [Paracchini *et al.*, 2006a]. *Kiaa0319* shRNA knock down resulting in apical dendritic hypertrophy and impaired neuronal migration in rats was shown by Peschansky *et al* (2010). Similarly, Adler and colleagues conducted a shRNA study on *Kiaa0319* in mice, resulting in failed migration of the neurons in the white matter of the brain [Adler *et al.*, 2013]. Additionally, the disruption of rat *Kiaa0319-like* (*Kiaa0319l*) (by knockdown, overexpression, or rescue) also resulted in impaired neuronal migration [Platt *et al.*, 2013], further strengthening the idea of neuronal migration being the cause for developmental dyslexia. Kim and colleagues performed a *Kiaa0319* knock down study on mice by *in utero* electroporation and showed the reduction of dendritic spine density [Kim, 2009]. There are no direct correlations between the spine density and dyslexia, however, it is known that the spine density does correlate to neurodevelopmental disorders schizophrenia and epilepsy [Ethell and Pasquale, 2005; Garey *et al.*, 1998].

In addition to several knock down *Kiaa0319* studies showing its involvement in neuronal migration [Peschansky *et al.*, 2010; Szalkowski *et al.*, 2012a; Adler *et al.*, 2013], Centanni *et al* (2014) created a knock down rat model and shown impaired discrimination in speech processing [Centanni *et al.*, 2014a, 2014b]. A recent characterisation of the *Kiaa0319* knockout mouse line shows no anatomical abnormalities in the brain layers [Martinez-Garay *et al.*, 2017]. Instead, the behavioural study indicates sensory impairment and alterations in anxiety-related behaviour [Martinez-Garay *et al.*, 2017]. A *Kiaa0319/Kiaa0319l* double knockout mouse mutant further confirmed the lack of neuronal migration phenotype in mice [Guidi *et al.*, 2017]. The study did however show significant sensory impairment in

double knockout specimen, suggesting *Kiaa0319* and *Kiaa0319l* together are important for auditory processing [Guidi et al., 2017].

1.3.1 Zebrafish as a model to study neurodevelopmental disorders

Due to the opposing outcomes (e.g. *Kiaa0319* role in neuronal migration) of functional studies using mammalian model systems, a different approach is needed to study the function of *KIAA0319*. Zebrafish (*Danio rerio*) is a well-established model organism used for genetic, pharmaceutical studies and behavioural analyses. The embryos are transparent, and they develop outside the womb, providing the ideal platform for the observations of embryogenesis *in vivo*. Embryogenesis requires 120 hours, enabling the observation of developing structures in a time-efficient manner. The handling of the embryos (collection, storage, microinjection, imaging) is time and cost efficient and relatively low effort. The well-studied embryonic development further adds to the popularity of this small teleost fish [Spence et al., 2007]. Due to a number of well-established techniques for genetic manipulation, the zebrafish poses an excellent opportunity for large scale forward- and reverse genetics analyses.

The zebrafish genome consists of 25 pairs of chromosomes coding for more than 26,000 proteins [Bhartiya et al., 2010]. The sequence homology to the human genome is approximately 70% and 84% of human disease genes have a zebrafish homologue, [Howe et al., 2013a]. An additional advantage of using zebrafish as a model organism to study genetics of human traits, is the simple application of transgenesis methods by microinjection in the single cell embryos. These characteristics allow performing different experiments, such as testing human regulatory sequences, performing knock down or knock out studies as well as studying mutations and their effects on gene function [Becker and Rinkwitz, 2012].

1.3.1.1 Zebrafish laterality

One of the regions I have selected to test for spatiotemporal activity throughout early development is the *PCSK6* intronic promoter. This bidirectional noncoding sequence entailing a rs11855415 variant has been recently shown to promote the expression of the shorter isoform of a *PCSK6* as well as the lncRNA transcripts [Shore et al., 2016]. The SNP is associated with handedness in dyslexic population, linking dyslexia to behavioural laterality. To test for the activity of said promoter region, I chose to use zebrafish as a model organism. Their highly conserved embryogenesis makes them an attractive model organism to study laterality and human developmental disorders [Onai et al., 2014].

The zebrafish laterality is thought to be set after the development of the Kupffer's vesicle, a transient teleost structure homologous to mammalian embryonic node [Cooper and D'Amico, 1996; D'Amico and Cooper, 1997]. It first appears around 12 hours post fertilisation (hpf). Kupffer vesicle is filled with ciliated cells generating a fluid flow, consequently regulating the LR patterning of the brain, heart and gut [Essner et al., 2005]. Following the activation of zebrafish Nodal pathway, members of Nodal family in zebrafish regulate the asymmetry of the brain development. The leftwards expression activates the asymmetry of the pineal gland complex, thus affecting the development of firstly left and then right habenulae [Concha et al., 2000, 2003; Liang et al., 2000; Gamse et al., 2002, 2003]. In the absence of Nodal leftward activity, the epithalamus develops asymmetries and the fish lateralised behaviour, "handedness", becomes randomised [Concha et al., 2000].

Further to the structural laterality of the zebrafish viscera, a lateralised behaviour such as preferential use of right eye when hunting or approaching to unfamiliar objects, has been reported [Miklosi et al., 1997, 1999]. A zebrafish "frequent *situs inversus*" (*fsi*) mutant line helped to link a part of structural, functional and behavioural asymmetries. It has been shown that *fsi* zebrafish simultaneously

exhibit visceral asymmetry reversal and the asymmetries in the diencephalon. Furthermore, some behaviours, such as mirror viewing and approach to target, are fully reversed [Barth et al., 2005]. Interestingly, not all behaviours tested have shown the reversal, indicating the involvement of more than one mechanisms in establishment of various asymmetries [Barth et al., 2005].

Despite the many benefits, zebrafish also possess some disadvantageous qualities. The teleost fish have undergone a genome duplication, adding to complexity of genetic analyses in zebrafish [Ekker et al., 1992; Prince et al., 1998; Amores et al., 1998]. The embryos development rate varies between embryos, even though they have been laid within a single batch. This poses a problem when dividing them into the same developmental stages as time is not the most reliable factor [Kimmel et al., 1995a]. Due to these differences in development it is important to use appropriate strategies when studying gene function throughout embryo development, as discussed in following section.

1.3.2 Tools to study disorders in zebrafish

1.3.2.1 Knock down morpholino studies

Morpholinos (MOs) are synthetic antisense oligonucleotides designed to knock down a gene with high specificity and low adverse effects [Summerton and Weller, 1997]. They consist of 25 morpholine (C₄H₉NO) subunits replacing the ribose ring of the DNA. Their structure (Figure 1.3 A) resembles the one of the standard nucleic acid with a change of phosphorodiamidate linkage (Figure 1.3 A red circle) with the anionic phosphodiester bond [Summerton and Weller, 1997]. These two modifications offer a high stability when studying gene function using MO knock down technique [Corey and Abrams, 2001; Heasman, 2002; Heasman et al., 2000; Nasevicius and Ekker, 2000; Summerton, 1999]. Morpholinos are designed to bind either to ATG translational start site of the sequence (translational blocking) or

between the exon-intron junction (splice junction), affecting the splicing of the premature messenger RNA into the matured mRNA (Figure 1.3 B). In both cases, MOs target the protein function thus creating a specific “knock-down” effect.

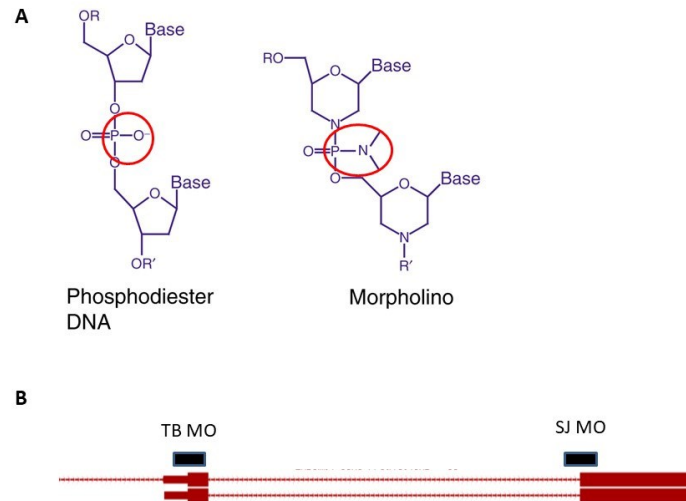


Figure 1.5 Morpholino oligonucleotides

A) Comparison of DNA and a morpholino structure as per Corey and Abrams (2001). The ribose ring in DNA structure is replaced by the morpholine ring and the phosphorodiamidate linkage with the anionic phosphodiester bond (red circles). R and R' indicate the continuation of the structure in the same manner. **B)** The position of translational blocking (TB) and splice junction (SJ) MO binding sites on the DNA sequence (red lines). TB MOs are complementary to the ATG translational start site, while SJ MOs bind to intron-exon junction and prevent efficient splicing of the pre-mRNA into mRNA. Red lines indicate DNA sequence. Thick lines indicate exons, thin lines indicate introns.

Due to their stability, nuclease resistance, water solubility and low toxicity, MO induced knock down is one of the most widely used reverse genetic approaches [Hosen et al., 2013]. For efficient ubiquitous delivery of MO molecules to target, microinjections need to be done between one and 8 cell stage of development [Nasevicius and Ekker, 2000]. The MOs can carry fluorescein label, which makes them visible under the GFP filter and enable fast phenotypical screening. The knock down effect is only temporary and depends on the concentration of injected MOs, which calls for initial dose optimisation before conducting a large scale KD analysis.

There are two classes of MO oligonucleotides: translational blocking and splice junction MOs. The translational blocking MOs (TB MOs) provide a more reliable knock down as they prevent the binding of the translational machinery to the mRNA, thus preventing protein translation to take place. Their effect can be validated by western blotting, and therefore requires specific antibodies which can be a limitation [Hutchinson and Eisen, 2006]. On the other hand, a simple RT-qPCR reaction provides the validation of splice junction MOs (SJ MOs). As the SJ MOs contribute to either exon skipping or intron retention, the resulting frameshift can be easily observed through reduced transcript levels [Draper et al., 2001].

The disadvantages of knock down by morpholino technique are mostly attributed to the off-target effects. Indeed, all the antisense techniques (RNAi, shRNA, MOs) suffer from the unwanted and unspecific effects on the organism development. Developmental delay, apoptosis and abnormal development of body axes are amongst non-target-related phenotypes [Egger et al., 2001]. In order to control for the specificity, stringent controls need to be put in place [Eisen and Smith, 2008]. One solution is to design a control sequence differing in five nucleotides from the target sequence (5-mismatch control). The mismatches between the bases disable the binding to the target sequence. When injected at the same concentration as the MOs, we can control for factors related to injection procedure or toxicity [Cornell and Eisen, 2002; Rana et al., 2006]. Furthermore, the more reliable control would be a “rescue” of the phenotype. It is common to many MO studies that zebrafish exhibit similar phenotypes. If however, these phenotypes can be reversed by adding mRNA of the knock down homolog, we can conclude that the effect were specific to the MO target sequence [Eisen and Smith, 2008].

1.3.2.2 CRISPR/Cas9 knock-out system

The Clustered, Regularly Interspaced, Short Palindromic Repeats (CRISPR) and the CRISPR-associated system (Cas) have recently been adapted for genome editing purposes [Sander and Joung, 2014]. The system has been used as efficient screening tool to study and assess multiple genes and their function in zebrafish [Shah et al., 2015]. The advantage of this system is the rapid generation of homozygous mutant lines, achieved in two generations or less [Li et al., 2016].

The CRISPR/Cas stems from bacterial immune system, providing bacterial defence against the virus invasion [Jinek et al., 2012]. Hwang *et al* (2013) developed a CRISPR/Cas9 system as easy and highly accessible tool for *in vivo* genome editing in zebrafish [Hwang et al., 2013a]. The system consists of a customized single guide RNA (sgRNA) and a single Cas9 enzyme. The sgRNA binds to the DNA sequence, providing a signal for the Cas9 cleavage. The *in vitro* transcribed, capped and polyadenylated Cas9 is translated into the protein. The Cas9 protein then creates a double strand break in the DNA, that can be repaired through the non-homologous end joining (NHEJ) [Chang et al., 2013; Hwang et al., 2013b]. The NHEJ repair mechanism introduces a variety of mutations and/or insertions or deletions (indels), disrupting the DNA sequence, hence preventing the proper translation of the mRNA and consequently, the protein sequence. As CRISPR/Cas9 system provides time and cost-efficient manner of creating knock out lines, it has become an invaluable complementary approach to morpholinos for protein function studies in zebrafish [Varshney et al., 2015; Gagnon et al., 2014; Jao et al., 2013].

1.3.2.3 Studying regulatory sequences using Gateway Tol2 technology

Regulatory sequences are functionally non-coding elements of the genome, alongside non-coding RNA and splicing elements [Chatterjee and Lufkin, 2012]. Previously, scientists have mostly been technically limited to studying conserved non-coding elements (CNEs) [Woolfe et al., 2004; Pennacchio et al., 2006; Sandelin et al., 2004]. However, with the advance in techniques, new enhancer regions have been identified, many of which have low levels of conservation between species [Roh et al., 2005, 2007, Heintzman et al., 2009, 2007; Visel et al., 2009; Blow et al., 2010]. To understand the role of such elements (conserved or non-conserved), functional analyses are needed. In zebrafish, the Tol2-based system for studying regulatory sequences (enhancers, promoters) has been established and optimised [Kawakami et al., 2004; Suster et al., 2009; Kawakami et al., 2000].

The Tol2 element is a transposon first discovered in the genome of the medaka fish (*Oryzias latipes*) [Koga et al., 1996]. The Tol2-mediated transgenesis is a highly efficient procedure, where more than 50% of the injected fish transmit the construct to the next generation [Kawakami et al., 2004, 2000]. The system consists of the donor plasmid carrying a Tol2 transposone backbone (Figure 1.6 A) and the *in vitro* transcribed transposase (Figure 1.6 B) [K. Kawakami et al., 2016]. The Tol2 system became widely used to screen and annotate human functional non-coding elements in the genome [Chatterjee and Lufkin, 2012]. The short DNA sequences flanking the transposon are recognised for cleavage by the transposase, enabling the integration of inserts into the zebrafish genome [Urasaki et al., 2006]. Tol2 can integrate almost everywhere in the genome as a single copy through a cut-and-paste mechanism, without any modifications at the target site (Kawakami et al., 2000). Recently, a mini Tol2 system has been developed, allowing the transposition of large (~10kb) sequences without affecting the transgenesis efficiency [Korz, 2011].

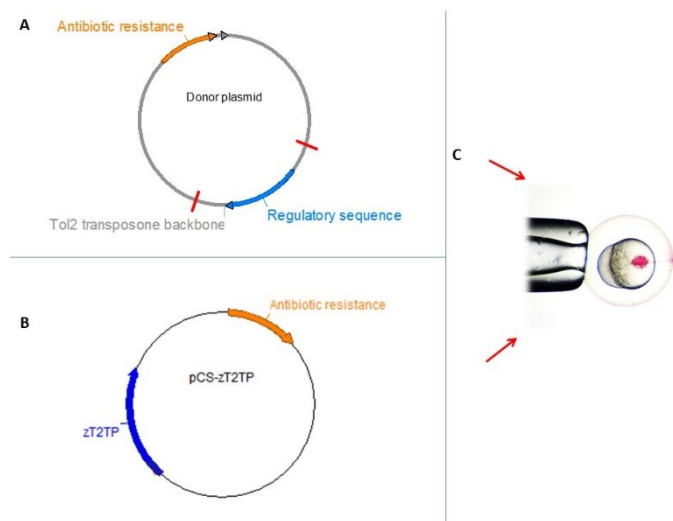


Figure 1.6 The Tol2 system

The donor plasmid (**A**) consists of the regulatory sequence (blue), carried on the zebrafish Tol2 transposone backbone (grey). The plasmid is cleaved at the recognition sites (red lines) for the transposase. **B**) The transposase plasmid pCS-zT2TP carries the zebrafish transposase enzyme (blue). After the *in vitro* transcription, the transposase mRNA is co-injected together with the donor plasmid DNA into the 1-4 cell stage embryo (**C**). There the transposase cleaves the plasmid, releasing the transposone backbone, which then randomly integrates into the zebrafish genome.

Using the Tol2 system, new transgenic lines are generated in time efficient manner [Fisher et al., 2006b, 2006a]. The co-injection of transposone backbone and the transposase enzyme enables effective low-mosaic construct integration thus enabling the analysis already in the injected embryos rather than waiting for the establishment of the transgenic line [Kwan et al., 2007].

Several studies (Table 1.2) have successfully used a nonconserved sequence and studied it in zebrafish using Tol2 system, therefore I am confident the system I have chosen for this analysis, is appropriate.

Table 1.2 An overview of a few recent studies, using non-conserved sequences in a Tol2 assay.

Gene	Gene region	Size [bp]	Species*	Conservation	Reference
Sox10	Enhancer	820	M-ZF	12%	[Antonellis et al., 2008]
MPZ	Enhancer Variant c.126-1086T>A	246	H-ZF	12%	[Antonellis et al., 2010]
AUTS2	Enhancer	1817	H-ZF	5%	[Oksenberg et al., 2013]
SIM1	Enhancer SCE2-CE-100658719 G>A	1882	H-ZF	7.5%	[Kim et al., 2013]
IRF4	rs12203592- [T/C] in enhancer region	451	H-ZF	17.5%	[Praetorius et al., 2013]

*Notes: H = Human, ZF = Zebrafish, M = mouse

Due to the ease of use and time saving properties of Tol2 Gateway system, I have chosen to use it to characterise the trait-associated afore-described regulatory sequences. The *KIAA0319* and *PCSK6* regulatory sequences have been shown to play a role in neurodevelopmental disorders and behavioural laterality [Dennis et al., 2009; Shore, 2015], which makes them attractive candidates to study their function throughout early embryonic development. The principle of the Tol2 Gateway system can be compared to the luciferase assay in the cell cultures, however, with the Tol2 we can not only observe the difference in expression levels, but also the spatiotemporal distribution throughout development.

1.4 Summary and aims

Dyslexia is a common developmental disorder, influenced by multiple genetic factors. Functional characterization of candidate genes suggest neuronal migration as an underlying cause of impaired reading, however, the results are not conclusive. The *KIAA0319* is a highly attractive candidate due a potential role in neuronal migration in the cortex and a number of genetic associations with dyslexia related traits.

The aim of this thesis is to map *kiaa0319* expression and to understand its function during zebrafish embryonic development.

I have used three different methods of *in situ* hybridisation to map the expression of zebrafish ortholog *kiaa0319* during the early development. I have applied a CRISPR/Cas9 knock out and a morpholino knock down technique to study the effect of *kiaa0319* on zebrafish development. As most of the associations with dyslexia phenotype reside in *KIAA0319* regulatory region, I have tested for the spatio-temporal expression of the promoter sequence during embryonic development. I have adjusted the Gateway Tol2 protocol to clone the human *KIAA0319* promoter into the zebrafish genome. Similar procedure has been carried out to test for the function of the *PCSK6* intronic promoter, a locus associated with degree handedness in cohorts selected for dyslexia.

2 Kiaa0319 expression in zebrafish embryo development

2.1 Summary

The role of *KIAA0319* during brain development remains unclear. To understand the function of this dyslexia candidate, the expression of the zebrafish orthologue during early neurogenesis was analysed. Firstly, the presence of *kiaa0319* sequence and copy number in the zebrafish genome were confirmed. Next, the expression pattern of *kiaaa0319* in developing zebrafish embryo was assessed, using three different ISH protocols: 1) digoxigenin uridine- 5'-triphosphate (DIG) labelled RNA probes, 2) fluorescence *in situ* Hybridisation, and 3) RNAScope. Due to similarity of human *KIAA0319* with *KIAA0319L* sequence and its involvement with dyslexia, I decided to test for the zebrafish *kiaa0319l* expression as well. I observed that *kiaa0319* and *kiaa0319l* have a similar expression pattern throughout the early stages of development. Both genes are expressed ubiquitously in the first 4 hours of development and then localise specifically to the developing brain, spinal cord and notochord. The expression of *kiaa0319* and *kiaa0319l* was also observed in the retina and otic vesicles, both of which include ciliated structures [Lepanto et al., 2016; Stooke-Vaughan et al., 2012]. Data from this chapter are described in a manuscript available as preprint (Appendix 6.7) and submitted for publication.

2.2 Methods

2.2.1 Genomic mapping of zebrafish *kiaa0319* and *kiaa0319l*

I used the University of California, Santa Cruz (UCSC <https://genome.ucsc.edu/>) and Ensembl (<http://www.ensembl.org>) genome browsers to identify the coordinates of the zebrafish orthologs of human *KIAA0319* gene. When mining for published work and expression data using zebrafish database (www.Zfin.org), no published data on *kiaa0319* was found (Appendix 7.3.2).

Mapping for *kiaa0319* expression throughout early development (first 5 days post fertilisation) was done by a reverse transcriptase PCR (RT PCR) reaction:

MyTaq Buffer	[50mM]	4 μ l
Fwd Primer	[10 μ M]	1 μ l
Rev Primer	[10 μ M]	1 μ l
zebrafish cDNA	[65ng/ μ l]	1.2 μ l
MyTaq DNA Polymerase	[5,000 units/ml]	0.2 μ l
H2O		12.6 μ l
Total Volume		20 μ l

The samples were run in the G-STORM thermocycler (Labtech international) under the following conditions:

Denaturation	95°C	30s,	}	30 cycles
Annealing	58°C	20s		
Elongation	72°C	1min		

Primer pair 416/417 (Appendix 7.1.6) resulting in 1024bp product were used for *kiaa0319* cDNA.

In order to test for potential *kiaa0319* isoforms, primer pairs (Appendix Table C1) were designed using Primer3web (<http://primer3.ut.ee/>) online software. Based on the cDNA sequences downloaded from Ensembl, the predicted differences in fragment sizes are in the range of 20 - 92bp, therefore the electrophoresis was performed using a 2% gel and ran for 2 hours at 50 volts.

Agarose gel was made using 1g of agarose and 50 mL of TAE Buffer (Tris-Acetate-EDTA). The mixture was heated in the microwave and left to cool. SYBR Safe DNA Gel Stain (ThermoFisher Scientific) was added to visualise DNA. Once the gel was poured into the mould, it was left to solidify. DNA was mixed with 6x loading buffer and loaded into wells. The appropriate timing and voltage were applied based on DNA size. The size of the resulting PCR product was assessed according to the 1kb and 100bp DNA ladder (NEB).

2.2.2 Quantitative Real time PCR

Once the presence of the *kiaa0319* was confirmed through the RT PCR, a quantitative RT-qPCR reaction was set in order to examine the genes' expression profile. Firstly, the cDNA was extracted (section 2.2.2.1) from the WIK WT zebrafish embryos and used for setting of the standard curve (section 2.2.2.2). The same settings were then used to quantify the level of *kiaa0319* expression throughout development.

2.2.2.1 cDNA preparation

The whole RNA from zebrafish developmental stages between 16 – 32 cells, 3 – 5 hours post fertilisation (hpf), 6hpf, 12hpf, 24hpf, 3hpf, 48hpf, 72hpf, 96hpf and 120hpf was extracted using RNeasy Mini kit (QIAGEN). To extract whole RNA from zebrafish embryos, 50 embryos were homogenized using TRIzol reagent (Thermo Fisher Scientific). The extraction of the RNA followed as per manufacturer instructions. Eluted RNA was further precipitated with 10µl of 3M Sodium Acetate Stop Solution and extracted with an equal volume of phenol/chloroform. The aqueous phase containing RNA was transferred to a new tube. RNA was once again precipitated by adding 1 volume of isopropanol. After overnight incubation at –20°C, RNA was centrifuged at 4°C for 15 minutes at maximum speed. All the excess liquid was removed and the RNA pellet was air dried for no more than 30 minutes. Purified RNA was resuspended in 20µl of RNase free water, quantified on Nanodrop and stored at -80°C until further use.

Following the extraction and purification of RNA, the PrimeScript RT reagent kit (Takara) was used to transcribe the RNA into the cDNA following the manufacturer's protocol:

PrimeScript Buffer	[5X]	2 µl
PrimeScript RT Enzyme Mix		0.5 µl
Oligo dT Primer	[50µM]	0.5 µl
Random Hexamers	[100µM]	0.5 µl
Total RNA	[500ng]	1.4 µl
RNase free water		5.1 µl

The reverse transcription was set for 15 minutes at 37°C and terminated for 5s at 85°C. The Resulting 50 ng/µl cDNA was stored at - 20°C until further use.

2.2.2.2 Standard curve

Quantitative real-time PCR (RT-qPCR) was used to quantify levels of gene expression. To test the efficiency of designed primer pairs, a standard curve (Appendix 7.3.3) was derived from serial dilutions with a known concentration. The standard curve was required to show a multiplying efficiency between 95% and 105% and a defined Cycle threshold (Ct).

The reaction was set using the cDNA obtained from the WIK WT strain of zebrafish in concentrations 12.5ng/μl, 6.25ng/μl, 3.125ng/μl, 1.56ng/μl and 0.78ng/μl. A final volume of 4μl of the cDNA was added to 6μl of the mastermix:

Primer 518	[10μM]	0.25 μl
Primer 519	[10μM]	0.25 μl
Luna Universal qPCR Master Mix		5 μl
Water		0.5 μl
Total Volume		6 μl

and ran on a Viia 7 thermocycler (Life technologies) under the following conditions:

Denaturation	95°C	60s,	} 30 cycles
Annealing	95°C	10s	
Elongation	60°C	30s	

Primer pairs 410/411 (Appendix 7.3.1) spanning 91bp through zebrafish eukaryotic translation elongation factor 1 alpha 1, like 2 (*eef1a1l2*) were used as positive control to assess cDNA quality.

2.2.2.2.1 RT-PCR analysis

Once the quality of designed primers was confirmed through the standard curve, the RT-qPCR mastermix was set for *kiaa0319* and *eef1a112* genes and repeated in triplicates. The positive control sample containing the adult zebrafish brain cDNA was run. As a negative control a triplicate of non-template control (NTC) was run on the same plate.

The RT-qPCR results for the Ct (Cycle threshold) values were used for further calculations of the relative quantification (RQ) factor. The mean values of *eef1a112* technical triplicates were calculated for each developmental stage. The individual mean Ct values of every *kiaa0319* sample triplicate were then subtracted from the mean value of the *eef1a112* (ΔCt). The individual values of the positive control Ct values (the *kiaa0319* expression in the adult zebrafish brain) were further subtracted from delta Ct (ΔCt). The result ($\Delta\Delta\text{Ct}$) was used to calculate the RQ using the following formula:

$$\text{RQ} = 2^{-\Delta\Delta\text{Ct}}$$

The relative quantification factor RQ was used to plot a graph, enabling the visual representation of the *kiaa0319* expression levels throughout development.

2.2.3 Whole-mount *in situ* hybridization (WISH) on zebrafish embryos

2.2.3.1 Zebrafish embryo collection

Zebrafish work using live embryos was done under the close supervision of Dr Carl Tucker, Zebrafish Facility Manager and Research Scientist at The Queen's Medical Research Institute at the University of Edinburgh. This includes zebrafish husbandry, embryo collection, embryo staging, microinjections (described in Chapter 3) and live imaging. Animals were handled in accordance with the guidelines from European Directive 2010/63/EU and euthanised in accordance with Schedule 1 procedures of the Home Office Animals (Scientific Procedures) Act 1986.

Wild type WIK or AB/TU zebrafish embryos were obtained from the mass egg production system (MEPS) and incubated at 28.5°C to enable developmental assessment according to the zebrafish standard staging series [Kimmel et al., 1995a] (Appendix G). Embryos younger than 48hpf were enzymatically dechorionated using 1 mg/ml pronase for 2-10 minutes (depending on developmental stage). The chorions of older embryos were manually broken with a pair of tweezers. After digestion, embryos were washed 3x for 5 minutes in Danieau solution and fixed in 4% PFA at 4°C overnight. The following day, fixed embryos were washed 3x in PBT and dehydrated using methanol series (25% MetOH/PBT, 50% MetOH/PBT, 75%MeOH/PBT, 2x 100% MetOH). Embryos in 100% methanol were stored at -20°C until further use.

2.2.3.2 Creating WISH riboprobe for detecting *kiaa0319* transcripts

A riboprobe was generated by amplifying a portion of the *kiaa0319* from the cDNA (For flow see Figure 2.1). To enable the consequent transcription into RNA, a T3 promoter sequence was attached to the reverse (T751) primer. A 1066bp cDNA sequence was obtained after a PCR reaction was set:

GoTaq Green	[2x]	25 μ l
Fwd T750 Primer	[10 μ M]	1 μ l
Rev T751 Primer	[10 μ M]	1 μ l
Zebrafish cDNA	[50ng/ μ l]	1 μ l
H2O		22 μ l
Total Volume		50 μ l

The samples were run in the G-STORM thermocycler (Labtech international) under the following conditions:

Denaturation	95°C	5 min	
Denaturation	95°C	30s,	} 30 cycles
Annealing	58°C	30s	
Elongation	72°C	72s	
Elongation	72°C	5 min	

The resulting ~1kb cDNA fragment with a T3 promoter at the 3' end of the sequence was gel purified and *in vitro* transcribed as described as follows:

PCR fragment	[333 ng/ μ l]	6 μ l
Transcription buffer	[5x]	4 μ l
DTT	[0.1 M]	2 μ l
DIG-NTP-Mix	[10X]	2 μ l
RNase Inhibitor, Murine	[40,000 units/ml]	2 μ l
H2O		2 μ l
T3 RNA polymerase	[50,000 units/ml]	2 μ l
Total Volume		20 μ l

The transcription mix was incubated for 2 hours at 37°C and then treated with DNaseI for 15 minutes at 37°C. The resulting riboprobe was precipitated by adding 5 μ l of NH₄OAc and 200 μ l of cold 100% ethanol and incubated at -20°C for 2 hours. The precipitated RNA was spun down at the highest speed for 30 minutes. The resulting supernatant was discarded. The RNA pellet was dried and resuspended in 20 μ l of RNase-free water. The concentration of the resulting riboprobe was measured on a Nanodrop instrument and ran on a standard 1% agarose gel to control for probe stability. In the final step, 17 μ l of RNA probe were diluted in 17 μ l of Hybridization buffer and stored at -20°C until further use.

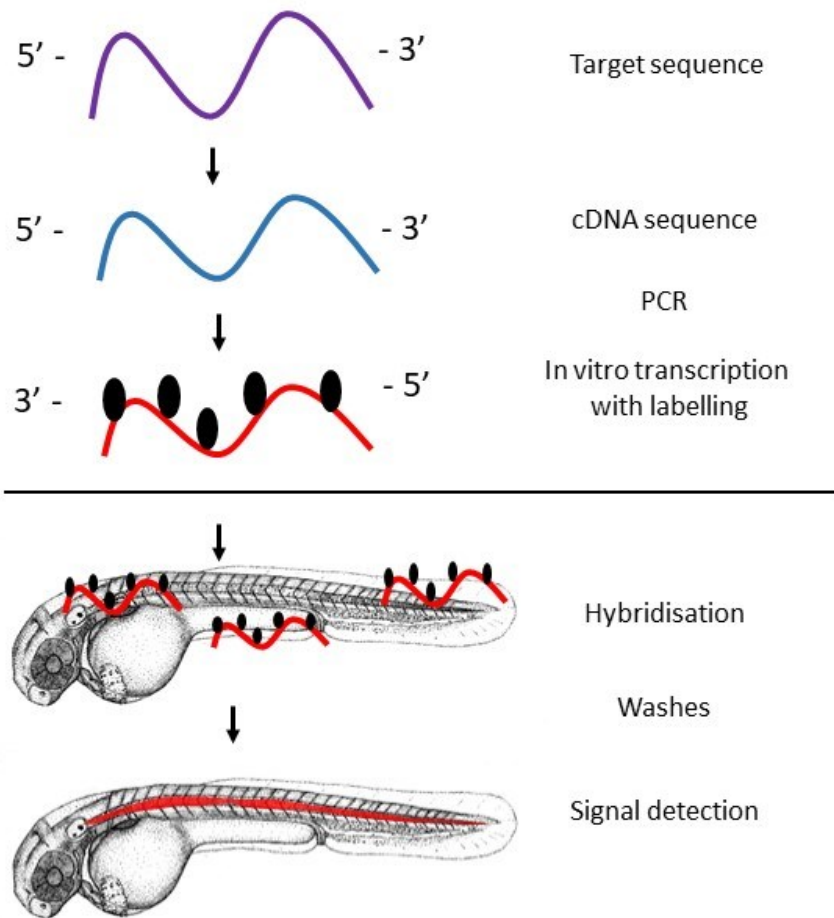


Figure 2.1 *In situ* Hybridisation procedure

A schematic representation of *in situ* Hybridisation flow. RNA sequence is read from 5' – 3' and a cDNA sequence transcribed. Target sequence is PCR amplified, *in vitro* transcribed and labelled accordingly to the protocol. Labelled riboprobe is synthesised antisense to the target RNA. The probe is introduced to the zebrafish embryo of chosen developmental stage and hybridised to target sequence. After a series of washes, the signal is detected using appropriate microscopy technique.

2.2.3.3 WISH Hybridisation protocol

Embryos at the appropriate stage were selected and rehydrated using reverse methanol series (75% MetOH/PBT, 50% MetOH/PBT, 25%MeOH/PBT, 2x PBT). Proteinase K (10µg/ml) treatment was applied (for duration, see Table 2.1) and then terminated by washing in PBT for 5 minutes. The Hybridisation solution (Appendix 7.1.2) was applied and incubated at 65°C for 2 hours. Before applying to the samples, the diluted riboprobe was heated at 65°C for 5 minutes, vortexed and spun down. Pre-warmed probe (200µl) was added to individual tubes and incubated at 65°C overnight.

Table 2.1 Duration of Proteinase K treatment according to zebrafish developmental stage

Time (min)	Embryo stage
8	24hpf
12	30hpf
30	48hpf
45	72hpf

The following day the probe was recovered and pre-warmed (65°C) wash-solutions were applied to the samples. The probe residues were washed out with 200µl hybridisation solution for 30 minutes. To further wash away any nonspecific binding, 1ml of 2x SSC buffer (Appendix 7.1.2) was added and incubated for 10 minutes with shaking. Additional two washes of 30 minutes with 0.2x SSC buffer were performed at 65°C, each with shaking. The samples were equilibrated for 5 minutes in Maleic Acid Buffer (MAB, Appendix 7.1.2) buffer and blocked in 2% MAB/blocking solution for at least 3 hours at room temperature on a shaker. To

detect incorporated DIG molecules, an anti-DIG antibody (Anti-Digoxigenin-AP, Fab fragments, Roche) was added to blocking mix in dilution of 1:5000 and incubated overnight at 4°C with shaking.

The samples were then washed 3x for 1 hour in MAB buffer. A fresh solution of alkaline phosphatase buffer (NTMT) was applied for at least 20 minutes. NTMT reacts with the added colouring solution (NBT + BCIP) and creates a colour signal where the antibody has bound to the riboprobe. Once the signal was visible, the embryos were post-fixed in 4% PFA for 20 minutes at RT and washed twice in PBT. The labelled embryos were finally stored in 80% glycerol until mounting.

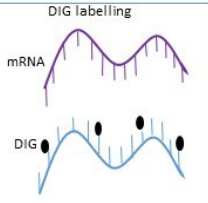
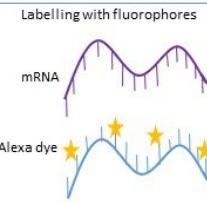
	WISH	FISH	RNAScope
Probe design	cDNA synthesis	✓	✗
	<i>In vitro</i> transcription		
Hybridisation	65 °C overnight	65 °C overnight	40 °C 2h - overnight
Signal amplification	✗	✗	✓
Antibody detection & Staining reaction	✓	✗	✗
Imaging	Bright field microscopy	Fluorescent microscopy	Fluorescent microscopy
Protocol duration	4 days	4 days	2 days

Figure 2.2 Comparison of three *in situ* Hybridisation protocols used in this study

Whole mount *In situ* Hybridisation (WISH), Fluorescence *In situ* Hybridisation (FISH) and RNAScope technology.

2.2.4 Fluorescence In situ Hybridisation (FISH)

2.2.4.1 Creating FISH riboprobe for detecting *kiaa0319* transcripts

The protocol for fluorescence *In situ* Hybridisation (FISH) was optimised from the Invitrogen FISH Tag™ RNA Multicolor Kit protocol (ThermoFisher Scientific). A 595bp cDNA sequence was obtained after a PCR reaction:

Phusion® GC Buffer	[5x]	10 µl
Forward 496 primer	[10µM]	2.5 µl
Reverse 497 primer	[10µM]	2.5 µl
dNTP mix	[10µM]	2.5 µl
cDNA	[50ng/µl]	2 µl
Phusion® High-Fidelity		
DNA Polymerase	[2,000 units/ml]	1.5 µl
H ₂ O		29 µl
Total Volume		50 µl

The samples were run in the G-STORM thermocycler (Labtech international) under the following conditions:

Denaturation	98°C	30s	
Denaturation	95°C	20s,	} 30 cycles
Annealing	65°C	20s	
Elongation	72°C	4min	
Elongation	72°C	10 min	

The resulting PCR product was gel extracted using the QIAquick Gel Extraction Kit (QIAGEN) and cloned into a pCRTM-Blunt II-TOPO[®] Vector containing SP6 and T7 promoter sequences. The cloning mix was transformed into One ShotTM TOP10 Chemically Competent *E. coli* cells. The resulting plasmid pCRTM-Blunt II-TOPO_kiaa0319 (Appendix 7.2) was isolated using QIAprep[®] Spin Miniprep Kit (QIAGEN) and stored at -20°C until further use.

To create an antisense riboprobe, 10µg of pCRTM-Blunt II-TOPO_kiaa0319 plasmid was linearised and purified using QIAprep[®] Spin Miniprep columns. The linear product was then *in vitro* transcribed using the mMESSAGING mMACHINE[®] T7 µLTRA Transcription Kit. As a positive control an *otx5* probe was transcribed, kindly provided by Blader group, Toulouse, France [Gamse et al., 2002]. The RNA was then purified and precipitated according to the manufacturer protocol. The kit provides an option for labelling the probe with four different Alexa Fluor dyes: 488, 555, 594 and 647. The *kiaa0319* and the *otx5* probes were labelled with Alexa Fluor 555 and 488, respectively. Fluorescently labelled RNA probes were again purified and precipitated as described in Section 2.2.2.1, before storing them at -80°C until further use. The same procedure was followed when transcribing the control sense probe.

The hybridisation protocol followed the same steps as the protocol for WISH (Figure 2.1 and Figure 2.2) with the exception of the antibody detection step. Instead, the embryos were incubated for 10 minutes per step in glycerol series (25% glycerol/PBT, 50%, and 75%) and finally incubated overnight in 75% glycerol. The following day, the embryos were deyolked and mounted on a single cavity microscope slides (Fisher Scientific).

2.2.5 RNAScope

RNAScope is a novel ISH protocol designed by Advanced Cell Diagnostics, Inc (ACD) to simultaneously detect up to four RNA transcripts in the same sample. In order to obtain the signal amplification, 20 target probe oligonucleotides (named double Z probes - ZZ) need to bind to the target sequence in tandem. The nucleotides need to bind next to each other in order to assure efficient binding of further amplification molecules. Two independent nucleotides will highly unlikely hybridize to a non-specific target right next to each other, thus preventing a high amplification of off-target signals.

RNAScope has primarily been developed for detection of RNA on tissue slices, but has recently been adapted for whole mount detection in zebrafish embryos [Gross-Thebing et al., 2014]. For our purposes, I have optimised the RNAScope® Multiplex Fluorescence Assay following the Gross-Thebing protocol.

2.2.5.1 RNAScope probe design

Custom-made oligonucleotides for *kiaa0319* and *kiaa0319l* were produced by the Advanced Cell Diagnostics (Figure 2.3, Appendix 7.4.4) . As a positive control, the probe for *myod1* as demonstrated in the Gross-Thebing protocol [Gross-Thebing et al., 2014] has been used. The negative control consists of a standardised triple negative sequence that doesn't bind to any of the sequences.

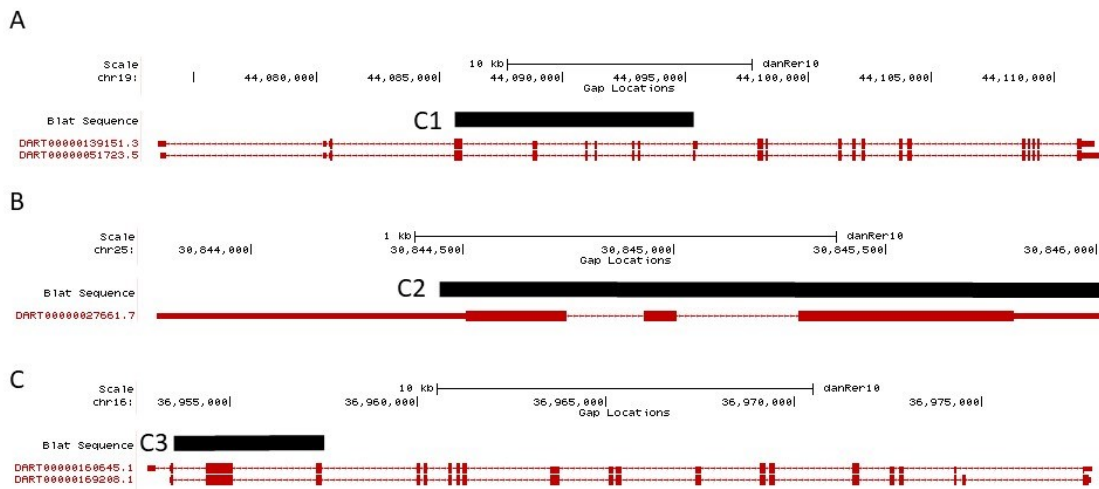


Figure 2.3 RNAScope probe design

Screenshot of the UCSC Blast nucleotide search results indicating the position of designed probes relative to the gene sequences. **A)** Probe C1 represents an 880bp sequence (black line) covering both *kaa0319l* isoforms (red). **B)** Probe C2 represents a 1081bp sequence (black line) covering zebrafish *myoD1* isoforms (red). **C)** Probe C3 represents a 908bp sequence (black line) covering both *kaa0319* isoforms (red).

2.2.5.2 RNAScope hybridisation protocol

Zebrafish embryos were collected and staged as described in section 2.2.3.1. The PFA treatment step was applied at the room temperature and incubated according to the developmental stage (See Table 2.2 **Error! Reference source not found.**). Following fixation, embryos were digested with the Pretreat 3 solution according to their developmental stage (See Table 2.2 **Error! Reference source not found.**). The embryos still remaining in chorions were treated with pronase prior to protease digestion.

Table 2.2 Duration of Pretreat 3 and PFA treatment according to zebrafish developmental stage

Duration of Pretreat 3 treatment (min)	Embryo stage	Duration of PFA treatment (h)
	>12hpf	4 (with chorion)
1.5	12hpf	1 (with chorion)
3	24hpf	0.5 (without chorion)
5	36hpf	0.5
7	48hpf	0.5
10	72hpf	0.5
12	96hpf	0.5
15	120hpf	0.5

The original protocol suggests the use of company-made and supplied wash buffer; however, based on previous reports of wash buffer being too aggressive on the embryos [Gross-Thebing et al., 2014], I chose to use SSCT solution (Appendix 7.1.2). Prior to hybridisation, all probes were warmed up to 40°C for 10 minutes, vortexed and spun down. A working solution in ratio 1:50 was prepared for each probe in company provided diluent and allowed to cool down to the room temperature. Following the digestion, the Pretreat 3 solution was removed and embryos were rinsed three times for 15 minutes in 1ml PBT at RT with shaking. After the third wash, a 100µl of target probes were added per tube and hybridised at 40°C overnight. The following day, used probes were collected and stored in a new tube in order to be reused in the following experiments. Three washes of 15

minutes with SSCT were followed by a 10 minute postfixation with 4% PFA. The embryos were then washed again and incubated with 100µl Amp1 solution for 30 minutes at 40°C. Three washes of 15 minutes with SSCT were followed by the Amp2 incubation for 15 minutes. Further three washes of 15 minutes with SSCT were followed by the Amp3 incubation for another 30 minutes. In order to label the probes with the correct combination of fluorescent dyes (Appendix Table 7.6), the *kiaa0319* (c3) and *kiaa0319l* (c1) probes were added to the same sample while the *myod* positive (c2) and a triple negative control to a separate one. Amp4 (option A, B or C) was added and incubated for 15 minutes at 40°C. After the three washes with SSCT, a company-provided DAPI solution was added to each sample and incubated overnight in the dark at 4°C with slow agitation. The following day, DAPI was removed with a quick PBT wash and the samples prepared for imaging with the fluorescence confocal microscope.

2.2.6 Imaging and Image reconstruction

Bright field images were taken on Leica MZ16F and MZFLIII microscopes. The fluorescence images were obtained with Leica TCS SP8 confocal microscope and processed in Leica Application Software X (LAS X). All images were taken under 20x magnification, some with manual zoom (see scale bars).

Imaging with the lightsheet microscope was conducted with an in-house built microscope designed on the basis of the project openSPIM [Pitrone et al., 2013a]. The original openSPIM design has both the illumination and detection objectives on a horizontal plane, but this was modified to achieve an inverted configuration to accommodate larger varieties of samples. The main setup fits on a 450 mm × 300 mm breadboard (MB3045/M, Thorlabs), as in the original openSPIM design. A 488nm wavelength laser (Solstis with frequency doubler, M Squared) provides illumination for the microscope through a single mode fibre. A beam expander is followed by an adjustable slit (VA100/M, Thorlabs) to adjust the width of the beam

and a cylindrical lens (LJ1695RM-A, FL 50mm, Thorlabs) to focus the beam to a light sheet. A steering mirror delivers the beam to the illumination objective (UMPLFLN 10XW, water dipping, NA 0.3, Olympus) through a relay lenses combination. The two objectives are mounted on a customized holder which not only simplifies the system but also minimizes adjustment required. This holder also allows a change of objective lens if needed. Excited fluorescent signal is collected by a detection objective (LUMPLFLN 20XW NA 0.5, water dipping, Olympus) and an achromatic lens (LA1708-A-ML, FL 200 mm, Thorlabs) as tube lens, then projected onto a sCMOS camera (ORCA-Flash4.0 sCMOS camera, Hamamatsu).

The imaging was done with a manual scanning stage. The 3D images were reconstructed using an arbitrary z step in ImageJ [Schindelin et al., 2012] and an open source software Icy [de Chaumont et al., 2012] with the VTK library Visualization Tool Kit [Schroeder et al., 2006a].

2.3 Results

2.3.1 Zebrafish *kiaa0319* and *kiaa0319l* throughout development

Zebrafish *kiaa0319* is located on Chromosome 16, spanning 25.135kb (Chromosome 16: 36,952,809-36,977,944) in antisense direction on the forward strand (Figure 2.4 A). It has two known isoforms. The chosen *kiaa0319* isoform (ENSDART00000160645.1) consists of 20 exons, of which 19 code for 955aa protein sequence. Zebrafish *kiaa0319l* exists in 2 isoforms, located on Chromosome 19 and is spanning 38.353kb (Chromosome 19: 44,073,525-44,111,878) in sense direction (Figure 2.4 B). The *kiaa0319l* isoform ENSDART00000139151.3 consists of 21 exons, of which 20 are coding for a 1,049aa protein sequence.

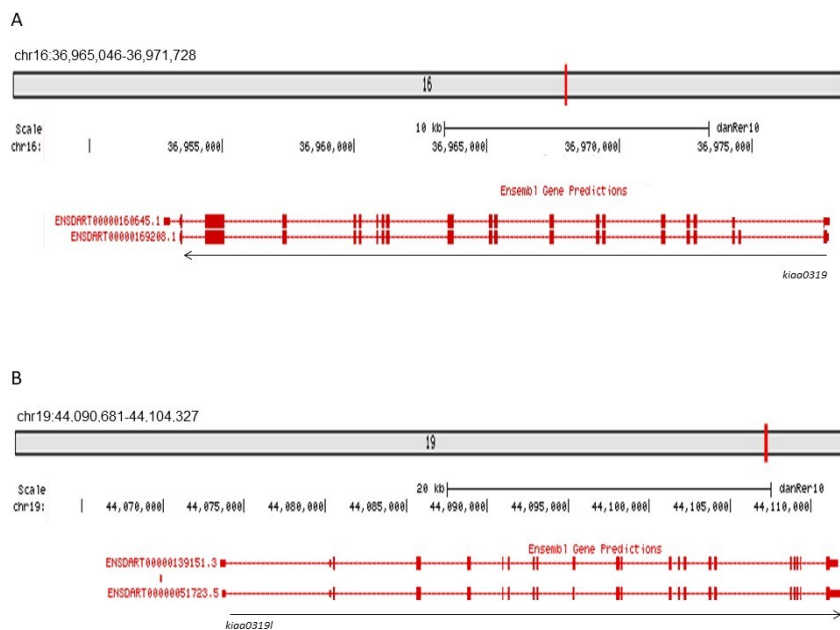


Figure 2.4 A schematic representation of zebrafish *kiaa0319* and *kiaa0319l* genes

A) Chromosome 16 as shown on the UCSC website. The red line marks the position containing both isoforms of *kiaa0319* (36.965.046 – 36.971.728). In red, isoform 201 (ENSDART00000160645.1) of *kiaa0319* gene with 20 exons spanning 25.135kb in antisense direction (black arrow). Isoform 202 (ENSDART00000169208.1) with 20 exons spanning 24.503kb in antisense direction **B)** Chromosome 19 as shown on the UCSC website. The red line marks the position containing both isoforms of *kiaa0319l* (44.090.681 – 44.104.327). In red, isoform 201 of *kiaa0319l* gene (ENSDART00000139151.3) with 22 exons spanning 38.140kb in sense direction (black arrow). Isoform 202 (ENSDART0000051723.5) with 22 exons spanning 38.254kb in sense direction.

In order to confirm zebrafish *kiaa0319* presence throughout embryonic development, a reverse transcription PCR reaction using the full cDNA was set as described in Section 2.2.1. The resulting ~1kb *kiaa0319* fragment was observed throughout all developmental stages (Figure 2.5). Human expression data confirm the highest expression of *KIAA0319* in the brain (Figure 1.2). To compare for *kiaa0319* gene expression in zebrafish tissues, adult zebrafish heart, brain and liver were dissected and whole RNA isolated. Following cDNA transcription, a reverse transcriptase PCR (Figure 2.5) was set. The results show *kiaa0319* expression throughout all tested developmental stages, as well as in the adult zebrafish brain. The level of *kiaa0319* expression in adult zebrafish liver and heart is substantially lower (Figure 2.5).

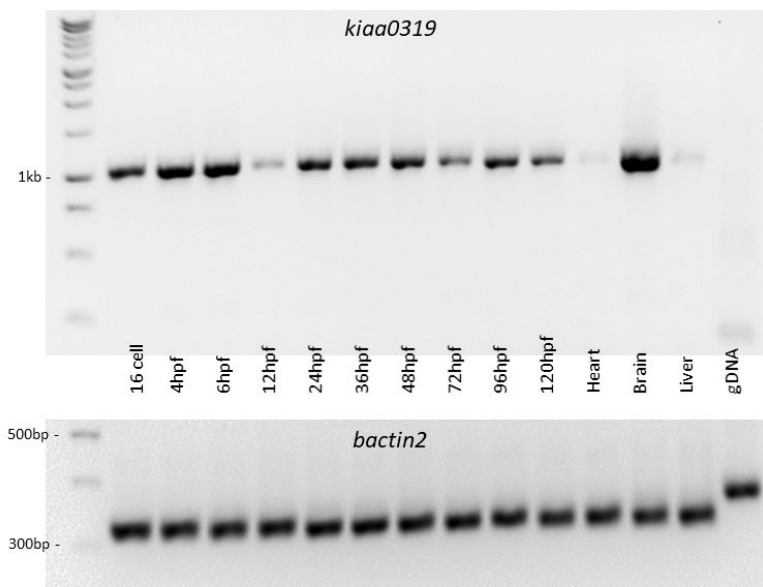


Figure 2.5 Zebrafish *kiaa0319* throughout embryo development

PCR reaction using primers 512/513 resulting in 1024bp *kiaa0319* (top panel). The expression level is low in adult zebrafish tissues other than brain. Genomic gDNA serves as a negative control. PCR reaction for zebrafish beta actin (*bacin2*) serves as positive control (Primer pairs 443/444 giving the expected fragment of 322bp)

Once the presence of *kiaa0319* was confirmed, the brain cDNA sample was used for further investigation of *kiaa0319* expression. When testing for *kiaa0319* isoforms as described in Section 2.2.1, no additional isoforms were found, and no alternative splicing discovered (Figure 2.6).

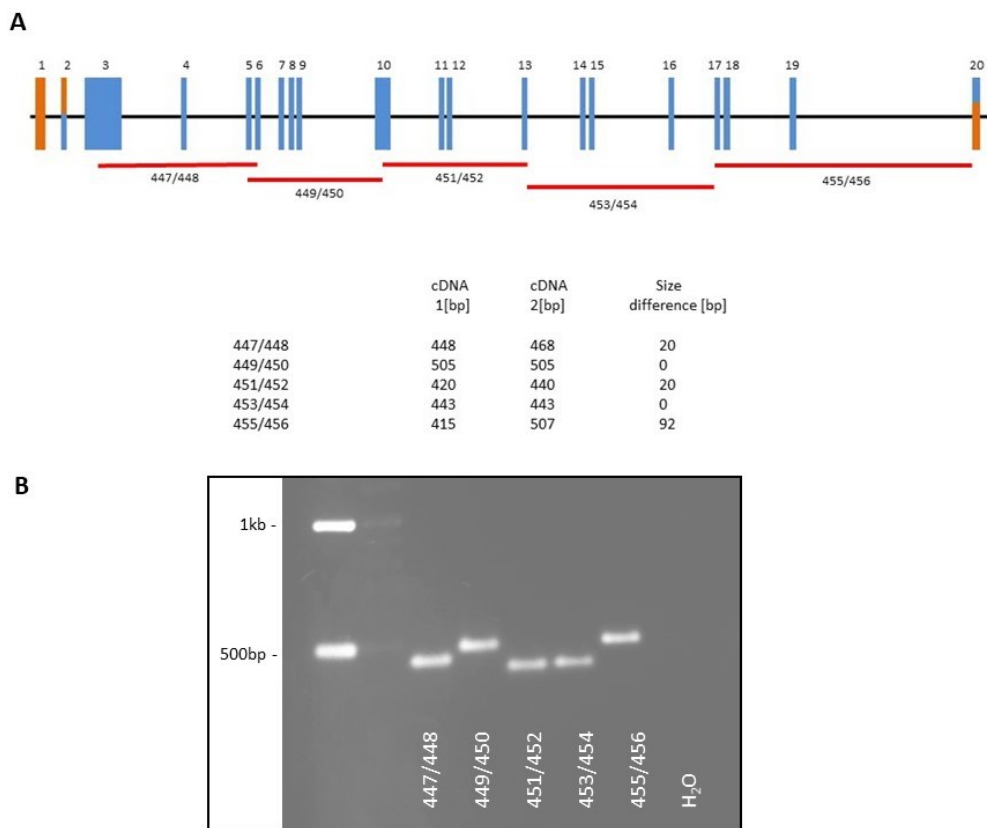


Figure 2.6 Primer design strategy for *kiaa0319* isoform screening

A) Analysis of *kiaa0319* gene with primer pairs (red) spanning from the beginning of coding sequence in Exon 3 to Exon 20. Orange coloured exons indicate untranslated region (UTR). Blue coloured exons indicate translated regions. Predicted cDNA fragment lengths for *kiaa0319* isoforms 1 and 2. **B)** A 2% agarose gel of PCR amplified *kiaa0319* fragments. No alternative splicing has been observed.

2.3.2 Quantification of *kiaa0319* expression levels

For more precise quantification of *kiaa0319* expression levels, a quantitative RT-qPCR was run for 10 different developmental stages. After optimising the reaction settings to obtain the standard curve within required measurements (Appendix Figure 7.3), the reaction was run and the ct values collected. The calculated RQ scores represent the amount of *kiaa0319* cDNA relative to the basal expression of the housekeeping gene *eef1a1l2*. The highest *kiaa0319* expression is observed in the first 5 hours post fertilisation (Figure 2.7 left panel). The expression level then drops significantly and hits the lowest scores at 12hpf (Figure 2.7 right panel). At 24hpf and 36hpf, the *kiaa0319* expression rises again, followed by another drop at 48hpf. At 96hpf, *kiaa0319* expression levels mark the highest score after 5hpf and then drops again at 120hpf.

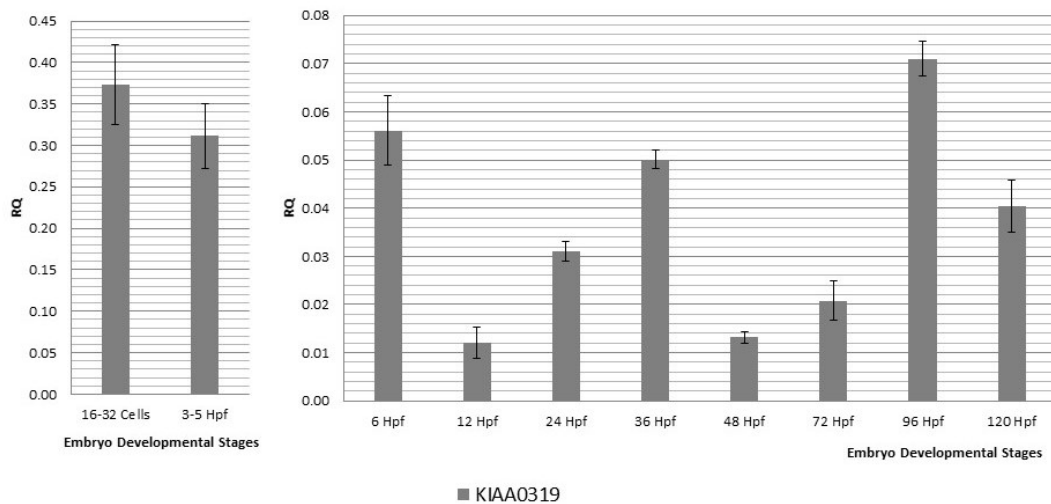


Figure 2.7 The expression levels of zebrafish *kiaa0319* throughout embryonic development

The RQ values represent the *kiaa0319* expression referenced against *eef1a1l2* values. Two panels shown here are due to a much higher expression of *kiaa0319* in the first 5 hpf.

2.3.3 *kiaa0319* WISH and FISH probe design

In order to design a riboprobe for *kiaa0319* transcript detection, a PCR reaction was set, followed by in vitro transcription of the probe. For the whole mount ISH (WISH) protocol, a 1066bp RNA sequence was DIG-labelled and ran on a 1% agarose gel to test for the transcription efficiency (Figure 2.8 A). Following the same principle, a 595bp fluorescently labelled ISH (FISH) riboprobe was transcribed (Figure 2.8 B).

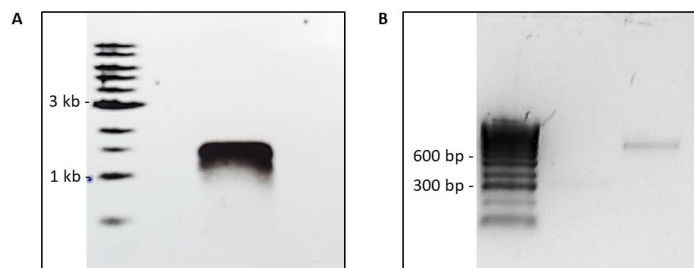


Figure 2.8 Agarose gels of transcribed WISH and FISH riboprobes

A) A 1066bp DIG-labelled WISH riboprobe. **B)** A 595bp fluorescently labelled FISH riboprobe. The bands appear larger due to incorporated labelling molecules.

Furthermore, the precise tissue localization of *kiaa0319* was investigated. In order to efficiently detect the transcript, a riboprobe was designed so that it binds transcripts from both isoforms. The highest and most ubiquitous expression of *kiaa0319* is observed in very early stages (Figure 2.9 A) then it becomes more brain specific with time. At 3 somite stage (Figure 2.9 A1, 2), *kiaa0319* is ubiquitously expressed. Already at 14 somite stage (16hpf), a localised distribution can be observed in the developing brain and spinal cord (Figure 2.9 A3, 4). The development of zebrafish otic vesicles, midbrain-hindbrain boundary and the pigmentation can be seen at 30hpf. The expression of *kiaa0319* at that stage is observed in the eyes (Figure 2.9 B1, 2 and 3), brain (Figure 2.9 B1, 2 and 4) and the otic vesicles (Figure 2.9 B2, 5).

Further along the embryo development, the *kiaa0319* expression becomes less abundant. At 48hpf, the *kiaa0319* expression was observed in the brain (Figure 2.9 C1, 2), more strongly in the forebrain area Figure 2.9 C2). Additionally, the *kiaa0319* expression is localised to the eyes (Figure 2.9 C1, 2, 3) and otic vesicles (Figure 2.9 C4). At all stages, the expression in the spinal cord and notochord can be observed (Figure 2.9 B6, C2).

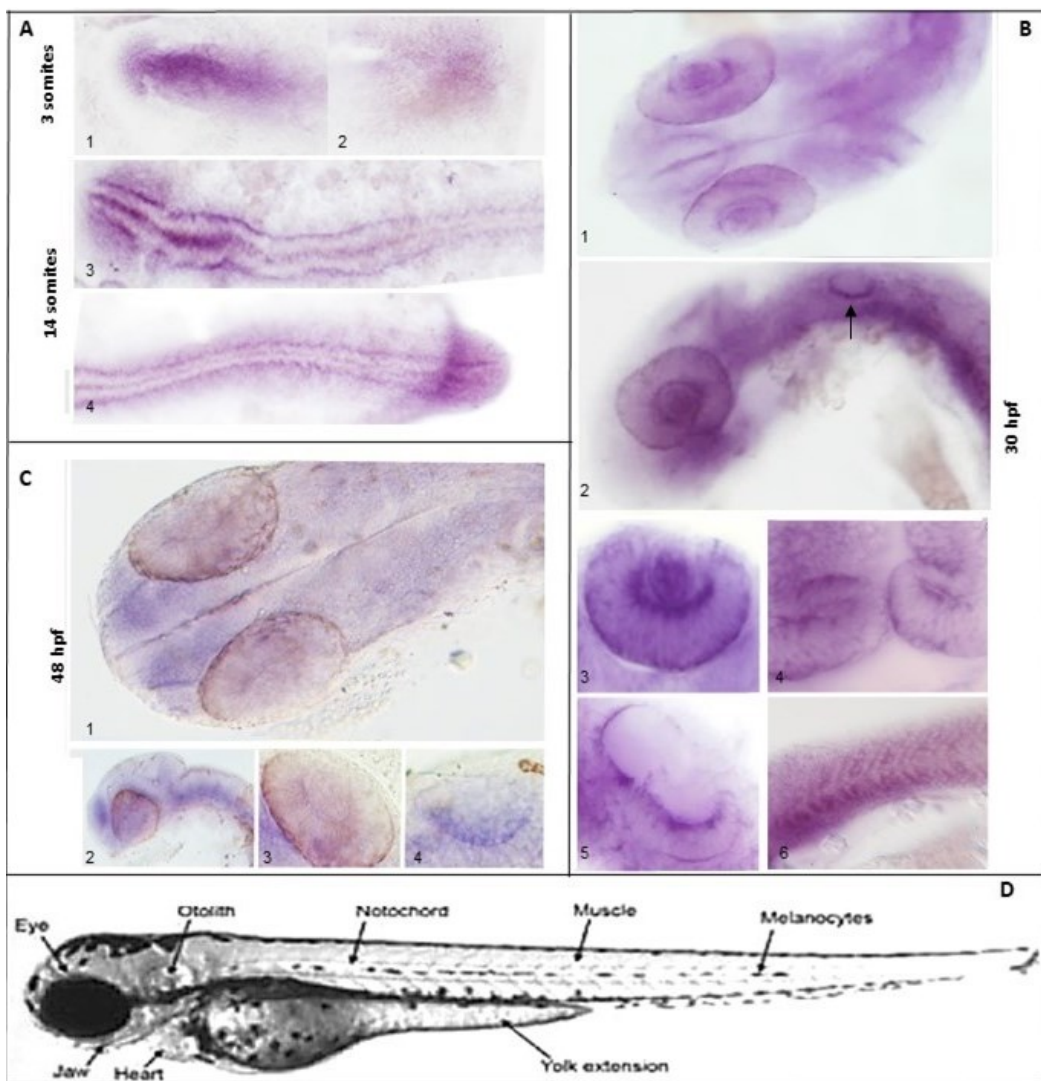


Figure 2.9 The expression of *kiaa0319* in early embryonic development

The purple stain indicates the location of *kiaa0319* transcripts in zebrafish embryos. **A)** Zebrafish embryo at 3 somite stage. The *kiaa0319* is ubiquitously expressed in the head (1) and is also present in the tail (2). *kiaa0319* is highly expressed in a 14 somite embryo head (A3) and throughout the developing spinal cord (A4). **B)** At 30hpf, the *kiaa0319* is localised to specific tissues, but still highly

expressed throughout the embryo. B1) The top view of the embryo showing the expression of *kiaa0319* in the brain structures and the eyes. B2) The lateral view of the embryo showing *kiaa0319* expression in the brain, eye and the otic vesicle (black arrow). Strong expression is seen in the notochord. The magnification of consistently strongly labelled structures: eyes (B3), midbrain-hindbrain barrier (B4), otic vesicle (B5) and the notochord (B6). C) *kiaa0319* expression in a 48hpf embryo. C1) The top view of the embryo showing *kiaa0319* expression in the whole embryo; C2) The lateral view of the embryo indicating *kiaa0319* expression in the telencephalon, eye (C3), spinal cord, notochord and the otic vesicle (C4). D) A zebrafish larva at three days post fertilisation as a reference indicating the main physiological culprits as labelled (black arrow).

2.3.4 *kiaa0319* FISH protocol

The WISH protocol was successfully applied to the developing embryos, but the accuracy of the information was not satisfactory. The wide distribution of the probe made it unclear to determine whether the detected signal was indeed *kiaa0319* transcript, or merely staining background. In order to obtain a more detailed information about *kiaa0319* localisation, I have optimised an ISH protocol with fluorescently labelled riboprobes, as described in section 2.2.4. Fluorescence from the FISH probes is predicted to be more accurate than DIG labelled riboprobes.

Two fluorescently labelled probes were designed: antisense probe labelled with Alexa Flour 555 and sense probe labelled with Alexa Flour 488. The antisense probe hybridises to the target mRNA sequence, whereas the sense probe does not bind at all. The sense probe is used as a negative control, testing for the efficiency of the protocol. As the fluorescence imaging makes it difficult to distinguish left from right, an additional control probe was applied. The zebrafish *otx5* proved to be an efficient control to test for both, the efficiency of the protocol and to control for the laterality of the zebrafish embryo. It has been shown that the *otx5* is expressed in the pineal and parapineal glands [Gamse et al., 2002] and can be detected as early as at 13-somite stage of the development. The pineal gland is located centrally, whereas the parapineal in 92% of the cases develops on the left side of the dorsal diencephalon [Gamse et al., 2002].

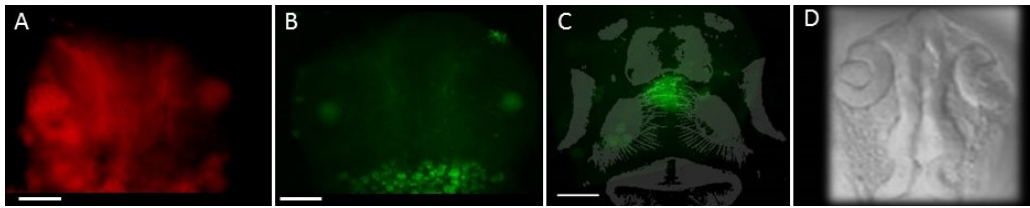


Figure 2.10 Fluorescence *in situ* hybridisation (FISH)

A) Expression of *kiaa0319* (red) in the head of 24 hpf embryo. **B)** No signal can be seen when applying sense riboprobe. **C)** A positive *otx5* control (green) relative to the embryo (grey). **D)** A head of a 24 hpf WT zebrafish embryo for reference. Scale bar 50µm

The FISH protocol has been optimised and the embryos imaged under the confocal microscope. The *kiaa0319* expression profile (Figure 2.10 A) was similar to the one obtained through WISH protocol. The probe labelled the majority of the embryo, making it unclear whether this is due to the transcript abundance or technical performance of the protocol. The negative control (Figure 2.10 B) proved to be unlabelled and only autofluorescence of the yolk cells could be detected. When imaging *otx5* positive control, a clear signal was obtained from the pineal and parapineal gland (Figure 2.10 C).

The FISH protocol is time consuming and the riboprobe hybridisation efficiency and stability depends on many factors. Therefore, the need for a shorter, more reliable and specific protocol arose. I have optimised the protocol for whole mount RNAScope based on the currently only published paper on this method [Gross-Thebing et al., 2014].

2.3.5 *kiaa0319* RNAScope protocol

The advantage of RNAScope is the ability to detect up to four independent transcripts in the same sample. The synthetic oligonucleotide tandems were designed to create probes C2 (*myod*) and C3 (*kiaa0319*) (Appendix 7.4.1 - 7.4.5). These tags enable us to simultaneously apply all probes to the sample and then detect them with one of three Amp4 dye combinations (Amp4 A, B or C). In order to avoid signal bleed through when detecting multiple probes simultaneously (Table 7.10), I have chosen to detect only two transcripts at once, leaving the detection of the positive control to a separate sample. The triple negative control was applied on its own. It consists of standardised probes bound to all three channels, leaving no space for other probes. The positive (*myod*) and negative controls were applied to the 5dpf embryos and imaged using the same settings as the samples with labelled *kiaa0319* (Figure 2.11 and Figure 2.11). There was a small amount of unspecific binding detected in the negative control (Figure 2.11). The positive control was labelled with Amp4 A, enabling its detection using the ATTO 550 settings on the confocal microscope. A strong and specific expression of *myod* in zebrafish muscle tissue was observed (Figure 2.11).

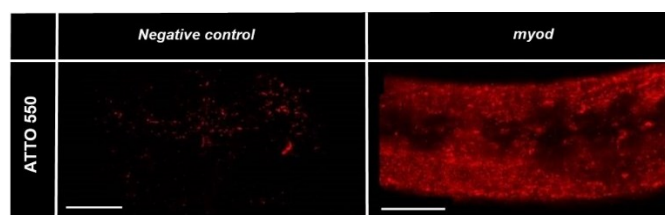


Figure 2.11 The 5dpf embryos labelled with triple negative and the positive control for RNAScope protocol

The negative control exhibits a small amount of unspecific binding. The positive (*myod*) control labels myogenic differentiation factor 1 in muscle tissue. Scale bar 50 μ m.

Once both controls were optimised, RNAScope protocol was carried out using zebrafish embryos from 16-cell stage to 120hpf. The whole mount embryos were imaged using the Leica TCS SP8 confocal microscope. To prevent the bleed-through of the fluorescence signals from multiple probes, a sequential scan was applied. The *kiaa0319* (Atto 647) was detected using a 633 laser and Myod (Atto 550) was detected using the argon laser. The ubiquitous expression of *kiaa0319* is observed in the first 24hpf, with the emphasis on developing nervous system (Figure 2.12). At 48hpf, the detection of *kiaa0319* transcripts can be localised to the developing brain structures, notochord, eyes and otic vesicles (Figure 2.12).

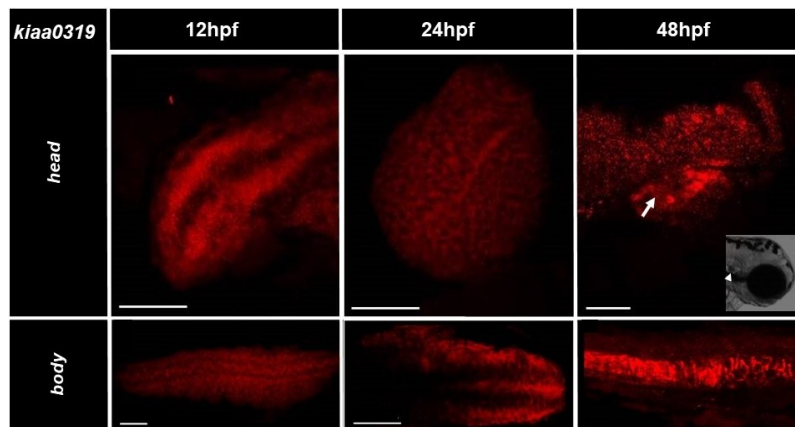


Figure 2.12 Confocal images of *kiaa0319* expression in three developmental stages

The RNAScope protocol was applied to whole zebrafish embryos. The *kiaa0319* (red) is strongly expressed in the brain throughout early development. At 48hpf, *kiaa0319* is strongly expressed in the zebrafish brain and otic vesicles (white arrow). Reference image of the zebrafish head at 48hpf. Black area in the brain due to the pigmentation of the embryo. White arrowhead indicates the otic vesicle. The scale bar is 50 μ m.

To closer investigate the *kiaa0319* expression in the sensory organs, a confocal z-stack images of RNAScope were taken for the eye and the otic vesicle (Figure 2.13). The *kiaa0319* transcripts are detected in the 48hpf left eye surface area (Figure 2.13 A) and concentrated on the top. The identity of the cells is so far unknown. The RNAScope protocol enables the application of several probes simultaneously, therefore I have used it to compare the expression of the *kiaa0319* to its homolog *kiaa0319-like* within the same sample. The *kiaa0319-l* is present on the surface of the eye; however, the signal rarely overlaps with the *kiaa0319* (Figure 2.13 A MERGE). In parallel, the triple negative control was applied to control for the background signals and unspecific binding of the probe (Figure 2.13 B). No signal was detected in Atto 550 (*kiaa0319*) or Alexa 488 (*kiaa0319-l*) channels.

Upon seeing the strong signal in the otic vesicle area (Figure 2.12 48hpf), I have performed additional RNASope on the 48hpf embryos to confirm whether the signal is reliable, or could it potentially be only due to the probe trapping. A confocal z-stack of the otic vesicle revealed a strong signal in both, the sample (Figure 2.13A') and the control (Figure 2.13 B'). These results indicate there is probe trapping present in the otic vesicle structures. However, when inspecting the RNAScope for the *kiaa0319* and *kiaa0319-l* sample, a clear signal can be observed in the brain area (above the vesicle), and in the vesicle itself (Figure 2.13 A'). As in the eye, the identity of the cells is unknown, however, the amount of overlaying signal is greater (Figure 2.13 A' MERGE). When analysing the triple negative control, no signal could be found, except for the probe trapping (Figure 2.13 B')

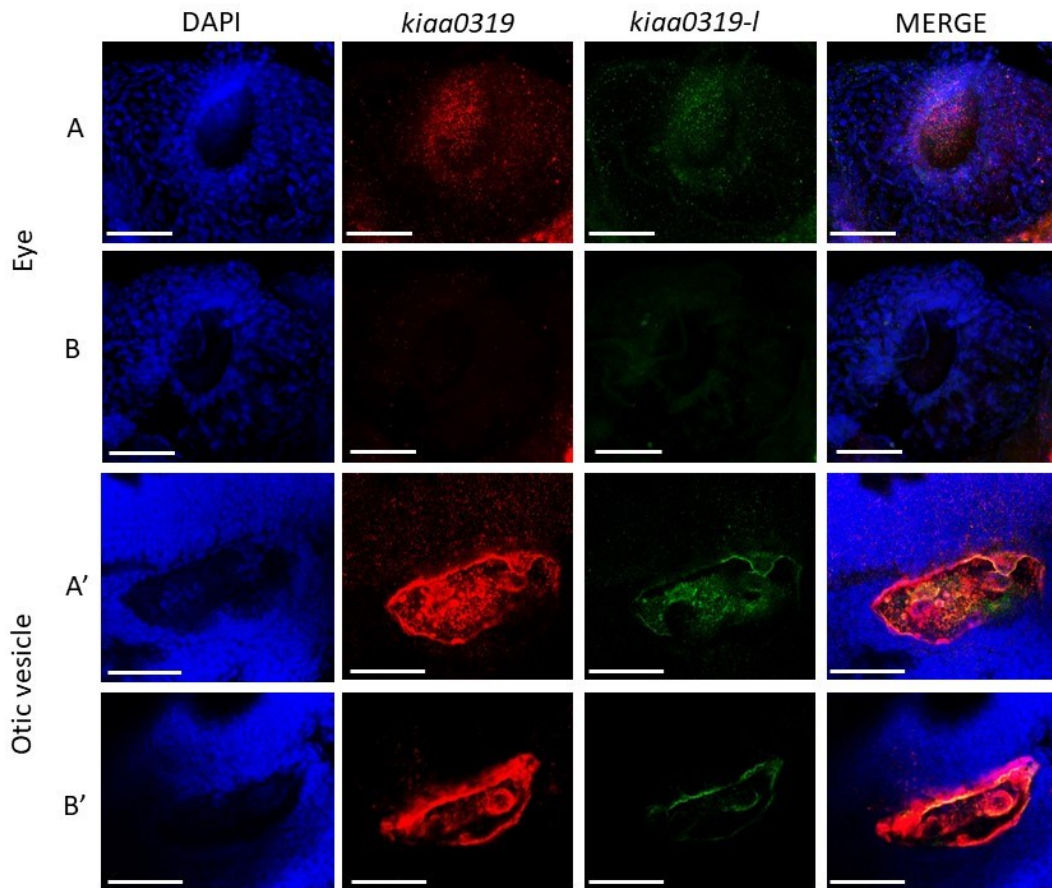


Figure 2.13 *kiaa0319* and *kiaa0319-like* signal in zebrafish eye and otic vesicle.

A) RNAScope of 48hpf zebrafish left eye. The *kiaa0319* (red) and *kiaa0319-like* (green) are expressed on the surface of the eyes and most strongly concentrated around the eye lens. **B)** Triple negative control of the left eye. There is no *kiaa0319* or *kiaa0319-like* expression. **A')** RNAScope at 48hpf zebrafish left otic vesicle. A strong *kiaa0319* (red) signal can be observed in the otic vesicle and in the brain (above the otic vesicle). *Kiaa0319-like* signal in green. **B')** Triple negative control of the left otic vesicle. Probe trapping is apparent in both channels, red and green. There is no signal in the brain. DAPI indicating nuclear staining. *Kiaa0319* is labelled with Atto 550 (red). *Kiaa0319-like* is labelled with Alexa 488 (green). Merge indicates a merge of all channels.

2.3.5.1 Light-sheet imaging

The light-sheet microscope is equipped only with a 488nm wavelength laser, restricting the *kiaa0319* labelling to Alexa 488 dye (Amp 4C). The images were then reconstructed as in section 2.2.6. Due to the inefficient light penetration through the tissue, the images could not be reconstructed in the highest resolution. As the stages on this in house build light sheet microscope are all manual, the specimen could not be turned during the imaging. This resulted in single-sided illumination of the sample.

The *myod* labelling in the 5dpf embryos showed a specific signal limited to the muscle tissue and was not seen in the spinal cord or in the notochord (Figure 2.14). When looking into the 5dpf embryo labelled with the triple negative control, no signal was detected (Figure 2.14).

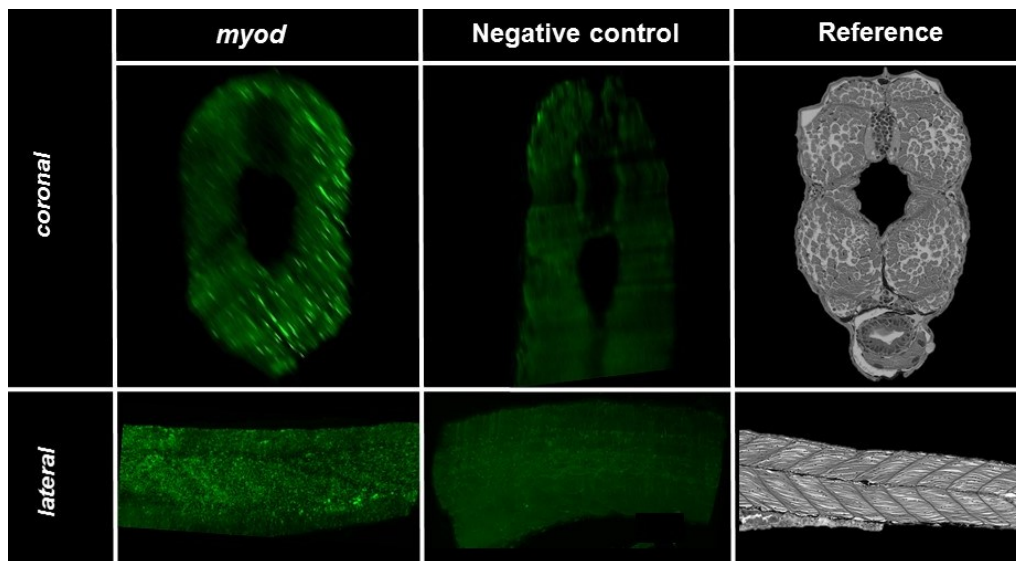


Figure 2.14 Lightsheet microscopy and 3D reconstruction of 5dpf zebrafish control embryos

The coronal and lateral view of a 3D reconstructed embryos. A positive *myod* and triple negative control indicating the accuracy of the protocol. The *myod* expression in a 120hpf embryo is limited to the muscle tissue, whereas the negative control shows no expression. The reference is an image of a coronal and lateral view of zebrafish body.

Furthermore, the embryos labelled for *kiaa0319* (Amp 4C) were imaged at three different developmental stages. Earlier in development, at 3dpf (72hpf), a clear and strong labelling of the notochord was observed, with the two spinal cord neuronal lines being strongly labelled (Figure 2.15). The spinal cord is clearly labelled but not as strongly as the notochord. There is also a low level of *kiaa0319* expression in the surrounding muscle. At 4dpf (96hpf), the *kiaa0319* was highly expressed in the spinal cord and more prominently present in the notochord. At 5dpf (120hf), a clear labelling of spinal cord neuronal lines was observed, and an additional signal was seen in the notochord and surrounding muscle tissue (Figure 2.15). The *kiaa0319* expression was also detected in the zebrafish gut at 120hpf (Figure 2.15).

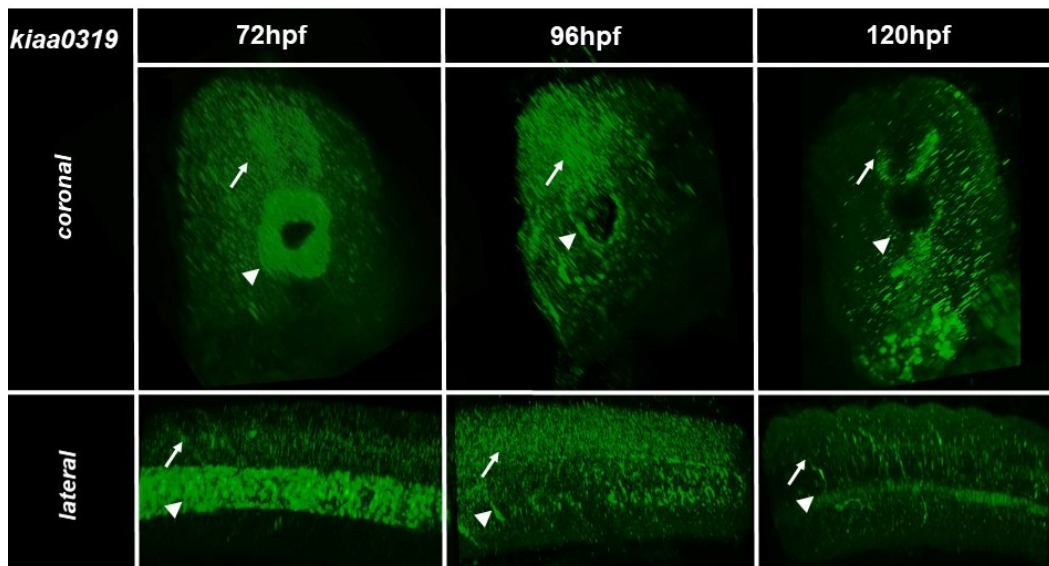


Figure 2.15 Lightsheet microscopy and 3D reconstruction of *kiaa0319* expression in three zebrafish developmental stages

A strong *kiaa0319* expression in the notochord (white arrowhead) and a well-defined signal in the spinal cord (white arrow) are visible in earlier developmental stages (72hpf). The expression in the spinal cord is stronger at 96hpf. A subset of *kiaa0319* positive cells can be observed in the notochord. At 120hpf, the *kiaa0319* is expressed in the spinal cord, notochord and gut lumen.

2.3.5.2 Imaging of transgenic lines

The localisation of Kiaa0319 to the notochord and spinal cord neuronal lines led me to investigate the identity of the *kiaa0319* – positive cells. In order to confirm the location of spinal cord in relation to *kiaa0319* positive cells, a tg(gfap:GFP; Oligo2:dsRed) double transgenic line was used in RNAScope protocol. In this transgenic zebrafish line the majority of secondary motoneurons, interneurons, and oligodendroglia cells are labelled with the GFP, whereas motor neurons and oligodendrocytes with DsRed. The tg(gfap:GFP; Oligo2:dsRed) zebrafish were kindly provided by Prof Bruce Appel [Shin et al., 2003].

When detecting the *kiaa0319* expression with the 488 laser, I obtained a strong GFP signal in the spinal cord. To identify the *kiaa0319* positive cells, I have performed an RNAScope on the above mentioned line and imaged with the confocal microscope. At 3dpf, the *kiaa0319* (labelled with Atto 647) could not be seen in the gfap:GFP positive cells in the spinal cord, but was strongly expressed in the notochord (Figure 2.16). In order to control for signal coverage due to the strong GFP in the spinal cord, a WT specimen was labelled in the same procedure. The notochord was labelled with *kiaa0319* probe, whereas the spinal cord remained very low on *kiaa0319* signal.

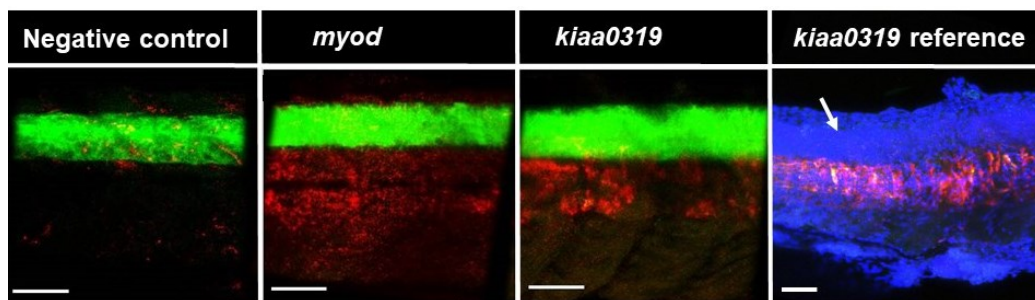


Figure 2.16 Confocal images of RNAScope on gfap:GFP Oligo2:dsRed transgenic zebrafish

The maximum projections of the RNAScope protocol on transgenic line. A 4dpf triple negative control exhibits low unspecific binding. A 3dpf *myod* positive control (red) in the muscle tissue. A 3dpf sample labelling *kiaa0319* (red) in the notochord. The spinal cord is GFP positive (green). A reference image indicating notochord (red) relative to spinal cord (white arrow) containing *kiaa0319*-positive red dots. Blue signal is DAPI. The scale bar is 50µm

2.3.6 *kiaa0319* is asymmetrically expressed at specific developmental stages

The WISH and FISH protocol both returned a minority of embryos (2 out of the pool of 20) with asymmetrically expressed *kiaa0319* in the eyes. The observed asymmetry was always in the favour of the left side of the embryo (Figure 2.17). The expression of *kiaa0319* is notably observed in the whole embryo, but appears stronger in the left eye, midbrain and midbrain-hindbrain barrier (Figure 2.17 arrows).

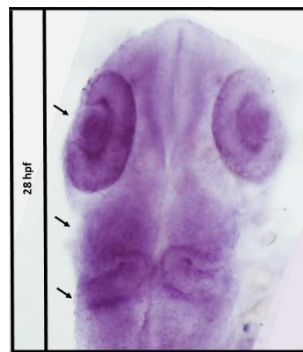


Figure 2.17 The asymmetric expression of *kiaa0319* in 28hpf zebrafish embryo

The DIG-labelled *kiaa0319* (purple) is expressed ubiquitously in developing embryo. Arrowheads indicate stronger expression in the left side of the embryo in the eye and brain.

The asymmetry observed through WISH was seen also after applying the FISH protocol (Figure 2.10 A). In order to test for asymmetrical gene expression, an RT-qPCR was run on zebrafish eyes. I staged 20 embryos of the WT strain AB.TU into 24hpf, 36hpf and 48hpf and dissected the eyes. The same was done on pool of 5 adult zebrafish (WIK strain). RT-qPCR was run and obtained data analysed manually, combining the Ct values from 9 technical replicates. As a reference I used the same cDNA samples and ran them for *eefla112*. The RQ scores were calculated as described in section 2.2.2.2.1. To see whether the difference in RQ scores reach the level of significance, a t.test was calculated for each RQ pair (L vs R). The value was then corrected from 0.05 to 0.01 using Bonferroni principle. The significant difference ($p < 0.01$) in asymmetry was therefore observed at 24hpf and 36hpf and interestingly, in adults (Figure 2.18).

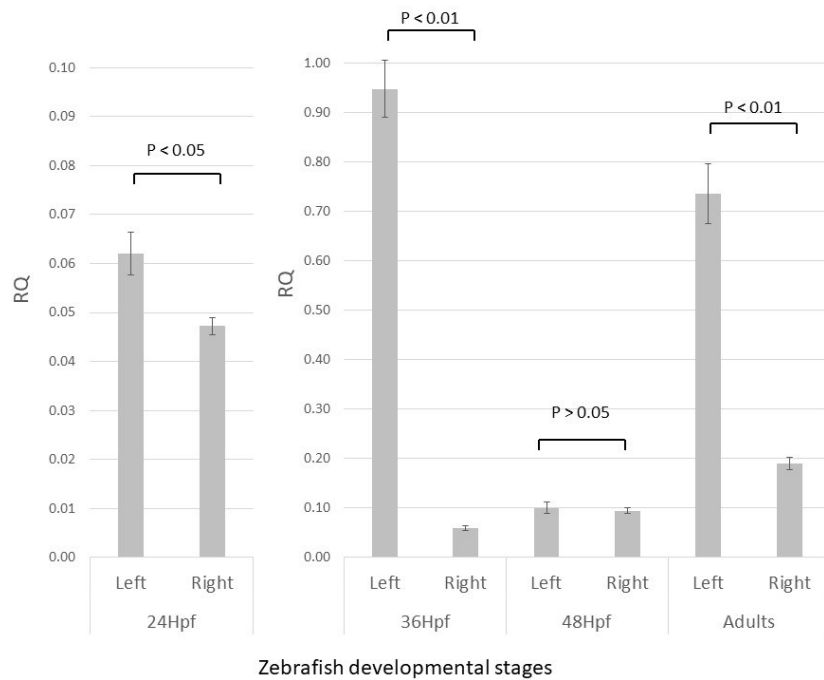


Figure 2.18 The RQ results of left vs right zebrafish eyes in three developmental stages

At 24hpf, there is a significant difference ($p < 0.05$) between *kiaa0319* expression in favour of the left eye. The highest and most significant ($p < 0.01$) expression is at 36hpf, where the left eye expresses almost 10x more *kiaa0319* than the right eye. At 48hpf there is no significant differences in *kiaa0319* expression when comparing left and right eye. Sample size 20 eyes per group. Three sets of three replicates. Scale difference due to lower levels of expression.

2.3.7 *kiaa0319*-like

The human *KIAA0319L* has been associated with dyslexia phenotype (discussed in Section 1.2.5). The PKD domains and high protein sequence similarity with *KIAA0319* are making it an attractive candidate for dyslexia susceptibility. In order to test whether the similarities in the expression profile between *kiaa0319* and *kiaa0319-like* exist also in zebrafish, the RT-PCR, qPCR and in situ hybridisation have been used in the same manner as described above.

RT-qPCR was performed as described in Sections 2.2.1 to 2.2.3. To confirm the presence of *kiaa0319l* transcripts throughout early embryonic development, primer pair 520/521 (Appendix A6) resulting in 119bp product were used for *kiaa0319l* cDNA (Figure 2.19).

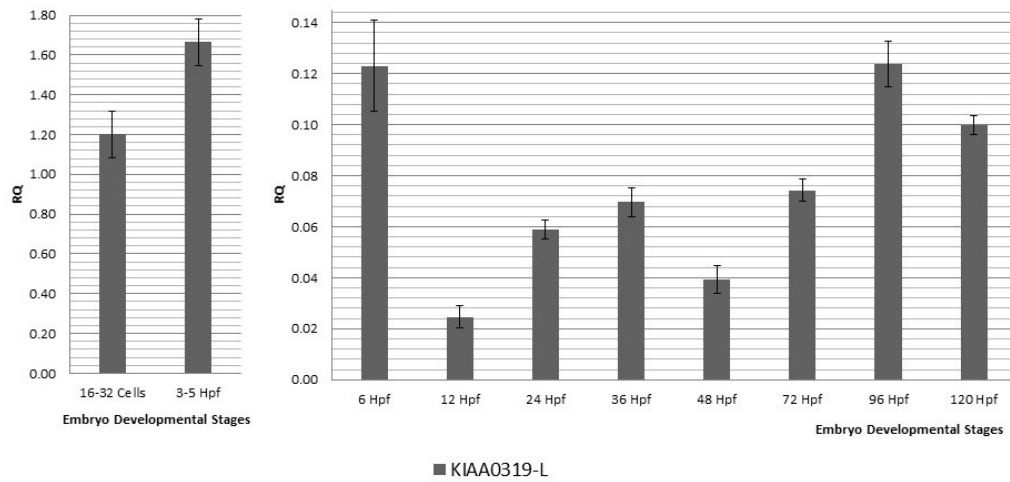


Figure 2.19 *Kiaa0319l* expression profile throughout embryonic development

The RQ scores indicate relative quantification of *kiaa0319l* expression throughout first 120hpf. The highest expression levels are within the first 6hpf. The *kiaa0319l* expression profile is similar to *kiaa0319* expression profile.

Following the RNAScope protocol (Section 2.3.5), a probe “C1” was created to detect *kiaa0319l* transcripts. The probe was applied simultaneously with the C2 (*myod*) and C3 (*kiaa0319*). The *kiaa0319l* transcripts were labelled with Alexa 488 and detected using a confocal microscope with argon laser. The triple negative control confirmed the efficient execution of the protocol, whereas the positive control (*myod*) returned a weak signal in the body (Figure 2.20 A).

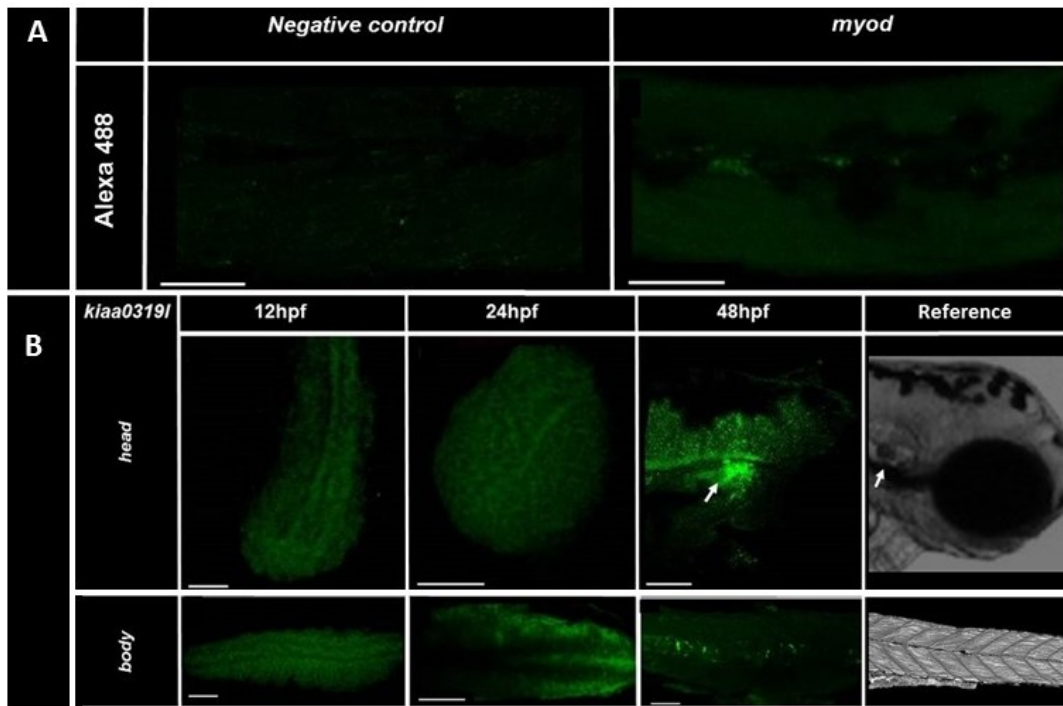


Figure 2.20 *kaa0319* expression profile of three developmental stages

A) Bodies of negative and positive control 5dpf embryo. Triple negative control is clear when observed under the argon laser, detecting Alexa 488. Positive control *myod* shows some unspecific binding in the body. **B)** 12hpf, 24hpf and 48hpf embryo expressing *kaa0319l* in the head and body. At 12hpf *kaa0319l* is ubiquitously expressed throughout throughout the nervous system. At 24hpf *kaa0319l* is strongly expressed in the brain midline. 48hpf embryo exhibits high presence of *kaa0319l* transcripts in the brain and the ciliated structure otic vesicle (white arrow). The *kaa0319l* expression is localised to zebrafish notochord at 48hpf. The grayscale image as a reference of 48hpf zebrafish head. White arrowhead indicates the otic vesicle. Reference image of a 24 hpf zebrafish embryo represents the area of imaged embryos. Scale bar 50µm.

The distribution of *kaa0319l* transcripts seems ubiquitous in the first 24hpf, however, the central nervous system tends to exhibit a stronger signal to the one in other tissues (Figure 2.20 B). At 48hpf, the *kaa0319l* is highly expressed in zebrafish brain and the otic vesicle (Figure 2.20 B white arrow), however the labelling of the notochord (48hpf body) seems to be limited to a specific subset of cells, which remain unidentified.

As the *kiaa0319l* expression profile highly resembles the one of the *kiaa0319*, I have decided to quantify the levels of transcripts in the zebrafish eyes (Figure 2.21). The eyes have been dissected from the pool of 20 embryos at three developmental stages (24hpf, 36hpf, 48hpf). The adult eyes have been dissected and pooled from 5 adult specimen. The *kiaa0319* has been shown to be asymmetrically expressed throughout the early development and in the adult zebrafish eyes (Figure 2.18). However, the *kiaa0319l* seems to only be asymmetrical at the 36hpf and 48hpf (Figure 2.21). Firstly, the left eye at 36hpf exhibits a significantly higher level of *kiaa0319l*. The asymmetry then turns towards the higher right expression at the 48hpf. When tested in adult zebrafish, there is no significant difference between left and right eye (Figure 2.21).

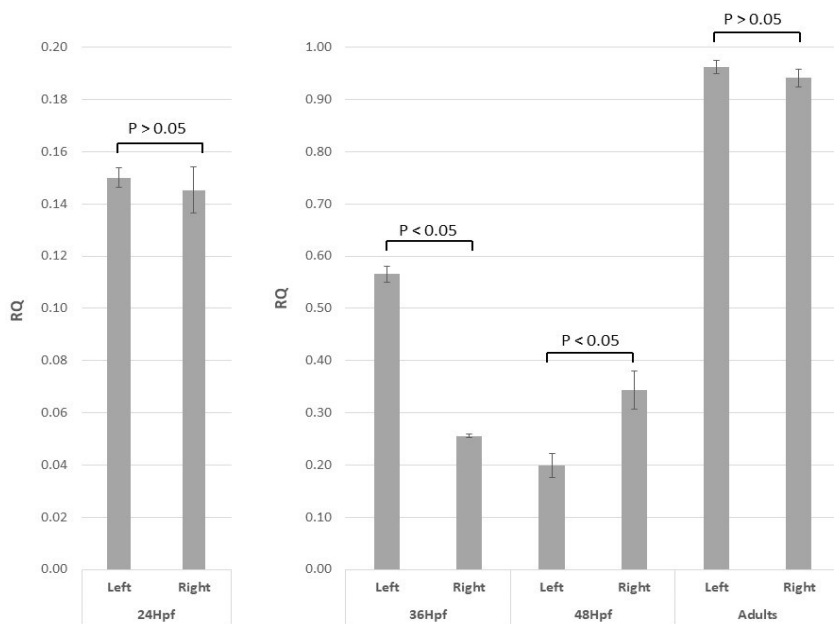


Figure 2.21 The RQ results of left vs right zebrafish eyes in three developmental stages

At 24hpf, there is no significant difference ($p > 0.05$) in *kiaa0319l* expression between left and right eyes. The significant ($p < 0.05$) difference in *kiaa0319l* expression is observed at 36hpf in the favour of the left eye. At 48hpf there, the direction of asymmetry of *kiaa0319* expression is reversed. Sample size 20 eyes per group. Two sets of three replicates. Scale difference due to lower levels of expression at 24hpf.

2.4 Concluding remarks

Zebrafish genome contains only one copy of *kiaa0319* and *kiaa0319l* genes. The expression of both genes peaks within the first 6 hours post fertilisation. Both genes are present during early embryo development and later appear limited to specific tissues, mainly the brain. The brain expression is in line with human data (Figure 1.2), where *KIAA0319* expression localises to cerebral neocortex, midbrain, hippocampus, and cerebellum of the developing human brain [Paracchini et al., 2006a]. *KIAA0319L* is expressed in the brain cortical neurons, hippocampus, telencephalon and other regions [Poon et al., 2011a].

Based on the expression profile of both, *kiaa0319* and *kiaa0319l*, we can assume they are somehow linked together. In the first 6 hours post fertilisation, the *kiaa0319* and *kiaa0319l* are widely expressed in the embryo (Figure 2.7 and Figure 2.19). The observed expression of *kiaa0319* and *kiaa0319l* in the eyes and the otic vesicles (Figure 2.9), the midbrain – hindbrain barrier (Figure 2.9), spinal cord and notochord (Figure 2.12 – Figure 2.15), support the suggestion of said genes being involved in functions other than neuronal migration.

The results obtained from lightsheet microscopy and a 3D reconstruction enabled me to see the distribution of *kiaa0319* in more detail (Figure 2.15). The expression of *kiaa0319* has consistently been observed in the spinal cord and notochord. To pinpoint the identity of *kiaa0319* labelled cells, I have performed the RNAScope protocol on the double transgenic line *gfap:GFP Olig2:DsRed*. This allowed for detection of the *gfap*-positive cells (peripheral glia and the majority of secondary motoneurons) with the 488 laser on the confocal microscope. The sequential scan with 633 laser provided for a reliable simultaneous imaging of *gfap*-positive cells and *kiaa0319* (labelled with Atto 647). The *kiaa0319* - labelled cells have not overlapped with the *gfap*-positive cells, excluding glia cells and secondary motoneurons as candidates. The transgenic line, however, enabled us to discriminate the location of the labelled cells. A strong *kiaa0319* signal was found

in the notochord rather than in spinal cord (Figure 2.16). Therefore, the identity of *kiaa0319* (and *kiaa0319l*) containing cells in the spinal cord still remains a subject of investigation.

When applying the probe for *kiaa0319l* transcript detection, a similar expression pattern was observed, with the exception of notochord labelling (Figure 2.20). The observed *kiaa0319l* expression was significantly lower compared to the one of the *kiaa0319* (Figure 2.12 and Figure 2.20 body). Notochord is a transient structure and is homologous to human cartilage tissue. The roles of notochord are in patterning the neural tube and developing of organs. It secretes proteins of Sonic Hedgehog family, which affects the embryo laterality development [Stemple, 2005]. High expression of *kiaa0319* in notochord could therefore be explained as additional indicator of *kiaa0319* involvement in LR organisation of the developing embryo.

RNAScope technology has proven to be a valuable technique for *in situ* detection of target transcripts. The major attribute of the RNAScope technique is the much shorter duration of the protocol. The protocol was highly efficient and straightforward in the older embryos (from 36hpf on), enabling the specific detection of *kiaa0319* and *kiaa0319l* transcripts. Younger embryos however, were a subject to further protocol optimisations as they were too fragile to withstand the harsh conditions of the washing buffers and chemicals provided by the ACD. Therefore, the focus of the RNAScope results is mostly on the embryos post-hatching, as their tissue managed to maintain integrity after the RNAScope was carried out. For further investigation, the focus of *kiaa0319* and *kiaa0319l* detection could be carried out on cryoslices. This would enable a more reliable detection on a cellular level by discriminating between different cell types throughout various tissues.

3 *Kiaa0319 function in zebrafish*

3.1 Abstract

Zebrafish *kiaa0319* is expressed ubiquitously in the early stages of development (up to 6hpf). At already 14 somite stage (16hpf), a specific and localised expression pattern can be observed in the head. Further along the development, *kiaa0319* specialises to the eyes, otic vesicle and the notochord. To understand *kiaa0319* function during the embryonic development, I have performed knock-out (KO) and knock-down (KD) studies using zebrafish as a model organism. Zebrafish genome conservation ranges up to 70% [Howe et al., 2013b] which makes it a great tool for studying gene functions in vivo and in vitro. The *kiaa0319* gene is presented in a single copy and codes for two transcripts. I have created three different CRISPR constructs to generate a *kiaa0319* KO zebrafish line. Additionally, I have performed a morpholino KD with two MOs affecting the translational start site and one affecting the splicing of the mRNA. No phenotype was observed in confirmed KD fish. The CRISPR/Cas9 protocol provided no KOs. While we cannot completely rule out technical artefacts, our results indicate *kiaa0319* does not play a major role during early development and is potentially subsidised by other factors.

3.2 Material and Methods

3.2.1 Morpholino experiments

3.2.1.1 Morpholino design and preparation

Morpholino (MO) antisense oligonucleotides were designed by the GeneTools LLC (<http://www.gene-tools.com/>), based on Ensembl mRNA transcript ID ENSDART00000160645 for zebrafish orthologue of KIAA0319. To target the translation of the protein, two different translation blocking (TB) MOs were designed, targeting the 5'UTR of the gene (Figure 3.1). A sequence for TB1 MO and its 5-mispair specificity control were designed, followed by the sequence for TB2 MO and its control (Table 3.1). An SJ MO affecting splicing of RNA into its mature form, was designed between the Intron 2 and Exon 3 of *kiaa0319* (Figure 3.1). All the MOs were labelled with fluorescein for efficient visualisation once delivered to the cells.

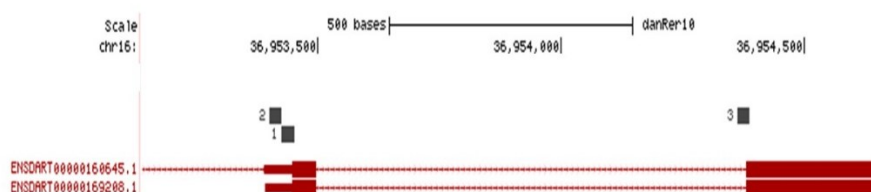
Lyophilised MOs were hydrated with 300µl of water to the stock concentration of 1mM and vigorously shaken before aliquoted. A dilution series was prepared for each MO separately. Working concentrations of 50µM, 100µM, 250µM, 500µM, 750µM and 1mM were stored in brown tubes in order to prevent bleaching of the fluorescein.

Table 3.1 Morpholino sequences for translational blocking (TB) and splice junction (SJ) targeting MOs.

MO	Morpholino sequence 5' -3'	5-mispair specificity control
TB1	CATGATGCCACTGCCGCCTTTTCAC	CATcATcCCAgTGCCcCgTTTTTCAC
TB2	GCGATGGTTTCTAACAGACATTACT	GCcATcGTTTgTAACAcAgATTACT
SJ	TCCTGATACTGAATGGGCCACAAAT	TCgTcATAgTGAATcGcCCACAAAT

3.2.1.2 Microinjection of morpholinos into zebrafish embryos

The zebrafish embryos were collected from the MEP system as described in Section 2.2.3.1 and prepared for microinjection. A microinjecting needle was filled with MO solution and calibrated to produce a 1µm diameter. This procedure was repeated for every new needle used in the experiment. Approximately a 100 embryos were injected per construct in order to provide suitable numbers for statistical analysis. Embryos were kept in embryo water with methylene blue at 28.5°C until further use. Prior overnight incubation, injected embryos were screened for death due to mechanical handling and affected embryos removed.

**Figure 3.1 USCS representation of morpholino locations on zebrafish *kiaa0319***

TB (1) and TB2 (2) MO sequences (black) are located in the 5' UTR region of zebrafish *kiaa0319* (red). SJ (3) sequence spans between the *kiaa0319* intron 2 and exon 3 and targets splicing of the RNA. The two red lines represent two isoforms of zebrafish *kiaa0319* gene.

3.2.1.3 Western Blot analysis of Morpholino injected embryos

Zebrafish embryos of the same developmental stage were collected into pools of 30 and fresh frozen on dry ice. Each tube was carefully defrosted, and tissue homogenized in 1 ml of homogenisation buffer (Appendix 7.1.2) using a Precellys homogeniser. A homogenate was spun down briefly to collect any connective tissue or large debris. Supernatant was removed, and the pellet was spun down for 90 min at 16.000rpm at 4°C. The remaining supernatant was removed and aliquots of 100µl membrane pellet were frozen at -20°C. Brain zebrafish homogenate, supernatant and membrane were used to test for the presence of Kiaa0319 protein. As a positive control, HEK293 cells with human KIAA0319-GFP overexpression has been used. KIAA0319 is a transmembrane protein, therefore I have chosen to test for its presence in the supernatant and the membrane of the cells.

A 100µl of homogenisation buffer was added to obtain 2 mg protein per ml of suspension. Samples were then diluted to 1mg protein/ml in Laemmli buffer containing β-mercaptoethanol and heated to 99°C for 10 minutes. The mix was vortexed and naturally cooled to room temperature. Collected samples were stored -20°C until further use.

Prior to loading on the gel, samples were incubated at 50°C for 5 min and spun down. Invitrogen NuPage 4% agarose gel was used to run 5µg of protein per well at 150 volts for 60 minutes. The gel was then blotted for 1h onto PVDF membrane at constant voltage of 150 volts. The membrane was immunostained according to ECL method. Solution 1 was applied to a square petri dish and incubated at room temperature for one hour with shaking. The Primary antibody (Table 3.2) was added to Solution 2 (Appendix 7.1.2) and incubated overnight at 4°C with shaking. The membrane was washed four times with quick succession in Solution 3 (Appendix 7.1.2) and then incubated in solution 3 twice for 15 minutes at room temperature with shaking. Secondary was added to Solution 4 (Appendix 7.1.2) and incubated for 1.5h at room temperature with shaking. The membrane was washed four times with quick succession in Solution 3 and then incubated in solution 3 twice for 15

minutes at room temperature with shaking as before. Solution 3 was replaced with PBS. The membrane was carefully blotted to a paper roll to remove all the excess liquid and placed facing down onto freshly made ECL reagent. After 3minute incubation in the dark, excess liquid was removed and the membrane placed between two layers of plastic film and imaged.

Table 3.2 List of antibodies used for western blot analysis

Antibody	Host species	Concentration
Anti-KIAA0319 R7	rabbit	1:1000
Anti-KIAA0319 70	guinea pig	1:200
Anti-human β actin	Mouse	1:10000
Anti-rabbit	*	1:35000
Anti-mouse	*	1:35000
Anti-guinea pig	*	1:10000

* Secondary antibodies were kindly provided by Dr Gordon Cramb, School of Medicine, St Andrews University

The antibodies R7, 70 and 74 were kindly provided by Antonio Velayos Baeza [Velayos-Baeza et al., 2008; Levecque et al., 2009]. All three antibodies are custom made. The R7 polyclonal antibody raised in rabbit targets the cytosolic domain of KIAA0319 with peptides ELRPKYGIKHRSTEH and EFESDQDTLFSRERM of the mouse KIAA0319 protein. The 70 polyclonal antibody raised in guinea pig targets the full intracellular C domain of human KIAA0319 protein. The 74 antibody has the same features as antibody 70, but has been made in a later batch. It should return the same results as the antibody 70, therefore we have used it as a control.

3.2.1.4 Quantitative Real time PCR of *kiaa0319* morphants

To assess the efficiency of the *kiaa0319* knock down, a qPCR reaction using primer pair 518/ 519 returning a 121bp fragment (Figure 3.2) was set as described in Section 2.2.2.2. Comparing the quantity of morphant *kiaa0319* mRNA relative to the WT embryos, the RNA from embryos injected with different MO concentrations has been transcribed into cDNA and the qPCR reaction set as previously described in Section 2.2.2.2.

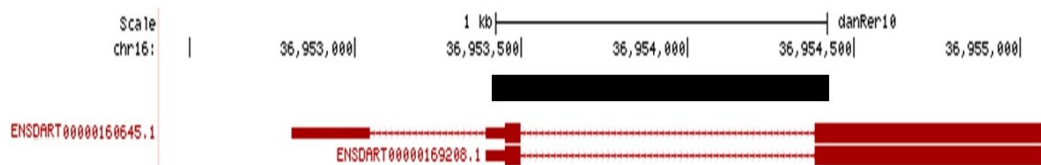


Figure 3.2 *kiaa0319* qPCR fragment

A screenshot of the UCSC genome browser for the region (thick black line) between Exons 2 and 3 in *kiaa0319* gene (upper red) and the same region in the *kiaa0319* isoform (lower red). When transcribed into cDNA, this region is 121bp long.

3.2.2 CRISPR genome editing protocol

The aim of this protocol was to introduce a point mutation to knock down the function of the *kiaa0319* gene. The CRISPR protocol was carried as described before [Hwang et al., 2013a]. The protocol requires the synthesis of Cas9 enzyme mRNA and its guide sequences. Once these constructs are made, the co-injection of both is required for efficient editing of zebrafish genome (Figure 3.3).

3.2.2.1 Synthesis of Cas9 mRNA

To synthesise the Cas9 mRNA, 10µg of the expression plasmid pMLM3613 was linearised for 3 hours at 37°C, using PmeI restriction enzyme reaction (NEB). The efficiency of the digestion reaction was verified on a 1% agarose gel. The successfully linearised plasmid was then purified using a QIAquick spin protocol (QIAGEN). To transcribe a capped RNA molecule, the reaction using Ambion mMMESSAGE mMACHINET7 ULTRA kit was set as follows:

T7 2X NTP/ARCA		10 µL
T7 Reaction Buffer	[10X]	2 µL
linear template DNA	[1µg]	6 µL
T7 Enzyme Mix		2 µL
Total volume		20 µL

The transcription reaction was incubated for 2 hours at 37°C and then terminated by the addition of 1µL TURBO DNase for 15 min at 37°C. The capped-RNA was then polyadenylated as follows:

Capping reaction		20 µL
Nuclease-free Water		36 µL
E-PAP Buffer	[5X]	20 µL
MnCl ₂	[25 mM]	10 µL
ATP Solution		10 µL

Four microliters of E-PAP enzyme were added to final reaction volume of 100 μ L, incubated at 37°C for 45 min and put on ice. The polyadenylation reaction was stopped, and RNA precipitated by adding 10 μ L of 3M Sodium Acetate Stop Solution (provided in the kit). The precipitated RNA was extracted by adding an equal volume (110 μ L) of phenol/chloroform, followed by centrifugation at the highest speed for 30 minutes. The aqueous phase was transferred to a new tube and added 1 volume of isopropanol. The mixture was put on -20°C overnight. To obtain the RNA pellet, the precipitated mix was centrifuged at 4°C for 15 min at maximum speed and supernatant carefully discarded. The pellet was then washed with 300 μ L of 70% ethanol, vortexed and centrifuged for 5min at 4°C. The ethanol was carefully removed by pipetting. The residual ethanol drops were left to dry out for 30 min at room temperature. Precipitated capped and polyadenylated RNA was finally resuspended in 20 μ L of RNase-free water and stored in 5 μ L aliquots at -80°C.

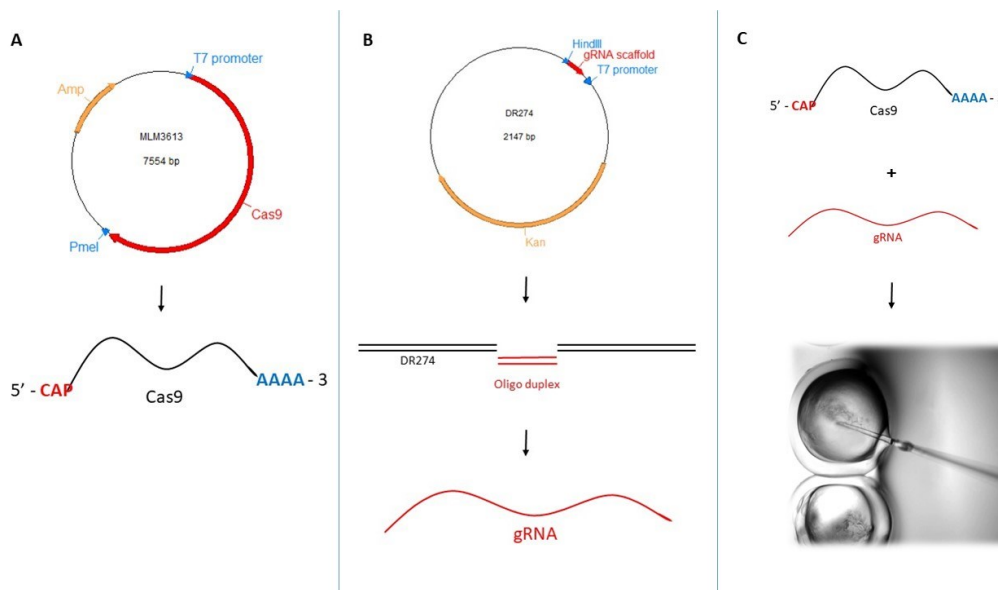


Figure 3.3 The CRISPR Cas9 protocol

A) Cas9 transcription. MLM3613 vector containing Cas9 was transcribed into capped and polyadenylated mRNA using T7 enzyme. **B)** gRNA design. DR274 vector (black) was restricted with HindIII and ligated with pre-made oligo duplexes (red) into the gRNA scaffold on the vector (red). The duplexes were then transcribed into gRNA through T7 transcription protocol. **C)** Delivery of CRISPR/Cas9 system. The Cas9 cap-mRNA-polyA and the gRNA have been co-injected into zebrafish embryos for efficient genome editing.

3.2.2.2 Guide RNA sequence design

The guide sequences were designed using ZiFiT Targeter software package (<http://zifit.partners.org/ZiFiT>). The target DNA sequence (zebrafish *kiaa0319*) was inserted in FASTA format which resulted in generation of primer pairs suitable to create guide RNA candidates. For our purpose, three primer pairs (Appendix 7.6.1) were chosen and ordered through Eurofins Genomic service (<https://www.eurofinsgenomics.eu/>).

To create the guide RNA sequence, primer pairs were firstly ligated into the pDR274 vector (Addgene) and then *in vitro* transcribed. Firstly, primer duplexes were created to ligate the primers into the vector. The phosphorylation of oligonucleotides was set as follows:

Primer I	[100 μ M]	1 μ l
Primer II	[100 μ M]	1 μ l
T4 Ligase buffer	[10X]	5 μ l
T4 PNK		1 μ l
ddH ₂ O		42 μ l
Total volume		50 μ l

The reaction was incubated at 37°C for 30 minutes followed by heat inactivation for 20min at 65°C. Phosphorylated primers were annealed into duplexes by mixing equal volumes of the equimolar oligonucleotides in a new tube and adding 2.5 μ l of 1M NaCl to the phosphorylated oligo pairs. The annealing reaction was incubated at 95°C for 5 min in a heat block. The tubes were left in the heat block and temperature was then set to 70°C. Once the temperature got to the set value, the heat block was switched off and allowed to cool to room temperature (1 hour).

Annealed primer duplexes were briefly vortexed, centrifuged and stored at 4°C until further use.

The pDR274 vector was used to ligate the oligonucleotide duplexes. Firstly, 10µg of DNA was linearised for 3 hours at 37°C, using HindIII restriction enzyme reaction (NEB). The vector was dephosphorylated using Shrimp Alkaline Phosphatase (rSAP, NEB). Linearised plasmid was then gel purified using QIAquick gel extraction protocol (QIAGEN).

To create the final construct for guide RNA transcription, the linearised dephosphorylated plasmid and phosphorylated oligonucleotide duplexes were ligated as follows:

pDR274	[100ng]	0.7 µl
phosphorylated oligo duplex		2 µl
T4 Ligase buffer	[10X]	1 µl
T4 ligase		1 µl
ddH ₂ O		5.3 µl
Total volume		10 µl

The ligation mix was incubated at room temperature for two hours and transformed into DH5α competent cells. The newly constructed plasmids were isolated using QIAprep Spin Miniprep (QIAGEN). For each of the three constructs of pDR274 vector containing oligonucleotide duplex, five clones were chosen at random and sent for sequencing using a standard M13 primer.

The positive clones were further in vitro transcribed using MAXIscript Kit Procedure (ThermoFisher). The amount of DNA added into the mix was dependant on the plasmid concentration:

DNA template	1 μ g	x μ l
Transcription Buffer	10X	2 μ l
ATP	10 mM	1 μ l
CTP	10 mM	1 μ l
GTP	10 mM	1 μ l
UTP	10 mM	1 μ l
T7 Enzyme mix		2 μ l
Nuclease-free Water		y μ l
Total volume		20 μ l

The transcription mix was incubated 1 hour at 37°C, followed by addition of 1 μ l TURBO DNase. The mix was further incubated at 37°C for 15min and finally purified using RNeasy Mini Kit (QIAGEN) columns. The end product resulted in three guide RNA molecules (81, 85, 89).

3.2.2.3 Microinjection of gRNA/Cas9 into zebrafish embryos

The zebrafish embryos were collected from the MEP system as described in Section 2.2.3.1 and prepared for microinjection. A mixture of guide RNA and Cas9 mRNA in the ratio 1:3 was injected into one to four cell stage embryos. Approximately 200 embryos per guide RNA have been injected with a gRNA/Cas9 mRNA mix. As a negative control, embryos with no Cas9 have been injected (gRNA only).

The following day, dead embryos were removed, and embryo water replaced with the fresh medium. The embryos were then left in the zebrafish facility for 3 months. To determine the fish with the successfully edited genome, the fin clipping genotyping protocol has been applied.

3.2.2.4 Genotyping of injected zebrafish embryos

The genotyping was performed using PCR and diagnostic restriction reaction. To obtain the genomic DNA, zebrafish tail fin was cut. The fin clipping was carried out under the close supervision of Dr Carl Tucker, the manager of the zebrafish facility at The Queen's Medical Research Institute at the University of Edinburgh. The fish were placed into the working tricaine solution (4.2ml tricaine solution in 100ml clean tank water; Appendix 7.1.2), until there was no movement observed. The anaesthetised fish were individually put on a cover of a petri dish, and the tail fin was cut away with the scalpel. The clipped fin was inserted into PCR tubes containing 100µl of tail buffer (Appendix 7.1.2) and individual fish placed into labelled tanks, where they remained until their genotype has been confirmed.

The PCR tubes containing tail clipping were added with Proteinase K solution (20 mg/ml) and incubated at 55°C overnight. To precipitate the SDS in the Tail Buffer, 12.5µl of 3M KOAc (Appendix 7.1.2) was added, vortexed and placed to 4°C for 2 hours. The tubes were then centrifuged at maximum speed for 15 minutes at 4°C. The supernatant was transferred to a clean tube and subsequently used in a standard MyTaq PCR reactions.

The primers to obtain the PCR fragment (Appendix 7.6.2) were designed simultaneously with guide sequences, using ZiFiT Targeter software package (<http://zifit.partners.org/ZiFiT>). The software returned the optimal genotyping primer pair for each guide sequence, which were then ordered through Eurofins Genomic service (<https://www.eurofinsgenomics.eu/>). When optimising the PCR reactions, gradient PCR was set run in the G-STORM thermocycler (Labtech international) under the following conditions:

Denaturation	95°C	1 min	
Denaturation	95°C	15s,	} 30 cycles
Gradient	58°C - 65°C	30s	
Elongation	72°C	72s	
Elongation	72°C	5 min	

The resulting DNA fragments were run on the gel in order to determine the optimal annealing temperature for each primer pair. The same procedure was repeated for the CRISPR/Cas9 constructs 81, 85 and 89.

The PCR fragments were further digested with according restriction enzymes (Appendix F1) and the fragments run on the 2% agarose gel. In the presence of CRISPR/Cas9 induced mutation, the fragments are not expected to be cleaved in the restriction reaction.

3.3 Results

3.3.1 Morpholino knock down of zebrafish *kiaa0319*

Morpholino (MO) system provides a non-transient knock down effect to study the function of the protein of choice. The application and analysis of such knock down (KD) is faster than the knock out (KO) techniques, therefore I have used it to study *kiaa0319* function during zebrafish early embryogenesis.

Splice junction MOs were injected with 50 μ M, 100 μ M, 250 μ M, 500 μ M, 750 μ M and 1mM concentration (Table 3.3). Approximately a 100 embryos per concentration have been injected and stored in embryo water with methylene blue at 28.5°C overnight. The following day the dead embryos were counted and cleaned away. In the first day post fertilisation normal death process occurs also in WT embryos. These embryos were not included in the calculation of the survival percentage as their mortality could be due to injection process or normal development.

Table 3.3 Titration of splice junction (SJ) MOs

Concentration	MO	#Dead 1dpf	#Dead 5dpf	#Live 5dpf	%live 5dpf
	WT	18	0	65	100
50 μ M	SJ	36	3	88	96.70
	SJ-C	28	0	62	100.00
100 μ M	SJ	47	0	65	100.00
	SJ-C	27	0	79	100.00
250 μ M	SJ	30	2	74	97.37
	SJ-C	23	3	62	95.38
500 μ M	SJ	46	1	77	98.72
	SJ-C	24	0	65	100.00
750 μ M	SJ	24	2	76	97.44
	SJ-C	38	1	74	98.67
1mM	SJ	45	3	48	94.12
	SJ-C	44	2	58	96.67

After the titration experiment, 20 embryos per MO were collected on day 1 and day 4 post fertilisation. Whole RNA was extracted and transcribed into cDNA. A qPCR reaction has been run for samples from 250µM to 1mM MO and referenced against WT level of *kiaa0319* expression (Figure 3.4). At all concentrations, the MOs provided a notable knock down (KD) effect on the mRNA level. The control MOs (mismatched morpholinos) caused no significant knock down. At 1mM concentration, the control MO has also provided a significant reduction in *kiaa0319* expression, possibly due to the saturation of the injected oligonucleotides. The levels of *kiaa0319* are lower at 1dpf than at 4dpf (Figure 3.4 light grey columns). At a concentration of 750µM, the KD effect persists to day 4 post fertilisation, suggesting this concentration is optimal for further experiments.

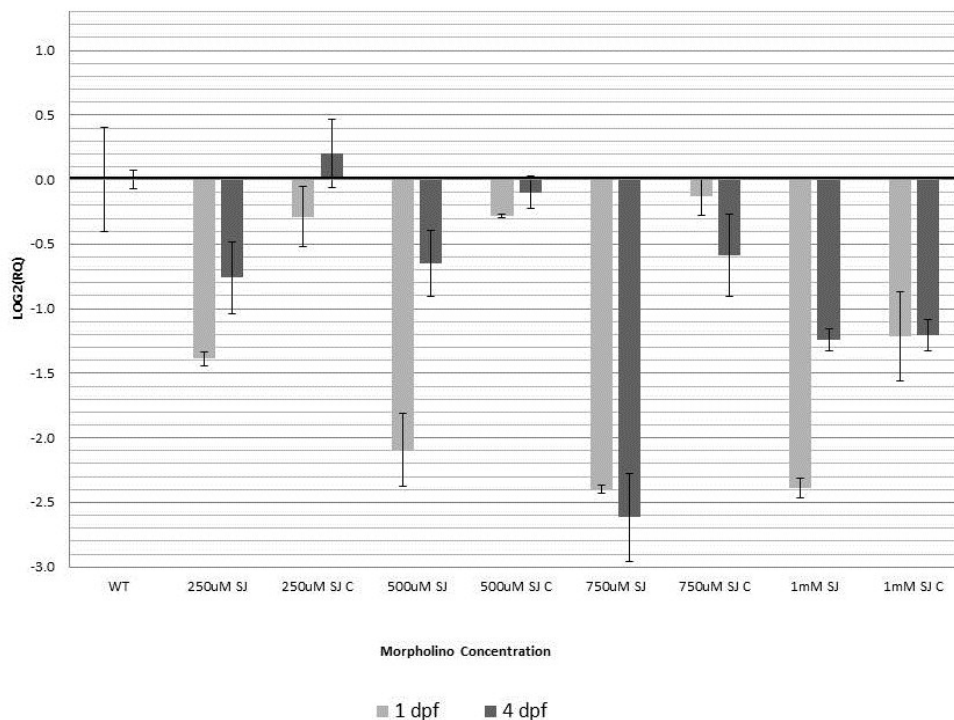


Figure 3.4 Splice Junction MO knock down in 1dpf vs 4dpf zebrafish embryos

Different concentrations of injected SJ MO and their controls referenced against the expression of *kiaa0319* in WT zebrafish embryos of the same developmental stage. The KD is the most efficient at 750µM concentration. The control MOs provide no significant KD effect with the exception of samples injected with 1mM MOs. Light grey represents MOs at 1dpf. Dark grey represents MOs at 4dpf. Error bars represent standard deviation SD.

Zebrafish embryos injected with translational blocking (TB1 and TB2) morpholinos were screened and imaged at 1dpf and 4dpf in order to observe any phenotypic differences during development. The TB MOs target the ATG translational start site, leading to more efficient KD. Following this, they should work efficiently at lower concentrations than SJ MO, therefore I have tested them from 50 μ M to 250 μ M. The observed survival rates have been over 90% (Table 3.4), suggesting the knock down has no negative effect on zebrafish development.

Table 3.4 Titration of translational blocking (TB1 and TB2) MOs

Concentration	MO	#Dead 1dpf	#Dead 5dpf	#Live 5dpf	%live 5dpf
50 μ M	TB1	40	0	48	100.0
	TB1-C	35	0	29	100.0
	TB2	32	0	50	100.0
	TB2-C	10	4	50	92.6
100 μ M	TB1	14	0	42	100.0
	TB1-C	22	0	29	100.0
	TB2	14	1	55	98.2
	TB2-C	17	1	25	96.2
250 μ M	TB1	19	0	36	100.0
	TB1-C	13	0	35	100.0
	TB2	38	0	46	100.0
	TB2-C	14	2	36	94.7

To observe the phenotypic change in development in KD zebrafish, the embryos were firstly anaesthetised with tricaine solution and then imaged under the epifluorescence microscope. Comparison images were taken at bright field (BF) and GFP channel (Figure 3.5). The injected zebrafish that have successfully taken up the morpholino oligonucleotides are easily distinguished under the GFP filter. WT embryos exhibit no GFP signal (Figure 3.5). I have chosen the MO concentration of 100 μ M in order to check for any phenotypic differences in development. At day 1 post fertilisation, all surviving embryos exhibit a GFP signal. This signal mellows off by the day 4 post fertilisation, where only autofluorescence can be observed in the zebrafish yolk. No phenotype was observed in the majority of embryos. To check whether the efficiency of the knock down improves with the co-injection of both TB morpholinos, an experiment injecting 100 μ M TB1, TB2 and the mixture of both was conducted (Table 6.18). No phenotype was observed.

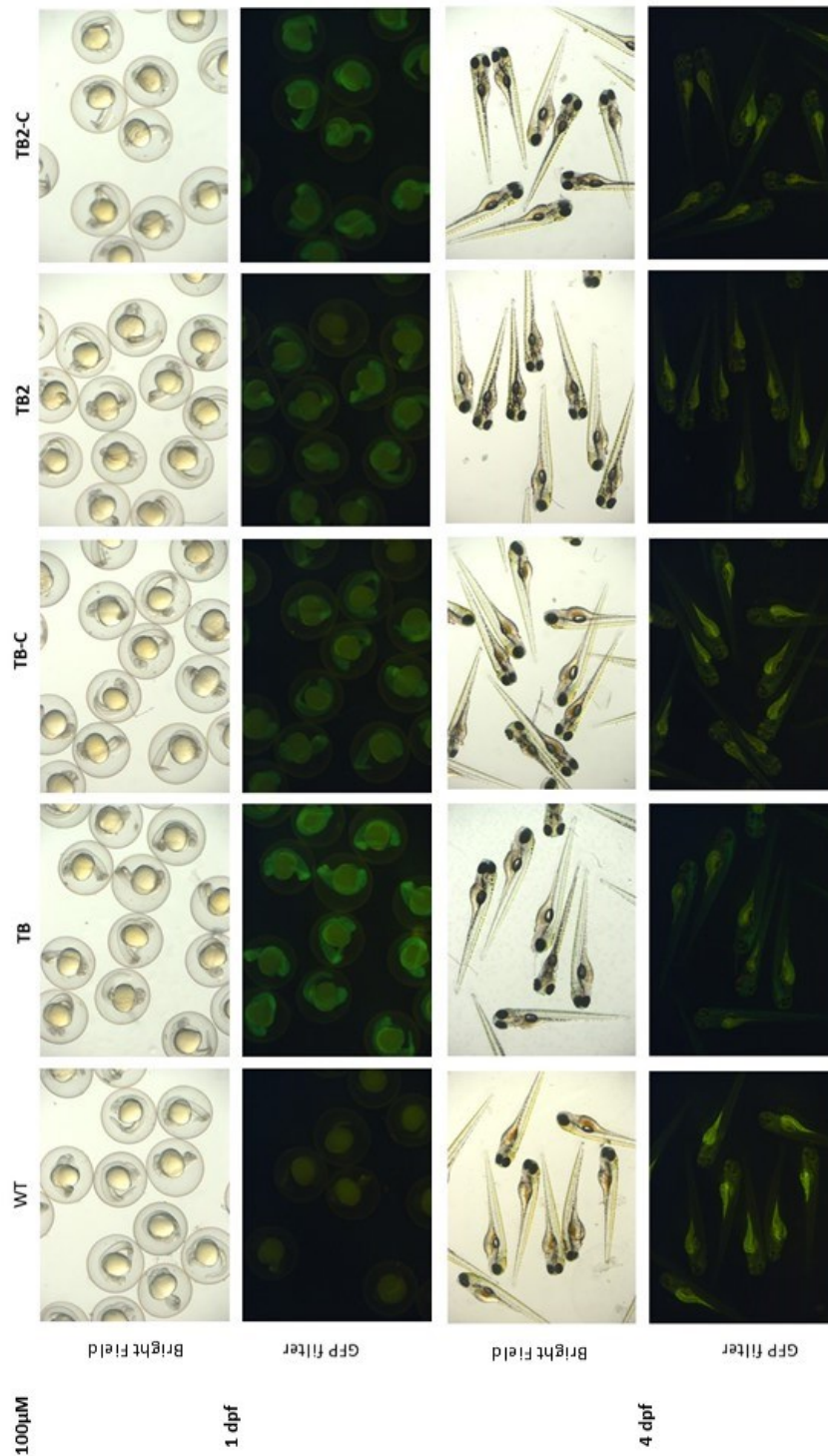


Figure 3.5 Translation blocking MOs at 1 dpf and 4 dpf

The embryos were injected with a 100µM concentration of the MOs. The TB1, TB1-c, TB2 and TB2-C injected embryos exhibit ubiquitously distributed GFP fluorescence signal at day 1 post fertilisation. The GFP fluorescence cannot be observed at day 4 post fertilisation. The WT embryos are imaged for reference. No phenotype can be observed in the injected embryos.

A specific phenotype was observed in a small number of embryos (Figure 3.6). The changes included tail curvature, pericardial oedema and hydrocephalus (Figure 3.6). These are the standard phenotypes, observed in most morpholino studies. As the WT zebrafish exhibit the same phenotype, the above-mentioned changes could not be attributed to *Kiaa0319* function, but rather to normal natural variation.

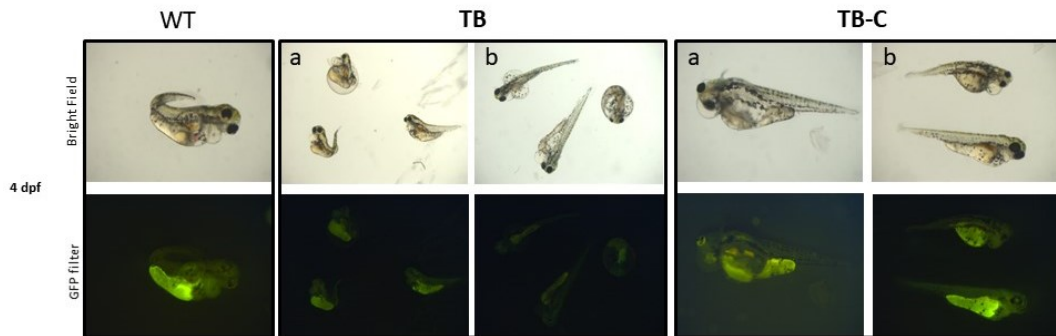


Figure 3.6 Zebrafish MO – injected embryos exhibiting phenotype

Zebrafish embryos were injected with a 100 μ M concentration of translational blocking (TB1) or its control (TB1-C) MOs. At 4dpf they are exhibiting phenotype including tail curvature, pericardial oedema and hydrocephalus. The WT control also exhibits listed phenotypes. a) and b) represent different batches of injection.

To further check whether the MO have an effect on zebrafish development at higher concentrations, I have injected around 100 embryos with the 250 μ M concentration of TB1 and the control MOs. The injected embryos exhibit the GFP signal due to the presence of hybridised oligonucleotides also at day 4 post fertilisation as do embryos with injected control MOs (Figure 3.7). The WT embryos only exhibit autofluorescence, best seen in the yolk.

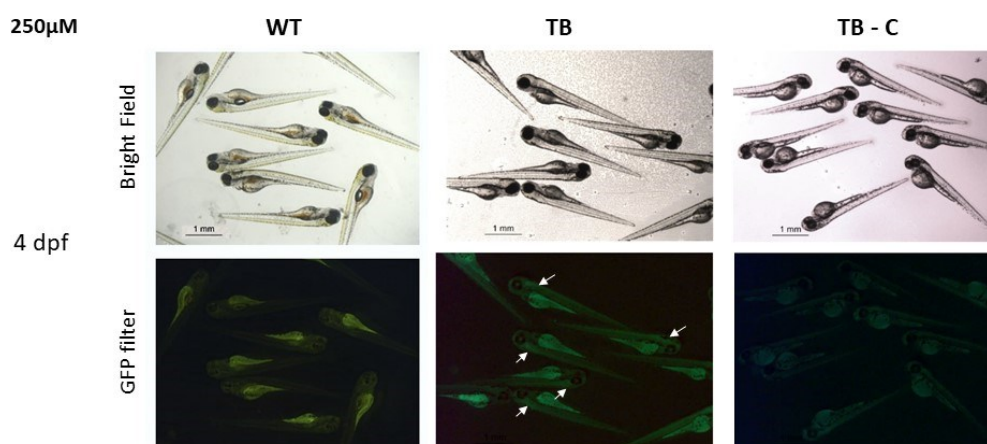


Figure 3.7 The zebrafish embryos injected with 250µM TB morpholino oligonucleotides

Translational blocking MO at 250µM concentration persists in the zebrafish embryos until day 4 post fertilisation. WT and TB-C MOs exhibit only autofluorescence GFP signal.

3.3.1.1 Western blot analysis of MO – injected embryos

To analyse whether the knock down of Kiaa0319 worked, a western blot protocol was applied to protein extracted from TB – injected embryos. As a positive control, HEK293 cells expressing KIAA0319-GFP have been used. The samples were prepared as described in Section 3.2.1.2. The samples were loaded on two membranes and detected with either anti-KIAA319 R7 primary antibody, anti-KIAA0319 70 or anti-KIAA0319 74 (Figure 3.8). Human and zebrafish Kiaa0319 are transmembrane proteins, therefore I have divided the samples into a homogenate (Figure 3.8A), a supernatant (Figure 3.8 B) and a membrane (Figure 3.8 C) for zebrafish brain sample. The HEK293 cells containing overexpressed Kiaa0319 with the fused GFP protein have been divided into the supernatant and the membrane (Figure 3.8 D, E). The samples were loaded on the gel and ran as described in Section 3.2.1.2. All antibodies have returned several strong bands in all of the samples (Figure 3.8) indicating the antibodies are not specific for the use in zebrafish. The zebrafish Kiaa0319 is a 955aa (105kDa) protein compared to the human orthologue which is 1063aa (115kDa). The human KIAA0319 is coupled

with the GFP protein (27kDa), modifying the size of the protein from 115kDa to 142kDa.

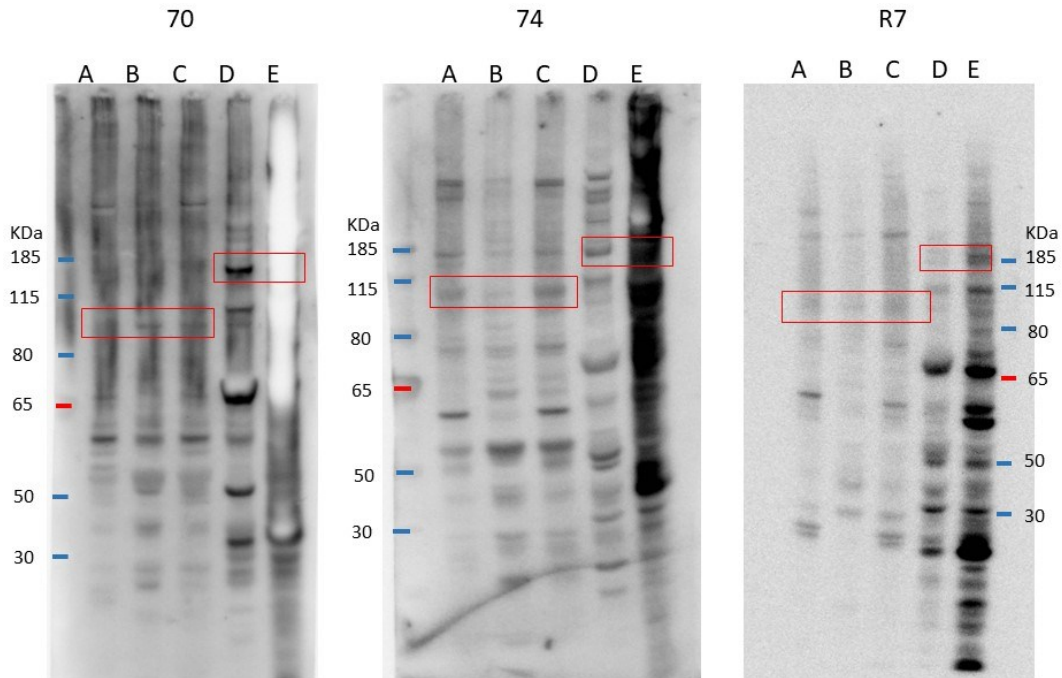


Figure 3.8 Western blot analysis of Kiaa0319

The WB analysis of zebrafish Kiaa0319 and human KIAA0319-GFP protein using three different antibodies: anti-KIAA0319 70, anti-KIAA0319 74 and anti-KIAA0319 R7. **A)** Zebrafish brain homogenate; **B)** Brain supernatant; **C)** Brain membrane; **D)** HEK293 supernatant with KIAA0319-GFP overexpression; **E)** HEK293 membrane. Red rectangle indicates predicted zebrafish Kiaa0319 protein at 105kDa and human KIAA0319-GFP protein at 142kDa.

The western blot did not return reliable results when using custom made antibodies against KIAA0319. The specificity of the antibody is too low to say with confidence that the detected protein is zebrafish Kiaa0319. The sequence comparison between antibody peptides and zebrafish Kiaa0319 (Appendix F4.3) has revealed a low percentage of identity (lower than 60%). When compared to Kiaa0319-like, the Kiaa0319 paralog, the homology percentage remains rather low with the exception of the anti-Kiaa0319 70 antibody (82.0%). Despite the low sequence identity, the similarity of sequences reaches over 50% in all peptides compared, always being higher when aligning to the Kiaa0319-like sequence (Figure 7.21).

To test the efficiency of the commercially available anti-KIAA0319 antibody (Abcam), the above described procedure has been applied. Two different developmental stages have been compared in order to control for the possible low expression of the protein at a specific stage. There are no visible bands around the expected 105kDa / 115kDa size in neither of the samples (Figure 3.9). At 24hpf, one of the samples has not worked, which is seen by the missing band of β actin control. The rest of the samples worked well with the control anti-actin antibody but failed to produce a band at expected size for Kiaa0319 protein.

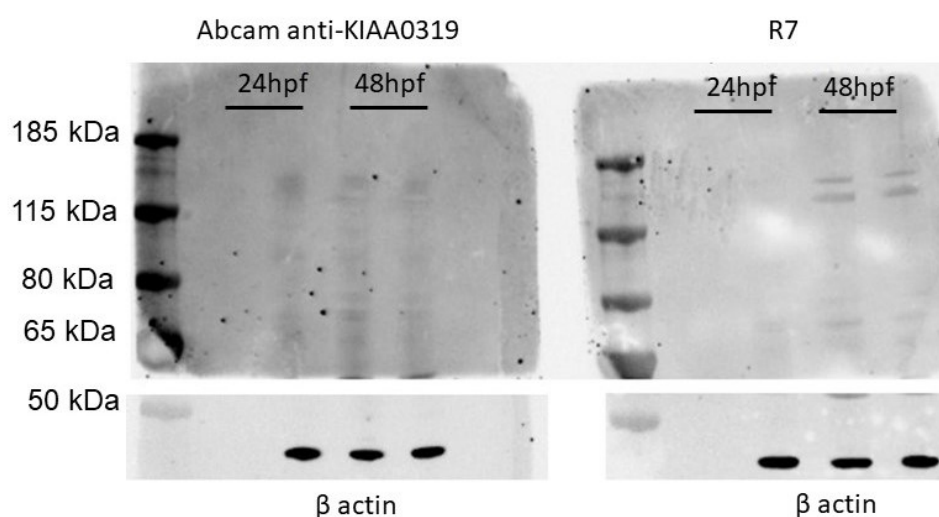


Figure 3.9 Comparison of commercial vs custom made anti-KIAA0319 antibody at 24hpf and 48hpf zebrafish

The commercially available anti-KIAA0319 (Abcam) has failed to produce any bands at any of the developmental stages (left). The custom-made antibody anti-KIAA0319 R7 has produced unspecific bands at 48hpf. No protein was detected at 24hpf. Beta actin (42kDa) as a positive control.

3.3.2 CRISPR/Cas9 knock-out of zebrafish *kiaa0319*

To efficiently edit zebrafish genome, a CRISPR/ Cas9 system has been optimised based on the protocol from Hwang et al., 2013 [Hwang et al., 2013b]. The Cas9 mRNA was capped and polyadenylated as described in Section 3.2.1.2 and the guide RNAs transcribed as per Section 3.2.2.2.

81 CCTCCCCAAGTGGAGCCAGTGTAGGTGATGCATCAGTAGCTGGAGTCTGAGGTCGCCTGAATGTACGCGACCGCCGGAGGGTGGCTTTGAGACGGGGACAGATC
CAGTCGCGCTGCTCTCGTCGATCCAAAGCTTTTTAAAAGCACCAGCTGGGCCACTTTTTCAAGTTGATAACGGACTAGCCTATTTAACTTGCTATTTCTAGCTCTAAAAC
CGCGGATCAGAGTGGGCTTTAGT GAGTCTGATTAAGCTAGCGGTGCGAGCGGATCGAGCATGTGCGATCCTACTGACCGCGAGCTGTGCTGGACCCGTCATCTTA
CGGCATTATACGTATGATCGGCCAGATCAGCTAGATATCTATCAGCTTGTGCTACTGTTCCGAGGTCATCTGACCATTTAAATCATACCTGACCTCCATAGCAAAAGC
AAAAGCCTCGACCGAGGCTTTGATTGATCGGCACGTAAAGAGGTTCCACTTTCCAAATGAATAAAGACACTACCGGGCGATTTTTGTAGTATCGAGATTTTCGAGTAAAG
GAAGCTAAATGAGCCTATTCACGGGAACGTTTGTGAGCCGGATTAATTCAGTGTGATTTATGGTTAATGTCCGAAATGCGGAACAGGGCCGACATCTTTGATGTTG
GCAACCATGCCGAGTGTCTGAACTTGTAGAGTACGTTCCATGATGTCGGATGAAATGAGTAAATGTTGAGAAATAGCTCTCCACTCAGATTTATCGATCTGTGATG
TGGTTCCATTGACCAAGGAACTTTCGTATTAATAATACC GTTCAGGAAA

85 GTTTTTTTTTAAACAGCTTGGTTCGCTGAGACGGATGTGAGCCAGTGAAGTTGTTGCACTCCAGTTACGCTGGAGTCTGAGGCTCGTGAATGATGCGACCGCCGG
AGGGTTGCGTTGAGACGGGACAGATCCAGTCCGCTGCTCTCGTCGATCCAAGCTTTTTAAAAGCACCAGCTGGTCCACTTTTTCAAGTTGATAACGGACTAGCCT
TATTTTAACTTGCATTTCTAGCTCTAAAACAGTGCCTGGGCTTTAGT GAGTCTGATTAAGCTAGCGGTGCGAGCGGATCGAGCAGGTGTCGATCACTACTGG
ACCGGAGCTGTGCTGCGACCCGTGATCTTTACGGCATTATACGCATGATCGGTCACGATCAGCTAGATTAATCTAGTACGCTTGTGTCATAGCTGTTTCTGAGGCTCAA
TACTGACCATTTAAATCATACCTGACCTCCATAGCAGAAAGTCAAAGCCCTCCGACCGGAGGCTTTGACTTGATCGGACGTAAGAGGTTCCAACTTTCAACATAATGAA
ATAAGTCACTACC GGGCGTATTTTGTGAGTTATCGAGATTTTCAGGAGCTAAAGGAAAGCTATATATGAGCCATATTC AACGAAAACGCTCTGCTTGAAGCCGTGATTA
ATTCCAACATGGATGTTGATTTATATGGGTATAACATGGGCTCTGCGATAATGTCGTGAAATCAGGCGCGACAATCTATCGATTGTAACGGGAAGCCCGATGCGCTAAG
TTGTTTCTGTATACTCGAAAAGGTAGCGCTGCCATGATGTCATCCG

89 GCGTCTCAACCCCTTTGGAGTGTGATTGAGCCAGTACGCTGATGCTGAGGTCGCTCTGATGATACGCGACCGCCGGAGGGTGC GTTGAGACGGGCGACAGATCCAGT
CGCGCTGCTCTCGTCGATCCAAAGCTTTTTAAAAGCACCAGCTCGGTGCCACTTTTTCAAGTTGATAACGGACTACCTATTTTAACTTGTCTATTCTAGCTCTAAAAC
CGCGGATCAGAGTGGGCTTTAGGAGTCTGATTAAGCTAGCGGTGCGAGCGGATCGAGCATGTGCGATCCTACTGACCGCGAGCTGTGCTGCGACCCGTCATCTTACGGATTA
TACGTATGTCGGCCAGATCAGCTAGATATCTATCAGTTGATGTTCTACTGTCCTGAGGCTCATCTGACCATTTAATCTACTGACTCCTACAGAAATCAAAGCTCCGA
CCGGAGGTTGAGTGTATCGGACGAAGAGGTTCCACTTTCCATATGAATAAGATACTACCGGGCGATTTTGATTATCGAGATTTCAAGGACTAAGC

Figure 3.10 gRNA oligo duplex sequencing results

Partial sequences of pDR274 vector obtained by using the standard primer M13 Fwd sequencing. Three different gRNAs were created and checked: 81, 85 and 89. The plasmids were then transcribed and the mRNAs co-injected with the Cas9 mRNA. The enzyme then recognised the gRNAs and introduced a double stranded break in the zebrafish gDNA.

Once co-injected into 200 zebrafish embryos per construct, the embryos were left to develop up to 3 months. At this time, they have fully developed their tail fin, which made it easier to clip. The genomic DNA was then extracted from the clipped tail fins and a PCR reaction run to check for indel mutations.

For the samples injected with constructs 81 and 89, the majority of PCR products returned the expected band size (Figure 3.11). In some cases (Figure 3.11 81: A, H, M, P; 89: G, H, J, K, L, M, N, O, U), no PCR product was obtained (Figure 3.11). Furthermore, the PCR products were digested with appropriate restriction enzyme

(Appendix 7.6.1) and ran next to the PCR products (lower case letters Figure 3.11). All the restriction reactions returned two bands, indicating the genome editing was unsuccessful. In the case of the introduced mutation, the restriction site would be deleted, and the reaction would return a single band of the same size as the PCR reaction.

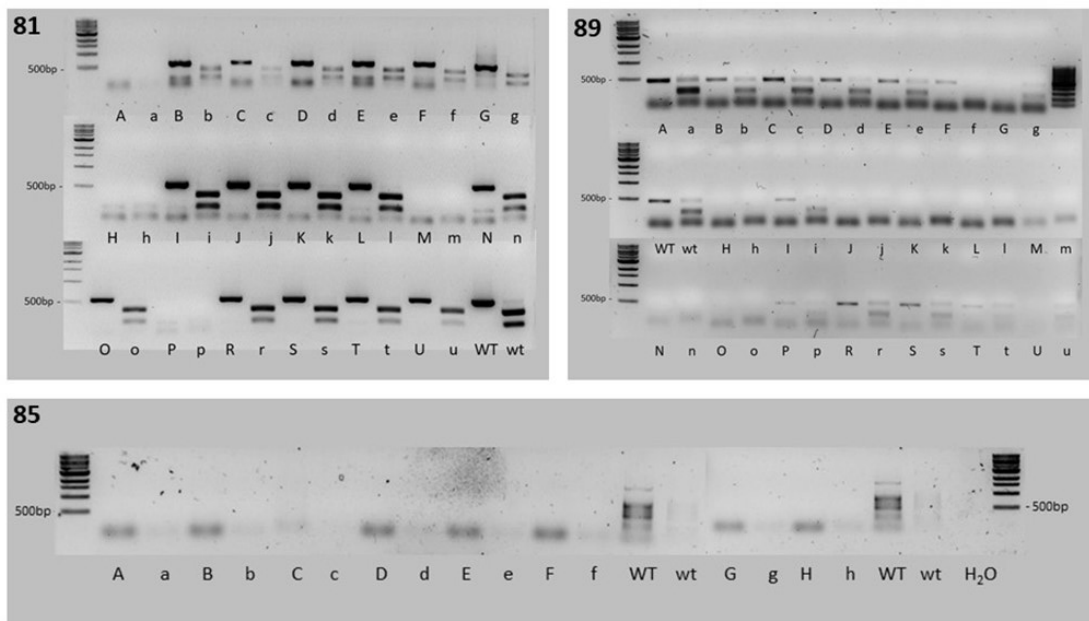


Figure 3.11 Genotyping results for CRISPR/Cas9 genome editing

The expected size of PCR product for construct 81 is 555bp, for 85 is 566bp and for 89 it is 461bp. **Sample 81)** The PCR reaction was successful in all cases except A, H, M, P. The restriction reaction returned two fragments, indicating there are no indel mutations in the screened fish. **Sample 85)** The PCR reaction was unsuccessful despite previous optimisation. The WT sample consists of more than 1 lane, indicating the unspecific binding of primers. None of the samples were successfully multiplied in the PCR reaction. **Sample 89)** The PCR reaction returned several positive and several negative results Sample sizes are as expected. The restriction reactions returned 2 bands, indicating no indel mutations in the screened fish. Capitalised letters indicate PCR product, lower case letters indicate restrictions of the PCR products.

3.4 Concluding remarks

Following the mapping of *kiaa0319* expression during early development (Chapter 2), I decided to test for the functional activity of *kiaa0319* in zebrafish. To test for *kiaa0319* function, I used a knock down (KD) morpholino and a knock out (KO) CRISPR/Cas9 techniques. Morpholinos (MOs) are synthetic oligonucleotides complementary to target sequence. In order to affect the formation of the protein, we have had MOs designed to target the ATG translational site of *kiaa0319*. Two different MOs (TB1 and TB2) target the ATG site, preventing the translation of the protein. Additional MO, targeting splice junction of *kiaa0319*, has been designed (SJ MO). The MOs have been provided at 1mM concentration and diluted to several working concentrations (50 μ M, 100 μ M, 250 μ M, 500 μ M, 750 μ M). Following the injection of working concentrations, the optimal concentration has been chosen at 750 μ M for SJ MO and 100 μ M for TB MO. Upon counting and image analysis, no phenotype has been determined at working concentration. A small number of embryos exhibited a phenotype (Figure 3.6), which could possibly be related to *kiaa0319* KD (tail curvature, hydrocephalus, pericardial oedema). Further analysis of WT embryos, however, has shown the same number of embryos with the same phenotype, discarding the significance of observed physiological changes of *kiaa0319* KD embryos. The lack of *kiaa0319* KD phenotype could be assigned to several factors. Knocking down the *kiaa0319* could potentially activate another gene, taking over the function of *kiaa0319*. The function of the KIAA0319 protein has been studied in human cell lines and in rodent models, however it has not been fully elucidated yet. The first functional characterization was conducted in rats and suggested a role in neuronal migration [Paracchini et al., 2006a] while more recent studies in mouse indicated the involvement in biological processes beyond brain development [Franquinho et al., 2017; Guidi et al., 2017]. Recent findings by Guidi *et al* suggest *kiaa0319* involvement in auditory processing [Guidi et al., 2017]. The lack of phenotype in developing brain of KD zebrafish and *kiaa0319* spatial distribution (See Chapter 2) support the idea of *kiaa0319* function in processes, different to neuronal migration.

Alongside the KD study, I conducted a genome editing CRISPR/Cas9 KO study, aiming to introduce a stop codon mutation into zebrafish *kiaa0319*. The three guide RNAs (gRNAs) have been designed in order to knock out the *kiaa0319*, following the protocol described in section 3.2.1. The co-injection of gRNA 81, 85 and 89 with the Cas9 enzyme was expected to change the amino acid sequence in the restriction enzyme cleavage site. A whole genome DNA has been extracted from the tail fin clippings of 3-month old zebrafish. The PCR reaction was followed by the restriction digest of the fragment in order to test for introduced mutations. The fragments returned two bands, indicating no mutation has been introduced. Failure of introducing the indel mutation to zebrafish genome could be attributed to the inappropriate concentration of injected RNA molecules. The suggested working concentration to obtain the highest mean frequency of mutations is 12.5ng/ μ l of gRNA and 300ng/ μ l of Cas-9 encoding RNA [Hwang et al., 2013b]. In order to determine the optimum concentration of the Cas9 and gRNA, a series of various concentrations should be injected into WT embryos and genotyped. The right concentration would then be injected in large scale and successful embryos left to grow to sexual maturity. Once they would be ready, pairing with WT zebrafish would return a F1 embryos. These embryos would be screened for introduced mutations. The positive specimen would then be crossed with each other, creating a knock out line. Once all the F2 (or further generations) zebrafish would carry a mutation, close observations would be made in early developmental stages. *In situ* hybridisation protocol would reveal the distribution of *kiaa0319* and any other genes of interest. I have chosen not to proceed with this protocol due to time restrictions.

4 Human regulatory sequence characterisation in zebrafish using Gateway Tol2 Protocol

4.1 Abstract

The Gateway Tol2 system uses a stable reporter gene transgenesis in zebrafish to test for functions of cis-regulatory sequences [Ishibashi et al., 2013]. For the purpose of this study, two different regulatory regions spanning genetic associations with neurodevelopmental traits were tested using the Gateway Tol2 system. The aim of this chapter was to test for the function of the human regulatory sequences using zebrafish as a model organism.

The promoter region of the human *KIAA0319* gene containing the rs9461045 variant was previously characterised by Dennis et al. [Dennis et al., 2009]. The minor allele, which was associated with dyslexia, is linked to lower expression of *KIAA0319* [Dennis et al., 2009; Paracchini et al., 2006a]. The adjusted minimal promoter sequence was cloned into the Gateway destination vector adjacent to the mCherry reporter cassette. The transposone was successfully integrated into the genome, however, no promoter activity was detected during the first 5 days of zebrafish development.

The promoter sequence containing rs11855145 SNP is located in the intron of the *PCSK6* gene [Brandler et al., 2013a; Scerri et al., 2011a; Shore et al., 2016]. The rs11855145 variant is associated with the better performance of the right hand in dyslexic population and also shown to affect the activity of the promoter. I cloned and screened the *PCSK6* promoter region in the same manner as the *KIAA0319* promoter. No mCherry expression could be observed during the first 5 days post injection.

4.2 Methods

Many vectors have been created for the Tol2 Gateway technology, enabling the expression of any foreign gene in zebrafish embryos [Kwan et al., 2007; Villefranc et al., 2015; Fisher et al., 2006b]. The Gateway technology enables the recombination of multiple inserts (entry clones) into a destination vector, a reaction called multisite recombination [Walhout et al., 2000; Cheo et al., 2004]. The inserts are generally divided to the 5' entry vector, the middle vector and the 3' vector. The 5' vectors usually consist of a promoter sequence, followed by the middle vector carrying a reporter cassette. The 3' entry vectors entail a polyadenylation signal or a 3' tag (fusion protein or an EGFP marker) [Kwan et al., 2007]. Each of the inserts is flanked by the required "att" recombination sequence. The att sequence recognises its analogue on the other insert and recombines with it, creating a single fragment consisting of several sequences. To successfully generate a clone that will integrate into the zebrafish genome, a destination vector containing the Tol2 transposone backbone needs to be included in the multisite recombination. Destination vector can carry additional reporter cassettes driven under minimal promoters for easier screening when integrated in the genome [Kwan et al., 2007].

4.2.1 The human KIAA0319 promoter

4.2.1.1 Analysis of KIAA0319 promoter sequence

The *KIAA0319* minimal promoter region as described in Dennis et al (2009) was adjusted using primer pair 516/517 (Appendix C1). The genomic DNA (gDNA) was extracted from human neural stem cells (gibco N7800100). The 1128bp fragment was obtained in the Touchdown PCR reaction as follows:

Phusion® GC Buffer	[50mM]	10 µl
dNTPs	[10µM]	1 µl
Fwd 516 Primer	[10µM]	2.5 µl
Rev 517 Primer	[10µM]	2.5 µl
Human gDNA	[65ng/µl]	3 µl
Phusion® High-Fidelity		
DNA Polymerase	[2,000 units/ml]	0.5 µl
H ₂ O		30.5 µl
Total Volume		50 µl

The reaction was run in the G-STORM thermocycler (Labtech international) under the following conditions:

Touchdown	72°C → 70°C	} 10 cycles
Denaturation	98°C 30s	
Annealing	70°C 30s	} 20 cycles
Elongation	72°C 50 s	

The reaction was run on a 1% agarose gel and the PCR fragment was purified using QIAquick Gel Extraction Kit as per manufacturers' guidelines. The purified DNA fragment was then cloned into pCR8-Blunt II-TOPO and transformed into One Shot® TOP10 Chemically Competent E. coli cells. The cloning mix with cells was incubated on ice for 30 min and heat shocked at 42°C for 30s. A 250µl of S.O.C. medium was added and incubated at 37°C with shaking for 1 hour. The pre-culture was then put on a selective plate and incubated overnight at 37°C. The next day, a single colony was inoculated into liquid LB broth containing 100µg/ml spectomycin antibiotic and incubated overnight at 37°C with shaking. Bacterial culture was then harvested, and plasmids isolated using QIAprep® Spin Miniprep Kit according to manufacturer's instructions.

4.2.1.2 Gateway cloning procedure

The Gateway Tol2 cloning enables precise and easy cloning of sequences due to the specially engineered recombination sites (att sites) flanking the region of interest. For the multisite recombination described in this chapter, attL and attR sites are required (for sequences see Appendix 7.5). The att sites recombine with the help of LR Clonase® II Plus enzyme and create a destination vector containing the chosen sequences of interest.

The entry vector p5E-MCS with special recombination sites attL4 and attR1 (For plasmid map see Appendix 7.5.5.2) was opened with a SmaI digestion (Figure 4.2 B):

DNA p5E-MCS	[340ng/µl]	14.7 µl
Restriction Enzyme Buffer	[10X]	3 µl
SmaI		4 µl
H ₂ O		11.3 µl

The restriction reaction was incubated for 2 hours at 37°C and dephosphorylated by adding 5µl of Shrimp Alkaline Phosphatase rSAP. Additional incubation at 37°C for 30–60 minutes prevented re-ligation of the linearised backbone. The reaction was heat-inactivated at 65°C for 5 min.

The *KIAA0319* promoter was excised from pCR8-Blunt II-TOPO (Figure 4.2 A) using restriction reaction with EcoRI as specified by the manufacturer (NEB) protocol. The 1146bp product was run on a 1% agarose gel and purified using QIAquick Gel Extraction Kit (QIAGEN). Gel purification was followed by blunting of the fragment with Quick Blunting™ Kit according to the manufacturer's protocol (QIAGEN). The blunt *KIAA0319* product was ligated into p5E-MCS overnight at 16°C using T4 DNA ligase (NEB). The following day, the reaction was transformed into DH5α competent cells.

The transformed cells were spread carefully on a pre-warmed kanamycin plate and incubated at 37°C overnight. Overnight colonies were selected for plasmid isolation using QIAprep® Spin Miniprep Kit according the standard protocol (QIAGEN). The resulting plasmids contain a PCR product flanked by the L4 and R1 att recombination sites (Figure 4.1 A, B).

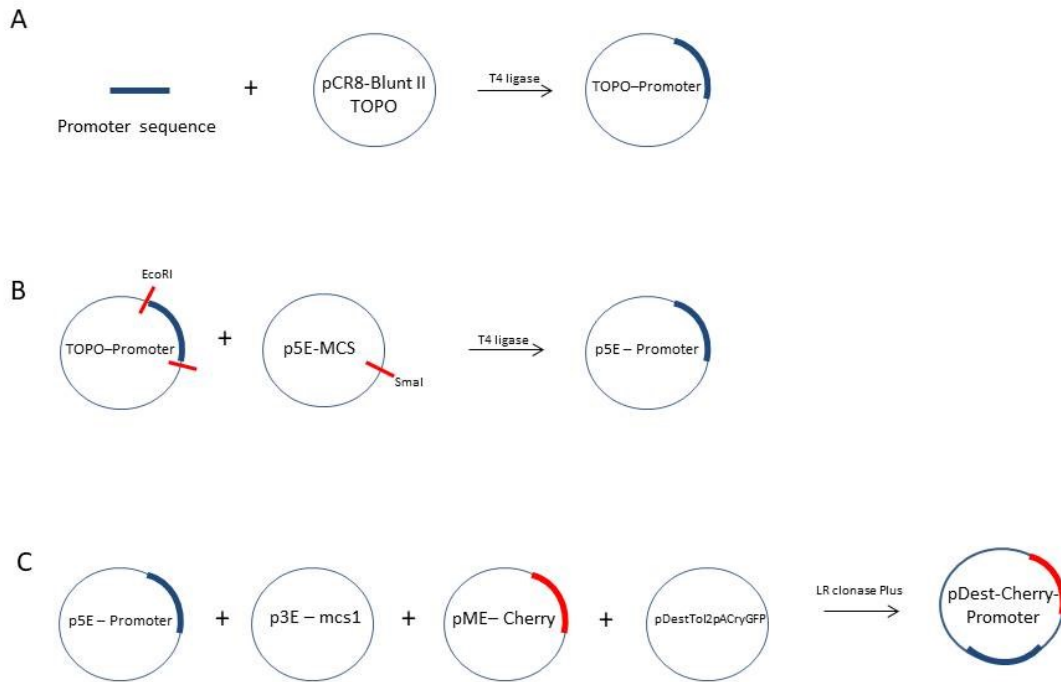


Figure 4.1 Gateway Multisite Recombination

A) The Human promoter (blue line) was cloned into pCR8 Blunt II TOPO vector using T4 DNA ligase. **B)** The TOPO vector was digested by EcoRI to excise the promoter. P5E MCS vector was opened with SmaI. Using T4 DNA ligase, the promoter was cloned into the p5E MCS, creating an Entry vector. **C)** The Entry vector was added to p3E-mcs1, pME-Cherry and pDestTol2pACryGFP vectors and recombined using LR clonase Plus enzyme. Red bars represent restriction sites. Red line represents mCherry reporter cassette. Blue line represents the promoter sequence.

In order to clone the mCherry reporter cassette next to the promoter region, a multisite recombination reaction (Figure 4.1 C) was set using an empty linker plasmid (p3E-mcs1), mCherry – containing plasmid (pME-Cherry) and *KIAA0319* promoter – containing plasmid (p5E-MCS-*KIAA0319*). Equimolar concentrations (150ng/μl) of p5E-MCS-*KIAA0319*, p3E-mcs1, pME-Cherry (Appendix 7.5.5.1) and pDestTol2pACryGFP (attR3/attR4) were used in a multisite Gateway recombination reaction to create pDest-Cherry-*KIAA0319* destination vector (Figure 4.1 C) as follows:

p3E-mcs1	[124 ng/μl]	1.2 μl
p5E-MCS-kiaa0319	[209 ng/μl]	0.7 μl
pME-cherry	[99 ng/μl]	1.5 μl
pDestTol2pACryGFP	[350 ng/μl]	0.4 μl
TE buffer		4.2 μl
TOTAL		8 μl

The mix was incubated at 25°C overnight with 2μl of LR Clonase® II Plus enzyme. The reaction was terminated with the addition of 1μl Proteinase K followed by brief vortexing and collection by short centrifugation. The solution was then incubated for 10 minutes at 37°C and transformed into One Shot® Mach1™ T1 Phage-Resistant Chemically Competent E. coli cells before overnight incubation on 100μg/ml ampicillin plates. The cells were inoculated into liquid LB broth and incubated overnight at 37°C with shaking (225 rpm). The bacterial culture was harvested and plasmids isolated using QIAprep® Spin Miniprep Kit. The resulting plasmids were digested with NotI to screen for positive colonies. Selected positive plasmids were then sequenced by the DNA Sequencing and Fragment Analysis Facility at the Medical Research Council Protein Phosphorylation and Ubiquitylation Unit (MRC PPU) services at the University of Dundee.

As a positive control, a human (Appendix 7.5.2) and zebrafish (Appendix 7.5.3) ubiquitous promoters were used in the same recombination reaction as described above. An p5E-MCS vector containing no regulatory sequences was cloned to control for phenotypes induced by the microinjection process (Appendix 7.5.4).

4.2.2 *PCSK6*

The Gateway Tol2 system was adapted to analyse a predicted 1.8kb intronic promoter. Recent data [Shore et al., 2016] showed that this promoter region regulates a novel *PCSK6* shorter isoform and potentially long non-coding RNA (lncRNA) in the opposite direction. To test for its activity throughout development, we have cloned the putative bidirectional promoter in to WT zebrafish using the Gateway Tol2 system.

4.2.2.1 *Analysis of PCSK6 intronic promoter sequence*

Human genomic DNA was obtained from a saliva sample of patients homozygous for the rs11855415 SNP (A/A). DNA was used as a template for a PCR reaction to produce a final 1.8kb fragment containing the intronic promoter (Figure 4.3). The PCR reaction was set as follows:

Phusion® GC Buffer	[50mM]	10
dNTPs	[10µM]	1
Fwd 281 Primer	[10µM]	2.5
Rev 275 Primer	[10µM]	2.5
Human gDNA	[65ng/µl]	3
Phusion® High-Fidelity		
DNA Polymerase	[2,000 units/ml]	0.5
H ₂ O		30.5
Total Volume		50 µl

The reaction was run in the G-STORM thermocycler (Labtech international) under the following conditions:

Denaturation	98°C	30s,	}	30 cycles
Annealing	58°C	20s		
Elongation	72°C	2min		

4.2.2.2 Gateway cloning procedure

The PCR product was firstly cloned into pCR8-GW-TOPO in order to obtain a stable stock for further experiments (For all vectors see Appendix Table 7.5). The empty p5E-MCS vector was opened and phosphorylated as described in section 4.2.1.2. The *PCSK6* PCR fragment was then cut from the pCR8-GW-TOPO vector using *PsiI*. The linear p5E-MCS and the PCR product were run on a 1% agarose gel and purified using QIAquick Gel Extraction Kit. Purified fragments were then ligated using T4 DNA ligase and transformed into DH5 α cells as described above. To select for constructs with correctly inserted PCR product, an *XbaI* restriction reaction was set as per manufacturers' protocol (NEB), followed by sequencing of positive p5E-MCS-*PCSK6* plasmids.

Multisite Gateway recombination using pME-Cherry, p5E-MCS-*PCSK6* and pMinTolR4R2 (*attR4att/R2*) led to a destination vector (Appendices 7.5.5.9 - 7.5.5.11), containing a PCR product adjacent to mCherry reporter cassette, both flanked by the zebrafish Tol2 transposone backbone. The pENTR5' *_ubi* vector (Appendix 7.5.5.12) was used as a positive control and to test for transposase efficacy. An empty p5E-MCS pMinTolR4R2 (Appendix 7.5.5.13) destination vector has been used in the multisite recombination as a negative control.

4.2.2.3 Generation of pCS-ZT2TP transposase

Zebrafish transposase plasmid (pCS-zT2TP) has been kindly provided by the Kawakami lab [Suster et al., 2011]. NotI-HF restriction enzyme was used to linearise 10µg of pCS-zT2TP for 3 hours at 37°C. To purify the reaction, the mixture was added 5x volume of PB buffer and applied to columns from QIAquick Gel Extraction Kit. The linearised DNA was then washed with 750µl of PE buffer and eluted in 30µl of water. Eluted DNA was quantified and stored at -20 °C until used for *in vitro* transcription:

T7 NTP/ARCA	[2X]	10µl
T7 Reaction Buffer	[10X]	2µl
linear template DNA	[9µg]	6µl
T7 Enzyme Mix		2µl

All the components were mixed together and incubated for 2h at 37°C. TURBO DNase (1µl) was added to terminate the capping *in vitro* transcription reaction and incubated 15 min at 37°C. Poly(A) tailing reaction was set in order to produce a more stable RNA molecule:

mMESSAGE mMACHINE® T7 Ultra reaction		20µl
Nuclease-free Water		36µl
E-PAP Buffer	[5X]	20µl
MnCl ₂	[25mM]	10µl
ATP Solution	[10µM]	10µl

E-PAP enzyme (4µl) was added to the reaction, reaching the final volume of 100 µl, and incubated at 37°C for 45 min. The reaction was immediately put on ice.

Resulting CAP-RNA-PolyA mix was transferred onto QIAGEN RNeasy Mini kit columns and centrifuged for 15s at 8000G. RNA was washed with 350µl of RW1buffer was added to individual tubes and centrifuged for 15s. DNase I was added to the membrane and left for 15 min at room temperature to degrade any residual DNA molecules. The RW1 wash buffer was added and spun down for 15s, followed by 500µl of wash buffer RPE. After 15s centrifugation, the flow through was discarded and additional 500µl buffer RPE were added to the spin column. The tubes were then centrifuged for 2 min to efficiently wash the RNA. The RNeasy column was placed in a new 2 ml collection tube and spun for 1 min. 30µl of Rnase-free water was added to the membrane and centrifuged 1min. Eluted RNA was quantified, aliquoted and stored at -80 °C.

4.2.2.4 Microinjection of zebrafish embryos

Destination vectors and transposase enzyme were diluted to 150ng/µl for both DNA and mRNA. Equimolar concentration of DNA and mRNA were then mixed together and put on dry ice. A control injection mix without transposase mRNA (DNA:H₂O) was prepared as a negative control to test for transposase activity.

The microinjection needle was calibrated to inject 1–2nl of DNA:RNA injection mix. This procedure was repeated for every new injection mix. Zebrafish embryos were kindly provided by Dr Carl Tucker (Queen's Medical Research Institute at the University of Edinburgh). The embryos were collected fresh from the MEP (mass egg production) system and injected at 1-4 cell developmental stage. Roughly, 100 injected eggs per construct were transferred to individual petri dish in a medium containing methylene blue at 28°C (50 embryos per dish). All dead and unfertilised embryos were removed and discarded. The removal of dead embryos was repeated on day 1 post-injection.

4.2.2.5 Analysis of expression patterns: Immunohistochemistry

Post injection embryos (20 embryos per stage) at 1-5 days post fertilisation (dpf) were collected and fixed using 4% PFA. Fixed embryos were incubated overnight at 4°C, followed by a methanol dehydration series. Each dehydration step (25% methanol, 50% methanol, 75% methanol, 100% methanol) was performed at room temperature for 5 min with shaking. At this point, embryos were stored at -20°C until further use.

On the day of immunohistochemistry, embryos were rehydrated by reverse methanol series (100% - 25% methanol) and finally incubated for 5 minutes in PBT at room temperature with shaking. To permeabilise the chorions we incubated embryos in 10ug/ml Proteinase K (PK) at room temperature. The duration of the permeabilisation is dependent on the developmental stage (see Table 4.1). We post fixed the embryos in 4% PFA for 20 minutes at room temperature and washed three times for five minutes with PBT. To prevent unspecific binding of the primary antibody, we incubated the embryos in blocking solution for 3 hours at room temperature with shaking. The primary mCherry Rat Monoclonal Antibody (Life Technologies). was diluted (1/1000) with the same blocking solution, applied to embryos and incubated at 4°C overnight with shaking.

The following day, the primary antibody was removed by washing briefly 3 times for 5 minutes, followed by 4x30 minute washes in PBT at room temperature with shaking. Secondary Alexa Fluor® 594 AffiniPure Donkey Anti-Rat IgG (H+L) was diluted 1000x in the blocking solution and applied overnight at 4°C with shaking in the dark.

On the last day of the immunohistochemistry, embryos were washed briefly 3 times for 5 minutes, followed by 4 washes of 30 minutes in PBT at room temperature with shaking. We performed glycerol series (25%, 50%, 75%) and incubated the embryos in 75% glycerol until mounting.

Table 4.1 Duration of Proteinase K treatment relative to zebrafish developmental stage

Developmental stage	PK treatment
>12 hpf	2 min
12 hpf	5 min
24 hpf	8 min
36 hpf	12 min
48hpf	15 min
72 hpf	20 min
96 hpf	22 min
120 hpf	25 min

Bright field and fluorescence images were taken on Leica MZ16F and MZFLIII under 5x magnification. The images were obtained with Leica DFC 450C and DFC300 FX camera system and processed in Leica Application Software X (LAS X).

4.3 Results

4.3.1.1 Analysis of KIAA0319 and control Gateway destination vectors

Four different constructs were built using the multisite Gateway recombination procedure. The control vectors p5E-MCS_pDestTol2pACryGFP (Figure 4.2 B), zUBI-promoter pDestTol2pACryGFP (Figure 4.2 C) and hUC-promoter pDestTol2pACryGFP (Figure 4.2 D) were generated through a one-step multisite recombination procedure. The sample vector *kiaa03919*-promoter pDestTol2pACryGFP (Figure 4.2 A) was produced as described in section 4.2.1. The vector backbone pDestTol2pACryGFP includes an additional reporter cassette coding for the green fluorescent protein (GFP) which is driven by the *cry* promoter. This promoter is specific for the zebrafish lens and drives the expression of the GFP from early stages of the lens development. The EGFP expression is a secondary control for successful integration of injected constructs. When designing the pDestTol2pACryGFP destination vectors, I checked for potential formation of out-of-frame shifts which could affect the promoter activity. The addition of the KIAA0319 promoter did not cause any rearrangements in the mCherry cassette and was successfully cloned into the destination vector. This procedure was repeated for all the constructs used for injections.

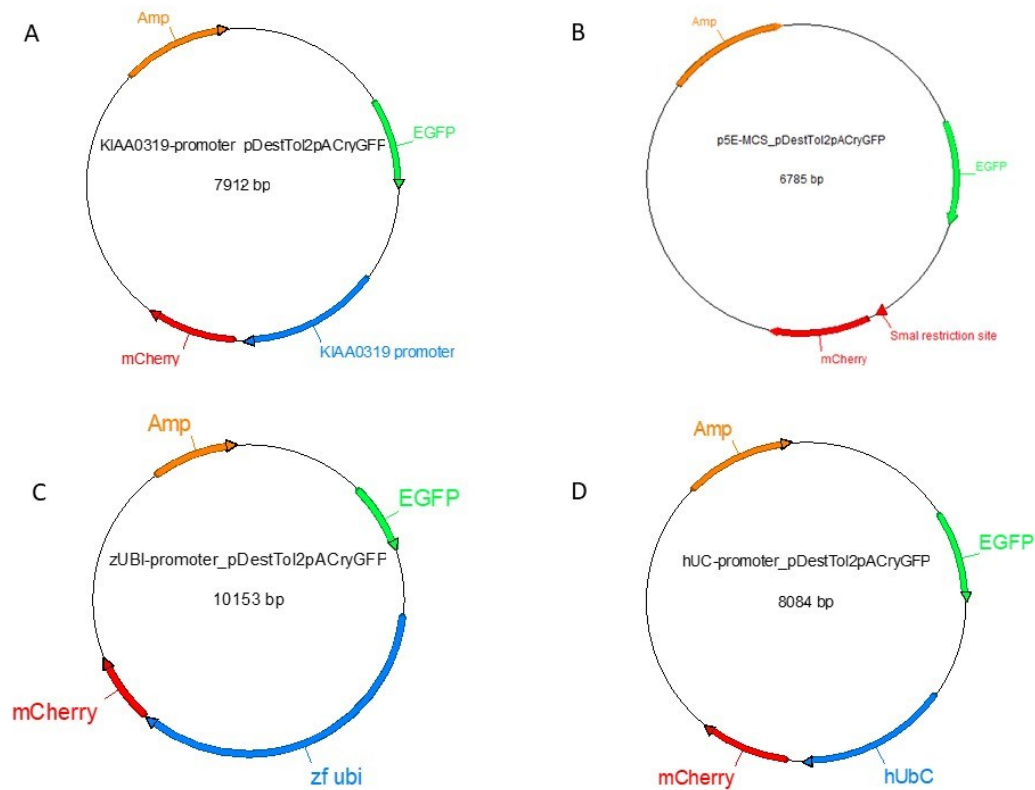


Figure 4.2 KIAA0319 and control Gateway destination vectors

A) *kiaa03919*-promoter pDestTol2pACryGFP destination vector. The 7912bp vector contains Amp resistance and an EGFP and mCherry cassettes. The EGFP expression is driven by the Cry promoter. The mCherry expression is driven by the human *kiaa0319* promoter. **B)** An empty p5E-MCS pDestTol2pACryGFP destination vector. The 76785bp vector contains Amp resistance and an EGFP and mCherry cassettes. The EGFP is driven by the Cry promoter. There are no additional promoters. The SmaI restriction site is indicated with an arrowhead. **C)** Zebrafish ubiquitous promoter in destination vector. The zebrafish zUBI-promoter pDestTol2pACryGFP is a 10153bp vector contains Amp resistance and an EGFP and mCherry cassettes. The EGFP is driven by the Cry promoter. The mCherry is driven by the zebrafish ubiquitin promoter. **D)** Human ubiquitin C promoter in destination vector. The human hUC-promoter pDestTol2pACryGFP vector is a 8084bp vector contains Amp resistance and an EGFP and mCherry cassettes. The EGFP is driven by the Cry promoter. The mCherry is driven by the human ubiquitinC promoter.

A reverse transcription PCR was used to test for the efficient integration of above mentioned constructs. The embryos have been collected at 4dpf and whole RNA extracted as described in section 2.2.2.1. The RNA was then transcribed into cDNA and a PCR ran using primers 524/525 (Appendix 7.1.6). These primers amplify the successfully integrated mCherry sequence in zebrafish genome. The resulting 187bp PCR product was run on a 1% agarose gel (Figure 4.3).

The embryos injected with the empty negative control vector (Figure 4.2 B) exhibit low mCherry transcription (Figure 4.3 MCS). Similar observation was made when injecting the embryos without the transposase (Figure 4.3 DNA only). Additionally, a low level of positive control (Figure 4.2 C) was also observed (Figure 4.3 zfUBI). Only a single zebrafish injected with zUBI-promoter pDestTol2pACryGFP survived this experiment. The highest level of mCherry cDNA was observed when the embryos were injected with constructs carrying the human ubiquitous (hUC-promoter pDestTol2pACryGFP) and *KIAA0319* promoters (*kiaa03919*-promoter pDestTol2pACryGFP) (Figure 4.3 huUBI and *KIAA0319* promoter). Non-injected WT embryos served to control for the accuracy of the experiment. A non-template control (Figure 4.3 H₂O) served as a negative control for the PCR reaction.

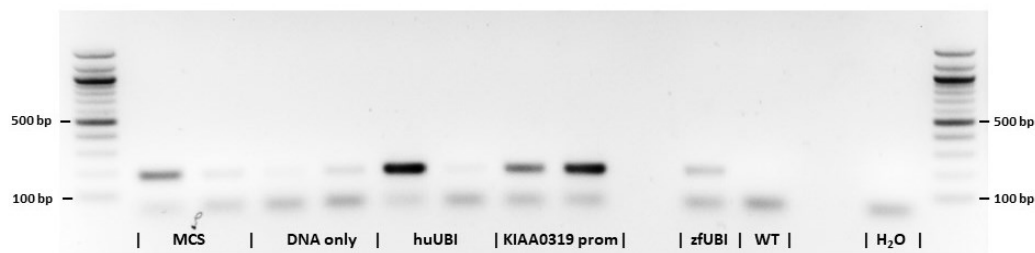


Figure 4.3 A reverse transcription PCR of 4dpf zebrafish embryos injected with different Tol2 constructs.

A 187 bp cDNA fragment confirming the presence or absence of mCherry construct in the zebrafish genome. A strong expression is observed in huUBI and KIAA0319prom samples. No bands are observed for H₂O and WT. The MCS and DNAonly negative controls exhibit low concentration of cDNA. A faint band is seen in zfUBI sample. Injected constructs: MCS = p5E-MCS pDestTol2pACryGFP vector; DNA only = a control p5E-MCS pDestTol2pACryGFP plasmid without transposase; huUBI = positive control human (hUC-promoter pDestTol2pACryGFP); KIAA0319 promoter = *kiaa03919*-promoter pDestTol2pACryGFP; zfUBI = positive control zebrafish (zUBI-promoter pDestTol2pACryGFP); WT = Un-injected WT negative control; H₂O = non-template PCR control. Marker for 100bp (NEB)

4.3.1.2 Imaging of zebrafish embryos

The injected embryos were imaged at 1dpf and at 4dpf (Figure 4.4). The imaging parameters were fixed, ensuring the same conditions of imaging for all embryos. The images were obtained using bright field (BF), TexasRed filter to detect mCherry and GFP filter to detect EGFP signal.

At 1dpf no EGFP or mCherry signal could be detected in any of the specimen. The dead embryos were discarded, and the embryo medium replaced with the fresh one. The embryos were then put back to incubation at 28.5°C and left to develop until 4 days post fertilisation. At 4dpf, the embryos were screened firstly under the GFP filter in order to select the embryos with integrated Tol2 constructs. The successful integration was determined by an EGFP signal in the zebrafish lens. As the EGFP is driven by the *cry* promoter on the vector backbone, only the integrated copies will drive the expression in the lens. In order to detect the mCherry, the filter on the microscope was set to TexasRed. Upon detailed observation at the 5x magnification, no mCherry signal was observed in any of the embryos injected with the constructs in the pDestTol2pACryGFP backbone (Figure 4.4).

To address the problem of no mCherry expression, the same sequences were cloned into the construct with pminTol-R4-R2 backbone as described in Section 4.2.2.2. No mCherry was detected, with the exception of the positive control, a zebrafish ubiquitous promoter driving the mCherry cassette on the pminTol-R4-R2 transposone backbone (Figure 4.4 zfUBI pminTol-R4-R2).

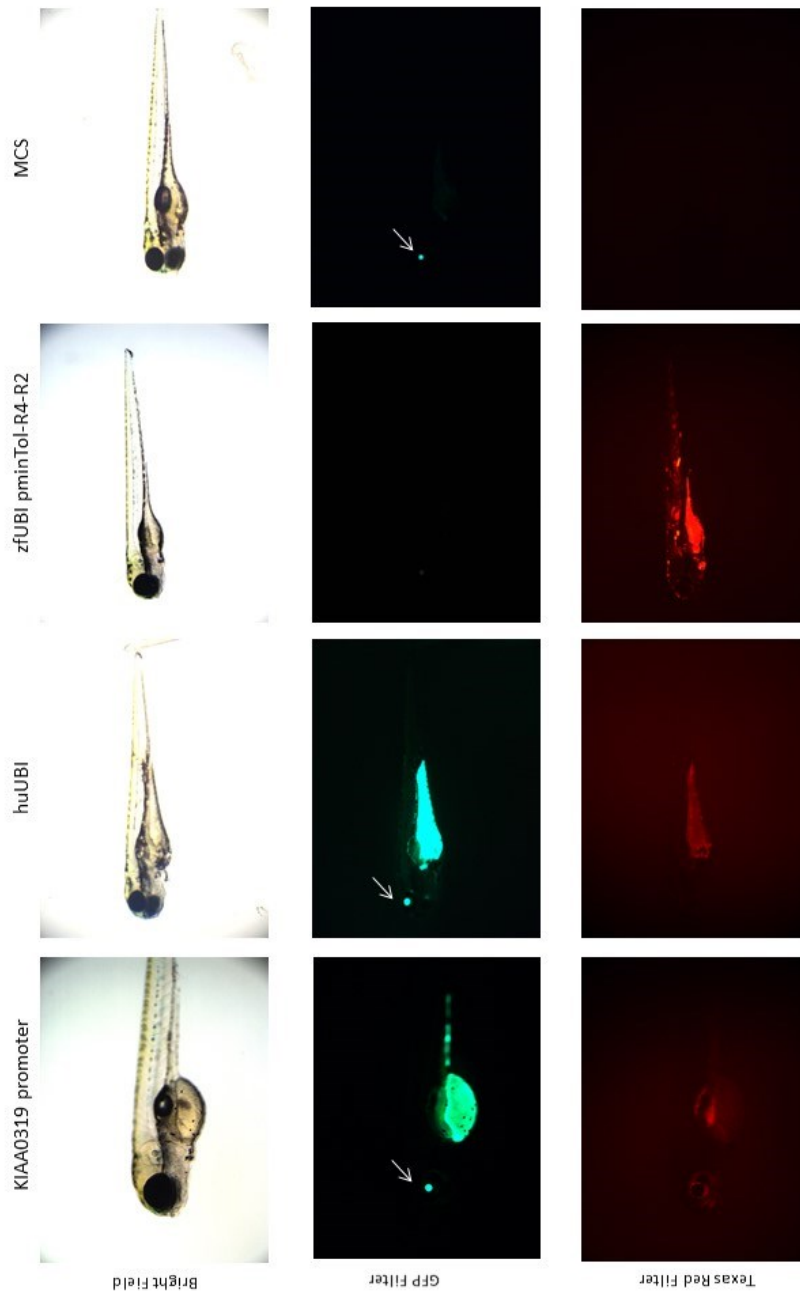


Figure 4.4 Bright field and fluorescence images of 4dpf zebrafish embryos injected with different pDestTol2pACryGFP Destination vectors

The sample (KIAA0319 promoter) construct was successfully integrated but no mCherry expression driven by the KIAA0319 promoter can be seen. The human ubiquitous promoter (huUBI) serves as a positive control for human sequences but drives no mCherry expression. The zebrafish ubiquitous promoter (zfUBI) in a pminTol-R4-R2 vector drives a mosaic mCherry expression at 4dpf. The negative control (MCS) drives no mCherry expression. Red signal corresponds to mCherry fluorescence detected under TexasRed Filter on Leica microscope. Green signal corresponds to EGFP fluorescence. Integration of the vector is confirmed with GFP positive lens (white arrows).

4.3.1.3 Analysis of handedness-associated PCSK6 locus

To test the *PCSK6* intronic regulatory sequence found to be associated with handedness, a series of destination vectors was generated, using a pMinTolR4R2 (Appendices 7.5.5.11– 7.5.5.13) vector as a backbone. The positive control destination vector (Figure 4.5 B) was injected into 1-4 cell stages of zebrafish embryonic development which presented with mosaic mCherry expression in F₀ embryos. The same procedure was repeated for the *PCSK6* promoter using the pminTol2R4-R2 (Figure 4.5 A) and p5E-MCS pMinTolR4R2 (Figure 4.5 C).

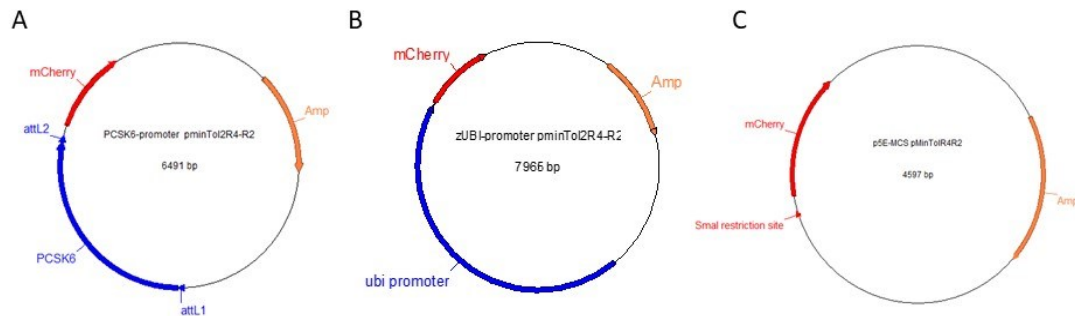


Figure 4.5 Gateway destination vectors used in *PCSK6* analysis

A) *PCSK6* promoter pminTol2R4-R2 vector. The 6491bp destination vector contains Amp resistance (orange) and a mCherry cassette (red) driven by the human *PCSK6* promoter (blue). It contains att/L1 and attL2 recombination sites. **B)** A zebrafish ubiquitous promoter in pminTol2R4-R2 destination vector. The zebrafish zUBI-promoter pminTol2R4-R2 is a 7965bp vector containing Amp resistance (orange) and a mCherry cassette (red). The mCherry is driven by the zebrafish ubiquitin promoter (blue). **C)** An empty p5E-MCS pMinTolR4R2 destination vector. The 4597bp vector contains Amp resistance (orange) and mCherry cassette (red). There are no promoters. Small restriction site is indicated with an arrowhead (red).

The *PCSK6* promoter-pminTol2R4-R2 integrated successfully as indicated by the RT PCR (Figure 4.6), however, following the image analysis, the level of mCherry expression was below detection at 2dpf or 5dpf (Figure 4.7 *PCSK6* promoter).

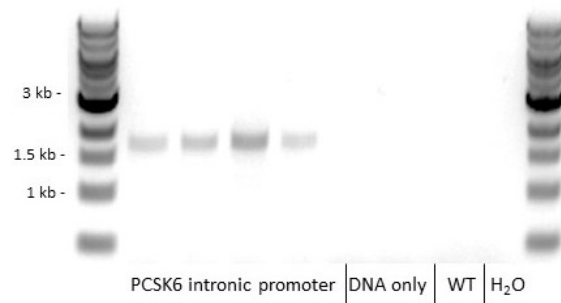


Figure 4.6 Agarose gel image of RT PCR products for PCSK6 and the controls

The RT PCR was performed using primers 275/281 in order to screen for successful integration of PCSK6 intronic promoter in zebrafish genome. A 1.8kb promoter region was integrated in the genome. When injection only with DNA (no transposase), the PCSK6 transcript could not be detected. There is no PCSK6 in the WT embryos. No template (H₂O) control is clean.

The injected embryos were imaged at 2dpf and 5dpf. The zUBI-promoter pminTol2R4-R2 drives a mosaic mCherry expression at 2dpf (Figure 4.7 A Positive control – UBI promoter), which was persisting up to 5dpf (Figure 4.7 B A Positive control – UBI promoter). When injected with the negative control, an empty p5E-MCS pMinTolR4R2 without added transposase (Figure 4.7 Negative control – DNA only), no mCherry expression could be detected using the same settings as for the positive control.



Figure 4.7 Bright field and fluorescence images of Zebrafish injected with different pminTol-R4-R2 Destination vectors

A) 2dpf zebrafish embryos injected with positive control (zebrafish ubiquitous promoter), negative control (DNA only) and test sequence (PCSK6 promoter). The mCherry expression is visible only in the positive control. **B)** 5dpf embryos injected with the same constructs as A. The mCherry signal can be observed in the positive control. Red signal in negative control and *PCSK6* promoter corresponds to mCherry autofluorescence detected under TexasRed Filter on Leica microscope.

4.3.2 Concluding remarks

In this chapter I describe the application of a complex protocol for testing the spatial and temporal effects on gene expression of human regulatory sequences in zebrafish embryos. The *KIAA0319* promoter sequence was chosen based on previous published work in which Dennis *et al.* identified single nucleotide polymorphisms (SNPs) associated with reading-related traits [Dennis *et al.*, 2009]. Paracchini *et al.* (2006) identified a reduction in *KIAA0319* expression influenced by risk haplotype for dyslexia on the chromosome 6p22.2. The reduction of *Kiaa0319* by shRNA led to impaired neuronal migration in rat cerebral neurocortex [Paracchini *et al.*, 2006a]. The SNP rs9461045 was identified close to *KIAA0319* transcription start site and shown to have an effect on binding of transcription factors. Additionally, Dennis *et al.* characterized a minimal promoter sequence, which I have altered for the purpose of this study [Dennis *et al.*, 2009] (see Figure 4.1).

Once the method was established, I applied it to the *PCSK6* locus, to study a regulatory region associated with handedness, as described by Shore *et al.* (2016). Firstly, I aimed to test for the activity of the human regulatory regions in zebrafish. If successful, the same protocol would then be used for testing the effects of above-mentioned variants on the activity of regulatory regions.

In order to control for the optimal effect of transposition, I have injected a mix of the positive control plasmid (zUBI-promoter pminTol2R4-R2) and the transposase mRNA in various concentrations. Through the imaging and the percentage of survival, I have acquired the optimal concentration of injected mixture. At the equimolar concentration of 150 ng/ μ l, the zebrafish embryos exhibit a clear mCherry signal and their survival rate remained over 80%. Approximately 100 embryos have been injected with the same construct. No mCherry signal was detected by any of these two regulatory sequences when inserted in the pDestTol2pACryGFP backbone. Despite the lack of mCherry expression, I could observe a clear EGFP signal in the zebrafish retina (Figure 4.4). The following RT PCR (Figure 4.3) confirmed the presence of the promoter sequence cDNA in all of the injected embryos. When using the pMinTolR4R2 backbone, the positive and

negative controls worked as expected (Figure 4.6). The vectors including *KIAA0319* or *PCSK6* regulatory region have been integrated in the genome (Figure 4.3) but did not drive any mCherry expression.

The results could be explained in different ways: 1) we have missed the time of *KIAA0319* and *PCSK6* Tol2 promoter activity (resulting in the lack of mCherry expression); 2) the promoters are active in single cells, which could be detected under the higher magnification and using a better imaging system. 3) The failure to detect the mCherry expression driven by the human regulatory sequences could also be due to zebrafish transcription machinery inability to recognise this particular sequence. This could be due to the conservation of the sequences, but as shown in the Section 1.3.2.3, the Tol2 protocol may work also for sequences with low conservation.

Based on the preliminary data obtained in Chapter 2, the highest expected activity of *KIAA0319* promoter sequence would be in the first 5 hours post fertilisation. Time constrains made it impossible to obtain data for the first 5 hpf, possibly missing the peak activity of the promoter. In addition to above mentioned reasons, the inability of the *KIAA0319* promoter sequence to drive mCherry expression could also be due to its design. The designed promoter sequence is not causing any out of frame rearrangements, however there might be certain zebrafish transcriptional factors that are not able to bind to the human promoter sequence.

Additional work on human promoter sequences is required. In order to say with confidence whether human *KIAA0319* promoter sequence drives a time and tissue specific expression in zebrafish, I would need to clone the exact sequence, as used in the previous study by Dennis et al. The promoter would then be tested for its activity during early zebrafish embryogenesis. Once characterised, I would design a new construct, containing the entire regulatory sequence, including the rs9461045. Furthermore, I would perform a point mutagenesis in order to change the rs9461045 variant. This would enable me to test for the effect of rs9461045 minor allele on *KIAA0319* activity in zebrafish neurodevelopment.

5 Discussion

The *KIAA0319* is a strong dyslexia candidate gene. It was shown to be highly expressed in human, mouse and rat brain [Paracchini et al., 2006a]. Independent association studies support *KIAA0319* role in dyslexia phenotype with the associated genetic variants residing mostly within the *KIAA0319* promoter region. [Luciano et al., 2007; Harold et al., 2006; Paracchini et al., 2008; Dennis et al., 2009; Cope et al., 2005; Paracchini et al., 2006a; Francks et al., 2004; Couto et al., 2010; Pinel et al., 2012]. In this thesis I have mapped zebrafish *kiaa0319* expression pattern throughout embryonic development using *in situ* hybridisation. Due to the sequence homology and its involvement in dyslexia [Couto et al., 2008], I have decided to map the expression of *kiaa0319-like* (*kiaa0319l*) in parallel. Additionally, I have attempted to generate *kiaa0319* knock out (CRISPR/Cas9) and knock down (morpholino) lines, to study *kiaa0319* function. As for most of genetic associations with complex traits, the *KIAA0319* variants associated with dyslexia reside in noncoding region. Cellular studies have shown that these variants affect gene expression regulation [Shore et al., 2016; Dennis et al., 2009]. Similarly, the genetic variants at the *PCSK6* locus have shown to affect the efficiency of an intronic promoter. I used the Tol2 Gateway system to test for spatio-temporal function of mentioned human promoters.

In this project I have aimed to 1) characterise zebrafish *kiaa0319* expression throughout development, 2) identify the function of *kiaa0319* throughout embryonic development and 3) test for temperospatial activity of human regulatory sequences using zebrafish as a model organism.

5.1 *Kiaa0319* and *Kiaa0319*-like expression pattern throughout zebrafish development

To date, there are no *kiaa0319* studies conducted in zebrafish. I have conducted the first ever study mapping zebrafish *kiaa0319* expression throughout early developmental stages. In Chapter 2, I have performed *in situ* hybridisation (ISH), using 3 different techniques: Whole mount ISH (WISH), Fluorescence ISH (FISH) and a novel technique: RNAScope. My results indicate the highest expression of *kiaa0319* (Figure 2.7) and *kiaa0319l* (Figure 2.19) in the first 5 hours post fertilisation (hpf). In the later embryonic development and especially at around 30 hpf, a strong and consistent signal is limited to the sensory organs (eyes, otic vesicle), brain and notochord (Figure 2.9 B and C). The notochord is a chordate embryonic midline structure leading to the development of vertebrae in zebrafish [Stemple, 2005]. It is a transient structure, which is also evident in the RNAScope *kiaa0319* expression data. The *kiaa0319* gene is expressed in the notochord of 2 and 3 days old zebrafish embryos but becomes less abundant the older the embryo becomes (Section 2.3.5). The 3D modelling of *kiaa0319*-labelled zebrafish indicates a strong expression in the notochord, more specifically in the notochord sheath at 72hpf (3 days). This expression almost completely disappears by day 5 post fertilisation (Figure 2.15). The pattern of *kiaa0319* expression is in line with the maturation of the notochord, where approximately 70% of notochord cells migrate outward to form the sheath epithelium [Dale and Topczewski, 2011; Yamamoto et al., 2010]. The residual signal is very scarce, consistent with the hypothesised transition of notochord into the vertebrae.

Interestingly, when comparing *kiaa0319* expression profile to the homologous dyslexia candidate gene *kiaa0319-like* (*kiaa0319l*), the levels of the *kiaa0319l* expression in the notochord are very low (Figure 2.20). The human data (Figure 1.2) and the data shown in this thesis (Figure 2.19) indicate *kiaa0319l* expression levels are much higher than *kiaa0319* (Figure 2.7). However, when testing for *kiaa0319l* expression with a more sensitive technique, such as qPCR, I have been

able to detect the expression in the eyes, with the expression levels pattern similar to the one of the *kiaa0319*. This finding indicates the *kiaa0319* and *kiaa0319l* could have a specific role in the development of the sensory organs, however, only the *kiaa0319* is involved in the notochord biology.

The strong expression of *kiaa0319* in the zebrafish brain and a subset of cells in the spinal cord opens a question of the cell identity. I have used a transgenic line tg(gfap:GFP; Oligo2:dsRed) with GFP labelled oligodendroglia cells and DsRed labelled motor neurons and oligodendrocytes to see whether the *kiaa0319* and GFP/DsRed signals in the cells overlap. Confocal imaging indicated that *kiaa0319*-positive cells are in fact not oligodendroglia, motor neurons or oligodendrocytes. Due to the large amount of data implicating *kiaa0319* in neuronal migration, it would be of importance to identify the *kiaa0319*-positive cells. This information would help us expand the understanding of the *kiaa0319* role, may it be involved in the neuronal migration or not.

5.2 *Kiaa0319* function in zebrafish development

To test for *Kiaa0319* function throughout zebrafish development, I have conducted a knockdown (morpholino, MO) and a knockout (CRISPR/Cas9) studies. The optimal concentration for the MO knockdown was confirmed through the qPCR reaction, comparing transcript levels of WT fish to the ones injected with various concentrations of splice junction (SJ) MOs (Figure 3.4). Analysis of ~100 MO injected zebrafish embryos returned no significant phenotype (Figure 3.7). The translational blocking (TB) MO knockdown remained unconfirmed. The characterisation of the protein levels was not possible due to the lack of appropriate antibodies. However, no phenotype was detected when injected with translational blocking TB1 or TB2 MOs (Figure 3.5).

Furthermore, the KO CRISPR/Cas9 study failed to produce a *kiaa0319* mutant zebrafish. The genotyping revealed no indel mutations in the ~200 embryos injected

with the gRNA plasmid and Cas9 mRNA (Figure 3.10). The fish were screened by fin clip genotyping, followed by a PCR and a diagnostic digest reaction. In the presence of the mutation, the restriction site in PCR fragment would be destroyed and the fragment would not be digested. However, all the digested PCR fragments returned a double strand indicating no successful mutation was introduced in the designed sites. Further knock out design, testing for a variety of conditions such as titrating the concentration of the mRNAs, would be necessary in order to say with confidence that CRISPR/Cas9 returned no successful knockout.

Taken together, while I cannot completely rule out technical artefacts leading to possible experimental failure, the MO results are in line with the latest research by Martinez-Garay and Guidi [Guidi et al., 2017; Martinez-Garay et al., 2017]. *Kiaa0319* knock out mice exhibit no phenotype in gross morphology and no impaired neuronal migration [Martinez-Garay et al., 2017]. Additionally, when *kiaa0319* and *kiaa0319l* are simultaneously knocked out, no phenotype was observed, however, novel behavioural changes in sensory processing have been displayed [Guidi et al., 2017]. These data are in line with the magnocellular theory of dyslexia, which suggests dyslexia is a result of the visual and auditory system impairment (reviewed in Section 1.1.1)

To check for behavioural changes in *kiaa0319* knock down and knock out zebrafish, we have established a collaboration with Dr Caroline Brennan at the Queen Mary University London, who studies learning and attention in the various zebrafish lines by the means of automated assays [Parker et al., 2012b, 2013b, 2012a, 2013a]. The Brennan lab is planning to conduct behavioural analyses on the knock down and knock out zebrafish with the emphasis on the sensory perception.

5.3 Testing for human regulatory sequences using zebrafish as a model organism

Dyslexia is a complex trait involving multiple genetic factors (reviewed in Section 1.2). An increasing amount of association studies revealed variations associated directly with dyslexia or dyslexia-related traits (reading, phonological awareness, phoneme recognition, etc). The *KIAA0319* minimal promoter sequence has so far been characterised using a cell culture model [Dennis et al., 2009]. To test for the human *KIAA0319* promoter region spatiotemporal function in zebrafish, I have cloned the minimal promoter region as characterised by Dennis et al (2009) in the Tol2 Gateway system. The Tol2 is a transposone system with random integration into the zebrafish genome through the assistance of the transposase enzyme [Kawakami et al., 2000]. The advantage of this system provides the integration of any regulatory sequence in the zebrafish genome, independent of the sequence conservation [Korzh, 2011]. The *KIAA0319* promoter was cloned upstream to the mCherry reporter cassette, aiming to activate mCherry expression when the promoter is active. I have designed a positive control containing zebrafish ubiquitous promoter, a human ubiquitin C promoter and a negative control containing no regulatory sequence. The zebrafish positive control manifested in mosaic mCherry expression, confirming the efficient cloning design. Finally, a *KIAA0319* promoter region was cloned upstream mCherry, however no mCherry signal was observed in the first 5 days post fertilisation.

In addition to the *KIAA0319* promoter, I have tested also for the recently characterised bidirectional promoter in the *PCSK6* intronic region [Shore et al., 2016]. The *PCSK6* has been associated with handedness in dyslexic population [Scerri et al., 2011a; Brandler et al., 2013b]. Furthermore, Shore *et al* (2016) characterised the variant rs11855145 within the intronic promoter region, which has been shown to alter the binding site for nuclear factor(s) [Shore et al., 2016]. In this thesis, I have taken the bidirectional promoter as characterised by Shore et al (2016)

and cloned it into the Tol2 Gateway system. As with the *KIAA0319* human promoter, no mCherry signal was observed in the first 5 days post fertilisation.

There could be several possible explanations to why mCherry signal was not present in the *KIAA0319* and *PCSK6* containing embryos:

1) The timing of detection was misaligned with the promoter activity. Considering the *kiaa0319* expression data from Chapter 2, the highest expression is observed within the first 5 hours post fertilisation (Figure 2.7) and in adult brain (Figure 2.5). However, when detecting for promoter activity, the first analysis was conducted at 24hpf and onward. This could well be the reason I have missed the peak of expression and would have to be looking into the specialised cells (notochord) to be able to detect mCherry signal. As the *PCSK6* is involved in the *Nodal* pathway and setting up the early embryonic asymmetry, the promoter would be expected to be active in the early time points of zebrafish development. The zebrafish laterality organ, the Kupffer's vesicle, develops around 12 hours post fertilisation [Essner et al., 2005]. As the Kupffer's vesicle is a transient structure, I might have missed the distribution of mCherry at 24hpf and later stages. However, the tested region is an intornic promoter and we cannot predict it to have the same function as the main promoter sequence.

2) The mCherry expression could not be detected due to the imaging settings I have been using. The integration of mCherry into the zebrafish genome has been confirmed through reverse transcription PCR at day 4 post fertilisation (Figure 4.5), which could not have been seen if there was only the residual plasmid of the unincorporated transposone. I can conclude the *KIAA0319* and *PCSK6* promoters' activity cannot be detected at an organism-wide level and advise for further, more detailed analysis.

3) The activity of the promoters could be regulated by distal regulatory sequences, which would work in tandem. Some promoters require the presence of cis or trans elements to function, such as enhancers. This, however, is not possible when the promoter sequence is cloned in isolation into the foreign genome.

5.4 Summary

I have conducted the first ever study of *kiaa0319* expression and function in zebrafish during early embryonic development. My data indicate *kiaa0319* is expressed ubiquitously in the first 5 hours post fertilisation and later becomes restricted to the eyes, otic vesicle and notochord. Assuming there were no technical issues, no obvious changes in zebrafish phenotype were pinpointed when *kiaa0319* function is knocked down. In parallel, I have tested for *kiaa0319l* expression, an additional dyslexia candidate gene with high homology to the *kiaa0319*. The expression is similar to the one of the *kiaa0319*, however no *kiaa0319l* was detected the notochord. This indicates *kiaa0319* has a specific role in early development of sensory organs and body axis formation (notochord) but is not necessary for the function of these structures. The localisation of *kiaa0319* to the sensory organs and the lack of phenotype in the knock down is in line with the magnocellular theory of dyslexia. This is the first time the zebrafish has been used to study these specific dyslexia genes. My data suggest that further work is required to test for potential *kiaa0319* involvement in sensory processing. More generally, I have demonstrated how zebrafish is a valid model organism to address important questions of gene expression distribution, its function and the function of noncoding sequences throughout time and tissue. My work suggest that zebrafish has the potential to advance the field on neurogenetics by providing a range of protocols to study both genes and genetic associations with neurodevelopmental disorders to overcome challenges presented by other more widely used models (i.d. cell lines and rodents) in this field.

6 References

- Adler WT, Platt MP, Mehlhorn AJ, Haight JL, Currier T a, Etchegaray M a, Galaburda AM, Rosen GD. 2013. Position of neocortical neurons transfected at different gestational ages with shRNA targeted against candidate dyslexia susceptibility genes. *PLoS One* 8: e65179.
- Amores A, Force A, Yan YL, Joly L, Amemiya C, Fritz A, Ho RK, Langeland J, Prince V, Wang YL, Westerfield M, Ekker M, Postlethwait JH. 1998. Zebrafish hox clusters and vertebrate genome evolution. *Science* 282: 1711–4.
- Amunts K, Schlaug G, Schleicher A, Steinmetz H, Dabringhaus A, Roland PE, Zilles K. 1996. Asymmetry in the Human Motor Cortex and Handedness. 222: 216–222.
- Antonellis A, Dennis MY, Burzynski G, Huynh J, Maduro V, Hodonsky CJ, Khajavi M, Szigeti K, Mukkamala S, Bessling SL, Pavan WJ, McCallion AS, Lupski JR, Green ED. 2010. A rare myelin protein zero (MPZ) variant alters enhancer activity in vitro and in vivo. *PLoS One* 5: e14346.
- Antonellis A, Huynh JL, Lee-Lin S-Q, Vinton RM, Renaud G, Loftus SK, Elliot G, Wolfsberg TG, Green ED, McCallion AS, Pavan WJ. 2008. Identification of neural crest and glial enhancers at the mouse Sox10 locus through transgenesis in zebrafish. *PLoS Genet.* 4: e1000174.
- Arning L, Ocklenburg S, Schulz S, Ness V, Gerding WM, Hengstler JG, Falkenstein M, Epplen JT, Güntürkün O, Beste C. 2013. PCSK6 VNTR Polymorphism Is Associated with Degree of Handedness but Not Direction of Handedness. *PLoS One* 8: e67251.
- Ashe HL, Briscoe J. 2006. The interpretation of morphogen gradients. *Development* 133.

- Badcock NA, Bishop DVM, Hardiman MJ, Barry JG, Watkins KE. 2012. Co-localisation of abnormal brain structure and function in specific language impairment. *Brain Lang.* 120: 310–320.
- Barth KA, Miklosi A, Watkins J, Bianco IH, Stephen W, Andrew RJ, Wilson SW, Andrew RJ. 2005. fsi Zebrafish Show Concordant Reversal of Laterality of Viscera , Neuroanatomy , and a Subset of Behavioral Responses. *Curr. Opin. Neurobiol.* 15: 844–850.
- Bates TC, Lind PA, Luciano M, Montgomery GW, Martin NG, Wright MJ. 2010. Dyslexia and DYX1C1: deficits in reading and spelling associated with a missense mutation. *Mol. Psychiatry* 15: 1190–1196.
- Becker TS, Rinkwitz S. 2012. Zebrafish as a genomics model for human neurological and polygenic disorders. *Dev. Neurobiol.* 72: 415–28.
- Bhartiya D, Maini J, Sharma M, Joshi P, Laddha S V, Jalali S, Patowary A, Purkanti R, Lalwani M, Singh AR, Chauhan R, Singh N, Bhardwaj A, Scaria V, Sivasubbu S. 2010. FishMap Zv8 update--a genomic regulatory map of zebrafish. *Zebrafish* 7: 179–80.
- Bishop DVM. 2013. Cerebral asymmetry and language development: cause, correlate or consequence? *Science.* 340.
- Blow MJ, McCulley DJ, Li Z, Zhang T, Akiyama JA, Holt A, Plajzer-Frick I, Shoukry M, Wright C, Chen F, Afzal V, Bristow J, Ren B, Black BL, Rubin EM, Visel A, Pennacchio LA. 2010. ChIP-Seq identification of weakly conserved heart enhancers. *Nat. Genet.* 42: 806–810.
- Boets B, Wouters J, van Wieringen A, De Smedt B, Ghesquière P. 2008. Modelling relations between sensory processing, speech perception, orthographic and phonological ability, and literacy achievement. *Brain Lang.* 106: 29–40.
- Bosse M-L, Tainturier MJ, Valdois S. 2007. Developmental dyslexia: The visual

- attention span deficit hypothesis. *Cognition* 104: 198–230.
- Bosse M-L, Valdois S. 2003. Patterns of developmental dyslexia according to a multi-trace memory model of reading. *Curr. Psychol. Lett.* 1.
- Brambati SM, Termine C, Ruffino M, Danna M, Lanzi G, Stella G, Cappa SF, Perani D. 2006. Neuropsychological deficits and neural dysfunction in familial dyslexia. *Brain Res.* 1113: 174–185.
- Brandler WM, Morris AP, Evans DM, Scerri TS, Kemp JP, Timpson NJ, St Pourcain B, Smith GD, Ring SM, Stein J, Monaco AP, Talcott JB, Fisher SE, Webber C, Paracchini S. 2013a. Common variants in left/right asymmetry genes and pathways are associated with relative hand skill. *PLoS Genet.* 9: e1003751.
- Brandler WM, Morris AP, Evans DM, Scerri TS, Kemp JP, Timpson NJ, St Pourcain B, Smith GD, Ring SM, Stein J, Monaco AP, Talcott JB, Fisher SE, Webber C, Paracchini S. 2013b. Common variants in left/right asymmetry genes and pathways are associated with relative hand skill. *PLoS Genet* 9: e1003751.
- Brandler WM, Paracchini S. 2013. The genetic relationship between handedness and neurodevelopmental disorders. *Trends Mol. Med.* 20: 1–8.
- Broca PM. 1861. REMARQUES SUR LE SIÈGE DE LA FACULTÉ DU LANGAGE ARTICULÉ, SUIVIES D'UNE OBSERVATION D'APHÉMIE (PERTE DE LA PAROLE). *Bicêtre Bull. la Société Anat.*: 330–357.
- Brown WE, Eliez S, Menon V, Rumsey JM, White CD, Reiss AL. 2001. Preliminary evidence of widespread morphological variations of the brain in dyslexia. *Neurology* 56: 781–3.
- Brunswick N, McCrory E, Price CJ, Frith CD, Frith U. 1999. Explicit and implicit processing of words and pseudowords by adult developmental dyslexics: A

- search for Wernicke's Wortschatz? *Brain*: 1901–17.
- Carrion-Castillo A, Franke B, Fisher SE. 2013. Molecular genetics of dyslexia: an overview. *Dyslexia* 19: 214–40.
- Centanni TM, Booker AB, Sloan AM, Chen F, Maher BJ, Carraway RS, Khodaparast N, Rennaker R, LoTurco JJ, Kilgard MP. 2014a. Knockdown of the dyslexia-associated gene *Kiaa0319* impairs temporal responses to speech stimuli in rat primary auditory cortex. *Cereb Cortex* 24: 1753–1766.
- Centanni TM, Chen F, Booker AM, Engineer CT, Sloan AM, Rennaker RL, LoTurco JJ, Kilgard MP. 2014b. Speech sound processing deficits and training-induced neural plasticity in rats with dyslexia gene knockdown. *PLoS One* 9: e98439.
- Chandrasekar G, Vesterlund L, Hultenby K, Tapia-Paez I, Kere J. 2013. The zebrafish orthologue of the dyslexia candidate gene *DYX1C1* is essential for cilia growth and function. *PLoS One* 8: e63123.
- Chang N, Sun C, Gao L, Zhu D, Xu X, Zhu X, Xiong J-W, Xi JJ. 2013. Genome editing with RNA-guided Cas9 nuclease in zebrafish embryos. *Cell Res*. 23: 465–72.
- Chatterjee S, Lufkin T. 2012. Regulatory genomics: Insights from the zebrafish. *Curr Top Genet*: 1–10.
- de Chaumont F, Dallongeville S, Chenouard N, Hervé N, Pop S, Provoost T, Meas-Yedid V, Pankajakshan P, Lecomte T, Le Montagner Y, Lagache T, Dufour A, Olivo-Marin J-C. 2012. Icy: an open bioimage informatics platform for extended reproducible research. *Nat. Methods* 9: 690–696.
- Cheo DL, Titus SA, Byrd DRN, Hartley JL, Temple GF, Brasch MA. 2004. Concerted Assembly and Cloning of Multiple DNA Segments Using In Vitro Site-Specific Recombination: Functional Analysis of Multi-Segment

- Expression Clones. *Genome Res.* 14: 2111–2120.
- Chuang H-C, Huang T-N, Hsueh Y-P. 2015. T-Brain-1 - A Potential Master Regulator in Autism Spectrum Disorders. *Autism Res.* 8: 412–426.
- Cohen L, Dehaene S. 2004. Specialization within the ventral stream: the case for the visual word form area. *Neuroimage* 22: 466–476.
- Cohen L, Dehaene S, Naccache L, Lehéricy S, Dehaene-Lambertz G, Hénaff M-A, Michel F. 2000. The visual word form area Spatial and temporal characterization of an initial stage of reading in normal subjects and posterior split-brain patients. *Brain* 123: 291–307.
- Concha ML, Burdine RD, Russell C, Schier a F, Wilson SW. 2000. A nodal signaling pathway regulates the laterality of neuroanatomical asymmetries in the zebrafish forebrain. *Neuron* 28: 399–409.
- Concha ML, Russell C, Regan JC, Tawk M, Sidi S, Gilmour DT, Kapsimali M, Sumoy L, Goldstone K, Amaya E, Kimelman D, Nicolson T, Gr??nder S, Gomperts M, Clarke JDW, Wilson SW. 2003. Local tissue interactions across the dorsal midline of the forebrain establish CNS laterality. *Neuron* 39: 423–438.
- Consortium GTe. 2013. The Genotype-Tissue Expression (GTEx) project. *Nat Genet* 45: 580–585.
- Constam DB, Robertson EJ. 1999. Regulation of bone morphogenetic protein activity by pro domains and proprotein convertases. *J. Cell Biol.* 144: 139–49.
- Cooper MS, D’Amico LA. 1996. A cluster of noninvoluting endocytic cells at the margin of the zebrafish blastoderm marks the site of embryonic shield formation. *Dev. Biol.* 180: 184–98.
- Cope N, Harold D, Hill G, Moskvina V, Stevenson J, Holmans P, Owen MJ, O’Donovan MC, Williams J. 2005. Strong evidence that KIAA0319 on

- chromosome 6p is a susceptibility gene for developmental dyslexia. *Am. J. Hum. Genet.* 76: 581–91.
- Corey DR, Abrams JM. 2001. Morpholino antisense oligonucleotides: tools for investigating vertebrate development. *Genome Biol.* 2: REVIEWS1015.
- Cornell RA, Eisen JS. 2002. Delta/Notch signaling promotes formation of zebrafish neural crest by repressing Neurogenin 1 function. *Development* 129: 2639–48.
- Couto JM, Gomez L, Wigg K, Cate-Carter T, Archibald J, Anderson B, Tannock R, Kerr EN, Lovett MW, Humphries T, Barr CL. 2008. The KIAA0319-Like (*KIAA0319L*) Gene on Chromosome 1p34 as a Candidate for Reading Disabilities. *J. Neurogenet.* 22: 295–313.
- Couto JM, Livne-Bar I, Huang K, Xu Z, Cate-Carter T, Feng Y, Wigg K, Humphries T, Tannock R, Kerr EN, Lovett MW, Bremner R, Barr CL. 2010. Association of reading disabilities with regions marked by acetylated H3 histones in KIAA0319. *Am. J. Med. Genet. Part B Neuropsychiatr. Genet.* 153: 447–462.
- D’Amico LA, Cooper MS. 1997. Spatially distinct domains of cell behavior in the zebrafish organizer region. *Biochem. Cell Biol.* 75: 563–77.
- Dahdouh F, Anthoni H, Tapia-Páez I, Peyrard-Janvid M, Schulte-Körne G, Warnke A, Remschmidt H, Ziegler A, Kere J, Müller-Myhsok B, Nöthen MM, Schumacher J, Zucchelli M. 2009. Further evidence for DYX1C1 as a susceptibility factor for dyslexia. *Psychiatr. Genet.* 19: 59–63.
- Dale RM, Topczewski J. 2011. Identification of an evolutionarily conserved regulatory element of the zebrafish *col2a1a* gene. *Dev. Biol.* 357: 518–531.
- Damasio AR, Damasio H. 1983. The anatomic basis of pure alexia. *Neurology* 33: 1573–83.
- Dassonville P, Zhu XH, Uurbil K, Kim SG, Ashe J. 1997. Functional activation in

- motor cortex reflects the direction and the degree of handedness. *Proc. Natl. Acad. Sci. U. S. A.* 94: 14015–8.
- DeFries JC, Fulker DW, LaBuda MC. 1987. Evidence for a genetic aetiology in reading disability of twins. *Lett. to Nat.* 329: 537–539.
- Dehaene S, Cohen L, Sigman M, Vinckier F. 2005. The neural code for written words: a proposal. *Trends Cogn. Sci.* 9: 335–341.
- Dejerine J. 1891. Sur un cas de cécité verbale avec agraphie, suivi d'autopsie. *C. R. Société du Biol.*: 197–201.
- Dennis MY, Paracchini S, Scerri TS, Prokunina-Olsson L, Knight JC, Wade-Martins R, Coggill P, Beck S, Green ED, Monaco AP. 2009. A common variant associated with dyslexia reduces expression of the KIAA0319 gene. *PLoS Genet.* 5: e1000436.
- Draper BW, Morcos PA, Kimmel CB. 2001. Inhibition of zebrafish *fgf8* pre-mRNA splicing with morpholino oligos: A quantifiable method for gene knockdown. *Genesis* 30: 154–156.
- Dubois J, Hertz-Pannier L, Cachia A, Mangin JF, Le Bihan D, Dehaene-Lambertz G. 2009. Structural Asymmetries in the Infant Language and Sensori-Motor Networks. *Cereb. Cortex* 19: 414–423.
- Echelard Y, Epstein DJ, St-Jacques B, Shen L, Mohler J, McMahon JA, McMahon AP. 1993. Sonic hedgehog, a member of a family of putative signaling molecules, is implicated in the regulation of CNS polarity. *Cell* 75: 1417–30.
- Eisen JS, Smith JC. 2008. Controlling morpholino experiments: don't stop making antisense. *Development* 135: 1735–1743.
- Ekker M, Wegner J, Akimenko MA, Westerfield M. 1992. Coordinate embryonic expression of three zebrafish engrailed genes. *Development* 116: 1001–10.

- Ekker SC, Larson JD, Gene MP, Strategies T, Effectiveness MOT, Controls E. 2001. Morphant technology in model developmental systems. *Genesis* 30: 89–93.
- Eliez S, Rumsey JM, Giedd JN, Schmitt JE, Patwardhan AJ, Reiss AL. 2000. Morphological alteration of temporal lobe gray matter in dyslexia: an MRI study. *J. Child Psychol. Psychiatry.* 41: 637–44.
- Essner JJ, Amack JD, Nyholm MK, Harris EB, Yost HJ. 2005. Kupffer’s vesicle is a ciliated organ of asymmetry in the zebrafish embryo that initiates left-right development of the brain, heart and gut. *Development* 132: 1247–60.
- Ethell IM, Pasquale EB. 2005. Molecular mechanisms of dendritic spine development and remodeling. *Prog. Neurobiol.* 75: 161–205.
- Farley EK, Olson KM, Zhang W, Rokhsar DS, Levine MS. 2016. Syntax compensates for poor binding sites to encode tissue specificity of developmental enhancers. *Proc. Natl. Acad. Sci. U. S. A.* 113: 6508–13.
- Filipek P. 1996. Structural variations in measures in the developmental disorders. In: R. Thatcher, G. Lyon, J. Rumsey, & N. Krasnegor (Eds.). *Developmental neuroimaging: Mapping the development of brain and behavior.* San Diego, CA: Academic Press., p 169–186.
- Finn ES, Shen X, Holahan JM, Scheinost D, Lacadie C, Papademetris X, Shaywitz SE, Shaywitz B a, Constable RT. 2014. Disruption of functional networks in dyslexia: a whole-brain, data-driven analysis of connectivity. *Biol. Psychiatry* 76: 397–404.
- Fisher S, Grice E a, Vinton RM, Bessling SL, McCallion AS. 2006a. Conservation of RET regulatory function from human to zebrafish without sequence similarity. *Science* 312: 276–9.
- Fisher S, Grice E a, Vinton RM, Bessling SL, Urasaki A, Kawakami K, McCallion

- AS. 2006b. Evaluating the biological relevance of putative enhancers using Tol2 transposon-mediated transgenesis in zebrafish. *Nat. Protoc.* 1: 1297–305.
- Fisher SE, Francks C, Marlow AJ, MacPhie IL, Newbury DF, Cardon LR, Ishikawa-Brush Y, Richardson AJ, Talcott JB, Gayán J, Olson RK, Pennington BF, Smith SD, DeFries JC, Stein JF, Monaco AP. 2002. Independent genome-wide scans identify a chromosome 18 quantitative-trait locus influencing dyslexia. *Nat. Genet.* 30: 86–91.
- Fletcher JM, Loveland K. 1986. Neuropsychology of arithmetic disabilities in children. *Focus Learn. Probl. Math.* 8: 23–40.
- Fletcher JM, Shaywitz SE, Shankweiler DP, Katz L, Liberman IY, Stuebing KK, Francis DJ, Fowler AE, Shaywitz BA. 1994. Cognitive profiles of reading disability: Comparisons of discrepancy and low achievement definitions. *J. Educ. Psychol.* 1: 6–23.
- Francks C, Fisher SE, MacPhie IL, Richardson AJ, Marlow AJ, Stein JF, Monaco AP. 2002. A genomewide linkage screen for relative hand skill in sibling pairs. *Am. J. Hum. Genet.* 70: 800–5.
- Francks C, Maegawa S, Laurén J, Abrahams BS, Velayos-Baeza A, Medland SE, Colella S, Groszer M, McAuley EZ, Caffrey TM, Timmusk T, Pruunsild P, Koppel I, Lind PA, Matsumoto-Itaba N, Nicod J, Xiong L, Joober R, Enard W, Krinsky B, Nanba E, Richardson AJ, Riley BP, Martin NG, Strittmatter SM, Möller H-J, Rujescu D, St Clair D, Muglia P, Roos JL, Fisher SE, Wade-Martins R, Rouleau GA, Stein JF, Karayiorgou M, Geschwind DH, Ragoussis J, Kendler KS, Airaksinen MS, Oshimura M, DeLisi LE, Monaco AP. 2007. LRRTM1 on chromosome 2p12 is a maternally suppressed gene that is associated paternally with handedness and schizophrenia. *Mol. Psychiatry* 12: 1129–39, 1057.
- Francks C, Paracchini S, Smith SD, Richardson AJ, Scerri TS, Cardon LR, Marlow

- AJ, MacPhie IL, Walter J, Pennington BF, Fisher SE, Olson RK, DeFries JC, Stein JF, Monaco AP. 2004. A 77-kilobase region of chromosome 6p22.2 is associated with dyslexia in families from the United Kingdom and from the United States. *Am. J. Hum. Genet.* 75: 1046–58.
- Franquinho F, Nogueira-Rodrigues J, Duarte JMJM, Esteves SSS, Carter-Su C, Monaco AP, Molnár Z, Velayos-Baeza A, Brites P, Sousa MMMM. 2017. The dyslexia-susceptibility protein KIAA0319 inhibits axon growth through Smad2 signaling. *Cereb Cortex* 27: In press.
- Frauenheim JG. 1978. Academic Achievement Characteristics of Adult Males Who Were Diagnosed as Dyslexic in Childhood. *J. Learn. Disabil.* 11: 476–483.
- Friedman RF, Ween JE, Albert ML. 1993. Alexia. In: K. M. Heilman & E. Valenstein (Eds.), 3e. New York: Oxford University Press., p 37~2.
- Gagnon J a., Valen E, Thyme SB, Huang P, Ahkmetova L, Pauli A, Montague TG, Zimmerman S, Richter C, Schier AF. 2014. Efficient mutagenesis by Cas9 protein-mediated oligonucleotide insertion and large-scale assessment of single-guide RNAs. *PLoS One* 9: 5–12.
- Galaburda AM, LoTurco J, Ramus F, Fitch RH, Rosen GD. 2006. From genes to behavior in developmental dyslexia. *Nat Neurosci* 9: 1213–1217.
- Galaburda AM, Sherman GF, Rosen GD, Aboitz F, Geschwind N. 1985. Developmental Dyslexia: Four consecutive patients with cortical anomaly. *Ann. Neurol.* 18: 222–223.
- Gamse JT, Shen Y-C, Thisse C, Thisse B, Raymond P a, Halpern ME, Liang JO. 2002. Otx5 regulates genes that show circadian expression in the zebrafish pineal complex. *Nat. Genet.* 30: 117–121.
- Gamse JT, Thisse C, Thisse B, Halpern ME. 2003. The parapineal mediates left-right asymmetry in the zebrafish diencephalon. *Development* 130: 1059–1068.

- Garey LJ, Ong WY, Patel TS, Kanani M, Davis A, Mortimer AM, Barnes TR, Hirsch SR. 1998. Reduced dendritic spine density on cerebral cortical pyramidal neurons in schizophrenia. *J. Neurol. Neurosurg. Psychiatry* 65: 446–53.
- Geschwind N. 1965. Disconnexion syndromes in animals and man. I. *Brain* 88: 237–94.
- Goswami U. 2015. Sensory theories of developmental dyslexia: three challenges for research. *Nat Rev Neurosci* 16: 43–54.
- Goswami U. 2014. Sensory theories of developmental dyslexia: three challenges for research. *Nat. Rev. Neurosci.* 16: 43–54.
- Grant CE, Bailey TL, Noble WS. 2011. FIMO: scanning for occurrences of a given motif. *Bioinformatics* 27: 1017–1018.
- Grati M, Chakchouk I, Ma Q, Bensaid M, Desmidt A. 2015. A missense mutation in DCDC2 causes human recessive deafness DFNB66 , likely by interfering with sensory hair cell and supporting cell cilia length regulation. 1–26.
- Gross-Thebing T, Paksa A, Raz E. 2014. Simultaneous high-resolution detection of multiple transcripts combined with localization of proteins in whole-mount embryos. *BMC Biol.* 12: 55.
- de Guibert C, Maumet C, Jannin P, Ferré J-C, Tréguier C, Barillot C, Le Rumeur E, Allaire C, Biraben A. 2011. Abnormal functional lateralization and activity of language brain areas in typical specific language impairment (developmental dysphasia). *Brain* 134: 3044–3058.
- Guidi LG, Mattley J, Martinez-Garay I, Monaco AP, Linden JF, Velayos-Baeza A, Molnár Z. 2017. Knockout Mice for Dyslexia Susceptibility Gene Homologs KIAA0319 and KIAA0319L have Unaffected Neuronal Migration but Display Abnormal Auditory Processing. *Cereb. Cortex* 27: 5831–5845.

- Guidi LG, Velayos-Baeza A, Martinez-Garay I, Monaco AP, Paracchini S, Bishop DVM, Molnár Z. 2018. The neuronal migration hypothesis of dyslexia: a critical evaluation thirty years on. *PeerJ Prepr.*: 1–49.
- Gutwinski S, Löscher A, Mahler L, Kalbitzer J, Heinz A, Bermpohl F. 2011. Understanding left-handedness. *Dtsch. Arztebl. Int.* 108: 849–53.
- Habas PA, Scott JA, Roosta A, Rajagopalan V, Kim K, Rousseau F, Barkovich AJ, Glenn OA, Studholme C. 2012. Early Folding Patterns and Asymmetries of the Normal Human Brain Detected from in Utero MRI. *Cereb. Cortex* 22: 13–25.
- Hannula-Jouppi K, Kaminen-Ahola N, Taipale M, Eklund R, Nopola-Hemmi J, Kääriäinen H, Kere J. 2005. The axon guidance receptor gene *ROBO1* is a candidate gene for developmental dyslexia. *PLoS Genet.* 1: e50.
- Harold D, Paracchini S, Scerri T, Dennis M, Cope N, Hill G, Moskvina V, Walter J, Richardson a J, Owen MJ, Stein JF, Green ED, O'Donovan MC, Williams J, Monaco a P. 2006. Further evidence that the *KIAA0319* gene confers susceptibility to developmental dyslexia. *Mol. Psychiatry* 11: 1085–91, 1061.
- Heasman J. 2002. Morpholino oligos: making sense of antisense? *Dev. Biol.* 243: 209–14.
- Heasman J, Kofron M, Wylie C. 2000. β Catenin Signaling Activity Dissected in the Early *Xenopus* Embryo: A Novel Antisense Approach. *Dev. Biol.* 222: 124–134.
- Heintzman ND, Hon GC, Hawkins RD, Kheradpour P, Stark A, Harp LF, Ye Z, Lee LK, Stuart RK, Ching CW, Ching KA, Antosiewicz-Bourget JE, Liu H, Zhang X, Green RD, Lobanenko V V., Stewart R, Thomson JA, Crawford GE, Kellis M, Ren B. 2009. Histone modifications at human enhancers reflect global cell-type-specific gene expression. *Nature* 459: 108–112.

- Heintzman ND, Stuart RK, Hon G, Fu Y, Ching CW, Hawkins RD, Barrera LO, Van Calcar S, Qu C, Ching KA, Wang W, Weng Z, Green RD, Crawford GE, Ren B. 2007. Distinct and predictive chromatin signatures of transcriptional promoters and enhancers in the human genome. *Nat. Genet.* 39: 311–318.
- Helenius P, Tarkiainen A, Cornelissen P, Hansen PC, Salmelin R. 1991. Dissociation of normal feature analysis and deficient processing of letter-strings in dyslexic adults. *Cereb. cortex* 9: 476–83.
- Hepper PG. 2013. The developmental origins of laterality: fetal handedness. *Dev. Psychobiol.* 55: 588–95.
- Hepper PG, McCartney GR, Shannon E a. 1998. Lateralised behaviour in first trimester human foetuses. *Neuropsychologia* 36: 531–4.
- Hervé P-Y, Crivello F, Perchey G, Mazoyer B, Tzourio-Mazoyer N. 2006. Handedness and cerebral anatomical asymmetries in young adult males. *Neuroimage* 29: 1066–79.
- Hildebrandt F, Benzing T, Katsanis N. 2011a. Ciliopathies. *N. Engl. J. Med.* 364: 1533–1543.
- Hildebrandt F, Benzing T, Katsanis N. 2011b. Ciliopathies. *N Engl J Med* 364: 1533–1543.
- Hoh RA, Stowe TR, Turk E, Stearns T. 2012. Transcriptional program of ciliated epithelial cells reveals new cilium and centrosome components and links to human disease. *PLoS One* 7: e52166.
- Horwitz B, Rumsey JM, Donohue BC. 1998. Functional connectivity of the angular gyrus in normal reading and dyslexia. *Proc. Natl. Acad. Sci. U. S. A.* 95: 8939–44.
- Hosen MJ, Vanakker OM, Willaert A, Huysseune A, Coucke P, De Paepe A. 2013. Zebrafish models for ectopic mineralization disorders: practical issues from

morpholino design to post-injection observations. *Front. Genet.* 4: 74.

Howe K, Clark M, Torroja C, Torrance J, Berthelot C, Muffato M, Collins JE, Humphray S, McLaren K, Matthews L, McLaren S, Sealy I, Caccamo M, Churcher C, Scott C, Barrett JC, Koch R, Al. E. 2013a. The zebrafish reference genome sequence and its relationship to the human genome. *Nature* 496: 498–503.

Howe K, Clark MMD, Torroja CCF, Torrance J, Berthelot C, Muffato M, Collins JJE, Humphray S, McLaren K, Matthews L, McLaren S, Sealy I, Caccamo M, Churcher C, Scott C, Barrett JC, Koch R, Al. E, Rauch G-J, White S, Chow W, Kilian B, Quintais LT, Guerra-Assunção J a, Zhou Y, Gu Y, Yen J, Vogel J-H, Eyre T, Redmond S, Banerjee R, Chi J, Fu B, Langley E, Maguire SF, Laird GK, Lloyd D, Kenyon E, Donaldson S, Sehra H, Almeida-King J, Loveland J, Trevanion S, Jones M, Quail M, Willey D, Hunt A, Burton J, Sims S, McLay K, Plumb B, Davis J, Clee C, Oliver K, Clark R, Riddle C, Elliot D, Elliott D, Threadgold G, Harden G, Ware D, Begum S, Mortimore B, Mortimer B, Kerry G, Heath P, Phillimore B, Tracey A, Corby N, Dunn M, Johnson C, Wood J, Clark S, Pelan S, Griffiths G, Smith M, Glithero R, Howden P, Barker N, Lloyd C, Stevens C, Harley J, Holt K, Panagiotidis G, Lovell J, Beasley H, Henderson C, Gordon D, Auger K, Wright D, Collins JJE, Raisen C, Dyer L, Leung K, Robertson L, Ambridge K, Leongamornlert D, McGuire S, et al. 2013b. The zebrafish reference genome sequence and its relationship to the human genome. *Nature* 496: 498–503.

Hulme C, Snowling MJ. 2009. *Developmental Disorders of Language Learning and Cognition*. Wiley-Blackwell. 37-89 p.

Humphreys P, Kaufmann WE, Galaburda AM. 1990. Developmental dyslexia in women: neuropathological findings in three patients. *Ann Neurol* 28: 727–738.

Hutchinson SA, Eisen JS. 2006. *Islet1 and Islet2 have equivalent abilities to*

- promote motoneuron formation and to specify motoneuron subtype identity. *Development* 133: 2137–47.
- Hwang WY, Fu Y, Reyon D, Maeder ML, Shengdar Q, Sander JD, Peterson RT, Yeh JJ, Keith J. 2013a. Efficient In Vivo Genome Editing Using RNA-Guided Nucleases. *Nat. Biotechnol.* 31: 227–229.
- Hwang WY, Fu Y, Reyon D, Maeder ML, Tsai SQ, Sander JD, Peterson RT, Yeh J-RJ, Joung JK. 2013b. Efficient genome editing in zebrafish using a CRISPR-Cas system. *Nat. Biotechnol.* 31: 227–9.
- Illingworth S, Bishop DVM. 2009. Atypical cerebral lateralisation in adults with compensated developmental dyslexia demonstrated using functional transcranial Doppler ultrasound. *Brain Lang.* 111: 61–65.
- Ishibashi M, Mechaly AS, Becker TS, Rinkwitz S. 2013. Using zebrafish transgenesis to test human genomic sequences for specific enhancer activity. *Methods* 62: 216–225.
- Ivliev AE, Hoen P a C, van Roon-Mom WMC, Peters DJM, Sergeeva MG, t Hoen PA, van Roon-Mom WMC, Peters DJM, Sergeeva MG. 2012a. Exploring the transcriptome of ciliated cells using in silico dissection of human tissues. *PLoS One* 7: e35618.
- Ivliev AE, t Hoen PA, van Roon-Mom WM, Peters DJ, Sergeeva MG. 2012b. Exploring the transcriptome of ciliated cells using in silico dissection of human tissues. *PLoS One* 7: e35618.
- J T, C W. 2002. A sensory linguistic approach to the development of normal and dysfunctional reading skills. In: Witruk E, Friederici A, and Lachmann T (Eds), *Basic Functions of Language, Reading and Reading Disability*. Boston: Kluwer, p 213–240.
- Jao L-E, Wenthe SR, Chen W. 2013. Efficient multiplex biallelic zebrafish genome

- editing using a CRISPR nuclease system. *Proc. Natl. Acad. Sci. U. S. A.* 110: 13904–9.
- Jinek M, Chylinski K, Fonfara I, Hauer M, Doudna JA, Charpentier E. 2012. A Programmable Dual-RNA-Guided DNA Endonuclease in Adaptive Bacterial Immunity. *Science* (80-.). 337: 816–821.
- K. Kawakami, Asakawa K, Muto. A, Wada H. 2016. Tol2-mediated Transgenesis, Gene Trapping, Enhancer Trapping, and the Gal4-UAS System, Third Edit. Elsevier Inc. 19-37 p.
- Kasprian G, Langs G, Brugger PC, Bittner M, Weber M, Arantes M, Prayer D. 2011. The Prenatal Origin of Hemispheric Asymmetry: An In Utero Neuroimaging Study. *Cereb. Cortex* 21: 1076–1083.
- Kawakami K, Shima a, Kawakami N. 2000. Identification of a functional transposase of the Tol2 element, an Ac-like element from the Japanese medaka fish, and its transposition in the zebrafish germ lineage. *Proc. Natl. Acad. Sci. U. S. A.* 97: 11403–8.
- Kawakami K, Takeda H, Kawakami N, Kobayashi M, Matsuda N, Mishina M. 2004. A transposon-mediated gene trap approach identifies developmentally regulated genes in zebrafish. *Dev. Cell* 7: 133–44.
- Kent WJ, Sugnet CW, Furey TS, Roskin KM, Pringle TH, Zahler AM, Haussler D. 2002. The human genome browser at UCSC. *Genome Res* 12: 996–1006.
- Kidd T, Bland KS, Goodman CS. 1999. Slit is the midline repellent for the robo receptor in *Drosophila*. *Cell* 96: 785–94.
- Kidd T, Brose K, Mitchell KJ, Fetter RD, Tessier-Lavigne M, Goodman CS, Tear G. 1998. Roundabout controls axon crossing of the CNS midline and defines a novel subfamily of evolutionarily conserved guidance receptors. *Cell* 92: 205–15.

- Kim DY. 2009. Knockdown of Kiaa0319 Reduces Dendritic Spine Density. Honor. Sch. Theses. 109.
- Kim MJ, Oksenberg N, Hoffmann TJ, Vaisse C, Ahituv N. 2013. Functional characterization of SIM1-associated enhancers. *Hum. Mol. Genet.*: 1–9.
- Kimmel CB, Ballard WW, Kimmel SR, Ullmann B, Schilling TF. 1995a. Stages of embryonic development of the zebrafish. *Dev. Dyn.* 203: 253–310.
- Kimmel CB, Ballard WW, Kimmel SR, Ullmann B, Schilling TF. 1995b. Stages of embryonic development of the zebrafish. *Dev. Dyn.* 203: 253–310.
- Kitaguchi T, Mizugishi K, Hatayama M, Aruga J, Mikoshiba K. 2002. *Xenopus* Brachyury regulates mesodermal expression of *Zic3*, a gene controlling left-right asymmetry. *Dev Growth Differ* 44: 55–61.
- Kivilevitch Z, Achiron R, Zalel Y. 2010. Fetal brain asymmetry: in utero sonographic study of normal fetuses. *Am. J. Obstet. Gynecol.* 202: 359.e1-359.e8.
- Knecht S. 2000. Handedness and hemispheric language dominance in healthy humans. *Brain* 123: 2512–2518.
- Koga A, Suzuki M, Inagaki H, Bessho Y, Hori H. 1996. Transposable element in fish. *Nature* 383: 30.
- Korzh VP. 2011. Search for tissue-specific regulatory elements using Tol2 transposon as an example of evolutionary synthesis of genomics and developmental biology. *Russ. J. Dev. Biol.* 39: 73–77.
- Kronbichler M, Hutzler F, Staffen W, Mair A, Ladurner G, Wimmer H. 2006. Evidence for a dysfunction of left posterior reading areas in German dyslexic readers. *Neuropsychologia* 44: 1822–1832.
- Kwan KM, Fujimoto E, Grabher C, Mangum BD, Hardy ME, Campbell DS, Parant

- JM, Yost HJ, Kanki JP, Chien C-B. 2007. The Tol2kit: a multisite gateway-based construction kit for Tol2 transposon transgenesis constructs. *Dev. Dyn.* 236: 3088–99.
- Lepanto P, Davison C, Casanova G, Badano JL, Zolessi FR. 2016. Characterization of primary cilia during the differentiation of retinal ganglion cells in the zebrafish. *Neural Dev.* 11: 10.
- Levecque C, Velayos-Baeza A, Holloway ZG, Monaco AP. 2009. The dyslexia-associated protein KIAA0319 interacts with adaptor protein 2 and follows the classical clathrin-mediated endocytosis pathway. *Am. J. Physiol. Cell Physiol.* 297: C160-8.
- Levin M. 2005. Left-right asymmetry in embryonic development: a comprehensive review. *Mech. Dev.* 122: 3–25.
- Li M, Zhao L, Page-Mccaw P, Chen W. 2016. Zebrafish genome engineering using the CRISPR-Cas9 system. *Trends* 32: 815–827.
- Liang JO, Etheridge a, Hantsoo L, Rubinstein a L, Nowak SJ, Izpisúa Belmonte JC, Halpern ME. 2000. Asymmetric nodal signaling in the zebrafish diencephalon positions the pineal organ. *Development* 127: 5101–5112.
- Lindamood P. 1994. Issues in researching the link between phonological awareness, learning disabilities, and spelling. In: G. R. Lyon (Ed.) *Frames of reference for the assessment of learning disabilities: New views on measurement issues.* Baltimore: Paul H. Brookes Publishing Company, p 351–373.
- Livingstone MS, Rosen GD, Drislane FW, Galaburda AM. 1991. Physiological and anatomical evidence for a magnocellular defect in developmental dyslexia. *Proc. Natl. Acad. Sci. U. S. A.* 88: 7943–7.
- Lovegrove WJ, Bowling A, Badcock D, Blackwood M. 1980. Specific reading disability: differences in contrast sensitivity as a function of spatial frequency.

Science 210: 439–40.

Luciano M, Lind PA, Duffy DL, Castles A, Wright MJ, Montgomery GW, Martin NG, Bates TC. 2007. A Haplotype Spanning KIAA0319 and TTRAP Is Associated with Normal Variation in Reading and Spelling Ability. *Biol. Psychiatry* 62: 811–817.

Ludwig KU, Mattheisen M, Mühleisen TW, Roeske D, Schmääl C, Breuer R, Schulte-Körne G, Müller-Myhsok B, Nöthen MM, Hoffmann P, Rietschel M, Cichon S. 2009. Supporting evidence for LRRTM1 imprinting effects in schizophrenia. *Mol. Psychiatry* 14: 743–745.

Marino C, Citterio A, Giorda R, Facchetti A, Menozzi G, Vanzin L, Lorusso ML, Nobile M, Molteni M. 2007. Association of short-term memory with a variant within DYX1C1 in developmental dyslexia. *Genes, Brain Behav.* 6: 640–646.

Martinez-Garay I, Guidi LG, Holloway ZG, Bailey MAG, Lyngholm D, Schneider T, Donnison T, Butt SJB, Monaco AP, Molnár Z, Velayos-Baeza A. 2017. Normal radial migration and lamination are maintained in dyslexia-susceptibility candidate gene homolog *Kiaa0319* knockout mice. *Brain Struct. Funct.* 222: 1367–1384.

Massinen S, Hokkanen M-EE, Matsson H, Tammimies K, Tapia-Paez I, Dahlstrom-Heuser V, Kuja-Panula J, Burghoorn J, Jeppsson KE, Swoboda P, Peyrard-Janvid M, Toftgard R, Castren E, Kere J, Tapia-Páez I, Dahlström-Heuser V, Kuja-Panula J, Burghoorn J, Jeppsson KE, Swoboda P, Peyrard-Janvid M, Toftgård R, Castrén E, Kere J. 2011a. Increased expression of the dyslexia candidate gene *DCDC2* affects length and signaling of primary cilia in neurons. *PLoS One* 6: e20580.

Massinen S, Hokkanen ME, Matsson H, Tammimies K, Tapia-Paez I, Dahlstrom-Heuser V, Kuja-Panula J, Burghoorn J, Jeppsson KE, Swoboda P, Peyrard-Janvid M, Toftgard R, Castren E, Kere J. 2011b. Increased expression of the

- dyslexia candidate gene DCDC2 affects length and signaling of primary cilia in neurons. *PLoS One* 6: e20580.
- Masuda T, Fukamauchi F, Takeda Y, Fujisawa H, Watanabe K, Okado N, Shiga T. 2004. Developmental regulation of notochord-derived repulsion for dorsal root ganglion axons. *Mol. Cell. Neurosci.* 25: 217–227.
- McCarthy MI, Abecasis GR, Cardon LR, Goldstein DB, Little J, Ioannidis JP a, Hirschhorn JN. 2008. Genome-wide association studies for complex traits: consensus, uncertainty and challenges. *Nat. Rev. Genet.* 9: 356–69.
- McKeever WF. 2000. A new family handedness sample with findings consistent with X-linked transmission. *Br. J. Psychol.* 91 (Pt 1): 21–39.
- McManus IC. 1991. The inheritance of left-handedness. *Ciba Found. Symp.* 162: 251-67; discussion 267-81.
- McManus IC, Davison A, Armour J a L. 2013. Multilocus genetic models of handedness closely resemble single-locus models in explaining family data and are compatible with genome-wide association studies. *Ann. N. Y. Acad. Sci.* 1288: 48–58.
- Medland SE, Duffy DL, Wright MJ, Geffen GM, Hay D a, Levy F, van-Beijsterveldt CEM, Willemsen G, Townsend GC, White V, Hewitt AW, Mackey D a, Bailey JM, Slutske WS, Nyholt DR, Treloar S a, Martin NG, Boomsma DI. 2009. Genetic influences on handedness: data from 25,732 Australian and Dutch twin families. *Neuropsychologia* 47: 330–7.
- Meng H, Smith SD, Hager K, Held M, Liu J, Olson RK, Pennington BF, DeFries JC, Gelernter J, Somlo S, Skudlarski P, Shaywitz SE, Shaywitz BA, Marchione K, Wang Y, Paramasivam M, LoTurco JJ, Page GP, Gruen JR, by Sherman Weissman CM. 2005. DCDC2 is associated with reading disability and modulates neuronal development in the brain. *PNAS Genet.* 102: 17053–17058.

- Metzakopian E, Lin W, Salmon-Divon M, Dvinge H, Andersson E, Ericson J, Perlmann T, Whitsett JA, Bertone P, Ang S-L. 2012. Genome-wide characterization of *Foxa2* targets reveals upregulation of floor plate genes and repression of ventrolateral genes in midbrain dopaminergic progenitors. *Development* 139: 2625–34.
- Miklosi A, Andrew R. J, Miklósi Á, Andrew R. J. 1999. Right eye use associated with decision to bite in zebrafish. *Behav. Brain Res.* 105: 199–205.
- Miklosi A, Andrew RJ, Savage H. 1997. Behavioural lateralisation of the tetrapod type in the zebrafish (*Brachydanio rerio*). *Physiol. Behav.* 63: 127–135.
- Moats L. 1994. Issues in researching the link between phonological awareness, learning disabilities, and spelling. In: G. R. Lyon (Ed.). *Frames of reference for the assessment of learning disabilities: New views on measurement issues*. Baltimore: Paul H. Brookes Publishing Company, p 333–349.
- Morillon B, Lehongre K, Frackowiak RSJ, Ducorps A, Kleinschmidt A, Poeppel D, Giraud A-L. 2010. Neurophysiological origin of human brain asymmetry for speech and language. *Proc. Natl. Acad. Sci. U. S. A.* 107: 18688–93.
- Morokuma J, Ueno M, Kawanishi H, Saiga H, Nishida H. 2002. *HrNodal*, the ascidian nodal-related gene, is expressed in the left side of the epidermis, and lies upstream of *HrPitx*. *Dev. Genes Evol.* 212: 439–446.
- Nasevicius a, Ekker SC. 2000. Effective targeted gene “knockdown” in zebrafish. *Nat. Genet.* 26: 216–220.
- Newbury DF, Monaco AP, Paracchini S. 2014. Reading and language disorders: the importance of both quantity and quality. *Genes (Basel).* 5: 285–309.
- Nicolson RI, Fawcett AJ. 1994. Reaction times and dyslexia. *Q. J. Exp. Psychol. A.* 47: 29–48.
- Nicolson RII, Fawcett AJJ. 1990. Automaticity: A new framework for dyslexia

- research? *Cognition* 35: 159–182.
- Nopola-Hemmi J, Taipale M, Haltia T, Lehesjoki AE, Voutilainen A, Kere J. 2000. Two translocations of chromosome 15q associated with dyslexia. *J. Med. Genet.* 37: 771–5.
- Oksenberg N, Stevison L, Wall JD, Ahituv N. 2013. Function and regulation of AUTS2, a gene implicated in autism and human evolution. *PLoS Genet.* 9: e1003221.
- Onai T, Irie N, Kuratani S. 2014. The Evolutionary Origin of the Vertebrate Body Plan: The Problem of Head Segmentation. *Annu. Rev. Genomics Hum. Genet.* 15: 443–459.
- Onuma Y, Takahashi S, Haramoto Y, Tanegashima K, Yokota C, Whitman M, Asashima M. 2005. Xnr2 and Xnr5 unprocessed proteins inhibit Wnt signaling upstream of dishevelled. *Dev. Dyn.* 234: 900–910.
- Paracchini S. 2011. Dissection of genetic associations with language-related traits in population-based cohorts. *J. Neurodev. Disord.* 3: 365–73.
- Paracchini S, Diaz R, Stein J. 2016a. Advances in Dyslexia Genetics—New Insights Into the Role of Brain Asymmetries. Elsevier Ltd. 53-97 p.
- Paracchini S, Diaz R, Stein J. 2016b. Chapter Two – Advances in Dyslexia Genetics—New Insights Into the Role of Brain Asymmetries. *Adv. Genet.* 96: 53–97.
- Paracchini S, Scerri T, Monaco AP. 2007. The genetic lexicon of dyslexia. *Annu. Rev. Genomics Hum. Genet.* 8: 57–79.
- Paracchini S, Steer CD, Buckingham L-L, Morris AP, Ring S, Scerri T, Stein J, Pembrey ME, Ragoussis J, Golding J, Monaco AP. 2008. Association of the KIAA0319 dyslexia susceptibility gene with reading skills in the general population. *Am. J. Psychiatry* 165: 1576–84.

- Paracchini S, Thomas A, Castro S, Lai C, Paramasivam M, Wang Y, Keating BJ, Taylor JM, Hacking DF, Scerri T, Francks C, Richardson AJ, Wade-Martins R, Stein JF, Knight JC, Copp AJ, Loturco J, Monaco AP. 2006a. The chromosome 6p22 haplotype associated with dyslexia reduces the expression of KIAA0319, a novel gene involved in neuronal migration. *Hum. Mol. Genet.* 15: 1659–66.
- Paracchini S, Thomas A, Castro S, Lai C, Paramasivam M, Wang Y, Keating BJ, Taylor JM, Hacking DF, Scerri T, Francks C, Richardson AJ, Wade-Martins R, Stein JF, Knight JC, Copp AJ, Loturco J, Monaco AP. 2006b. The chromosome 6p22 haplotype associated with dyslexia reduces the expression of KIAA0319, a novel gene involved in neuronal migration. *Hum Mol Genet* 15: 1659–1666.
- Parker MO, Brock AJ, Millington ME, Brennan CH. 2013a. Behavioral Phenotyping of Casper Mutant and 1-Pheny-2-Thiourea Treated Adult Zebrafish. *Zebrafish* 10: 466–471.
- Parker MO, Gaviria J, Haigh A, Millington ME, Brown VJ, Combe FJ, Brennan CH. 2012a. Discrimination reversal and attentional sets in zebrafish (*Danio rerio*). *Behav. Brain Res.* 232: 264–268.
- Parker MO, Ife D, Ma J, Pancholi M, Smeraldi F, Straw C, Brennan CH. 2013b. Development and automation of a test of impulse control in zebrafish. *Front. Syst. Neurosci.* 7: 65.
- Parker MO, Millington ME, Combe FJ, Brennan CH. 2012b. Development and implementation of a three-choice serial reaction time task for zebrafish (*Danio rerio*). *Behav. Brain Res.* 227: 73–80.
- Paulesu E, Danelli L, Berlingeri M, Zoccolotti P, Pernet CR, Klaver P. 2014. Reading the dyslexic brain: multiple dysfunctional routes revealed by a new meta-analysis of PET and fMRI activation studies.

- Paulesu E, Démonet J-F, Fazio F, McCrory E, Chanoine V, Brunswick N, Cappa SF, Cossu G, Habib M, Frith CD, Frith U. 2001. Dyslexia: Cultural Diversity and Biological Unity. *Science* (80-). 291.
- Pennacchio LA, Ahituv N, Moses AM, Prabhakar S, Nobrega MA, Shoukry M, Minovitsky S, Dubchak I, Holt A, Lewis KD, Plajzer-Frick I, Akiyama J, De Val S, Afzal V, Black BL, Couronne O, Eisen MB, Visel A, Rubin EM. 2006. In vivo enhancer analysis of human conserved non-coding sequences. *Nature* 444: 499–502.
- Pennington BF, Bishop DVM. 2009. Relations among speech, language, and reading disorders. *Annu. Rev. Psychol.* 60: 283–306.
- Peschansky VJ, Burbidge TJ, Volz AJ, Fiondella C, Wissner-Gross Z, Galaburda AM, Turco JJ Lo, Rosen GD. 2010. The Effect of Variation in Expression of the Candidate Dyslexia Susceptibility Gene Homolog Kiaa0319 on Neuronal Migration and Dendritic Morphology in the Rat. *Cereb. Cortex* April 20: 884–897.
- Peterson RL, Pennington BF. 2015. Developmental dyslexia. *Annu Rev Clin Psychol* 11: 283–307.
- Phan ML, Vicario DS. 2010. Hemispheric differences in processing of vocalizations depend on early experience. *Proc. Natl. Acad. Sci.* 107: 2301–2306.
- Pinel P, Fauchereau F, Moreno A, Barbot A, Lathrop M, Zelenika D, Le Bihan D, Poline J-B, Bourgeron T, Dehaene S. 2012. Genetic Variants of FOXP2 and KIAA0319/TTRAP/THEM2 Locus Are Associated with Altered Brain Activation in Distinct Language-Related Regions. *J. Neurosci.* 32: 817–825.
- Pini A. 1993. Chemorepulsion of axons in the developing mammalian central nervous system. *Science* 261: 95–8.

- Pitrone PG, Schindelin J, Stuyvenberg L, Preibisch S, Weber M, Eliceiri KW, Huisken J, Tomancak P. 2013a. OpenSPIM: an open-access light-sheet microscopy platform. *Nat. Methods* 10: 598–599.
- Pitrone PG, Schindelin J, Stuyvenberg L, Preibisch S, Weber M, Eliceiri KW, Huisken J, Tomancak P. 2013b. OpenSPIM: an open-access light-sheet microscopy platform. *Nat. Methods* 10: 598–599.
- Platt MP, Adler WT, Mehlhorn a J, Johnson GC, Wright K a, Choi RT, Tsang WH, Poon MW, Yeung SY, Waye MMY, Galaburda a M, Rosen GD. 2013. Embryonic disruption of the candidate dyslexia susceptibility gene homolog Kiaa0319-like results in neuronal migration disorders. *Neuroscience* 248C: 585–593.
- Poon M-W, Tsang W-H, Waye MM-Y, Chan S-O. 2011a. Distribution of Kiaa0319-like immunoreactivity in the adult mouse brain--a novel protein encoded by the putative dyslexia susceptibility gene KIAA0319-like. *Histol. Histopathol.* 26: 953–63.
- Poon MW, Tsang WH, Chan SO, Li HM, Ng HK, Waye MMY. 2011b. Dyslexia-associated Kiaa0319-Like protein interacts with axon guidance Receptor Nogo Receptor 1. *Cell. Mol. Neurobiol.* 31: 27–35.
- des Portes V, Francis F, Pinard JM, Desguerre I, Moutard ML, Snoeck I, Meiners LC, Capron F, Cusmai R, Ricci S, Motte J, Echenne B, Ponsot G, Dulac O, Chelly J, Beldjord C. 1998. doublecortin is the major gene causing X-linked subcortical laminar heterotopia (SCLH). *Hum. Mol. Genet.* 7: 1063–70.
- Praetorius C, Grill C, Stacey SN, Metcalf AM, Gorkin DU, Robinson KC, Van Otterloo E, Kim RSQ, Bergsteinsdottir K, Ogmundsdottir MH, Magnusdottir E, Mishra PJ, Davis SR, Guo T, Zaidi MR, Helgason AS, Sigurdsson MI, Meltzer PS, Merlino G, Petit V, Larue L, Loftus SK, Adams DR, Sobhiafshar U, Emre NCT, Pavan WJ, Cornell R, Smith AG, McCallion AS, Fisher DE,

- Stefansson K, Sturm R a, Steingrimsson E. 2013. A polymorphism in IRF4 affects human pigmentation through a tyrosinase-dependent MITF/TFAP2A pathway. *Cell* 155: 1022–33.
- Price CJ, Devlin JT. 2011. The Interactive Account of ventral occipitotemporal contributions to reading. *Trends Cogn. Sci.* 15: 246–253.
- Price CJ, Mechelli A. 2005. Reading and reading disturbance. *Curr. Opin. Neurobiol.* 15: 231–238.
- Prince VE, Joly L, Ekker M, Ho RK. 1998. Zebrafish hox genes: genomic organization and modified colinear expression patterns in the trunk. *Development* 125: 407–20.
- Rabin M, Wen XL, Hepburn M, Lubs HA, Feldman E, Duara R. 1993. Suggestive linkage of developmental dyslexia to chromosome 1p34-p36. *Lancet (London, England)* 342: 178.
- Ramus F, Ahissar M. 2012. Developmental dyslexia: The difficulties of interpreting poor performance, and the importance of normal performance. *Cogn. Neuropsychol.* 29: 104–122.
- Ramus F, Rosen S, Dakin SC, Day BL, Castellote JM, White S, Frith U. 2003. Theories of developmental dyslexia: insights from a multiple case study of dyslexic adults. *Brain* 126: 841–865.
- Rana AA, Collart C, Gilchrist MJ, Smith JC. 2006. Defining synphenotype groups in *Xenopus tropicalis* by use of antisense morpholino oligonucleotides. *PLoS Genet.* 2: 1751–1772.
- Ray NJ, Fowler S, Stein JF. 2005. Yellow filters can improve magnocellular function: Motion sensitivity, convergence, accommodation, and reading. *Ann. N. Y. Acad. Sci.* 1039: 283–293.
- Raymond M, Pontier D, Dufour A-B, Moller AP. 1996. Frequency-Dependent

- Maintenance of Left Handedness in Humans. *Proc. R. Soc. B Biol. Sci.* 263: 1627–1633.
- Rendall AR, Tarkar A, Contreras-Mora HM, LoTurco JJ, Fitch RH. 2017. Deficits in learning and memory in mice with a mutation of the candidate dyslexia susceptibility gene *Dyx1c1*. *Brain Lang.* 172: 30–38.
- Richlan F. 2012. Developmental dyslexia: dysfunction of a left hemisphere reading network. *Front. Hum. Neurosci.* 6: 120.
- Richlan F, Kronbichler M, Wimmer H. 2011. Meta-analyzing brain dysfunctions in dyslexic children and adults.
- Roh T-Y, Cuddapah S, Zhao K. 2005. Active chromatin domains are defined by acetylation islands revealed by genome-wide mapping. *Genes Dev.* 19: 542–552.
- Roh T, Wei G, Farrell CM, Zhao K. 2007. Genome-wide prediction of conserved and nonconserved enhancers by histone acetylation patterns. *Genome Res.* 17: 74–81.
- Rosen GD, Bai J, Wang Y, Fiondella CG, Threlkeld SW, LoTurco JJ, Galaburda AM. 2007. Disruption of neuronal migration by RNAi of *Dyx1c1* results in neocortical and hippocampal malformations. *Cereb. Cortex* 17: 2562–72.
- Rumsey JM, Andreason P, Zametkin AJ, Aquino T, King AC, Hamburger SD, Pikus A, Rapoport JL, Cohen RM. 1992. Failure to activate the left temporoparietal cortex in dyslexia. An oxygen 15 positron emission tomographic study. *Arch. Neurol.* 49: 527–34.
- Rumsey JM, Nace K, Donohue B, Wise D, Maisog JM, Andreason P. 1997. A Positron Emission Tomographic Study of Impaired Word Recognition and Phonological Processing in Dyslexic Men. *Arch. Neurol.* 54: 562–573.
- Salmelin R, Kiesilä P, Uutela K, Service E, Salonen O. 1996. Impaired visual word

- processing in dyslexia revealed with magnetoencephalography. *Ann. Neurol.* 40: 157–162.
- Sandelin A, Bailey P, Bruce S, Engström PG, Klos JM, Wasserman WW, Ericson J, Lenhard B. 2004. Arrays of ultraconserved non-coding regions span the loci of key developmental genes in vertebrate genomes. *BMC Genomics* 5: 99.
- Sander JD, Joung JK. 2014. CRISPR-Cas systems for editing, regulating and targeting genomes. *Nat. Biotechnol.* 32: 347–355.
- Scerri TS, Brandler WM, Paracchini S, Morris AP, Ring SM, Richardson AJ, Talcott JB, Stein J, Monaco AP. 2011a. PCSK6 is associated with handedness in individuals with dyslexia. *Hum. Mol. Genet.* 20: 608–14.
- Scerri TS, Fisher SE, Francks C, MacPhie IL, Paracchini S, Richardson a J, Stein JF, Monaco a P. 2004. Putative functional alleles of DYX1C1 are not associated with dyslexia susceptibility in a large sample of sibling pairs from the UK. *J. Med. Genet.* 41: 853–857.
- Scerri TS, Morris AP, Buckingham LL, Newbury DF, Miller LL, Monaco AP, Bishop DVM, Paracchini S. 2011b. DCDC2, KIAA0319 and CMIP are associated with reading-related traits. *Biol. Psychiatry* 70: 237–245.
- Schier AF. 2003. Nodal signaling in vertebrate development. *Annu. Rev. Cell Dev. Biol.* 19: 589–621.
- Schilling TF, Concordet J-P, Ingham PW. 1999. Regulation of Left–Right Asymmetries in the Zebrafish by Shh and BMP4. *Dev. Biol.* 210: 277–287.
- Schindelin J, Arganda-Carreras I, Frise E, Kaynig V, Longair M, Pietzsch T, Preibisch S, Rueden C, Saalfeld S, Schmid B, Tinevez J-Y, White DJ, Hartenstein V, Eliceiri K, Tomancak P, Cardona A. 2012. Fiji: an open-source platform for biological-image analysis. *Nat. Methods* 9: 676–682.
- Schroeder W, Martin K, Lorensen B. 2006a. *The Visualization Toolkit* (4th ed.).

- Schroeder W, Martin K, Lorensen B, Kitware I. 2006b. The visualization toolkit : an object-oriented approach to 3D graphics. Kitware. 512 p.
- Schueler M, Braun DA, Chandrasekar G, Gee HY, Klasson TD, Halbritter J, Bieder A, Porath JD, Airik R, Zhou W, LoTurco JJ, Che A, Otto EA, Bockenbauer D, Sebire NJ, Honzik T, Harris PC, Koon SJ, Gunay-Aygun M, Saunier S, Zerres K, Bruechle NO, Drenth JP, Pelletier L, Tapia-Paez I, Lifton RP, Giles RH, Kere J, Hildebrandt F. 2015a. DCDC2 Mutations Cause a Renal-Hepatic Ciliopathy by Disrupting Wnt Signaling. *Am J Hum Genet* 96: 81–92.
- Schueler M, Braun DA, Chandrasekar G, Gee HY, Klasson TD, Halbritter J, Bieder A, Porath JD, Airik R, Zhou W, LoTurco JJ, Che A, Otto EA, Böckenbauer D, Sebire NJ, Honzik T, Harris PC, Koon SJ, Gunay-Aygun M, Saunier S, Zerres K, Bruechle NO, Drenth JPH, Pelletier L, Tapia-Páez I, Lifton RP, Giles RH, Kere J, Hildebrandt F, Bockenbauer D, Sebire NJ, Honzik T, Harris PC, Koon SJ, Gunay-Aygun M, Saunier S, Zerres K, Bruechle NO, Drenth JPH, Pelletier L, Tapia-Paez I, Lifton RP, Giles RH, Kere J, Hildebrandt F. 2015b. DCDC2 Mutations Cause a Renal-Hepatic Ciliopathy by Disrupting Wnt Signaling. *Am. J. Hum. Genet.* 96: 1–12.
- Schulte-Körne G, Bruder J. 2010. Clinical neurophysiology of visual and auditory processing in dyslexia: A review. *Clin. Neurophysiol.* 121: 1794–1809.
- Schumacher J, Anthoni H, Dahdouh F, König IR, Hillmer AM, Kluck N, Manthey M, Plume E, Warnke A, Remschmidt H, Hülsmann J, Cichon S, Lindgren CM, Propping P, Zucchelli M, Ziegler A, Peyrard-Janvid M, Schulte-Körne G, Nöthen MM, Kere J. 2006. Strong genetic evidence of DCDC2 as a susceptibility gene for dyslexia. *Am. J. Hum. Genet.* 78: 52–62.
- Schumacher J, Hoffmann P, Schmal C, Schulte-Körne G, Nöthen MM. 2007. Genetics of dyslexia: the evolving landscape. *J. Med. Genet.* 44: 289–97.
- Seeger M, Tear G, Ferres-Marco D, Goodman CS, Jan LY, Jan YN, Goodman CS,

- Carretto R, Uemara T, Grell EH, Jan LY, Jan YN. 1993. Mutations affecting growth cone guidance in *Drosophila*: genes necessary for guidance toward or away from the midline. *Neuron* 10: 409–26.
- Shah AN, Davey CF, Whitebirch AC, Miller AC, Moens CB. 2015. Rapid reverse genetic screening using CRISPR in zebrafish. *Nat Methods* 12: 535–540.
- Shaywitz BA, Shaywitz SE, Pugh KR, Mencl WE, Fulbright RK, Skudlarski P, Constable RT, Marchione KE, Fletcher JM, Lyon GR, Gore JC. 2002. Disruption of Posterior Brain Systems for Reading in Children with Developmental Dyslexia. *Biol Psychiatry* 52: 101–110.
- Shaywitz SAES. 1998. Dyslexia. *N. Engl. J. Med.*: 307–312.
- Shaywitz SE. 2003. *Overcoming dyslexia: a new and complete science-based program for reading problems at any level*. A.A. Knopf. 416 p.
- Shaywitz SE, Fletcher JM, Holahan JM, Shneider AE, Marchione KE, Stuebing KK, Francis DJ, Pugh KR, Shaywitz BA. 1999. Persistence of Dyslexia: The Connecticut Longitudinal Study at Adolescence. *Pediatrics* 104.
- Shaywitz SE, Shaywitz BA. 2005. Dyslexia (Specific Reading Disability). *Biol. Psychiatry* 57: 1301–1309.
- Shaywitz SE, Shaywitz BA. 2004. Reading Disability and The Brain. *What Res. Says about Read.* 61: 630–633.
- Shaywitz SE, Shaywitz BA, Fulbright RK, Skudlarski P, Mencl WE, Constable RT, Pugh KR, Holahan JM, Marchione KE, Fletcher JM, Lyon GR, Gore JC. 2003. Neural systems for compensation and persistence: young adult outcome of childhood reading disability. *Biol. Psychiatry* 54: 25–33.
- Shen MM. 2007. Nodal signaling: developmental roles and regulation. *Development* 134: 1023–1034.

- Shin J, Park H-C, Topczewska JM, Mawdsley DJ, Appel B. 2003. Neural cell fate analysis in zebrafish using olig2 BAC transgenics Neural cell fate analysis in zebrafish using olig2 BAC transgenics. *Methods Cell Sci.*: 7–14.
- Shore R. 2015. A functional characterisation of the PCSK6 locus associated with handedness Robert Shore at the University of St Andrews Date of Submission : November 30 2015.
- Shore R, Covill L, Pettigrew KA, Brandler WM, Diaz R, Xu Y, Tello JA, Talcott JB, Newbury DF, Stein J, Monaco AP, Paracchini S. 2016. The handedness-associated PCSK6 locus spans an intronic promoter regulating novel transcripts. *Hum. Mol. Genet.* 25: 1771–1779.
- Simos PG, Breier JI, Fletcher JM, Bergman E, Papanicolaou AC. 2000. Cerebral Mechanisms Involved in Word Reading in Dyslexic Children: a Magnetic Source Imaging Approach. *Cereb. Cortex* 10: 809–816.
- Skaper SD. 2012. Neuronal Growth-Promoting and Inhibitory Cues in Neuroprotection and Neuroregeneration. In: *Methods in molecular biology* (Clifton, N.J.), p 13–22.
- Smith SD, Kimberling WJ, Pennington BF, Lubs HA. 1983. Specific reading disability: identification of an inherited form through linkage analysis. *Science* 219: 1345–7.
- Sommer IEC, Ramsey NF, Mandl RCW, Kahn RS. 2002. Language lateralization in monozygotic twin pairs concordant and discordant for handedness. 2710–2718.
- Spence R, Gerlach G, Lawrence C, Smith C. 2007. The behaviour and ecology of the zebrafish, *Danio rerio*. *Biol. Rev.* 83: 13–34.
- Stein J. 2001a. The magnocellular theory of developmental dyslexia. *Dyslexia* 7: 12–36.

- Stein J. 2001b. The Sensory Basis of Reading Problems. *Dev. Neuropsychol.* 20: 509–534.
- Stemple DL. 2005. Structure and function of the notochord: an essential organ for chordate development. *Development* 132: 2503–2512.
- Stoodley CJ, Stein JF. 2011. The cerebellum and dyslexia. *Cortex* 47: 101–116.
- Stooke-Vaughan GA, Huang P, Hammond KL, Schier AF, Whitfield TT. 2012. The role of hair cells, cilia and ciliary motility in otolith formation in the zebrafish otic vesicle. *Development* 139: 1777–1787.
- Summerton J. 1999. Morpholino antisense oligomers: The case for an RNase H-independent structural type. *Biochim. Biophys. Acta - Gene Struct. Expr.* 1489: 141–158.
- Summerton J, Weller D. 1997. Morpholino antisense oligomers: design, preparation, and properties. *Antisense Nucleic Acid Drug Dev.* 7: 187–195.
- Sun Y-F, Lee J-S, Kirby R. 2010. Brain Imaging Findings in Dyslexia. *Pediatr. Neonatol.* 51: 89–96.
- Suster ML, Abe G, Schouw A, Kawakami K. 2011. Transposon-mediated BAC transgenesis in zebrafish. *Nat. Protoc.* 6: 1998–2021.
- Suster ML, Kikuta H, Urasaki A, Asakawa K, Kawakami K. 2009. Transgenesis in zebrafish with the tol2 transposon system. 561.
- Szalkowski CE, Booker AB, Truong DT, Threlkeld SW, Rosen GD, Fitch RH. 2013. Knockdown of the candidate dyslexia susceptibility gene homolog *dyx1c1* in rodents: effects on auditory processing, visual attention, and cortical and thalamic anatomy. *Dev. Neurosci.* 35: 50–68.
- Szalkowski CE, Fiondella CG, Galaburda AM, Rosen GD, Loturco JJ, Fitch RH. 2012a. Neocortical disruption and behavioral impairments in rats following in

- utero RNAi of candidate dyslexia risk gene Kiaa0319. 30: 293–302.
- Szalkowski CE, Fiondella CG, Galaburda AM, Rosen GD, Loturco JJ, Fitch RH. 2012b. Neocortical disruption and behavioral impairments in rats following in utero RNAi of candidate dyslexia risk gene Kiaa0319. *Int J Dev Neurosci* 30: 293–302.
- Taipale M, Kaminen N, Nopola-Hemmi J, Haltia T, Myllyluoma B, Lyytinen H, Muller K, Kaaranen M, Lindsberg PJ, Hannula-Jouppi K, Kere J. 2003. A candidate gene for developmental dyslexia encodes a nuclear tetratricopeptide repeat domain protein dynamically regulated in brain. *Proc. Natl. Acad. Sci. U. S. A.* 100: 11553–8.
- Tamplin OJ, Cox BJ, Rossant J. 2011. Integrated microarray and ChIP analysis identifies multiple Foxa2 dependent target genes in the notochord. *Dev. Biol.* 360: 415–425.
- Tarkar A, Loges NT, Slagle CE, Francis R, Dougherty GW, Tamayo J V, Shook B, Cantino M, Schwartz D, Jahnke C, Olbrich H, Werner C, Raidt J, Pennekamp P, Abouhamed M, Hjeij R, Köhler G, Griese M, Li Y, Lemke K, Klena N, Liu X, Gabriel G, Tobita K, Jaspers M, Morgan LC, Shapiro AJ, Letteboer SJF, Mans D a, Carson JL, Leigh MW, Wolf WE, Chen S, Lucas JS, Onoufriadis A, Plagnol V, Schmidts M, Boldt K, Roepman R, Zariwala M a, Lo CW, Mitchison HM, Knowles MR, Burdine RD, Loturco JJ, Omran H, Kohler G, Griese M, Li Y, Lemke K, Klena N, Liu X, Gabriel G, Tobita K, Jaspers M, Morgan LC, Shapiro AJ, Letteboer SJF, Mans D a, Carson JL, Leigh MW, Wolf WE, Chen S, Lucas JS, Onoufriadis A, Plagnol V, Schmidts M, Boldt K, Roepman R, Zariwala M a, Lo CW, Mitchison HM, Knowles MR, Burdine RD, Loturco JJ, Omran H. 2013b. DYX1C1 is required for axonemal dynein assembly and ciliary motility. *Nat. Genet.* 45: 995–1003.
- Thisse C, Thisse B. 2008. High-resolution in situ hybridization to whole-mount zebrafish embryos. *Nat. Protoc.* 3: 59–69.

- Thompson PM, Cannon TD, Narr KL, van Erp T, Poutanen V-P, Huttunen M, Lönngqvist J, Standertskjöld-Nordenstam C-G, Kaprio J, Khaledy M, Dail R, Zoumalan CI, Toga AW. 2001. Genetic influences on brain structure. *Nat. Neurosci.* 4: 1253–1258.
- Threlkeld SW, McClure MM, Bai J, Wang Y, LoTurco JJ, Rosen GD, Fitch RH. 2007. Developmental Disruptions and Behavioral Impairments in Rats Following In Utero RNAi of *Dyx1c1*. *Brain Res Bull* 71: 508–514.
- Toga AW, Thompson PM. 2003. Mapping brain asymmetry. *Nat. Rev. Neurosci.* 4: 37–48.
- Truong DT, Che A, Rendall AR, Szalkowski CE, LoTurco JJ, Galaburda AM, Holly Fitch R. 2014. Mutation of *Dcdc2* in mice leads to impairments in auditory processing and memory ability. *Genes Brain Behav* 13: 802–811.
- Urasaki A, Morvan G, Kawakami K. 2006. Functional dissection of the Tol2 transposable element identified the minimal cis-sequence and a highly repetitive sequence in the subterminal region essential for transposition. *Genetics* 174: 639–49.
- Varshney GK, Pei W, LaFave MC, Idol J, Xu L, Gallardo V, Carrington B, Bishop K, Jones M, Li M, Harper U, Huang SC, Prakash A, Chen W, Sood R, Ledin J, Bruggess SM. 2015. High-throughput gene targeting and phenotyping in zebrafish using CRISPR / Cas9. *Genome Res.*: 1030–1042.
- Velayos-Baeza A, Toma C, Paracchini S, Monaco AP. 2008. The dyslexia-associated gene KIAA0319 encodes highly N- and O-glycosylated plasma membrane and secreted isoforms. *Hum. Mol. Genet.* 17: 859–871.
- Velayos-Baeza A, Toma C, da Roza S, Paracchini S, Monaco AP. 2007. Alternative splicing in the dyslexia-associated gene KIAA0319. *Mamm Genome* 18: 627–634.

- Villefranc JA, Amigo J, Lawson ND. 2015. Gateway Compatible Vectors for Analysis of Gene Function in the Zebrafish. *73*: 389–400.
- Vinckier F, Dehaene S, Jobert A, Dubus JP, Sigman M, Cohen L. 2007. Hierarchical Coding of Letter Strings in the Ventral Stream: Dissecting the Inner Organization of the Visual Word-Form System. *Neuron* 55: 143–156.
- Visel A, Blow MJ, Li Z, Zhang T, Akiyama JA, Holt A, Plajzer-Frick I, Shoukry M, Wright C, Chen F, Afzal V, Ren B, Rubin EM, Pennacchio LA. 2009. ChIP-seq accurately predicts tissue-specific activity of enhancers. *Nature* 457: 854–858.
- Walhout a J, Temple GF, Brasch M a, Hartley JL, Lorson M a, van den Heuvel S, Vidal M. 2000. GATEWAY recombinational cloning: application to the cloning of large numbers of open reading frames or ORFeomes. *Methods Enzymol.* 328: 575–592.
- Wang Y, Paramasivam M, Thomas A, Bai J, Kaminen-Ahola N, Kere J, Voskuil J, Rosen GD, Galaburda AM, Loturco JJ. 2006. DYX1C1 functions in neuronal migration in developing neocortex. *Neuroscience* 143: 515–22.
- Weinberg ES, Allende ML, Kelly CS, Abdelhamid A, Murakami T, Andermann P, Doerre OG, Grunwald DJ, Riggelman B. 1996. Developmental regulation of zebrafish MyoD in wild-type, no tail and spadetail embryos. *Development* 122: 271–80.
- Wernicke C. 1874. *Der aphasische Symptomencomplex eine psychologische Studie auf anatomischer Basis.* Breslau: Cohn & Weigert.
- Wigg KG, Couto JM, Feng Y, Anderson B, Cate-Carter TD, Macciardi F, Tannock R, Lovett MW, Humphries TW, Barr CL. 2004. Support for EKN1 as the susceptibility locus for dyslexia on 15q21. *Mol. Psychiatry* 9: 1111–1121.
- Wong K, Park HT, Wu JY, Rao Y. 2002. Slit proteins: molecular guidance cues for

- cells ranging from neurons to leukocytes. *Curr. Opin. Genet. Dev.* 12: 583–91.
- Woolfe A, Goodson M, Goode DK, Snell P, McEwen GK, Vavouri T, Smith SF, North P, Callaway H, Kelly K, Walter K, Abnizova I, Gilks W, Edwards YJK, Cooke JE, Elgar G. 2004. Highly Conserved Non-Coding Sequences Are Associated with Vertebrate Development. *PLoS Biol.* 3: e7.
- Wu JY, Rao Y, Wu W, Wong K, Chen J, Jiang Z, Dupuis S. 1999. Directional guidance of neuronal migration in the olfactory system by the protein Slit. *Nature* 400: 331–336.
- Yamamoto M, Morita R, Mizoguchi T, Matsuo H, Isoda M, Ishitani T, Chitnis AB, Matsumoto K, Crump JG, Hozumi K, Yonemura S, Kawakami K, Itoh M. 2010. Mib-Jag1-Notch signalling regulates patterning and structural roles of the notochord by controlling cell-fate decisions. *Development* 137: 2527–2537.
- Zhang Z, Liu S, Lin X, Teng G, Yu T, Fang F, Zang F. 2011. Development of fetal brain of 20 weeks gestational age: Assessment with post-mortem Magnetic Resonance Imaging. *Eur. J. Radiol.* 80: e432–e439.
- Zhu Y, Li H, Zhou L, Wu JY, Rao Y. 1999. Cellular and molecular guidance of GABAergic neuronal migration from an extracortical origin to the neocortex. *Neuron* 23: 473–85.

7 Appendices

7.1 Appendix A

7.1.1 Appendix A1 Enzyme catalogue

Table 7.1 List of enzymes with reference numbers and the company

Enzyme	Reference number	Company
DNaseI	79254	QIAGEN
EcoRI	R0101S	NEB
GoTaq Green	M7122	Promega
LR Clonase® II Plus enzyme	12538120	Life Technologies Ltd
NotI-HF	R3189S	NEB
Poly-A tailed	M0276S	NEB
Pronase	101659210-01	Roche Diagnostics Ltd.
Proteinase K	11588916	ThermoFisher Scientific
RNase Inhibitor, Murine	M0314S	NEB
Shrimp Alkaline Phosphatase rSAP	M0371S	NEB
SmaI	R0141S	NEB
SP6 polymerase	M0207S	NEB
T3 RNA polymerase	M0378S	NEB
T4 DNA ligase	M0202S	NEB
Vaccinia Capping System	M2080S	NEB

7.1.2 Appendix A2 Buffers and solutions

Table 7.2 List of buffers and solutions

Name	Recipe
0.1% Methylene Blue Stock Solution	0.1 g methylene blue-trihydrate, H ₂ O to 100mL
0.2x SSCT	SSC + 0.01% Tween20
3M KOAc pH 4.8	Mix 29.4 g of potassium acetate, 40 mL of dH ₂ O, add HCl to pH 4.8, and dH ₂ O to 100 mL (Filter sterilize) (store at 4°C)
10x PBS	80g NaCl, 2g KCl, 7.62g Na ₂ HPO ₄ , 0.77g KH ₂ PO ₄ , H ₂ O to 1000mL (pH 7.4)
1M Tris-HCl	27g Tris-HCl, 23g Tris base, H ₂ O to 1000mL (pH 9)
20x SSC	175,3g NaCl, 88,2g Na Citrate, H ₂ O to 1000mL (pH 7.0)
4% PFA	4 g Paraformaldehyde powder, H ₂ O to 100mL PBS
Alkaline phosphatase buffer (NTMT)	1ml NaCl 5M, 2.5ml (2M) Tris-HCl pH9.5, 1.25ml MgCl ₂ (2M), 5ml Tween20 10%, Top up to 50ml with H ₂ O
Blocking solution	10% normal goat serum (NGS), 1% DMSO, 0.5-0.8% Triton-X100 in PBS
Danieau solution	101.7g NaCl (1740mM), 1.56g KCl (21mM), 2.96g MgSO ₄ •7H ₂ O (12mM), 4.25g Ca(NO ₃) ₂ (18 mM), 35.75g HEPES buffer (150 mM)
Hybridisation solution	50% formamide, 5X SSC, 1%Tween20, 0.5mg/ml Torula yeast mRNA, 50µg/ml heparin
Homogenisation buffer	50 mM Hepes, 0.25M sucrose, 5 mM MgCl ₂ (0.5 mM EDTA, optional) and 1 x Roche Complete protease cocktail inhibitors, pH 7.4

Maleic Acid Buffer (MAB)	150 mM NaCl, 100mM Malic Acid, pH 7.5
Methanol series	100% MeOH, 75% MeOH:25% PBT, 50% MeOH:50% PBT, 25% MeOH: 75% PBT, 1x PBT
Methylene Blue Working Solution	2ml of 0.1% methylene blue, Danieau solution to 1000mL
MS-222 (Tricaine)	400mg Tricaine, 2.1mL Tris-HCl (1M), H ₂ O to 100mL (pH 7)
Solution 1	40 ml PBS, 4g non-fat milk powder, 0.08 ml Tween 20
Solution 2	16 ml PBS, 4 ml Solution 1, 0.1 ml Tween 20
Solution 3	500 ml PBS, 1 ml Tween 20
Solution 4	10 ml PBS, 10 ml Solution 1, 0.1 ml Tween 20
Tail Buffer	100mM TrisHCl, pH 8.5, 200mM NaCl, 5mM EDTA, 0.2% SDS

7.1.3 Appendix A3 Catalogue of Cells used in experiments

Table 7.3 List of competent cells use for transformations

Cells	Reference number	Company
One Shot® TOP10 Chemically Competent E. coli cells	C4040-06	Invitrogen
Subcloning Efficiency™ DH5α™ Competent Cells	18265-017	Life Technologies Ltd
One Shot® Mach1™ T1 Phage-Resistant Chemically Competent E. coli	C862003	Life Technologies Ltd

7.1.4 Appendix A4 catalogue of Kits used in experiments

Table 7.4 List of kits with reference number and the company

Kit	Reference number	Company
FISH Tag™ RNA Multicolor Kit	F32956	ThermoFisher Scientific
mMESSAGE mMACHINE® T7 ULTRA Transcription Kit	AM1345	ThermoFisher Scientific
PrimeScript RT reagent kit	RR037A	TAKARA
QIAprep® Spin Miniprep Kit	27104	QIAGEN
QIAquick Gel Extraction Kit	28704	QIAGEN
Quick Blunting™ Kit	E1201S	QIAGEN
RNeasy columns	74106	QIAGEN

7.1.5 Appendix A5 Plasmids

Table 7.5 List of plasmids used in the Gateway Tol2 cloning protocol

Plasmid name	Reference number	Company	att sites
p5E-MCS	26029	Addgene	L4/R1
p3E-mcs1	49004	Addgene	R2/L3
pME-Cherry	26028	Addgene	L1/L2
pDestTol2pACryGFP	64022	Addgene	R3/R4
pCR TM -Blunt Vector	II-TOPO® K280002	ThermoFisher Scientific	
pUB-GFP	11155	Addgene	
pENTR5'_ubi	27320	Addgene	
pCS-zT2TP		Kawakami lab	

7.1.6 Appendix A6 Primer catalogue

Table 7.6 List of primers used in this thesis

Primer number	Primer sequence 5' - 3'
275	ACCCCGAGTACTACTGCTTTT
281	CTGGCTCTAAATGGCAGCCT
410	TTGAGAAGAAAATCGGTGGTGCTG
411	GGAACGGTGTGATTGAGGGAAATTC
443	GCAGAAGGAGATCACATCCCTGGC
444	CATTGCCGTCACCTTCACCGTTC
496	CCGCAACCTACTCTGAAAGC
497	TGACTTGGGGTAATGGTGCT
512	ACCAGCAAACGTGTCCTTTC
513	CCTGTGCTGCAAGTATCCAC
516	CACAGGTGGAGCAAGGTTG
517	CTGGCTAACACGGTGAAACC
518	AACCATCGCTGTGAAAAGGC
519	CTTTCAGAGTAGGTTGCGGC
520	CGCAGCCACATGTAGAGTCT
521	AGAAGACATGTCCTGCTCCG
524	CGACATCCCCGACTACTTGA
525	CTTCTTCTGCATTACGGGGC
T750	AGGGTCAGTACACGTTTCAGC
T751	CGCAATTAACCCTCACTAAAGGGACA CAGAGGGTCACAGGAACAG

7.2 Appendix B

A map of pCR™-Blunt II-TOPO® vector containing *kiaa0319* cDNA sequence

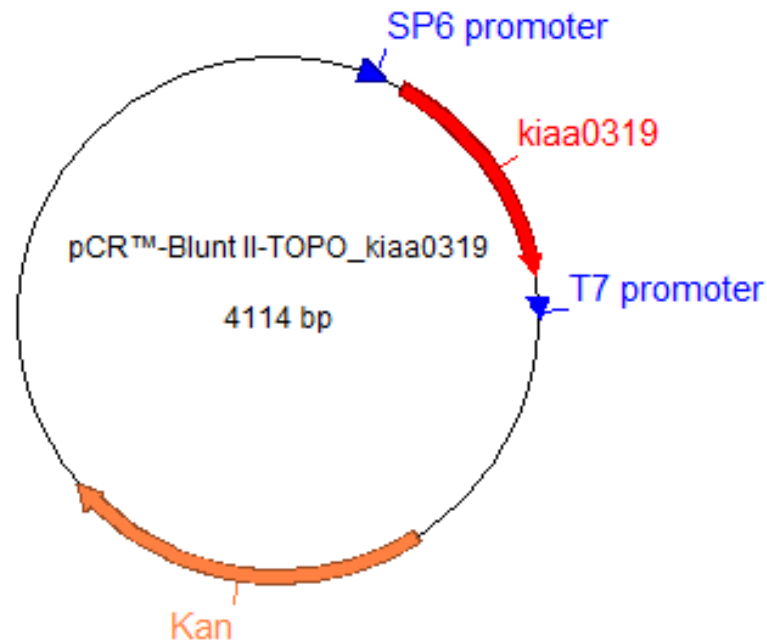


Figure 7.1 A zebrafish *kiaa0319* cDNA sequence in pCR™-Blunt II-TOPO® vector

A 4114bp pCR™-Blunt II-TOPO® vector containing kanamycin resistance (Kan), SP6 and T7 promoters (blue) and a 595bp *kiaa0319* cDNA sequence (red). SP6 drives the sense transcription, T7 drives antisense transcription.

7.2.1 Appendix B1 A standard PCR reaction using Phusion DNA Polymerase

Table 7.7 PCR mastermix for obtaining PCSK6 promoter sequence

Compound	Concentration	1 reaction [μ l]	1 reaction [μ l]
Phusion® GC Buffer	50mM	4	10
dNTPs	10 μ M	0.4	1
Fwd 281 Primer	10 μ M	1	2.5
Rev 275 Primer	10 μ M	1	2.5
Human gDNA	65ng/ μ l	1.2	3
Phusion® High-Fidelity DNA Polymerase	2,000 units/ml	0.2	0.5
H₂O		12.4	30.5
Total Volume		20 μ l	50 μ l

The mastermix was incubated in the thermocycler under the following conditions:

Denaturation	98°C	30s,	} 30 cycles
Annealing	58°C	20s	
Elongation	72°C	2min	

7.3 Appendix C

kiaa0319 isoform profiling

7.3.1 Appendix C1 Primer catalogue

Table 7.8 List of primers used in *kiaa0319* isoform analysis

Primer number	Primer name	Primer sequence 5' - 3'
447	<i>kiaa_iso_Fwd_1</i>	AGGGCCCTGTTGAAAGTAGC
448	<i>kiaa_iso_Rev_1</i>	CAGATTTGTTGTGCTGCCCC
449	<i>kiaa_iso_Fwd_2</i>	CATGCTGCCCCAAAACACTG
450	<i>kiaa_iso_Rev_2</i>	GCTCAGCCCCTCAGAATCAG
451	<i>kiaa_iso_Fwd_3</i>	CTGCCTCTCAACCACCTCAC
452	<i>kiaa_iso_Rev_3</i>	ATCCCAGATCTCAGGCCTGT
453	<i>kiaa_iso_Fwd_4</i>	CCCTCCAGGCTTGAAGATGA
454	<i>kiaa_iso_Rev_4</i>	GCGGATCAGGTCGTACTIONTCC
455	<i>kiaa_iso_Fwd_6</i>	ATTCAGGTTCTCGGTGCAGG
456	<i>kiaa_iso_Rev_6</i>	TGTTCACTGTCCAGCTCTGAT
506	<i>kiaa_iso_1F</i>	ATCAGCTCTTCACCACAGCT
507	<i>4kiaa_iso_1R</i>	TCTGAAGTCATCTGCGGTGT
508	<i>kiaa_iso_2F</i>	GCCCTGTTGAAAGTAGCACC
509	<i>kiaa_iso_2R</i>	ACTGCGTAAACACCCTCTGA
510	<i>kiaa_iso_3F</i>	GCTGCCCCAAAACACTGTTA
511	<i>kiaa_iso_3R</i>	AGTGCGATGTCTGAGTCCAA
512	<i>kiaa_iso_4F</i>	ACCAGCAAACGTGTCTTTC
513	<i>kiaa_iso_4R</i>	CCTGTGCTGCAAGTATCCAC

7.3.2 Appendix C2 Screenshot of zfin.org database on *kiaa0319* and *kiaa0319l*

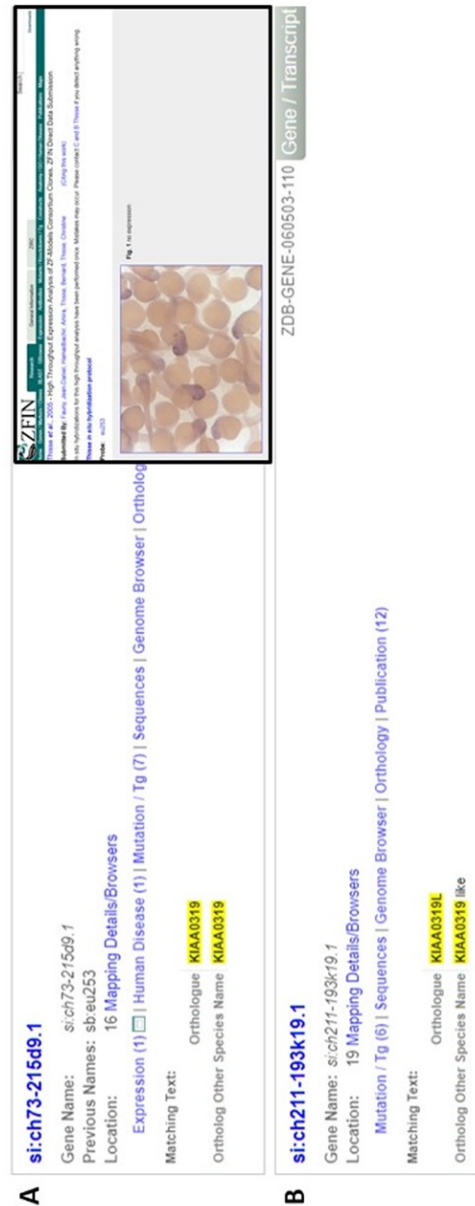


Figure 7.2 *kiaa0319* and *kiaa0319l* information as in *zfin.org* database

A) The *zfin.org* database screenshot shows the official gene name for *kiaa0319*, the previous name, location on the chromosome and the data published. There is a single expression data study by Thisse et al (2005) on AB.TU strain claiming there is no expression (black box on the right). B) The *zfin.org* database screenshot for *kiaa0319l*. No expression studies have been performed to date

7.3.3 Appendix C3 RT-qPCR standard curve

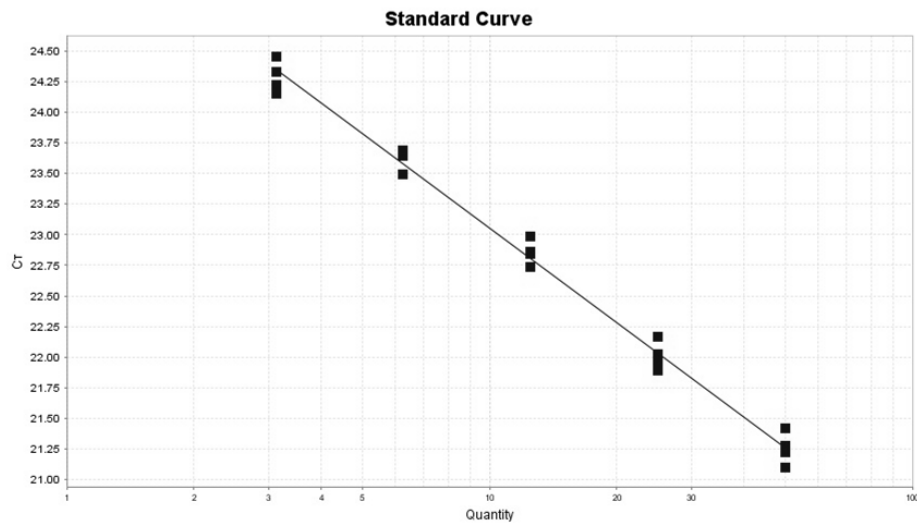


Figure 7.3 Standard curve using kias0319 primers 518 and 519

Square points represent individual replicate of the same dilution. Ct is the cycle threshold. Quantity represents the number of cycles.

7.4 Appendix D

7.4.1 Appendix D1 RNAScope

The RNAScope probes were created by the Advanced Cell Diagnostics, Inc. (ACD) based on the Ensembl accession numbers. The probes consist of 20 double Z (ZZ) oligonucleotides and are targeting approximately 1kb sequence all together (see below). The channels represent the labelling combination options for each probe. The *kiaa0319l* was linked to C1 channel, *myod* to C2 and *kiaa0319* to C3 channel.

Table 7.9 RNAScope probes with their name and Ensembl accession number

Channel	Name	Ensembl accession number	Target	Probe size
C1	<i>kiaa0319l</i>	ENSDART00000051723.5	545- 1425	880bp
C2	<i>myod1</i>	ENSDART00000027661.7	2-1083	1081bp
C3	<i>kiaa0319</i>	ENSDART000000160645	239- 1147	908bp

7.4.4 Appendix D4 RNAScope probe design *myod*

```

1 CTCTTACCAGCAACAAGTACCTGAGGGGTACATGCAAAAGAAACCCCTCCGAGGTCTCGGAATTTTAGACTGTAGT
76 TTTGAAACGTACGTTATTTGGGGATCTGAAGGACTTTGTCTTACTATTCCCTAATTTTGGTTTTATTTTTTTTAC
151 AAAATTTACTACTTTGGAAACATTCAAGTACATTTCTTGCTTTTAAACTTTAACACAAAAAGATGGAGTTGTCCG
226 GATATCCCCTTCCCCATCCCATCAGCTGATGACTTCTACGACGACCCCTTGCTTCAACACCAACGACATGCACTTC
301 TTTGAAGACTTGGACCCAGGCTTGTTCACGTGAGCCTGCTCAAACCCGACGAGCATCACCACATCGAGGACGAG
376 CACGTGAGGGCCGCCAGTGGGCATCATCAGGCCGGCAGGTGCCTACTGTGGGCATGCAAAGCTTCAAAGAGAAA
451 ACTACCAATGCTGACCGTGCAAAGCCGCCACCATGAGGGAGAGGGCGACTGAGCAAGGTCAACGACGCTTTG
526 GAGACCCCTCAAGAGATGCACGTCCACCAACCCGAACCCAGAGGCTGCCCAAAGTGGAGATTTCTGAGAAAACGCCATT
601 AGTTATATCGAGTCTCTGCAGGCTCTTCTCAGAAAGTCAAGAGGATAACTACTATCCCGTTCTGGAACATTACAGT
676 GGAGACTCTGATGCTTCCAGTCCGAGATCCAAGTCTGCTGATGGCATGATGGATTTATGGGCCCAACGTTGTCAG
751 ACGAGAAGACGGAAACAGCTATGACAGCTCTTACTTCAATGACACACCAAAATGCTGACGCACGGAATAATAAAAAC
826 TCAGTGGTGTGAGTGTGGATTGTCTGTCCAGCATCGTGGAGCGAATTTCCACAGAGACTCCTGCATGTCCCGTG
901 CTGTGAGTACCCGAGGGGCACGAAGAGAGCCCGTGTCTCCGATGAGGGATCTGTCTGAGTACACCCGGAACC
976 ACCGCACCGTCCCCGACAGCTGCCTCAACAGCAGGCTCAGGAAACCAATTTATCAAGTGTCTTAAAAATCTGCA
1051 ACATTTCAAACAATTTGAAAAAGACAATCTGAAAGGAAACTTTGAGCAAAAAAGGCGAATCCGACCTTTAA
1126 CGACAAAAGAAAGACTTTTATCCACTGCTGGAAACTAGGAAAGAATGCTTTCTTTCTTTCTTTCTTTCTTTCT
1201 TCTTTCTTTCTTTCTTTCTTTCTTTCTTTCTTTCTTTCTTTCTTTCTTTCTTTCTTTCTTTCTTTCTTTCTTT
1276 TTCTTTCTTTCTTTCTTTCTTTCTTTCTTTCTTTCTTTCTTTCTTTCTTTCTTTCTTTCTTTCTTTCTTTCTTT
1351 TTTCTTTCTTTCTTTCTTTCTTTCTTTCTTTCTTTCTTTCTTTCTTTCTTTCTTTCTTTCTTTCTTTCTTTCTTT
1426 ATCAGCAGAAGTGAATTTCTTAAGTCTTATTTATATTGTTATATCCAGTGAAGATGTGACCATATTTTTTT
1501 CCCTTTGTGAATATATTTCTGTCAACATCACCTTTTATTTTCTAATTTTACGAAAAAATCGTAATCCAGA
1576 TACGAATAGTAGGACCATTTTGTATATGTGTAATAAGATCTGTTTTGTTAAAGCGACGAAAACGAACAAACAT
1651 ATTATTGTATTTAATGATGCCTGTTTGAACACTAGTTTGTGTGCTTGTGTTAAACTTTTATATTTACTTCT
1726 TAAACGAGTGAATGACGGATAAATAAAAACAATATTTATACTGGAA
    
```

Figure 7.5 *myod* cDNA sequence

The 20ZZ RNAScope probe is labelled purple.

7.4.5 Appendix D5 RNAScope probe design *kiaa0319*

```

1 GTCTTTATCTGCTGACACTCCCTCCCGCAGACAAACACACACACACTCCAGCATCTTCCAGCTATATCAGAGCTTTCATTACAAGATCATTGCCGCAATATCAGCTCTTACCACAGCTTT
123 AGTTTACTCCATCAGCTTGTGTCAGCAGCAATTCGCCATGGAGTAGCAGCAGCGAAGCAGATCCCTCGATATCATGGAACACAGATGCTTGAATAAGAGCGTCACATCCCTCTGGGTTGAAG
245 AAGTAAATGCTGTGTAAGAACCATCGCTGAAAGGGCCAGTGGCATCATGAATCTTTACCAGTCTTTCCACTTTTGATACCTTTATGATCAGAGTATCAGGACAGTCTGGCAGGCGCC
367 CAACCTACTCTGAAGCGTGGTGTCTCCGGAGCTGAGGAGCAGCAGTATTTACGTGTCCGGATGTGTCGTCCTCGCTCAGTGTCCGGGGCTGCTGTGATCTCCGGGGCTGTGACCTG
489 SCCTGGTTTTTGGACCCAGTGTATGTCTCAGTGTGTGACGACACAGAAAACGCCAGCGGAGAGAGACCTGGTACAGACTCTTACCTGGCTTCTGCAACGTGGGCCCCCAAAAC
611 ACTTGTCTCGACTCCCTGGTTGAGAGAGACTTTCCAAACCAATGGCAGCCTCTGCCCAGACACCGGGGATCCGAGGATCCCATGAAGGATCTCGCTCTGCTTGAAGGGATTCAAGATT
733 CGGACAACTTGGAGCTGAGTATGACAGAGATTTTCAAGTGTGGAAGCAAAAAGAGCTGAGACATAGACTAAAAGCGGTAGAGCAAGAGAGCAAACTGGGCTTTATGATGGCCACT
855 TTCAAAGAAAAGGAAATCAACCAATCAGAGACGGAGAGGCGAGTAAAGATTGACACTGTTCAGGGCCCTGTTGAAAGTAGCACCAATACCCCAAGTCACTTTTCAGAAAGAGAGAAA
977 TGAAGCAGATCAACCAATTAAGAGCAGAACTAATGTTACGGTACCATCAACCTCTGATTTGACATTAAGGTTGAAGAGAGCCACAGACACACTGTGCAACTACTGCACCTTAAG
1099 TCGTGAAGACTCAGTACAGAGACCGCAACTTAGTGCAGTCAACGGTTTCAATCATCACTCCAGCCACACTGAAGCTACACCGCAGATGACTTCAGAACAGCCAGTAAAGCTCTGACT
1221 GTGTCCATGGAAGCCCTGTGGAAGCCATGTCGCCCAAAACACTGTAAACTAACAGCTTTAGTTAGTCCAGATGATACTCCGGAATCTCCTTACACATATGAGTGGACTTTTGTGATCTC
1343 ACCAGAAGCAACCTAGGGGTGATGGAGGGCCAGCACACAAATCTGTCTACTTTCTGAAGTGTGAGGGGTGTTACGCACTCAGAGTGATTTGAAAGCAGATCAAGCATATGGAGAAG
1465 GTTCTGTGGACTTGACCGTACACCTGCGAGAGAAAATAAACAGCTTCTAAAGCAGTGTCTTCCCAAGAGCCAGATGTGCTTCAAAAAAGATTCTGTCTTAATCAITTAACGGAAAT
1587 GAGAGTATGGATGATGACAGGATTTGTCAGTTATCTGTGAAAAGGTTGGACGGCCGCTTTGGACACTGAAGTCTGTTAAACAACTGTACTGACGCTGAAAATCTTTTACCTGGAA
1709 ATATACCTTCGAGCTGACAGTGTCTGATTCTGAGGGGCTGAGCGACTCCAGCACTGCCACTTTGAGGGTCAAGCATCCCAAAAGATGAGCTTCTCTGGCCAGAGCGGGCACAGACCGGTC
1831 TTACCTGCTCTCAACCACTCACCTCTGAGGGGAAACCAAGCAGACAGATGACAGGCAATACAGACTACTCTGGACACTCCATCCGACAGCCGACCCGAAAGTCCACATGACGAGT
1953 GTGAGATCAGCAATTTCTGTAGTCTCTGATCTGATCTGAGGGGGTCACTACAGCTTTCAGCTCAGACTCACTGACTCAAGAGGTCAACAGGATTCAGACAGCACTCTGTCACTGTCTGCTG
2075 AAACAGACCCAGTGGCTGTAACAGSACACACATACAGTACTTCTGCCGTCAACAGCATCACTGAATGGCAGCGCAGCACTGATGATCAGGCCATCAGCAGATACCAGTGGGACG
2197 TGATGAGTGGCCCTCCAGCTTGAAGATGAAGATGCCAATAAGCGGTTGCCATCCGACAGCCGCTGAGATCTGGGATTTACAAGTTGAAGTTGACTGTGGTGGATGAGCAGGGAGAAACA
2319 GACAGTGCAGTCTGAGCATCACAGTTAAAGAGCTAAAAGCTGCCACTGGTGGCTCATGCCAGCGCAGCCATACACTCACTTTGCCCAACAACCTCTCTGGTGTCTCAGAGGTTCAAGTGT
2441 CAACAGCGGACCGCAACCGTGTCTTCTGTGGGTTAGAGATGAACAGAGCCCTGCTCGGGGGATGTGTTGATGGTTAGATCAGCAGGGCTCGCTTACCTTCCCAACCTGTTAGAG
2563 GAACATACCTGTTCCAGCTGCGGGTCAACGATGTCAGGGCCGCTCAAGCAGCGCTACAGCCACTGTGGAAGTACGACTGATCCGCTGAGCAGAGAGGAGTGAACCTGAGCTGCAAGTG
2685 AGCGTGGCTCAAGTCACTCAGCAACAGAGAGACAGTGTATCAGACAGTGGCCGCACTTCTGCAATGTTGGACTCAGACATCGCACTAAAGGCTCTACATGGACAGTCTGACATCAGAC
2807 AGTATTCAGGTTCTCGGTGCGGGTCTGATGGTTGATCCCTGGCCCTAAACTTGGCCGCTGCTGAGAAACCAAGCTGTTGAGAGAGAAAAGCGACTTCTGCTCTTAGGGTCTTAAGAG
2929 TGGACACAGTCAATGTTTGTGCTGTGTTCTGGGGTGTGTCAGTGTGACCCATACAAAAGCTGTTCTGTGACCTCTGTGGATGGAGAACCCCATCCGCTCTCTCATAGCAGTGA
3051 GAGAGCAATTTGACTGAGTGTGCTGTATGTCACAACTCTGTTTGTGACCAATCATTTTCACTTGTCCGTCAGCTGGATCTGCTGTGCTGCTGTTAAAAGCAATTAACACAGAGACA
3173 CAGACCAACTCTAGCTGATGATGTCTGAATCAGAGCTGACAGTGAACAGSACAACTTACAATTAAGCGAGATCCAAAAGCTCATAACGAATCAGAAAGCGAGACACTCTCAGC
3295 CTTTGCCTGTGGAGATTTGAGTCCATGGACAAAAGGACATTTCTTCATCGTGATACTTGCAGCACAGGGGTATTGCTGAAITTTACCCTAATAACAAAGACAGACAGATTTGAAT
    
```

Figure 7.6 *kiaa0319* cDNA sequence

The 20ZZ RNAScope probe is labelled green.

7.5 Appendix E

Multisite recombination

Table 7.11 List of att recombination site sequences

att recombination sites	sequence
attL1	CAAATAATGATTTTATTTTGACTGATAGTGACCTGTTCGT TGCAACAMATTGATGAGCAATGCTTTTTTATAATGCCAAC TTTGTACAAAAAGCAGGCT
attL2	ACCCAGCTTCTTGTACAAAGTTGGCATTATAAGAAAGCA TTGCTTATCAATTTGTTGCAACGAACAGGTCACTATCAGT CAAATAAAAATCATTATTTG
attL3	CAACTTTATTATACAAAGTTGGCATTATAAAAAAGCATTG CTTATCAATTTGTTGCAACGAACAGGTCACTATCAGTCAA AATAAAAATCATTATTT
attL4	AAATAATGATTTTATTTTGACTGATAGTGACCTGTTCGTT GCAACAAATTGATAAGCAATGCTTTTTTATAATGCCAACT TTGTATAGAAAAGTTG
attR1	CAAGTTTGTACAAAAAGTTGAACGAGAAACGTAAAATG ATATAAATATCAATATATTTAAATTAGATTTTGCATAAAAA ACAGACTACATAATACTGTAAAACACAACATATGCAGTC ACTATGAATCAACTACTTAGATGGTATTAGTGACCTGTA
attR2	TACAGGTCACTAATACCATCTAAGTAGTTGR TTCATAGTG ACTGCATATGTTGTGTTTTACAGTATTATGTAGTCTGTTTT TTATGCAAAATCTAATTTAATATATTGATATTTATATCATT TTACGTTTCTCGTTCAACTTTCTTGTACAAAGTGG
attR3	CCATAGTGACTGGATATGTTGTGTTTTACAGTATTATGTA GTCTGTTTTTTATGCAAAATCTAATTTAATATATTGATATT TATATCATTTTACGTTTCTCGTTCAACTTTATTATACATAG TTG
attR4	CAACTTTGTATAGAAAAGTTGAACGAGAAACGTAAAATG ATATAAATATCAATATATTTAAATTAGATTTTGCATAAAAA ACAGACTACATAATACTGTAAAACACAACATATCCAGTC ACTATGG

7.5.1 Appendix E1 *kiaa0319* human promoter

Table 7.12 The components and the volume needed for the multisite recombination creating a pDest-Cherry-*kiaa0319* destination vector

COMPONENT	VOLUME
p3E-mcs1 [124 ng/μl]	1.2 μl
p5E-MCS- <i>kiaa0319</i> [209 ng/μl]	0.7 μl
pME-cherry [99 ng/μl]	1.5 μl
pDestTol2pACryGFP [350 ng/μl]	0.4 μl
TE buffer	4.2 μl
TOTAL	8 μl

7.5.2 Appendix E2 Positive control HUMAN

Table 7.13 The components and the volume needed for the multisite recombination creating a pDest-Cherry-hUBI destination vector

COMPONENT		VOLUME
p3E-mcs1 [124 ng/μl]		1.2 μl
p5E-mcs_hUbi [105 ng/μl]		1.4 μl
pME-cherry [99 ng/μl]		1.5 μl
pDestTol2pACryGFP [350 ng/μl]		0.4 μl
TE buffer		4.5 μl
TOTAL		8 μl

7.5.3 Appendix E3 Positive control ZEBRAFISH

Table 7.14 The components and the volume needed for the multisite recombination creating a pDest-Cherry-zfUBI destination vector

COMPONENT	VOLUME
p3E-mcs1 [124 ng/μl]	1.2 μl
pENTR5'_ubi [177 ng/μl]	0.8 μl
pME-cherry 2 [99 ng/μl]	1.5 μl
pDestTol2pACryGFP [350 ng/μl]	0.4 μl
TE buffer	4.1 μl
TOTAL	8 μl

7.5.4 Appendix E4 Negative control

Table 7.15 The components and the volume needed for the multisite recombination creating a pDest-Cherry-MCS destination vector

COMPONENT	VOLUME
p3E-mcs1 [124 ng/ μ l]	1.2 μ l
p5E-mcs [150 ng/ μ l]	1 μ l
pME-cherry [99 ng/ μ l]	1.5 μ l
pDestTol2pACryGFP [350 ng/ μ l]	0.4 μ l
TE buffer	3.9 μ l
TOTAL	8 μl

7.5.5 Appendix E5 Catalogue of multisite recombination plasmids

7.5.5.1 Appendix E5.1 *pME-Cherry*

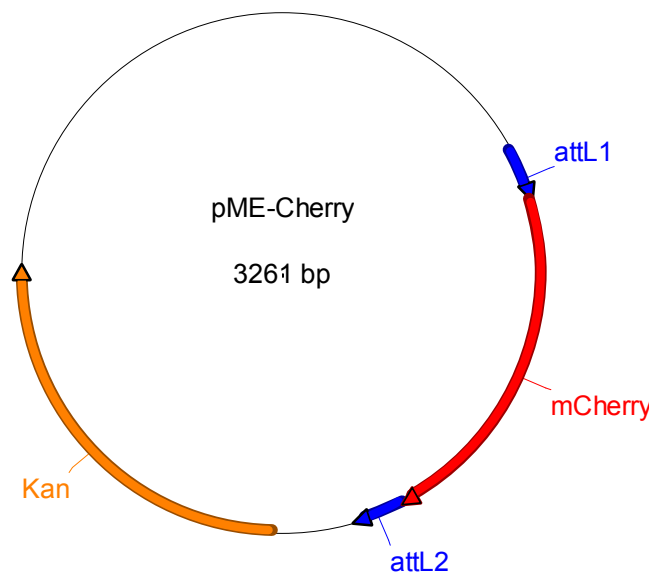


Figure 7.7 A pME-cherry vector

The 3261bp vector contains Kan resistance (orange) and an mCherry cassette (red), flanked by attL1 and attL2 recombination sites (blue).

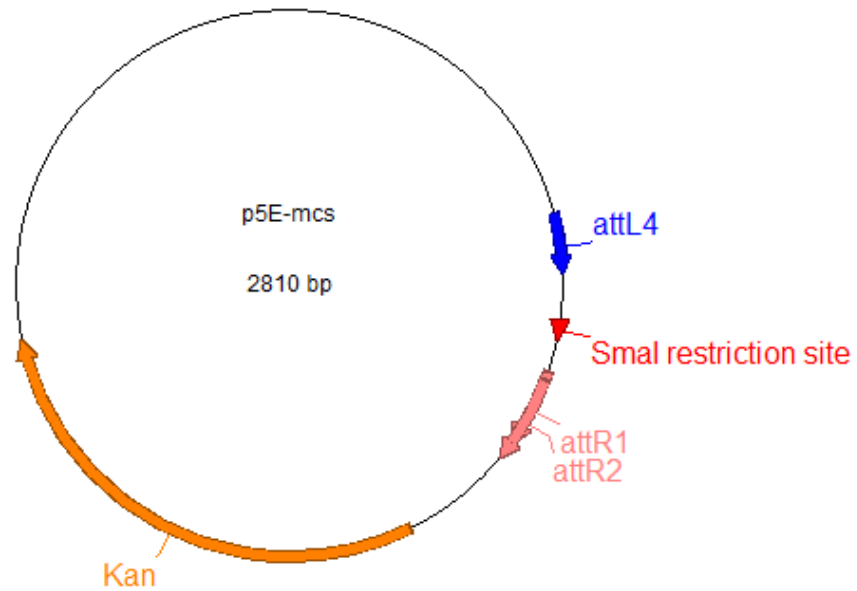
7.5.5.2 Appendix E5.2 *p5E-MCS*

Figure 7.8 A p5E-MCS vector

The 2810bp vector contains Kan resistance (orange) and a SmaI restriction site (red). It contains attL4 (blue) and attR1 and R2 (pink) recombination sites.

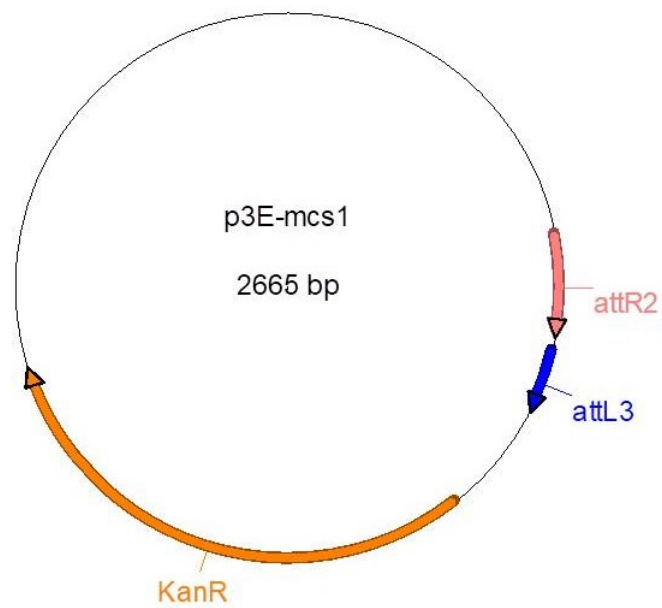
7.5.5.3 Appendix E5.3 *p3E-mcs1*

Figure 7.9 A p3E-mcs 1 vector

The 2665bp vector contains Kan resistance (orange) and a attL3 (blue) and R2 (pink) recombination sites.

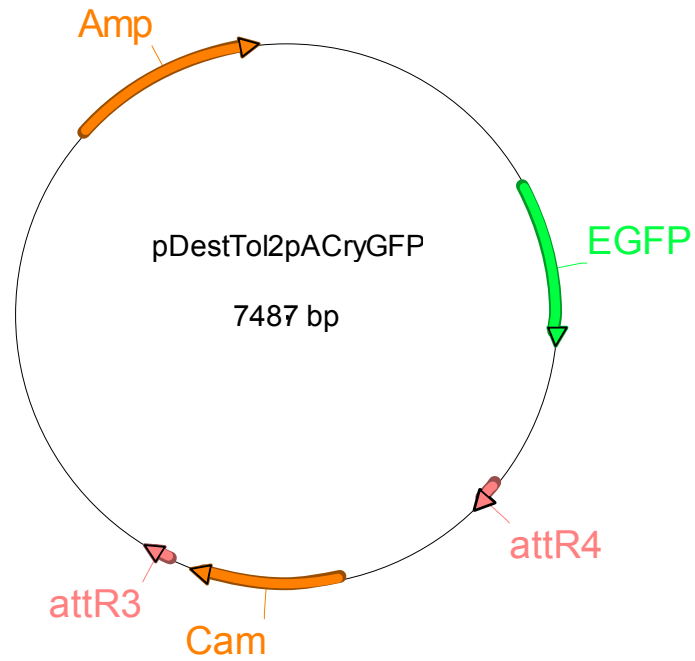
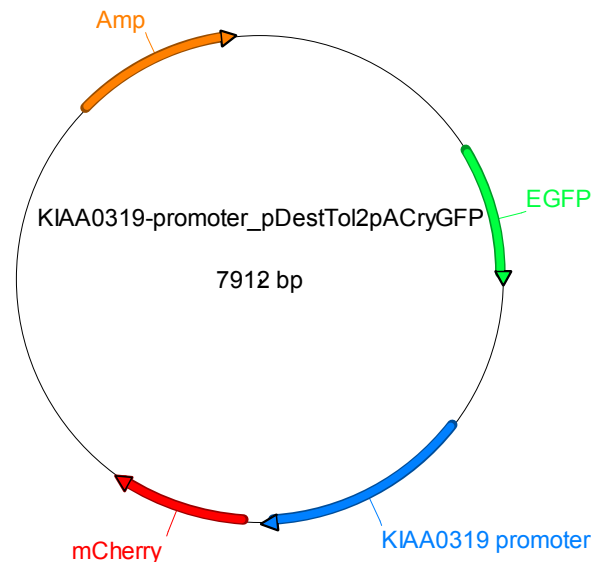
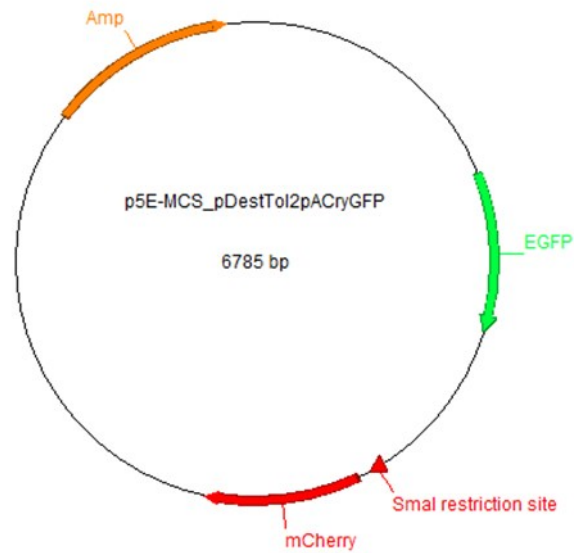
7.5.5.4 Appendix E5.4 *pDestTol2pACryGFP*

Figure 7.10 A *pDestTol2pACryGFP* vector

The 7487bp vector contains Kan and Cam resistance (orange) and an EGFP cassette (green). It contains attR3 and attR4 recombination sites (pink).

7.5.5.5 Appendix E5.5 *kiaa0319*-promoter pDestTol2pACryGFP**Figure 7.11 A *kiaa0319*-promoter pDestTol2pACryGFP destination vector**

The 7912bp vector contains Amp resistance (orange) and an EGFP (green) and mCherry (red) cassettes. The mCherry is driven by the human *kiaa0319* promoter (blue).

7.5.5.6 Appendix E5.6 p5E-MCS_pDestTol2pACryGFP**Figure 7.12 An empty p5E-MCS pDestTol2pACryGFP destination vector**

The 6785bp vector contains Amp resistance (orange) and an EGFP (green) and mCherry (red) cassettes. SmaI restriction site is indicated with an arrowhead (red).

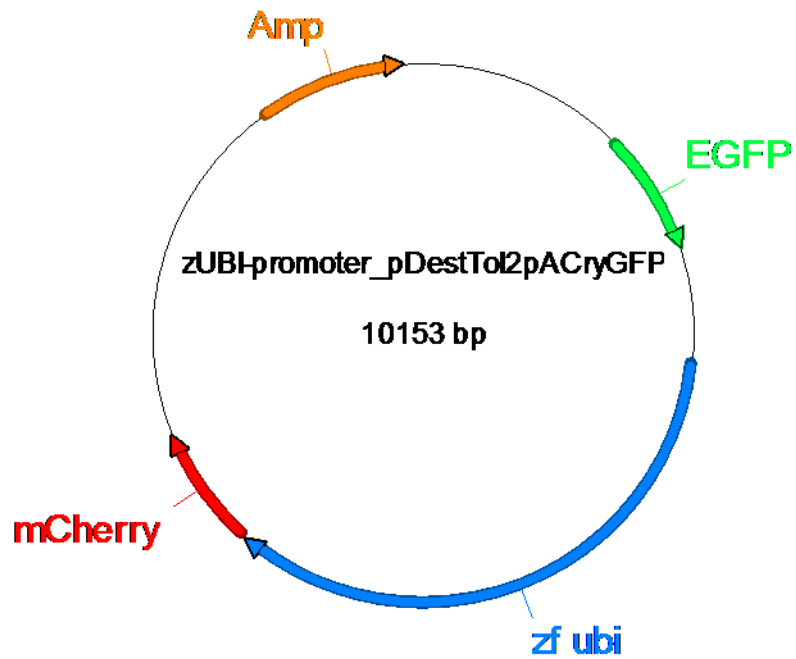
7.5.5.7 Appendix E5.7 *zUBI-promoter pDestTol2pACryGFP*

Figure 7.13 A zebrafish ubiquitous promoter in destination vector

The zebrafish zUBI-promoter pDestTol2pACryGFP is a 10153bp vector contains Amp resistance (orange) and an EGFP (green) and mCherry (red) cassettes. The mCherry is driven by the zebrafish ubiquitin promoter (blue).

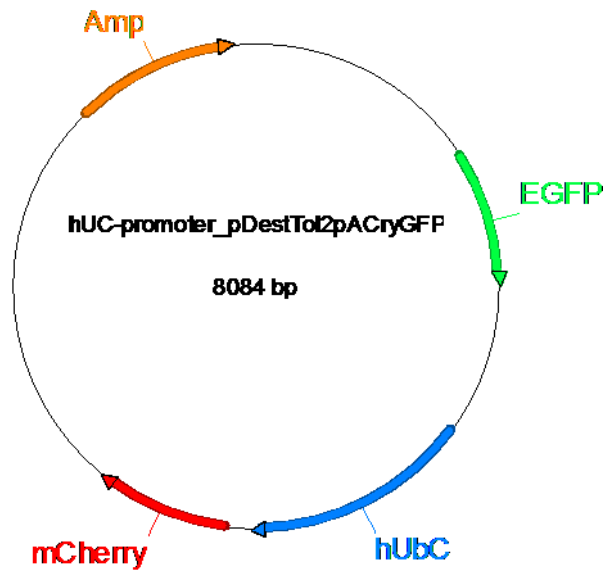
7.5.5.8 Appendix E5.8 hUC-promoter pDestTol2pACryGFP

Figure 7.14 A human ubiquitous promoter in destination vector

The human hUC-promoter pDestTol2pACryGFP vector is a 8084bp vector contains Amp resistance (orange) and an EGFP (green) and mCherry (red) cassettes. The mCherry is driven by the human ubiquitin C promoter (blue).

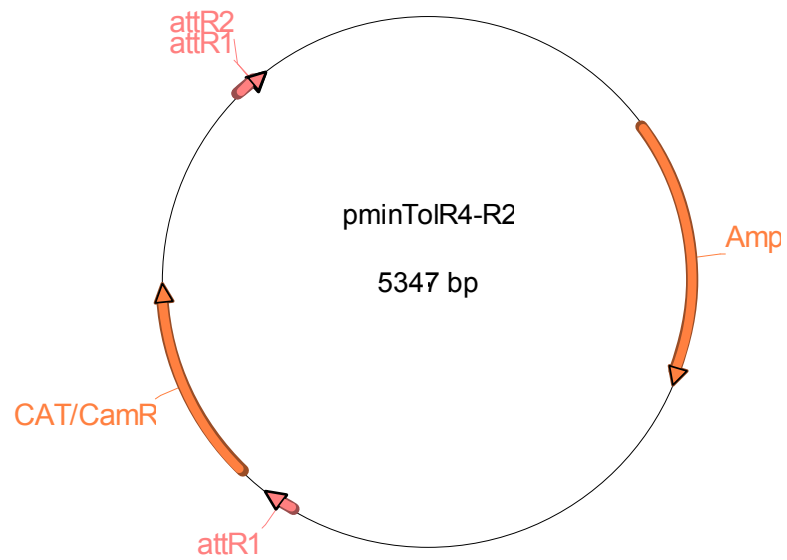
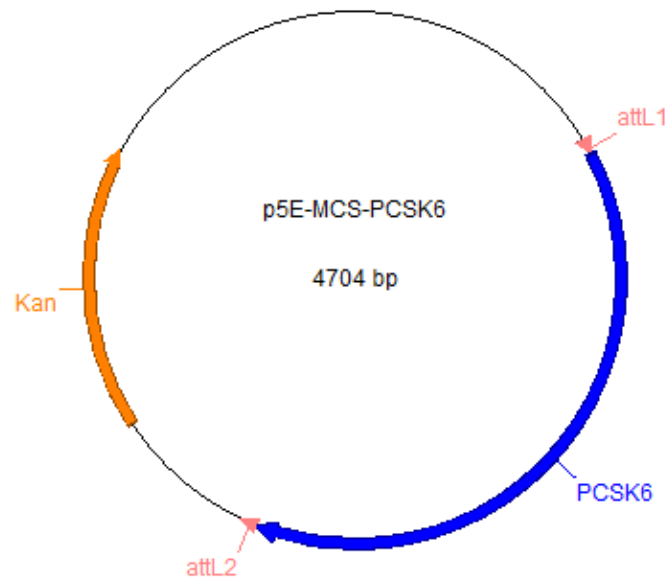
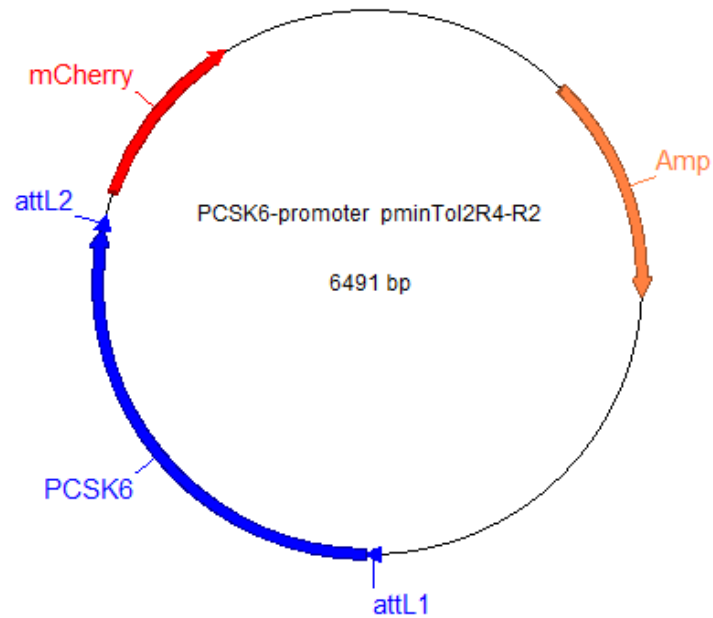
7.5.5.9 Appendix E5.9 *pminTol2R4-R2*

Figure 7.15 A *pminTol2R4-R2* vector

The 5347bp vector contains Amp and CAT/CamR resistance (orange). It contains attR1 and attR1/R2 recombination sites (pink).

7.5.5.10 Appendix E5.10 p5E-MCS-PCSK6**Figure 7.16 A p5E-MCS-PSK6 vector**

The 4704bp entry vector contains Kan resistance (orange). It contains attR1 and attR1/R2 recombination sites (pink) flanking a human *PCSK6* promoter sequence (blue)

7.5.5.11 Appendix E5.11 PCSK6-promoter pminTol2R4-R2**Figure 7.17 A PCSK6 promoter pminTol2R4-R2 vector**

The 6491bp destination vector contains Amp resistance (orange) and an mCherry (red) cassette driven by the human PCSK6 promoter (blue). It contains att/L1 and attL2 recombination sites (blue arrowheads).

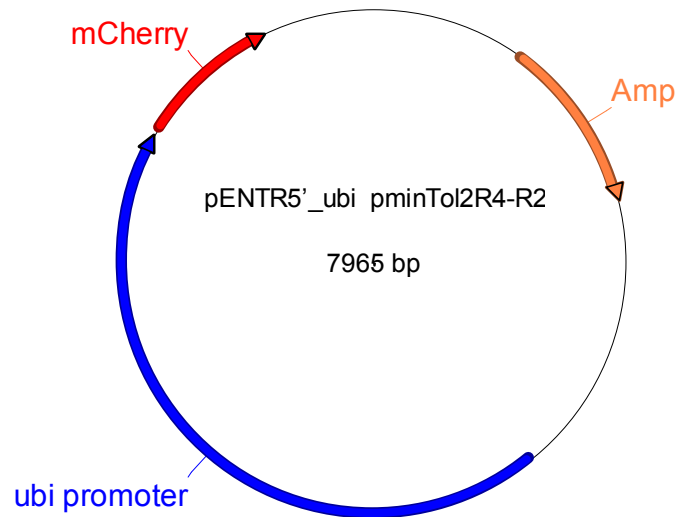
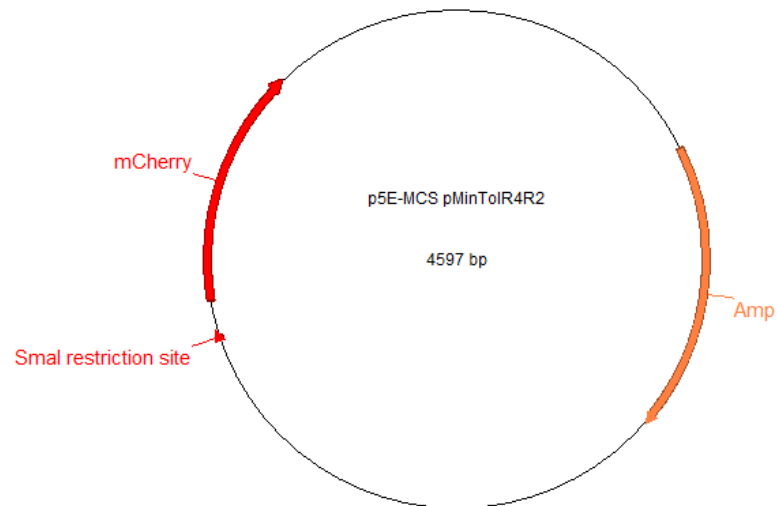
7.5.5.12 Appendix E5.12 *pENTR5'_ubi pminTol2R4-R2*

Figure 7.18 A zebrafish ubiquitous promoter in pminTol2R4-R2 destination vector

The zebrafish zUBI-promoter pminTol2R4-R2 is a 7965bp vector containing Amp resistance (orange) and an mCherry cassette (red). The mCherry is driven by the zebrafish ubiquitin promoter (blue).

7.5.5.13 Appendix E5.13 p5E-MCS pMinTolR4R2**Figure 7.19 An empty p5E-MCS pMinTolR4R2 destination vector**

The 4597bp vector contains Amp resistance (orange) and mCherry (red) cassette. There are no promoters. SmaI restriction site is indicated with an arrowhead (red).

7.6 Appendix F

kiaa0319 Knock out – CRISPR/Cas9

7.6.1 Appendix F1

Table 7.16 The list of primers used to create oligo duplexes for gRNA

Construct name	number	sequence	Enzyme
81	T780	ATAGGGGCCTGCTGTGATCTCCC	SmaI/XmaI
	T781	AAACGGGAGATCACAGCAGGCC	
85	T784	ATAGCTCCTCGAACCAGGGACTGC	PstI/SfcI
	T785	AAACGCAGTCCCTGGTTCGAGGAG	
89	T788	ATAGAGATCCTTCATGGGATCCT	BamHI
	T789	AAACAGGATCCCATGAAGGATCTC	

7.6.2 Appendix F2

Table 7.17 List of primers for PCR genotyping of CRISPR/Cas9 injected embryos

Construct name	number	sequence	Sequence length
81	T782	GCAATTGTGCGGTGAAGAGA	555
	T783	CAGAGGCTGCCAATGGTTTG	
85	T786	TCTGAAAGCGTGGTGTCTCC	566
	T787	GCTACTTTCAACAGGGCCCT	
89	T790	TGTGACCTGGCCTGGTTTTT	461
	T791	GCTACTTTCAACAGGGCCCT	

7.6.3 Appendix F3 *kiaa0319* Knock down – Morpholino

7.6.3.1 Appendix F3.1 *Morpholino sequences in kiaa0319* genome

GTCTTTATCTGCTGACACTCCCTCCCGCAGACAAACACACACACCTCAGCATCTTTCCAGCTATATCAGAGCTTTCATTACA
 AGATCATTGCCGCAATATCAGCTCTTACCACAGCTTTAGTTTACTCCATCAGCTTGTGTCCAGCACGAATTCGCCATGGAGTA
 GCAGCACGGAAGCAGATCTCGATATCATGAAACAGATGCTTGAATAAGAGCGTCACATCCCTCTGgtactgtaggctacagctaaaacta
 atacattttgatgcttcccaagGGTTGAAGA**CGTAAAGCTGCTGAGAAATCATCTCT**TGTGAAAAGCGCGCAGTGGCATCATGAACTTCT
 TACCAGTCTTTCACCTTTGATACTCTTATGTATCAGAGgccaagtataaaattctgattattctgtttattgtggccattcagTATCAGGACAGTGTGG
 CAGGCCCAACTACTCTGAAAGCGTGGTGTCTCCGGAGCTGAGGAGCAGAGTATTTACGTGTCCCGGATGTGTCTGCCCT
 GGCTCAGTGTGCCGGGGCTGTGTGATCTCCCGGGTGTGACCTGGCTGGTTTTTTGAGCACCGGATGTGTCTCAGTTG
 TCAGCACAGAAAACCTGCCAGCCGAAGAAGAGACTGGTACAGACTCTTACCTGGCTTCCTGCAACGTGGGCCCCCAAA
 ACACTGTCTCAGTCCCTGGTTCGAGGAGAGTCTTTCCAAACCATTGGCAGCTCTGGCCAGACACCGGGGATCCGAGGA
 TCCCATGAAGGATCTCGCTCTGCTTGAAGGATTCAGGATTCGGACAACCTGAGCTGAGTATGCAGAGAGTTTTCGAAGTT
 TGAAGACAAAAGAGCTGAAGACATAGACCTAAAAGCGGTAGAGCAAGAAGAGCAAATGGGCTTTATGATTGGCCACTG
 TTCAAAGAAAAGAGGAATTAACCAATCAGAGACGGAGAGAGGCAGTAAAAGATTGACAACGTTCAGGGCCCTGTGAAA
 GTAGCACCATTACCCAAGTCACTTTTCAAGAGAGAAAATGAAAGCAGATCAACCATTATTGAAGCAGAATCTAATGTTAC
 GGTACCATCAACCCTGTATTTGACATTAAGgtgagatttttttaagataatgaatagaacacttttatcattaagGTTGAAGAAGAGCCACAGAACAC
 ATCGTCTGCAACTACTGCACCTAAAGTCGTGGAAGACCTCAGTACAGAGACCGCAAACCTTGTGCAGTCAACGGTTCATTCA
 TCACTCCAGCCAACACTGAAGTACACCGCAGATGACTTCAAGACAGCCAGgtactgtgcgcaatattgggaaaagtctgttattctctctttgtcagTA
 AGAGCTGTACTGTGCCATTGAAGGCCCTGTTGAAGCCTGCTGCCCCAAAACACTGTTAAACTAACAGCTTTAGTTAGTCC
 AGATGTACTGCCGgtacgacctctacattctgaatttttttttaatttcaattctctagAATCTCCTTACACATATGAGTGGACTTTTGTGATCTCACCAGA
 AGGACAACGTAGGGTGTAGGAGGGGACGACAACAACTGTCTACTTTCTGAAgtgagatttaattcatttaatacacagatttctgtatctttatcca
 gCTGTGAGAGGGTGTACACGAGTCAGAGTGTATTGAAAGCACATCAAGCATATGGAGAAGTTCGTGGACTTGACCGTAC
 ACCCTGgtacaactataacctctttgcatcaaatggcttctctttcaattctacagCAGAGAAAATAAACAAGCCCTCTAAAGCAGTCTTCTCCCAAGAGCC
 AAGATGTGCTGTTCAAAAAGATTCTGTCTTAATCATTAAACGGAAGTgtatgtggcctgtttctttttctgttttaactaaattgcatccagAGAGTAT
 GGATGATGCAGGGATTGTCAGTTATCTGTGAAAAAGGTGGACGGCCGTTTTGGACACCTGAAGGTCTGTTAACAACCT
 GTACTGCAGCTGAAAAATCTTTTACCTGGAGAATATACCTTCGAgtaaaggactttgtttacaaaaactgattttgcttggctacattagGCTGCAGTG
 TCTGATCTGAGGGGCTGAGCGACTCCAGCACTGCCACCTTGAGGGTCAGCATCCCAAAAGATGAGCCTCCTCTGGCCAGAG
 CGGGCACAGACCGGGTCAATACCCTGCCTCAACCACCTACCTGTGGGGAAACCAAAGCACAGATGACCAGGCCATTAC
 AAGTACCTTGGACTCCATCCCAGCAGCCGACCCGAAAGGTACCATGCAGgttaattagatcttacttaccagatgtttcatalgtctccattta
 gGATGTGAGATCAGCATTCTGTAGTCTGTACTGTAGAGGGGTCAGTACACGTTTCAGCTCACAGTCACTGACTCAAGAG
 GTCAACAGGATTCAGACACCATCTCTGTACTGTGCTGCTGTgtaaaacacacccccggccaataagttgacattttattattgtggcagCAAACAGAGCA
 CCAGTGGCTGTAACAGGACCAGACATACAGTACTCTGCCGTCAACAGCATCACACTGAATGGCAGCGGCAGCACTGATG
 ATCAGCCATCAGCAGATACCAGTGGGACGTGATGAGgtattgtttattattattatttctctcttatataatgatgaagTGGCCCTCCAGGCTTGAAG
 ATGAAAGATGCCAATAAAGCGGTTGCCATCGCAGACGGCCTGAGATCTGGGATTTACAAGTTGAAGTTGACTGTGGTGGATG
 AGCAGGGAGAAACAGACAGTGCAGTCTGAGCATCACAGTTAAAGAAAGgtgagctgaaacatgcacatgcataaacagttctaatgttaaatcacagCTA
 AAAGCCTGCCACTGGTGGCTCATGCCAGCGGCAGCCATACACTACTTTGCCAACAACTCTCTGGTGTCTCAGAGTTGATG
 TCCAACAGCGGACCAGCAAACGTGTCTTTCTGTGGGTTAGAGATGAACAGAGCCCTGTGCGGGGgtgagtgatattgttgattgtttttgttt
 tcacatctttgagagtagGATGTGTTGATGGTTCAGATCACGAGCCCTCGCTTTACCTTGCCAACCTGGTAGAAGGAACATACCTGTTC
 CAGCTGCGGGTACCGATGTCCAGGGCCGCTCAAGCACGGCTACAGCCACTGTGGAAGTACGACCTGgtaaatattacttacttttaataaggc
 tttttgtgatattgatgtcagAT**NC**CGCTGAGC**NA**AGAGGAGGTGGAACCTTGAGCTGCAGGTGAGCGTGGCTCAAGTCAGTCAGCAACAGA
 GAGACACAGTATCAGACAGCTGGCCGCACTTCT**NC**ATGTGTTGACTCAGACATCGCACTAAAGGCTCTACATGGACAGTC
 TGACATCAGgtacagtacatctcacacattagccttataaatgtgectctctgttttagCACAGTATTCAGGTTCTCGGTGACGGGTCCTGATGGTTTATCCC
 TGGCCCTAAACTTGCCCGCTGTGAGAAACAGCTGTTGAGAGAGAAAAGCGACTTCTGTCTTTAGGGTCTTAAGAGTGG
 ACACAGTCAgtgagtgacttgaatcctttactaataatattatcttaataagaaactcagTGTTGTTGTCTGTGTTCTGGCGGTGGTCACTGTGACCCATTAC
 AAAAAGCTGTCTCTGTGACCTCTGTGGATGGAGAACCCATCCGCTCTTCATAGACGATGGAGAGAGCAATTGTGgittatgatga
 cctttctatttaactgagatgctgtgctctctcagACTGGAGTGTGCTGATGTGCAAACTCTTGTGTTTGTGACAATCATTTTCATCTGTCCGT
 CAGCTGGATCTGCGTCTGCTGTGTAAGgtgataaagggtttatcgtcattatgtgtgtgtgtttgtctcttccagACATTAACACAGAAGCACAGAGC
 ACAACTCTAGCCTGATGATGCTGAATCAGAGCTGGACAGTGAACAGGACAACATTTACAATTACGGGAGAGTCCAAAAAGC
 TCATAACAGAATCAGAAACGGAGACACTCTCAGCCTTTGCCCTGTGGAGAGTTGAGTCGCATGGACAAAAGGACATTTCTC
 ATCGTGGATACTTGCAGCACAGGGGTATTGCTGAATTTACCACTAATACAAAAGACAGACAGAATTGAATG

Figure 7.20 The location of morpholino sequences in zebrafish *kiaa0319* gene

Turquoise colour represents translational blocking morpholino (TB MO) sequence located between the 5' UTR and exon 2. Green colour represents TB2 located upstream of TB. Blue colour represents exon sequences, grey are intron sequences, brown are UTRs. Missense and synonymous variants are labelled yellow and green respectively.

7.6.3.2 Appendix F3.2 Comparison of single to co-injected TB MOs survival rates

Table 7.18 The survival rate and the number of embryos exhibiting phenotype of embryos injected with TB1 MOs, TB2 MOs and a coinjection of both MOs at a 100 μ M concentration

Concentration	MO	#Dead 1dpf	#Dead 5dpf	#Live 5dpf	%live 5dpf	#Phenotype
100 μ M	TB1	37	1	112	99.1	0
	TB1©	24	2	123	98.4	4
100 μ M	TB2	18	0	155	100.0	1
	TB2©	35	0	132	100.0	1
100 μ M	TB+TB2	38	2	129	98.5	2
	TB©+TB2©	33	0	138	100.0	1

7.6.4 Appendix F4 Sequence alignment of Kiaa0319 protein and Kiaa0319-like protein against the peptide sequences of the chosen antibodies.

7.6.4.1 Appendix F4.1 Zebrafish Kiaa0319 protein sequence

MNFLPVLSLLILLCIRVSGQCWQAATYSESVVPELRSSSILRVPDVSSLAQCAGACCDLPGCDLAWFFEHRCYVL
 SCQHTENCQPKKRPGETSYLAFLQRGPPQTLVLQSLVRGESFPNHWQPLARHRGSEDPMKDLALLEGIQSDNPE
 PEYAESFRSLEDKRAEDIDLKAVEQEEQTGLYDWPPVQRKEEFNQSETERGSKRLTTVQGPVVESTITPSHLSEERN
 ESRSTIIEAESNVTVPSTTVFDIKVEEPPQNTSSATTAPKVVEDLSTETANFSAVNGSFITPANTEATPQMTSEQPVR
 ALTVSIEGPVEAMLPQNTVKLTALVSPDDTAESPYTYEWFVISPEGQRRVMEGQHNSVILSELSEGVIYAVRVIV
 KAHQAYGEGSVDLTVHPAEKINKPPKAVVLPKSDVLFKDKSVLIINGSESMD DAGIVSYLWKKVDGPFWTPEGP
 VNKPVQLKNLLPGEYTFELTVSDSEGLSDSSTATLRVSIPKDEPLARAGTDRVITLPLNHLTLWGNQSTDDQAIT
 SYLWTLHPSSPTRKVTMQDVRSAFLLVSDLEEGQYTFQLTVTDSRGQQSDTISVTVLPANRAPVAVTGPDQLLL
 PVNSITLNGSGSTDDQAISRYQWDVMSGPPGLKMKDANKAVAIATGLRSGIYKLLKLTVVDEQGETDSAVLSITVK
 EAKSLPLVAHASGSHTLTLPNNSLVLRGVSNVSGPANVSFLVWRDEQSPAAGDVLYGSDHEASLYLANLVEGTYL
 FQLRVTDVQGRSSTATATVEVRPDPREEREVELELQVSVAAQVQQQRDTVIRQLAALLHVLDSDIALKALHGQSD
 ISTVFRFSVQGPDLIPGPKLARLLRNQLLREKSDFLFRVLRVDTVMCLLLCSGRGQCDPITKSCSDPLWMENPI
 RLFIDDGESNCDWSVLYVTISCFVTIIFILSVSWICVCCCKRH

7.6.4.2 Appendix F4.2 Zebrafish Kiaa0319-like protein sequence

MPNVELRMHRWKWQTRFTSLYLSCVYLLCSVSGVSGSICSVTGGVLGIIHSSVIGLWQPLAVDQGGSRCWESC
 CLEPSCGAVVSLGGRCVLLACSQRETCGISSLPQPHVESLGLLQLLNKSRRKTRSAQDIRAIRDTEQDMSSNPSEP
 LTTSNSAASSSSSSEQTAEHNTLSDAANHSTLNNSNQSPQSTVAPATTPAVTVRELVVSAGQNVEVTLPRNEV
 KLSAYVVPAPPTGTNYDFDWRILITHPKDYSGEMEGKHTMTLKLKSLTVGLYEFVVDGEGAHGEGYVNVTVK
 PEPRVKNPPVAVVSPKYQEISLPTSSTVIDGSRSTDDDKVVLWHWEEVKGPLREEKASGDTDILTTLNLVPGNYTF
 SLTVTDSGDAQNSTQAMLLVNKATDYRPTANAGPNQVITLPHNYITLNGNQSTDDHDNLSYEWLSPEKGGKVV
 EMQGVRTPTLQLSAMQEGDYTFELTVTDSGQDQTQVTVIVQPENNPVADAGPDKELTLPVDHTLTDGGKS
 TDDQKIVTYHWKKTGPEGVKLDNAETVVATVTGLQEGEYIFMLTVTDERNLESSDTVSVIVREENDQPPVAKV
 VSSPPITLPVRTAVLDGSRSSDDKGSISYLWRENSPAAGDVLNHSQHQAFLGFLGVLVEGKYSFTLTVTDSKGGT
 SSDSGVVDVRPDVYERDLVELILEVAVAQVSRQKDMYIRQVGVLLGVLDSDITIREISAFNEHSTRLVFLVSGGP
 GRPPLTGHSVAMELRNFRKQKNEFLIFKARRVDTVICQLNCSGHGECDSFTRRCVCHLFWMENLFSTYFGDAES
 NCEWSVLYVTIASFMIVVAIATVIWGLVCCRRRKSQVRRKSRKMLNEDDQETMELKLRPGRKLSVPAPTSSA
 LMHSDSDLESDDGQAGIPWSDRERGRKLLPPQNGSLRNGQGPHPKPKKTREELL

7.6.4.3 Appendix F4.3 Pairwise sequence alignment for R7, 70 and Abcam anti-KIAA0319 antibody

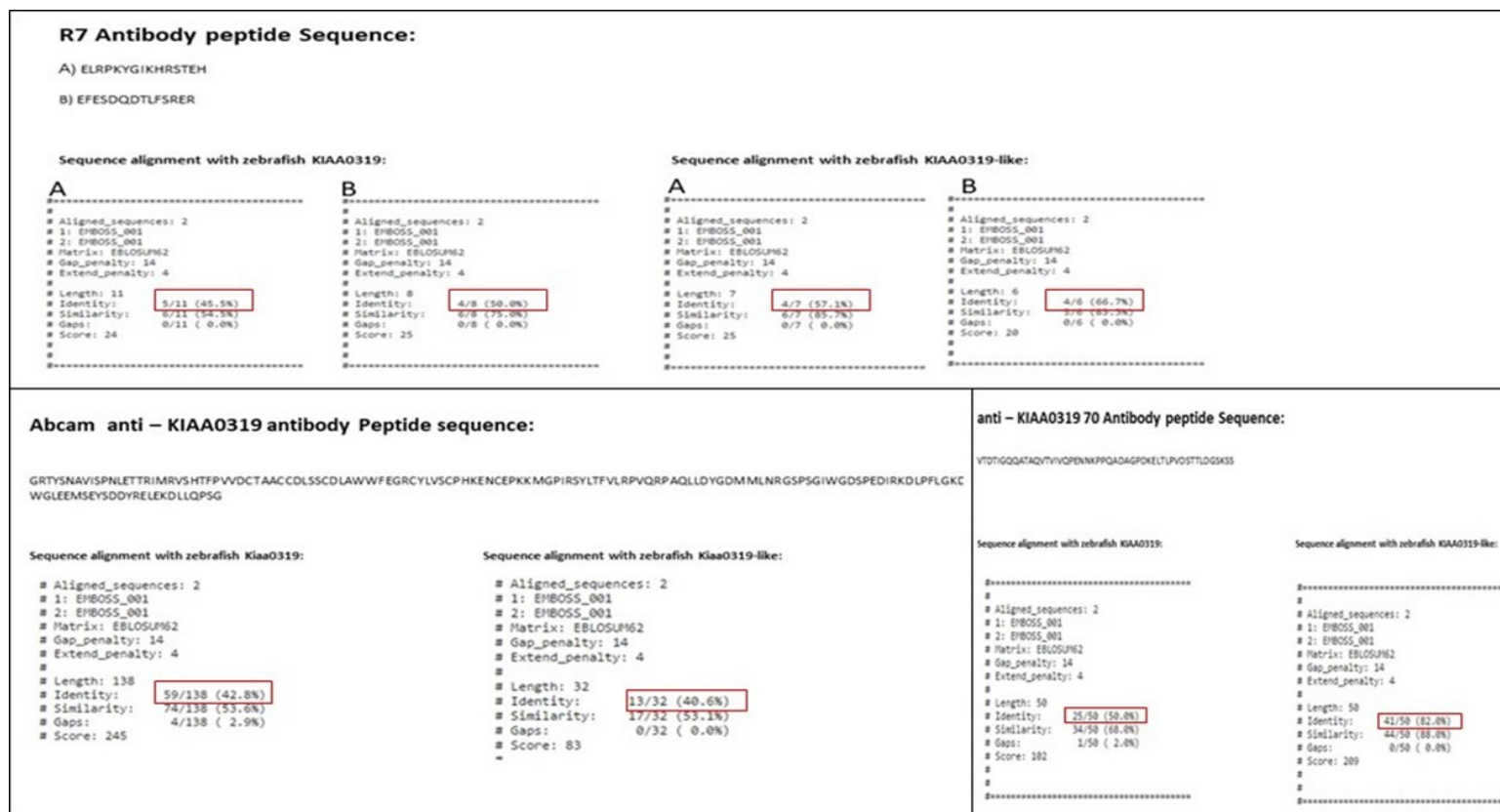


Figure 7.21 Pairwise sequence alignment for R7, 70 and Abcam anti-KIAA0319 antibody

The anti-KIAA0319 R7 antibody consists of 2 peptide sequences (A, B), which are 45.5% and 50.0% identical to the Kiaa0319 sequence and 57.1% and 66.7% identical to Kiaa0319-like sequence. The Abcam anti-KIAA0319 antibody exhibits 42.8% identity with Kiaa0319 protein sequence and 40.6% identity with Kiaa0319-like sequence. The anti-KIAA0319 70 antibody is in 50% identical to the Kiaa0319 sequence and 82.0% to Kiaa0319-like protein sequence.

7.7 Appendix G

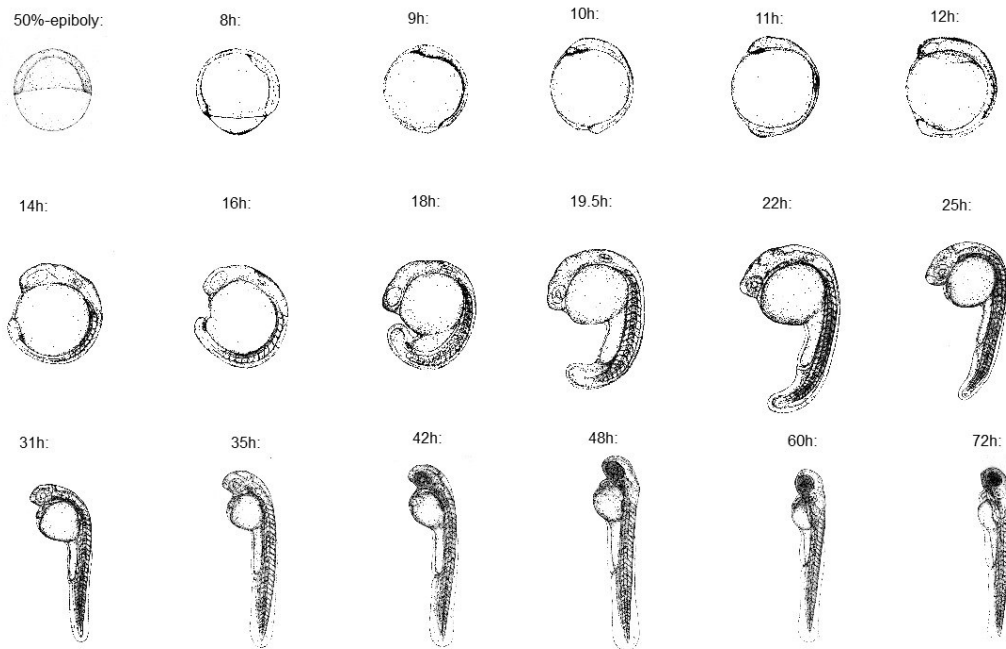


Figure 7.22 Zebrafish developmental stages as per Kimmel et al (1995)

Developmental stages of zebrafish embryos ranging from 50% epiboly to 72 hours post fertilisation. [Kimmel et al., 1995a]

8 PUBLICATION

The dyslexia susceptibility *KIAA0319* gene shows a specific expression pattern during zebrafish development supporting a role beyond neuronal migration.

Monika Gostic^{1,2}, Angela Martinelli^{1,2}, Carl Tucker³, Zhengyi Yang⁴, Federico Gasparoli¹, Jade-Yi Ewart^{1,5}, Kishan Dholakia^{4,2}, Keith Sillar⁵, Javier A. Tello^{1,2}, and Silvia Paracchini^{1,2*}

¹School of Medicine, University of St Andrews, St Andrews, KY16 9TF, UK

²Biomedical Sciences Research Complex, University of St Andrews, North Haugh St Andrews, KY16 9ST, UK

³College of Medicine and Veterinary Medicine, The University of Edinburgh, Edinburgh EH16 4TJ, UK

⁴SUPA, School of Physics and Astronomy, University of St Andrews, St Andrews, KY16 9SS, UK

⁵School of Psychology and Neuroscience, University of St Andrews, St Andrews, KY16 9JP, UK

*Correspondence to: Silvia Paracchini, sp58@st-andrews.ac.uk

Abstract

Dyslexia is a common neurodevelopmental disorder caused by a significant genetic component. The *KIAA0319* gene is one of the most robust dyslexia susceptibility factors but its function remains poorly understood. Initial RNA-interference studies in rats suggested a role in neuronal migration whereas subsequent work with double knock-out mouse models for both *Kiaa0319* and its paralogue *Kiaa0319-like* reported effects in the auditory system but not in neuronal migration. To further understand the role of *KIAA0319* during neurodevelopment, we carried out an expression study of its zebrafish orthologue at different embryonic stages. We used different approaches including RNAscope *in situ* hybridization combined with light sheet microscopy. The results show particularly high gene expression during the first few hours of development. Later, expression becomes localised in well-defined structures. In addition to high expression in the brain, we report for the first time expression in the eyes and the notochord. Surprisingly, *kiaa0319-like*, which generally shows a similar expression pattern, was not expressed

in the notochord suggesting a role specific to *kiaa0319* in this structure. This observation was supported by the identification of notochord enhancers enriched upstream of the *KIAA0319*, both in zebrafish and in humans. This study supports a developmental role for *KIAA0319* in the brain as well as in other developing structures, particularly in the notochord which is key for establishing the body patterning in vertebrates.

Keywords: dyslexia, neurodevelopment, zebrafish, KIAA0319, gene expression, notochord.

Introduction

Developmental dyslexia is a specific impairment in learning to read in the absence of any other obvious impairing factors. It affects at least 5% of school-aged children and its heritability is estimated to be above 60% [Shaywitz and Shaywitz, 2005]. Studying the genetic contribution to dyslexia may help to dissect the underlying neuropsychological mechanisms, which remain hotly debated [Goswami, 2014]. While a phonological deficit is the most commonly accepted cause for dyslexia, sensory dysfunction in the visual and auditory systems have also been observed in a number of studies [Ramus and Ahissar, 2012; Shaywitz and Shaywitz, 2005; Goswami, 2014].

The *DYX1C1*, *DCDC2*, *ROBO1* and *KIAA0319* genes are known as the classical dyslexia susceptibility genes and they are supported by a number of independent replication studies [Newbury et al., 2014; Carrion-Castillo et al., 2013]. A role in cortical development, and specifically in neuronal migration, has been proposed for these genes [Paracchini et al., 2007], in line with earlier *post-mortem* observations that reported subtle cortical defects in individuals with dyslexia [Humphreys et al., 1990; Galaburda et al., 2006]. In particular, *KIAA0319* variants have been found to be associated with dyslexia and reading abilities in multiple clinical and epidemiological cohorts [Paracchini, 2011; Newbury et al., 2014]. A specific dyslexia-associated variant was shown to affect *KIAA0319* transcription regulation and gene expression levels, providing a mechanism to link genetic variation with the disorder [Dennis et al., 2009; Paracchini et al., 2006b]. Its paralogous gene, *KIAA0319-LIKE* or *KIAA0319L*,

has also been reported to be associated with dyslexia but with weaker evidence [Couto et al., 2008]. Both *KIAA0319* and *KIAA0319L* are transmembrane proteins [Velayos-Baeza et al., 2007], but their exact cellular functions remain unclear.

A new role in cilia biology is emerging for dyslexia candidate genes [Brandler and Paracchini, 2013; Paracchini et al., 2016b]. A transcriptome study showed differential regulation for *KIAA0319*, *DCDC2* and *DYX1C1* in ciliated tissues [Ivliev et al., 2012b]. Functional studies for *Dyx1c1* and *Dcdc2* showed a role in ciliogenesis in different biological models, including zebrafish, [Tarkar et al., 2013a; Chandrasekar et al., 2013; Massinen et al., 2011b] and some patients with ciliopathies have been found to harbour mutations in both genes [Schueler et al., 2015a; Tarkar et al., 2013a]. While there is no direct evidence supporting a role for *KIAA0319* in cilia, the presence of five PKD domains in *KIAA0319* lends support to this notion [Velayos-Baeza et al., 2008]. Mutations in PKD genes, which play key roles in cilia, lead to ciliopathies and laterality defects [Hildebrandt et al., 2011b]. *KIAA0319* has been shown to be a target of T-Brain-1 (TBR1), a transcription factor implicated in autism which regulates different brain developmental processes, such as neuronal migration, axon guidance [Chuang et al., 2015] and the determination of left-right asymmetries in bilaterians [Kitaguchi et al., 2002]. *KIAA0319* has been shown to be involved in axon growth and regeneration supporting a role in the adult peripheral nervous system [Franquinho et al., 2017].

Both *KIAA0319* and *KIAA0319L* have been implicated in neuronal migration following knockdown experiments that specifically targeted neurons at the early stages of brain development using *in utero* shRNA in rats [Peschansky et al., 2010; Szalkowski et al., 2012b; Adler et al., 2013; Platt et al., 2013; Paracchini et al., 2006b]. However, knockout (KO) mouse models do not display any cortical abnormalities that could be explained by defective neuronal migration [Martinez-Garay et al., 2017; Guidi et al., 2017]. Instead, the KO mice presented auditory system defects [Guidi et al., 2017] in line with observations reported in adult rats that underwent *KIAA0319* knockdown *in utero* [Centanni et al., 2014b, 2014a; Szalkowski et al., 2012b]. Therefore, while a role for *KIAA0319* in neurodevelopment is supported by different lines of evidence, its exact function remains largely unclear.

Here, we report a gene expression study for the *kiaa0319* gene in zebrafish to further understand the role of this gene during vertebrate development. We observed

a spatiotemporal expression pattern beyond the brain including in the eyes and the notochord. Surprisingly, *kiaa0319-like*, which presents a widespread expression in other species, was not expressed in the notochord, suggesting role specific to *kiaa0319*. These data support a role for *KIAA0319* both in the brain and in other structures and suggest for the first time a function in the notochord.

Materials and Methods

Fish care. All the experimental procedures were approved by the Animal Welfare Ethics Committee (AWEC) at the University of St Andrews in compliance with the Home Office regulations. All researchers who conducted work with animals held a Personal License issued by the Home Office.

Wild type zebrafish (*Danio rerio*) (WIK and AB/TU) and the double transgenic Tg(gfap:GFP);Tg(Oligo2:dsRed) were raised at The Queen's Medical Research Institute at the University of Edinburgh according to standard procedures in a Home Office approved facility. Developmental stages, maintained at 28.5°C, were identified as previously described [Kimmel et al., 1995b]. Animals were handled in accordance with the guidelines from European Directive 2010/63/EU and euthanised in accordance with Schedule 1 procedures of the Home Office Animals (Scientific Procedures) Act 1986. Zebrafish embryos were obtained using the Mass Embryo production system (MEPs) of the wild type line Wik.

PCR and qPCR. Total RNA from developmental stages between 16 – 32 cells, up to 120 hours post-fertilisation (hpf) was extracted using the RNeasy Mini kit according to the manufacturer's instructions (QIAGEN) using at least 50 embryos at each stage. The heart, liver and brain were dissected from five adult fish, flash-frozen on dry ice and stored at -80°C until the RNA was extracted. Eyes were dissected (N= 40 eyes total) at 48hpf stage and flash frozen on dry ice.

The PrimeScript RT reagent kit (Takara) was used to transcribe the RNA into the cDNA following the manufacturer's protocol. The presence of *kiaa0319* transcripts was verified by electrophoresis following PCR amplification. Gene expression was assessed by quantitative PCR (qPCR) conducted with the Luna Universal RT-qPCR Kit (NEB) and using a Vii7 instrument (Life Technologies, Paisley, UK). For protocol

details see Supplementary materials. Primer sequences and accession numbers are shown in Supplementary Table S1.

Whole-mount in situ hybridization (WISH). WISH was carried out following a previously described protocol [Thisse and Thisse, 2008]. Briefly, a DIG-labelled riboprobe targeting *kiaa0319* was transcribed using a T3 Polymerase with a DIG RNA Labelling Mix (Roche) according to the manufacturer's instructions and, as a template, a 1066 bp PCR fragment amplified from cDNA (Supplementary Table S1). Zebrafish embryos were collected and processed at 3 somite, 14 somite, 30 hpf and 48 hpf. Embryos were imaged with a Leica MZ16F or MZFLIII bright field microscopes following treatment with an anti-DIG antibody (Roche, diluted 1:5000 in blocking buffer) and a staining solution (NBT and BCIP, Roche).

RNAscope. RNAscope in situ hybridization (ISH; Advanced Cell Diagnostics) was modified from a previously described protocol [Gross-Thebing et al., 2014]. Samples were fixed in 4% PFA at room temperature for a length of time dependent on the developmental stage (Supplementary Table S2). Samples were hybridized with RNAscope target probes (*kiaa0319l*, nt 545-1425 of ENSDART00000051723.5, Channel 1; *myoD1*, nt 2-1083 of ENSDART00000027661.7, Channel 2; *kiaa0319*, nt 239-1147 of ENSDART00000160645, Channel 3) overnight at 40°C. Images were taken with a Leica TCS SP8 confocal microscope under 20x magnification and processed in Leica Application Software X (LAS X), unless otherwise specified. Light sheet microscopy (LSM) was conducted with a bespoke microscope built in-house (Supplementary Materials).

Sequence analysis. The zebrafish orthologues of the human KIAA0319 and KIAA0319L genes were identified in the zebrafish genome using the UCSC genome browser [Kent et al., 2002]. The 10kb regions upstream of the zebrafish and human *KIAA0319* (danRer10 chr16:36946809-36952809; hg38 range= chr6:24645946-24652021) and *KIAA0319L* (danRer10 range= chr19:4401525-44013525; hg38 range= chr1:35,557,338-35563413) transcription start sites (TSS) were scanned for the presence of *FOXA2* (a key regulator for genes expressed in the notochord [Tamplin et al., 2011]) consensus sequences (5'-T(G/A)TTT(A/G)(C/T)T-3') with the FIMO software [Grant et al., 2011].

Results

Exploratory analysis. As a first step of our analysis, we verified the expression of *kiaa0319* during early zebrafish development using RT-PCR (Figure 1A). The expression of *kiaa0319* was observed across all the developmental stages that were analysed. In the adult, expression was much higher in the brain compared to heart and liver, where it is barely detectable. The brain-specific expression pattern is consistent with the expression profile observed for *KIAA0319* in humans in contrast to *KIAA0319L* which is widespread across human tissues (Supplementary Figure S1). Quantification of expression by qPCR confirmed *kiaa0319* expression at different developmental stages and showed that the highest level was detected in the earliest stages of development (Figure 1B), whereas the lower expression was observed at 12hpf.

For an initial localization assessment we conducted WISH (Supplementary Figure S2). Consistent with the qPCR data, we observed high *kiaa0319* expression during the early stages of embryonic development (Supplementary Figure S2A). As development progresses, this widespread expression becomes restricted to specific structures. At the 14 somite stage (16 hpf), *kiaa0319* expression can be visualized in the developing brain and the body midline (Supplementary Figure S2A.3 and S2A.4). At 30 hpf, expression is detected in the eye, the otic vesicle and in the midbrain-hindbrain boundary (Supplementary Figure S2B). The midline expression appears localised to the notochord rather than the spinal cord. At 48 hpf expression becomes weaker in the eyes and otic vesicles and is more pronounced in the telencephalon (Supplementary Figure S2C). The WISH analysis therefore confirmed expression of *kiaa0319* both in the brain, as expected, as well as in other tissues where a role for *KIAA0319* was not described before.

RNAscope analysis. To verify this expression pattern and to achieve higher resolution, and specificity we used the highly sensitive RNAscope Fluorescent Multiplex Assay (Figure 2). In particular, we focussed on tissues other than brain. These included the body midline, the otic vesicles and the eyes following the observations made by WISH. For comparison, we included in the analysis the *kiaa0319-like* gene. Consistent with the qPCR and the WISH results, at 24 hpf *kiaa0319* expression is widespread but stronger in the brain and body midline (Figure

2A). Expression in specific structures, such as the otic vesicles was visible at 48 hpf. The *kiaa0319-like* presented a similar pattern of expression but, surprisingly, a much weaker signal was observed in the notochord (Figure 2B). Therefore, we further investigated the expression of *kiaa0319* in the notochord with fluorescence LSM combined with RNAscope probes targeting *kiaa0319* (Figure 3C). Transverse and lateral images at different developmental stages allowed us to accurately distinguish the spinal cord from the notochord. We detected much higher *kiaa0319* signal intensity in the notochord which became weaker as development progressed. Although weaker, a signal in the spinal cord was also observed. This was strongest at 96 hpf but, rather than increasing or stabilising as development progressed, it became weaker at 120 hpf. Finally, analysis in the double Tg(gfap:GFP);Tg(Oligo2:dsRed) transgenic embryos further confirmed localization of *kiaa0319* expression in the notochord (Figure 2D). This line presents i) secondary motor neurons, interneurons, and oligodendroglia cells labelled with GFP and ii) motor neurons and oligodendrocytes labelled with DsRed [Shin et al., 2003] and therefore is useful to distinguish the developing neural tube.

Among the elements controlling gene expression in the notochord, *FOXA2* is a key transcription factor [Tamplin et al., 2011]. We scanned the genomic sequences upstream of the *KIAA0319* and *KIAA0319L* TSS in both humans and zebrafish for *FOXA2* consensus motifs (Figure 3; Supplementary Table S3). We analysed the 10 kb region upstream of the TSS, which is the genomic interval that would most likely regulate the downstream genes [Metzakopian et al., 2012]. In zebrafish, six and three *FOXA2* motifs were found upstream of *kiaa0319* and *kiaa0319-like*, respectively. Three out of the six motifs upstream of *kiaa0319* were within the 6 kb upstream of the TSS, while all three of the *FOXA2* motifs were more distant to the *kiaa0319-like* TSS. In humans, *FOXA2* motifs were found only upstream of *KIAA0319* (N=2) and not of *KIAA0319L*. Figure 3B shows the position of these two motifs relatively to *KIAA0319* and to the dyslexia-associated SNPs [Paracchini et al., 2006b; Newbury et al., 2014].

Both the WISH and RNAscope analyses suggested expression of *kiaa0319* at the otic vesicles (Figure 4), which is of interest in the context of previous reports of a possible role of *Kiaa0319* in the auditory system of rodents [Guidi et al., 2017; Centanni et al., 2014b, 2014a; Szalkowski et al., 2012b]. However, this structure tends

to accumulate non-unspecific signal when conducting *in situ* hybridization because of technical artefacts, such as probe trapping. Detailed RNAscope analysis showed a signal for both *kiaa0319* (Figure 4.2) and *kiaa0319-like* (Figure 4.3) in the otic vesicles, however a signal was detected also in the negative controls (Figure 4.6 and 4.7). In comparison to the controls, both genes showed stronger expression and a signal characterised by a speckled pattern including within the main structures, suggestive of a genuine expression. In contrast, the controls showed a weaker signal, mainly localised along the contour of the otic vesicles suggesting probe trapping. However, given this background noise, we cannot confirm with confidence that *kiaa0319* and *kiaa0319l* are expressed at these structures.

The WISH analysis also suggested expression in the eyes, another structure that might lead to unspecific signals. The RNAscope analysis at the eyes showed expression for both *kiaa0319* (Figure 5A.2 and 5B.2) and *kiaa0319-like* (Figure 5A.3 and 5B.4). Both genes are expressed on the surface of the eyes and, most strongly, around the eye lens. The negative controls had no signal confirming the specificity of the probes. Expression in the eyes was further confirmed by qPCR (Figure 5C).

Discussion

We conducted the first zebrafish characterization of the dyslexia susceptibility *KIAA0319* gene. The expression pattern described in our study supports a specific role for *kiaa0319* in neurodevelopmental processes and adds novel findings towards our understanding of its function. We found that *kiaa0319* is highly expressed at the very first stages and, in addition to the expected expression in the brain, we show that it is expressed in the notochord, the eyes and possibly the otic vesicles. For comparison, we analysed the *kiaa0319-like* gene, which showed a similar expression pattern but presented a very weak signal in the notochord. This observation is surprising given the generally higher and ubiquitous expression of *KIAA0319-LIKE* reported in human tissues (Supplementary Figure S1) and suggests a specific role to *kiaa0319*. To the best of our knowledge, this is the first study reporting expression of *kiaa0319* during the very first hours of development and clearly showing its expression in specific structures other than the brain.

The function of the KIAA0319 protein has been studied in human cell lines and in rodent models, however it is not yet fully understood. The first functional characterization was conducted in rats and suggested a role in neuronal migration [Paracchini et al., 2006b] while more recent studies in mice indicate an involvement in biological processes beyond brain development [Guidi et al., 2018, 2017; Franquinho et al., 2017].

Consistent with the latest studies, we observed expression in the brain, but also observed expression in other organs. Guidi and colleagues [Guidi et al., 2017] generated a double KO mouse model for the *Kiaa0319* and *Kiaa0319l* genes and the most notable phenotype reported was an impairment of the auditory system. Analysis of individual KO for both genes showed mild effects for *Kiaa0319l* but no effects for *Kiaa0319* alone. Rodent models for other dyslexia candidate genes (i.e. *Dcdc2* and *Dyx1c1*) have also suggested an impairment in auditory processing [Truong et al., 2014; Szalkowski et al., 2013]. The potential expression of both *Kiaa0319* and *Kiaa0319l* in the otic vesicles (Figure 2, Figure 4 and Supplementary Figure S2) would be interesting in the context of the rodent data. However, further work will be required to establish whether these genes are expressed at the otic vesicles given possible probe trapping in these structures (Figure 4). Instead, given the eye-specific expression observed in our study (Figure 5), it would be expected for vision-related phenotypes to have also been observed in the rodent models. Accordingly, we recommend conducting a thorough visual assessment in future studies of *Kiaa0319* knock-out models.

Whether dyslexia is the result of a deficit in sensory systems, as predicted by the magnocellular theory [Stein, 2001a], remains highly debated [Paracchini et al., 2016b]. Defects in both the visual and auditory systems have been reported in individuals with dyslexia across different studies, but heterogeneity and inconsistency across studies remain significant challenges [Goswami, 2014]. The *kiaa0319* expression in the eyes during zebrafish development could be considered in line with a role of sensory organs. While it would be tempting to reach conclusions, it is worth noting that it is not possible to generalise and make strong assumptions based on observations for genes analysed in isolation. Moreover, the *KIAA0319* genetic associations (as with most

genetic associations with complex traits) explains only a small fraction of dyslexia heritability [Paracchini et al., 2016b].

The most compelling observation of our study is the notochord expression of *kiaa0319*, which instead was very weak for *kiaa0319-like* (Figure 2). The notochord is a transient embryonic structure in zebrafish essential for guiding the development and patterning of the early embryo [Stemple, 2005]. Because of the important functions of the notochord, the identification of the notochord-expressed genes is important to understand these developmental processes. The notochord is a source of signalling to the surrounding tissues to guide structural development, particularly for the spinal cord. For example, the notochord is the source of sonic hedgehog (SHH) signalling which controls many processes including the development of motor neurons, the establishment of the dorsal-ventral axis and left/right asymmetries [Echelard et al., 1993; Schilling et al., 1999]. The notochord also controls in a highly specific spatiotemporal manner the trajectories of dorsal root ganglion (DRG) axons through repressive signals mediated by aggrecan, one of the chondroitin sulfate proteoglycans (CSPGs) specifically found in the cartilage [Masuda et al., 2004]. A similar repressive role has been described for *Kiaa0319* in mice, including the repression of axon growth in hippocampal and DRG neurons [Franquinho et al., 2017]. The same study also showed that *Kiaa0319* was expressed in sensory and spinal cord neurons in post-natal and adult mice. Our data are consistent with these findings suggesting an evolutionary conserved function for *kiaa0319* beyond brain development.

A specific expression pattern is likely to result from a fine-tuned regulation. Most of markers associated with dyslexia map to the *KIAA0319* regulatory regions (Figure 3; [Paracchini et al., 2006b; Newbury et al., 2014]. Previously, we showed that a dyslexia-associated allele (rs9406145) at this region affects the affinity for a transcription factor and reduce the expression of *KIAA0319* [Dennis et al., 2009]. *FOXA2* is a key transcription factor involved in the regulation of genes expressed in the notochord [Tamplin et al., 2011]. However, *FOXA2* motifs are not sufficient to predict expression in the notochord as other transcription factors (e.g. Brachyury, GLIS3 and RFX3) might be required and would function through enhancer located at specific distances [Farley et al., 2016]. Nevertheless, the *FOXA2* consensus motifs upstream of *KIAA0319* TSS support the patterns observed in Figure 2 showing a much

stronger expression for *kiaa0319* in the notochord compared to *kiaa0319l*. The region upstream of *kiaa0319* had more FOXA2 consensus sequences and in more proximal position compared to *kiaa0319l*. In humans, FOXA2 motifs were found for *KIAA0319* only suggesting a conserved role for *KIAA0319* across vertebrates. These observations also provide a framework to interpret the genetic associations with dyslexia reported in *KIAA0319* non-coding regions (Figure 3)[Paracchini et al., 2006b; Dennis et al., 2009]. Genetic variation at this locus might affect not only gene expression levels as previously shown [Dennis et al., 2009] but also perturb the regulation of a specific spatiotemporal pattern.

In summary, our characterization of the *KIAA0319* dyslexia susceptibility gene in zebrafish reveals a specific pattern of expression during development. In addition to the expected expression in the brain, we show for the first time high embryonic expression during the first hours of development and, later on, at specific structures such as the eyes and the notochord. Our study therefore supports a developmental role for *KIAA0319* which is not restricted to the brain and may contribute to the ongoing discussion around the role of neuronal migration in dyslexia. While our data do not exclude a role in the developing brain and in neuronal migration, they suggest an involvement in other developmental processes as well.

Acknowledgements

SP is a Royal Society University Research Fellow. This work was supported by Royal Society [RG160373], Carnegie Trust [50341] and Northwood Trust awards to SP. MG was supported by a 600th Anniversary University of St Andrews PhD scholarship and is the recipient of EuFishBioMed scholarship used to visit the Centre de Biologie du Développement (CBD), in Toulouse, France. KD and ZY were supported by a UK Engineering and Physical Sciences Research Council (EPSRC) grant [EP/R004854/1]. The authors are grateful to Prof Caterina Becker for access to zebrafish facilities, to Prof. Bruce Appel for the *Tg(gfap:GFP);Tg(Oligo2:dsRed)* transgenic line, to Drs Patrick Blader and Julie Batut for mentoring on zebrafish experiments during MG stay at the CBD and to Dr Luiz Guidi for comments to the manuscript.

Conflict of interest

The author(s) declare no competing interests.

References

- Adler WT, Platt MP, Mehlhorn AJ, Haight JL, Currier T a, Etchegaray M a, Galaburda AM, Rosen GD. 2013. Position of neocortical neurons transfected at different gestational ages with shRNA targeted against candidate dyslexia susceptibility genes. *PLoS One* 8: e65179.
- Amores A, Force A, Yan YL, Joly L, Amemiya C, Fritz A, Ho RK, Langeland J, Prince V, Wang YL, Westerfield M, Ekker M, Postlethwait JH. 1998. Zebrafish hox clusters and vertebrate genome evolution. *Science* 282: 1711–4.
- Amunts K, Schlaug G, Schleicher A, Steinmetz H, Dabringhaus A, Roland PE, Zilles K. 1996. Asymmetry in the Human Motor Cortex and Handedness. *222*: 216–222.
- Antonellis A, Dennis MY, Burzynski G, Huynh J, Maduro V, Hodonsky CJ, Khajavi M, Szigeti K, Mukkamala S, Bessling SL, Pavan WJ, McCallion AS, Lupski JR, Green ED. 2010. A rare myelin protein zero (MPZ) variant alters enhancer activity in vitro and in vivo. *PLoS One* 5: e14346.
- Antonellis A, Huynh JL, Lee-Lin S-Q, Vinton RM, Renaud G, Loftus SK, Elliot G, Wolfsberg TG, Green ED, McCallion AS, Pavan WJ. 2008. Identification of neural crest and glial enhancers at the mouse Sox10 locus through transgenesis in zebrafish. *PLoS Genet.* 4: e1000174.
- Arning L, Ocklenburg S, Schulz S, Ness V, Gerding WM, Hengstler JG, Falkenstein M, Epplen JT, Güntürkün O, Beste C. 2013. PCSK6 VNTR Polymorphism Is Associated with Degree of Handedness but Not Direction of Handedness. *PLoS One* 8: e67251.
- Ashe HL, Briscoe J. 2006. The interpretation of morphogen gradients. *Development* 133.
- Badcock NA, Bishop DVM, Hardiman MJ, Barry JG, Watkins KE. 2012. Co-localisation of abnormal brain structure and function in specific language impairment. *Brain*

Lang. 120: 310–320.

Barth KA, Miklosi A, Watkins J, Bianco IH, Stephen W, Andrew RJ, Wilson SW, Andrew RJ. 2005. fsi Zebrafish Show Concordant Reversal of Laterality of Viscera , Neuroanatomy , and a Subset of Behavioral Responses. *Curr. Opin. Neurobiol.* 15: 844–850.

Bates TC, Lind PA, Luciano M, Montgomery GW, Martin NG, Wright MJ. 2010. Dyslexia and DYX1C1: deficits in reading and spelling associated with a missense mutation. *Mol. Psychiatry* 15: 1190–1196.

Becker TS, Rinkwitz S. 2012. Zebrafish as a genomics model for human neurological and polygenic disorders. *Dev. Neurobiol.* 72: 415–28.

Bhartiya D, Maini J, Sharma M, Joshi P, Laddha S V, Jalali S, Patowary A, Purkanti R, Lalwani M, Singh AR, Chauhan R, Singh N, Bhardwaj A, Scaria V, Sivasubbu S. 2010. FishMap Zv8 update--a genomic regulatory map of zebrafish. *Zebrafish* 7: 179–80.

Bishop DVM. 2013. Cerebral asymmetry and language development: cause, correlate or consequence? *Science.* 340.

Blow MJ, McCulley DJ, Li Z, Zhang T, Akiyama JA, Holt A, Plajzer-Frick I, Shoukry M, Wright C, Chen F, Afzal V, Bristow J, Ren B, Black BL, Rubin EM, Visel A, Pennacchio LA. 2010. ChIP-Seq identification of weakly conserved heart enhancers. *Nat. Genet.* 42: 806–810.

Boets B, Wouters J, van Wieringen A, De Smedt B, Ghesquière P. 2008. Modelling relations between sensory processing, speech perception, orthographic and phonological ability, and literacy achievement. *Brain Lang.* 106: 29–40.

Bosse M-L, Tainturier MJ, Valdois S. 2007. Developmental dyslexia: The visual attention span deficit hypothesis. *Cognition* 104: 198–230.

Bosse M-L, Valdois S. 2003. Patterns of developmental dyslexia according to a multi-trace memory model of reading. *Curr. Psychol. Lett.* 1.

- Brambati SM, Termine C, Ruffino M, Danna M, Lanzi G, Stella G, Cappa SF, Perani D. 2006. Neuropsychological deficits and neural dysfunction in familial dyslexia. *Brain Res.* 1113: 174–185.
- Brandler WM, Morris AP, Evans DM, Scerri TS, Kemp JP, Timpson NJ, St Pourcain B, Smith GD, Ring SM, Stein J, Monaco AP, Talcott JB, Fisher SE, Webber C, Paracchini S. 2013a. Common variants in left/right asymmetry genes and pathways are associated with relative hand skill. *PLoS Genet.* 9: e1003751.
- Brandler WM, Morris AP, Evans DM, Scerri TS, Kemp JP, Timpson NJ, St Pourcain B, Smith GD, Ring SM, Stein J, Monaco AP, Talcott JB, Fisher SE, Webber C, Paracchini S. 2013b. Common variants in left/right asymmetry genes and pathways are associated with relative hand skill. *PLoS Genet* 9: e1003751.
- Brandler WM, Paracchini S. 2013. The genetic relationship between handedness and neurodevelopmental disorders. *Trends Mol. Med.* 20: 1–8.
- Broca PM. 1861. REMARQUES SUR LE SIÈGE DE LA FACULTÉ DU LANGAGE ARTICULÉ, SUIVIES D'UNE OBSERVATION D'APHÉMIE (PERTE DE LA PAROLE). *Bicêtre Bull. la Société Anat.*: 330–357.
- Brown WE, Eliez S, Menon V, Rumsey JM, White CD, Reiss AL. 2001. Preliminary evidence of widespread morphological variations of the brain in dyslexia. *Neurology* 56: 781–3.
- Brunswick N, McCrory E, Price CJ, Frith CD, Frith U. 1999. Explicit and implicit processing of words and pseudowords by adult developmental dyslexics: A search for Wernicke's Wortschatz? *Brain*: 1901–17.
- Carrion-Castillo A, Franke B, Fisher SE. 2013. Molecular genetics of dyslexia: an overview. *Dyslexia* 19: 214–40.
- Centanni TM, Booker AB, Sloan AM, Chen F, Maher BJ, Carraway RS, Khodaparast N, Rennaker R, LoTurco JJ, Kilgard MP. 2014a. Knockdown of the dyslexia-associated gene *Kiaa0319* impairs temporal responses to speech stimuli in rat primary auditory cortex. *Cereb Cortex* 24: 1753–1766.

- Centanni TM, Chen F, Booker AM, Engineer CT, Sloan AM, Rennaker RL, LoTurco JJ, Kilgard MP. 2014b. Speech sound processing deficits and training-induced neural plasticity in rats with dyslexia gene knockdown. *PLoS One* 9: e98439.
- Chandrasekar G, Vesterlund L, Hultenby K, Tapia-Paez I, Kere J. 2013. The zebrafish orthologue of the dyslexia candidate gene *DYX1C1* is essential for cilia growth and function. *PLoS One* 8: e63123.
- Chang N, Sun C, Gao L, Zhu D, Xu X, Zhu X, Xiong J-W, Xi JJ. 2013. Genome editing with RNA-guided Cas9 nuclease in zebrafish embryos. *Cell Res.* 23: 465–72.
- Chatterjee S, Lufkin T. 2012. Regulatory genomics: Insights from the zebrafish. *Curr Top Genet*: 1–10.
- de Chaumont F, Dallongeville S, Chenouard N, Hervé N, Pop S, Provoost T, Meas-Yedid V, Pankajakshan P, Lecomte T, Le Montagner Y, Lagache T, Dufour A, Olivo-Marin J-C. 2012. Icy: an open bioimage informatics platform for extended reproducible research. *Nat. Methods* 9: 690–696.
- Cheo DL, Titus SA, Byrd DRN, Hartley JL, Temple GF, Brasch MA. 2004. Concerted Assembly and Cloning of Multiple DNA Segments Using In Vitro Site-Specific Recombination: Functional Analysis of Multi-Segment Expression Clones. *Genome Res.* 14: 2111–2120.
- Chuang H-C, Huang T-N, Hsueh Y-P. 2015. T-Brain-1 - A Potential Master Regulator in Autism Spectrum Disorders. *Autism Res.* 8: 412–426.
- Cohen L, Dehaene S. 2004. Specialization within the ventral stream: the case for the visual word form area. *Neuroimage* 22: 466–476.
- Cohen L, Dehaene S, Naccache L, Lehéricy S, Dehaene-Lambertz G, Hénaff M-A, Michel F. 2000. The visual word form area Spatial and temporal characterization of an initial stage of reading in normal subjects and posterior split-brain patients. *Brain* 123: 291–307.
- Concha ML, Burdine RD, Russell C, Schier a F, Wilson SW. 2000. A nodal signaling pathway regulates the laterality of neuroanatomical asymmetries in the zebrafish

- forebrain. *Neuron* 28: 399–409.
- Concha ML, Russell C, Regan JC, Tawk M, Sidi S, Gilmour DT, Kapsimali M, Sumoy L, Goldstone K, Amaya E, Kimelman D, Nicolson T, Gr??nder S, Gomperts M, Clarke JDW, Wilson SW. 2003. Local tissue interactions across the dorsal midline of the forebrain establish CNS laterality. *Neuron* 39: 423–438.
- Consortium GTe. 2013. The Genotype-Tissue Expression (GTEx) project. *Nat Genet* 45: 580–585.
- Constam DB, Robertson EJ. 1999. Regulation of bone morphogenetic protein activity by pro domains and proprotein convertases. *J. Cell Biol.* 144: 139–49.
- Cooper MS, D'Amico LA. 1996. A cluster of noninvoluting endocytic cells at the margin of the zebrafish blastoderm marks the site of embryonic shield formation. *Dev. Biol.* 180: 184–98.
- Cope N, Harold D, Hill G, Moskvina V, Stevenson J, Holmans P, Owen MJ, O'Donovan MC, Williams J. 2005. Strong evidence that KIAA0319 on chromosome 6p is a susceptibility gene for developmental dyslexia. *Am. J. Hum. Genet.* 76: 581–91.
- Corey DR, Abrams JM. 2001. Morpholino antisense oligonucleotides: tools for investigating vertebrate development. *Genome Biol.* 2: REVIEWS1015.
- Cornell RA, Eisen JS. 2002. Delta/Notch signaling promotes formation of zebrafish neural crest by repressing Neurogenin 1 function. *Development* 129: 2639–48.
- Couto JM, Gomez L, Wigg K, Cate-Carter T, Archibald J, Anderson B, Tannock R, Kerr EN, Lovett MW, Humphries T, Barr CL. 2008. The KIAA0319-Like (*KIAA0319L*) Gene on Chromosome 1p34 as a Candidate for Reading Disabilities. *J. Neurogenet.* 22: 295–313.
- Couto JM, Livne-Bar I, Huang K, Xu Z, Cate-Carter T, Feng Y, Wigg K, Humphries T, Tannock R, Kerr EN, Lovett MW, Bremner R, Barr CL. 2010. Association of reading disabilities with regions marked by acetylated H3 histones in KIAA0319. *Am. J. Med. Genet. Part B Neuropsychiatr. Genet.* 153: 447–462.

- D'Amico LA, Cooper MS. 1997. Spatially distinct domains of cell behavior in the zebrafish organizer region. *Biochem. Cell Biol.* 75: 563–77.
- Dahdouh F, Anthoni H, Tapia-Páez I, Peyrard-Janvid M, Schulte-Körne G, Warnke A, Remschmidt H, Ziegler A, Kere J, Müller-Myhsok B, Nöthen MM, Schumacher J, Zucchelli M. 2009. Further evidence for DYX1C1 as a susceptibility factor for dyslexia. *Psychiatr. Genet.* 19: 59–63.
- Dale RM, Topczewski J. 2011. Identification of an evolutionarily conserved regulatory element of the zebrafish *col2a1a* gene. *Dev. Biol.* 357: 518–531.
- Damasio AR, Damasio H. 1983. The anatomic basis of pure alexia. *Neurology* 33: 1573–83.
- Dassonville P, Zhu XH, Uurbil K, Kim SG, Ashe J. 1997. Functional activation in motor cortex reflects the direction and the degree of handedness. *Proc. Natl. Acad. Sci. U. S. A.* 94: 14015–8.
- DeFries JC, Fulker DW, LaBuda MC. 1987. Evidence for a genetic aetiology in reading disability of twins. *Lett. to Nat.* 329: 537–539.
- Dehaene S, Cohen L, Sigman M, Vinckier F. 2005. The neural code for written words: a proposal. *Trends Cogn. Sci.* 9: 335–341.
- Dejerine J. 1891. Sur un cas de cécité verbale avec agraphie, suivi d'autopsie. *C. R. Société du Biol.*: 197–201.
- Dennis MY, Paracchini S, Scerri TS, Prokunina-Olsson L, Knight JC, Wade-Martins R, Coghill P, Beck S, Green ED, Monaco AP. 2009. A common variant associated with dyslexia reduces expression of the KIAA0319 gene. *PLoS Genet.* 5: e1000436.
- Draper BW, Morcos PA, Kimmel CB. 2001. Inhibition of zebrafish *fgf8* pre-mRNA splicing with morpholino oligos: A quantifiable method for gene knockdown. *Genesis* 30: 154–156.
- Dubois J, Hertz-Pannier L, Cachia A, Mangin JF, Le Bihan D, Dehaene-Lambertz G.

2009. Structural Asymmetries in the Infant Language and Sensori-Motor Networks. *Cereb. Cortex* 19: 414–423.
- Echelard Y, Epstein DJ, St-Jacques B, Shen L, Mohler J, McMahon JA, McMahon AP. 1993. Sonic hedgehog, a member of a family of putative signaling molecules, is implicated in the regulation of CNS polarity. *Cell* 75: 1417–30.
- Eisen JS, Smith JC. 2008. Controlling morpholino experiments: don't stop making antisense. *Development* 135: 1735–1743.
- Ekker M, Wegner J, Akimenko MA, Westerfield M. 1992. Coordinate embryonic expression of three zebrafish engrailed genes. *Development* 116: 1001–10.
- Ekker SC, Larson JD, Gene MP, Strategies T, Effectiveness MOT, Controls E. 2001. Morphant technology in model developmental systems. *Genesis* 30: 89–93.
- Eliez S, Rumsey JM, Giedd JN, Schmitt JE, Patwardhan AJ, Reiss AL. 2000. Morphological alteration of temporal lobe gray matter in dyslexia: an MRI study. *J. Child Psychol. Psychiatry.* 41: 637–44.
- Essner JJ, Amack JD, Nyholm MK, Harris EB, Yost HJ. 2005. Kupffer's vesicle is a ciliated organ of asymmetry in the zebrafish embryo that initiates left-right development of the brain, heart and gut. *Development* 132: 1247–60.
- Ethell IM, Pasquale EB. 2005. Molecular mechanisms of dendritic spine development and remodeling. *Prog. Neurobiol.* 75: 161–205.
- Farley EK, Olson KM, Zhang W, Rokhsar DS, Levine MS. 2016. Syntax compensates for poor binding sites to encode tissue specificity of developmental enhancers. *Proc. Natl. Acad. Sci. U. S. A.* 113: 6508–13.
- Filipek P. 1996. Structural variations in measures in the developmental disorders. In: R. Thatcher, G. Lyon, J. Rumsey, & N. Krasnegor (Eds.). *Developmental neuroimaging: Mapping the development of brain and behavior*. San Diego, CA: Academic Press., p 169–186.
- Finn ES, Shen X, Holahan JM, Scheinost D, Lacadie C, Papademetris X, Shaywitz

- SE, Shaywitz B a, Constable RT. 2014. Disruption of functional networks in dyslexia: a whole-brain, data-driven analysis of connectivity. *Biol. Psychiatry* 76: 397–404.
- Fisher S, Grice E a, Vinton RM, Bessling SL, McCallion AS. 2006a. Conservation of RET regulatory function from human to zebrafish without sequence similarity. *Science* 312: 276–9.
- Fisher S, Grice E a, Vinton RM, Bessling SL, Urasaki A, Kawakami K, McCallion AS. 2006b. Evaluating the biological relevance of putative enhancers using Tol2 transposon-mediated transgenesis in zebrafish. *Nat. Protoc.* 1: 1297–305.
- Fisher SE, Francks C, Marlow AJ, MacPhie IL, Newbury DF, Cardon LR, Ishikawa-Brush Y, Richardson AJ, Talcott JB, Gayán J, Olson RK, Pennington BF, Smith SD, DeFries JC, Stein JF, Monaco AP. 2002. Independent genome-wide scans identify a chromosome 18 quantitative-trait locus influencing dyslexia. *Nat. Genet.* 30: 86–91.
- Fletcher JM, Loveland K. 1986. Neuropsychology of arithmetic disabilities in children. *Focus Learn. Probl. Math.* 8: 23–40.
- Fletcher JM, Shaywitz SE, Shankweiler DP, Katz L, Liberman IY, Stuebing KK, Francis DJ, Fowler AE, Shaywitz BA. 1994. Cognitive profiles of reading disability: Comparisons of discrepancy and low achievement definitions. *J. Educ. Psychol.* 1: 6–23.
- Francks C, Fisher SE, MacPhie IL, Richardson AJ, Marlow AJ, Stein JF, Monaco AP. 2002. A genomewide linkage screen for relative hand skill in sibling pairs. *Am. J. Hum. Genet.* 70: 800–5.
- Francks C, Maegawa S, Laurén J, Abrahams BS, Velayos-Baeza A, Medland SE, Colella S, Groszer M, McAuley EZ, Caffrey TM, Timmusk T, Pruunsild P, Koppel I, Lind PA, Matsumoto-Itaba N, Nicod J, Xiong L, Joober R, Enard W, Krinsky B, Nanba E, Richardson AJ, Riley BP, Martin NG, Strittmatter SM, Möller H-J, Rujescu D, St Clair D, Muglia P, Roos JL, Fisher SE, Wade-Martins R, Rouleau GA, Stein JF, Karayiorgou M, Geschwind DH, Ragoussis J, Kendler KS,

- Airaksinen MS, Oshimura M, DeLisi LE, Monaco AP. 2007. LRRTM1 on chromosome 2p12 is a maternally suppressed gene that is associated paternally with handedness and schizophrenia. *Mol. Psychiatry* 12: 1129–39, 1057.
- Francks C, Paracchini S, Smith SD, Richardson AJ, Scerri TS, Cardon LR, Marlow AJ, MacPhie IL, Walter J, Pennington BF, Fisher SE, Olson RK, DeFries JC, Stein JF, Monaco AP. 2004. A 77-kilobase region of chromosome 6p22.2 is associated with dyslexia in families from the United Kingdom and from the United States. *Am. J. Hum. Genet.* 75: 1046–58.
- Franquinho F, Nogueira-Rodrigues J, Duarte JMJM, Esteves SSS, Carter-Su C, Monaco AP, Molnár Z, Velayos-Baeza A, Brites P, Sousa MMMM. 2017. The dyslexia-susceptibility protein KIAA0319 inhibits axon growth through Smad2 signaling. *Cereb Cortex* 27: In press.
- Frauenheim JG. 1978. Academic Achievement Characteristics of Adult Males Who Were Diagnosed as Dyslexic in Childhood. *J. Learn. Disabil.* 11: 476–483.
- Friedman RF, Ween JE, Albert ML. 1993. Alexia. In: K. M. Heilman & E. Valenstein (Eds.), 3e. New York: Oxford University Press., p 37~2.
- Gagnon J a., Valen E, Thyme SB, Huang P, Ahkmetova L, Pauli A, Montague TG, Zimmerman S, Richter C, Schier AF. 2014. Efficient mutagenesis by Cas9 protein-mediated oligonucleotide insertion and large-scale assessment of single-guide RNAs. *PLoS One* 9: 5–12.
- Galaburda AM, LoTurco J, Ramus F, Fitch RH, Rosen GD. 2006. From genes to behavior in developmental dyslexia. *Nat Neurosci* 9: 1213–1217.
- Galaburda AM, Sherman GF, Rosen GD, Aboitz F, Geschwind N. 1985. Developmental Dyslexia: Four consecutive patients with cortical anomaly. *Ann. Neurol.* 18: 222–223.
- Gamse JT, Shen Y-C, Thisse C, Thisse B, Raymond P a, Halpern ME, Liang JO. 2002. Otx5 regulates genes that show circadian expression in the zebrafish pineal complex. *Nat. Genet.* 30: 117–121.

- Gamse JT, Thisse C, Thisse B, Halpern ME. 2003. The parapineal mediates left-right asymmetry in the zebrafish diencephalon. *Development* 130: 1059–1068.
- Garey LJ, Ong WY, Patel TS, Kanani M, Davis A, Mortimer AM, Barnes TR, Hirsch SR. 1998. Reduced dendritic spine density on cerebral cortical pyramidal neurons in schizophrenia. *J. Neurol. Neurosurg. Psychiatry* 65: 446–53.
- Geschwind N. 1965. Disconnexion syndromes in animals and man. I. *Brain* 88: 237–94.
- Goswami U. 2015. Sensory theories of developmental dyslexia: three challenges for research. *Nat Rev Neurosci* 16: 43–54.
- Goswami U. 2014. Sensory theories of developmental dyslexia: three challenges for research. *Nat. Rev. Neurosci.* 16: 43–54.
- Grant CE, Bailey TL, Noble WS. 2011. FIMO: scanning for occurrences of a given motif. *Bioinformatics* 27: 1017–1018.
- Grati M, Chakchouk I, Ma Q, Bensaid M, Desmidt A. 2015. A missense mutation in DCDC2 causes human recessive deafness DFNB66 , likely by interfering with sensory hair cell and supporting cell cilia length regulation. 1–26.
- Gross-Thebing T, Paksa A, Raz E. 2014. Simultaneous high-resolution detection of multiple transcripts combined with localization of proteins in whole-mount embryos. *BMC Biol.* 12: 55.
- de Guibert C, Maumet C, Jannin P, Ferré J-C, Tréguier C, Barillot C, Le Rumeur E, Allaire C, Biraben A. 2011. Abnormal functional lateralization and activity of language brain areas in typical specific language impairment (developmental dysphasia). *Brain* 134: 3044–3058.
- Guidi LG, Mattley J, Martinez-Garay I, Monaco AP, Linden JF, Velayos-Baeza A, Molnár Z. 2017. Knockout Mice for Dyslexia Susceptibility Gene Homologs KIAA0319 and KIAA0319L have Unaffected Neuronal Migration but Display Abnormal Auditory Processing. *Cereb. Cortex* 27: 5831–5845.

- Guidi LG, Velayos-Baeza A, Martinez-Garay I, Monaco AP, Paracchini S, Bishop DVM, Molnár Z. 2018. The neuronal migration hypothesis of dyslexia: a critical evaluation thirty years on. *PeerJ Prepr.*: 1–49.
- Gutwinski S, Löscher A, Mahler L, Kalbitzer J, Heinz A, Bempohl F. 2011. Understanding left-handedness. *Dtsch. Arztebl. Int.* 108: 849–53.
- Habas PA, Scott JA, Roosta A, Rajagopalan V, Kim K, Rousseau F, Barkovich AJ, Glenn OA, Studholme C. 2012. Early Folding Patterns and Asymmetries of the Normal Human Brain Detected from in Utero MRI. *Cereb. Cortex* 22: 13–25.
- Hannula-Jouppi K, Kaminen-Ahola N, Taipale M, Eklund R, Nopola-Hemmi J, Kääriäinen H, Kere J. 2005. The axon guidance receptor gene *ROBO1* is a candidate gene for developmental dyslexia. *PLoS Genet.* 1: e50.
- Harold D, Paracchini S, Scerri T, Dennis M, Cope N, Hill G, Moskvina V, Walter J, Richardson a J, Owen MJ, Stein JF, Green ED, O'Donovan MC, Williams J, Monaco a P. 2006. Further evidence that the *KIAA0319* gene confers susceptibility to developmental dyslexia. *Mol. Psychiatry* 11: 1085–91, 1061.
- Heasman J. 2002. Morpholino oligos: making sense of antisense? *Dev. Biol.* 243: 209–14.
- Heasman J, Kofron M, Wylie C. 2000. β Catenin Signaling Activity Dissected in the Early *Xenopus* Embryo: A Novel Antisense Approach. *Dev. Biol.* 222: 124–134.
- Heintzman ND, Hon GC, Hawkins RD, Kheradpour P, Stark A, Harp LF, Ye Z, Lee LK, Stuart RK, Ching CW, Ching KA, Antosiewicz-Bourget JE, Liu H, Zhang X, Green RD, Lobanenkov V V., Stewart R, Thomson JA, Crawford GE, Kellis M, Ren B. 2009. Histone modifications at human enhancers reflect global cell-type-specific gene expression. *Nature* 459: 108–112.
- Heintzman ND, Stuart RK, Hon G, Fu Y, Ching CW, Hawkins RD, Barrera LO, Van Calcar S, Qu C, Ching KA, Wang W, Weng Z, Green RD, Crawford GE, Ren B. 2007. Distinct and predictive chromatin signatures of transcriptional promoters and enhancers in the human genome. *Nat. Genet.* 39: 311–318.

- Helenius P, Tarkiainen A, Cornelissen P, Hansen PC, Salmelin R. 1991. Dissociation of normal feature analysis and deficient processing of letter-strings in dyslexic adults. *Cereb. cortex* 9: 476–83.
- Hepper PG. 2013. The developmental origins of laterality: fetal handedness. *Dev. Psychobiol.* 55: 588–95.
- Hepper PG, McCartney GR, Shannon E a. 1998. Lateralised behaviour in first trimester human foetuses. *Neuropsychologia* 36: 531–4.
- Hervé P-Y, Crivello F, Perchey G, Mazoyer B, Tzourio-Mazoyer N. 2006. Handedness and cerebral anatomical asymmetries in young adult males. *Neuroimage* 29: 1066–79.
- Hildebrandt F, Benzing T, Katsanis N. 2011a. Ciliopathies. *N. Engl. J. Med.* 364: 1533–1543.
- Hildebrandt F, Benzing T, Katsanis N. 2011b. Ciliopathies. *N Engl J Med* 364: 1533–1543.
- Hoh RA, Stowe TR, Turk E, Stearns T. 2012. Transcriptional program of ciliated epithelial cells reveals new cilium and centrosome components and links to human disease. *PLoS One* 7: e52166.
- Horwitz B, Rumsey JM, Donohue BC. 1998. Functional connectivity of the angular gyrus in normal reading and dyslexia. *Proc. Natl. Acad. Sci. U. S. A.* 95: 8939–44.
- Hosen MJ, Vanakker OM, Willaert A, Huysseune A, Coucke P, De Paepe A. 2013. Zebrafish models for ectopic mineralization disorders: practical issues from morpholino design to post-injection observations. *Front. Genet.* 4: 74.
- Howe K, Clark M, Torroja C, Torrance J, Berthelot C, Muffato M, Collins JE, Humphray S, McLaren K, Matthews L, McLaren S, Sealy I, Caccamo M, Churcher C, Scott C, Barrett JC, Koch R, Al. E. 2013a. The zebrafish reference genome sequence and its relationship to the human genome. *Nature* 496: 498–503.

Howe K, Clark MMD, Torroja CCF, Torrance J, Berthelot C, Muffato M, Collins JJE, Humphray S, McLaren K, Matthews L, McLaren S, Sealy I, Caccamo M, Churcher C, Scott C, Barrett JC, Koch R, Al. E, Rauch G-J, White S, Chow W, Kilian B, Quintais LT, Guerra-Assunção J a, Zhou Y, Gu Y, Yen J, Vogel J-H, Eyre T, Redmond S, Banerjee R, Chi J, Fu B, Langley E, Maguire SF, Laird GK, Lloyd D, Kenyon E, Donaldson S, Sehra H, Almeida-King J, Loveland J, Trevanion S, Jones M, Quail M, Willey D, Hunt A, Burton J, Sims S, McLay K, Plumb B, Davis J, Clee C, Oliver K, Clark R, Riddle C, Elliot D, Elliott D, Threadgold G, Harden G, Ware D, Begum S, Mortimore B, Mortimer B, Kerry G, Heath P, Phillimore B, Tracey A, Corby N, Dunn M, Johnson C, Wood J, Clark S, Pelan S, Griffiths G, Smith M, Glithero R, Howden P, Barker N, Lloyd C, Stevens C, Harley J, Holt K, Panagiotidis G, Lovell J, Beasley H, Henderson C, Gordon D, Auger K, Wright D, Collins JJE, Raisen C, Dyer L, Leung K, Robertson L, Ambridge K, Leongamornlert D, McGuire S, et al. 2013b. The zebrafish reference genome sequence and its relationship to the human genome. *Nature* 496: 498–503.

Hulme C, Snowling MJ. 2009. *Developmental Disorders of Language Learning and Cognition*. Wiley-Blackwell. 37-89 p.

Humphreys P, Kaufmann WE, Galaburda AM. 1990. Developmental dyslexia in women: neuropathological findings in three patients. *Ann Neurol* 28: 727–738.

Hutchinson SA, Eisen JS. 2006. Islet1 and Islet2 have equivalent abilities to promote motoneuron formation and to specify motoneuron subtype identity. *Development* 133: 2137–47.

Hwang WY, Fu Y, Reyon D, Maeder ML, Shengdar Q, Sander JD, Peterson RT, Yeh JJ, Keith J. 2013a. Efficient In Vivo Genome Editing Using RNA-Guided Nucleases Woong. *Nat. Biotechnol.* 31: 227–229.

Hwang WY, Fu Y, Reyon D, Maeder ML, Tsai SQ, Sander JD, Peterson RT, Yeh J-RJ, Joung JK. 2013b. Efficient genome editing in zebrafish using a CRISPR-Cas system. *Nat. Biotechnol.* 31: 227–9.

Illingworth S, Bishop DVM. 2009. Atypical cerebral lateralisation in adults with

- compensated developmental dyslexia demonstrated using functional transcranial Doppler ultrasound. *Brain Lang.* 111: 61–65.
- Ishibashi M, Mechaly AS, Becker TS, Rinkwitz S. 2013. Using zebrafish transgenesis to test human genomic sequences for specific enhancer activity. *Methods* 62: 216–225.
- Ivliev AE, Hoen P a C, van Roon-Mom WMC, Peters DJM, Sergeeva MG, t Hoen PA, van Roon-Mom WMC, Peters DJM, Sergeeva MG. 2012a. Exploring the transcriptome of ciliated cells using in silico dissection of human tissues. *PLoS One* 7: e35618.
- Ivliev AE, t Hoen PA, van Roon-Mom WM, Peters DJ, Sergeeva MG. 2012b. Exploring the transcriptome of ciliated cells using in silico dissection of human tissues. *PLoS One* 7: e35618.
- J T, C W. 2002. A sensory linguistic approach to the development of normal and dysfunctional reading skills. In: Witruk E, Friederici A, and Lachmann T (Eds), *Basic Functions of Language, Reading and Reading Disability*. Boston: Kluwer, p 213–240.
- Jao L-E, Wente SR, Chen W. 2013. Efficient multiplex biallelic zebrafish genome editing using a CRISPR nuclease system. *Proc. Natl. Acad. Sci. U. S. A.* 110: 13904–9.
- Jinek M, Chylinski K, Fonfara I, Hauer M, Doudna JA, Charpentier E. 2012. A Programmable Dual-RNA-Guided DNA Endonuclease in Adaptive Bacterial Immunity. *Science* (80-.). 337: 816–821.
- K. Kawakami, Asakawa K, Muto. A, Wada H. 2016. *Tol2-mediated Transgenesis, Gene Trapping, Enhancer Trapping, and the Gal4-UAS System*, Third Edit. Elsevier Inc. 19-37 p.
- Kasprian G, Langs G, Brugger PC, Bittner M, Weber M, Arantes M, Prayer D. 2011. The Prenatal Origin of Hemispheric Asymmetry: An In Utero Neuroimaging Study. *Cereb. Cortex* 21: 1076–1083.

- Kawakami K, Shima a, Kawakami N. 2000. Identification of a functional transposase of the Tol2 element, an Ac-like element from the Japanese medaka fish, and its transposition in the zebrafish germ lineage. *Proc. Natl. Acad. Sci. U. S. A.* 97: 11403–8.
- Kawakami K, Takeda H, Kawakami N, Kobayashi M, Matsuda N, Mishina M. 2004. A transposon-mediated gene trap approach identifies developmentally regulated genes in zebrafish. *Dev. Cell* 7: 133–44.
- Kent WJ, Sugnet CW, Furey TS, Roskin KM, Pringle TH, Zahler AM, Haussler D. 2002. The human genome browser at UCSC. *Genome Res* 12: 996–1006.
- Kidd T, Bland KS, Goodman CS. 1999. Slit is the midline repellent for the robo receptor in *Drosophila*. *Cell* 96: 785–94.
- Kidd T, Brose K, Mitchell KJ, Fetter RD, Tessier-Lavigne M, Goodman CS, Tear G. 1998. Roundabout controls axon crossing of the CNS midline and defines a novel subfamily of evolutionarily conserved guidance receptors. *Cell* 92: 205–15.
- Kim DY. 2009. Knockdown of Kiaa0319 Reduces Dendritic Spine Density. *Honor. Sch. Theses.* 109.
- Kim MJ, Oksenberg N, Hoffmann TJ, Vaisse C, Ahituv N. 2013. Functional characterization of SIM1-associated enhancers. *Hum. Mol. Genet.*: 1–9.
- Kimmel CB, Ballard WW, Kimmel SR, Ullmann B, Schilling TF. 1995a. Stages of embryonic development of the zebrafish. *Dev. Dyn.* 203: 253–310.
- Kimmel CB, Ballard WW, Kimmel SR, Ullmann B, Schilling TF. 1995b. Stages of embryonic development of the zebrafish. *Dev. Dyn.* 203: 253–310.
- Kitaguchi T, Mizugishi K, Hatayama M, Aruga J, Mikoshiba K. 2002. *Xenopus* Brachyury regulates mesodermal expression of Zic3, a gene controlling left-right asymmetry. *Dev Growth Differ* 44: 55–61.
- Kivilevitch Z, Achiron R, Zalel Y. 2010. Fetal brain asymmetry: in utero sonographic study of normal fetuses. *Am. J. Obstet. Gynecol.* 202: 359.e1-359.e8.

- Knecht S. 2000. Handedness and hemispheric language dominance in healthy humans. *Brain* 123: 2512–2518.
- Koga A, Suzuki M, Inagaki H, Bessho Y, Hori H. 1996. Transposable element in fish. *Nature* 383: 30.
- Korzh VP. 2011. Search for tissue-specific regulatory elements using Tol2 transposon as an example of evolutionary synthesis of genomics and developmental biology. *Russ. J. Dev. Biol.* 39: 73–77.
- Kronbichler M, Hutzler F, Staffen W, Mair A, Ladurner G, Wimmer H. 2006. Evidence for a dysfunction of left posterior reading areas in German dyslexic readers. *Neuropsychologia* 44: 1822–1832.
- Kwan KM, Fujimoto E, Grabher C, Mangum BD, Hardy ME, Campbell DS, Parant JM, Yost HJ, Kanki JP, Chien C-B. 2007. The Tol2kit: a multisite gateway-based construction kit for Tol2 transposon transgenesis constructs. *Dev. Dyn.* 236: 3088–99.
- Lepanto P, Davison C, Casanova G, Badano JL, Zolessi FR. 2016. Characterization of primary cilia during the differentiation of retinal ganglion cells in the zebrafish. *Neural Dev.* 11: 10.
- Levecque C, Velayos-Baeza A, Holloway ZG, Monaco AP. 2009. The dyslexia-associated protein KIAA0319 interacts with adaptor protein 2 and follows the classical clathrin-mediated endocytosis pathway. *Am. J. Physiol. Cell Physiol.* 297: C160-8.
- Levin M. 2005. Left-right asymmetry in embryonic development: a comprehensive review. *Mech. Dev.* 122: 3–25.
- Li M, Zhao L, Page-Mccaw P, Chen W. 2016. Zebrafish genome engineering using the CRISPR-Cas9 system. *Trends* 32: 815–827.
- Liang JO, Etheridge a, Hantsoo L, Rubinstein a L, Nowak SJ, Izpisua Belmonte JC, Halpern ME. 2000. Asymmetric nodal signaling in the zebrafish diencephalon positions the pineal organ. *Development* 127: 5101–5112.

- Lindamood P. 1994. Issues in researching the link between phonological awareness, learning disabilities, and spelling. In: G. R. Lyon (Ed.) *Frames of reference for the assessment of learning disabilities: New views on measurement issues*. Baltimore: Paul H. Brookes Publishing Company, p 351–373.
- Livingstone MS, Rosen GD, Drislane FW, Galaburda AM. 1991. Physiological and anatomical evidence for a magnocellular defect in developmental dyslexia. *Proc. Natl. Acad. Sci. U. S. A.* 88: 7943–7.
- Lovegrove WJ, Bowling A, Badcock D, Blackwood M. 1980. Specific reading disability: differences in contrast sensitivity as a function of spatial frequency. *Science* 210: 439–40.
- Luciano M, Lind PA, Duffy DL, Castles A, Wright MJ, Montgomery GW, Martin NG, Bates TC. 2007. A Haplotype Spanning KIAA0319 and TTRAP Is Associated with Normal Variation in Reading and Spelling Ability. *Biol. Psychiatry* 62: 811–817.
- Ludwig KU, Mattheisen M, Mühleisen TW, Roeske D, Schmääl C, Breuer R, Schulte-Körne G, Müller-Myhsok B, Nöthen MM, Hoffmann P, Rietschel M, Cichon S. 2009. Supporting evidence for LRRTM1 imprinting effects in schizophrenia. *Mol. Psychiatry* 14: 743–745.
- Marino C, Citterio A, Giorda R, Facoetti A, Menozzi G, Vanzin L, Lorusso ML, Nobile M, Molteni M. 2007. Association of short-term memory with a variant within DYX1C1 in developmental dyslexia. *Genes, Brain Behav.* 6: 640–646.
- Martinez-Garay I, Guidi LG, Holloway ZG, Bailey MAG, Lyngholm D, Schneider T, Donnison T, Butt SJB, Monaco AP, Molnár Z, Velayos-Baeza A. 2017. Normal radial migration and lamination are maintained in dyslexia-susceptibility candidate gene homolog Kiaa0319 knockout mice. *Brain Struct. Funct.* 222: 1367–1384.
- Massinen S, Hokkanen M-EE, Matsson H, Tammimies K, Tapia-Paez I, Dahlstrom-Heuser V, Kuja-Panula J, Burghoorn J, Jeppsson KE, Swoboda P, Peyrard-Janvid M, Toftgård R, Castren E, Kere J, Tapia-Páez I, Dahlström-Heuser V, Kuja-Panula J, Burghoorn J, Jeppsson KE, Swoboda P, Peyrard-Janvid M, Toftgård R, Castrén E, Kere J. 2011a. Increased expression of the dyslexia

candidate gene DCDC2 affects length and signaling of primary cilia in neurons. *PLoS One* 6: e20580.

Massinen S, Hokkanen ME, Matsson H, Tammimies K, Tapia-Paez I, Dahlstrom-Heuser V, Kuja-Panula J, Burghoorn J, Jeppsson KE, Swoboda P, Peyrard-Janvid M, Toftgard R, Castren E, Kere J. 2011b. Increased expression of the dyslexia candidate gene DCDC2 affects length and signaling of primary cilia in neurons. *PLoS One* 6: e20580.

Masuda T, Fukamauchi F, Takeda Y, Fujisawa H, Watanabe K, Okado N, Shiga T. 2004. Developmental regulation of notochord-derived repulsion for dorsal root ganglion axons. *Mol. Cell. Neurosci.* 25: 217–227.

McCarthy MI, Abecasis GR, Cardon LR, Goldstein DB, Little J, Ioannidis JP a, Hirschhorn JN. 2008. Genome-wide association studies for complex traits: consensus, uncertainty and challenges. *Nat. Rev. Genet.* 9: 356–69.

McKeever WF. 2000. A new family handedness sample with findings consistent with X-linked transmission. *Br. J. Psychol.* 91 (Pt 1): 21–39.

McManus IC. 1991. The inheritance of left-handedness. *Ciba Found. Symp.* 162: 251-67; discussion 267-81.

McManus IC, Davison A, Armour J a L. 2013. Multilocus genetic models of handedness closely resemble single-locus models in explaining family data and are compatible with genome-wide association studies. *Ann. N. Y. Acad. Sci.* 1288: 48–58.

Medland SE, Duffy DL, Wright MJ, Geffen GM, Hay D a, Levy F, van-Beijsterveldt CEM, Willemsen G, Townsend GC, White V, Hewitt AW, Mackey D a, Bailey JM, Slutske WS, Nyholt DR, Treloar S a, Martin NG, Boomsma DI. 2009. Genetic influences on handedness: data from 25,732 Australian and Dutch twin families. *Neuropsychologia* 47: 330–7.

Meng H, Smith SD, Hager K, Held M, Liu J, Olson RK, Pennington BF, DeFries JC, Gelernter J, Somlo S, Skudlarski P, Shaywitz SE, Shaywitz BA, Marchione K,

- Wang Y, Paramasivam M, LoTurco JJ, Page GP, Gruen JR, by Sherman Weissman CM. 2005. DCDC2 is associated with reading disability and modulates neuronal development in the brain. *PNAS Genet.* 102: 17053–17058.
- Metzakopian E, Lin W, Salmon-Divon M, Dvinge H, Andersson E, Ericson J, Perlmann T, Whitsett JA, Bertone P, Ang S-L. 2012. Genome-wide characterization of *Foxa2* targets reveals upregulation of floor plate genes and repression of ventrolateral genes in midbrain dopaminergic progenitors. *Development* 139: 2625–34.
- Miklosi A, Andrew R. J, Miklósi Á, Andrew R. J. 1999. Right eye use associated with decision to bite in zebrafish. *Behav. Brain Res.* 105: 199–205.
- Miklosi A, Andrew RJ, Savage H. 1997. Behavioural lateralisation of the tetrapod type in the zebrafish (*Brachydanio rerio*). *Physiol. Behav.* 63: 127–135.
- Moats L. 1994. Issues in researching the link between phonological awareness, learning disabilities, and spelling. In: G. R. Lyon (Ed.). *Frames of reference for the assessment of learning disabilities: New views on measurement issues*. Baltimore: Paul H. Brookes Publishing Company, p 333–349.
- Morillon B, Lehongre K, Frackowiak RSJ, Ducorps A, Kleinschmidt A, Poeppel D, Giraud A-L. 2010. Neurophysiological origin of human brain asymmetry for speech and language. *Proc. Natl. Acad. Sci. U. S. A.* 107: 18688–93.
- Morokuma J, Ueno M, Kawanishi H, Saiga H, Nishida H. 2002. *HrNodal*, the ascidian nodal-related gene, is expressed in the left side of the epidermis, and lies upstream of *HrPitx*. *Dev. Genes Evol.* 212: 439–446.
- Nasevicius a, Ekker SC. 2000. Effective targeted gene “knockdown” in zebrafish. *Nat. Genet.* 26: 216–220.
- Newbury DF, Monaco AP, Paracchini S. 2014. Reading and language disorders: the importance of both quantity and quality. *Genes (Basel).* 5: 285–309.
- Nicolson RI, Fawcett AJ. 1994. Reaction times and dyslexia. *Q. J. Exp. Psychol. A.* 47: 29–48.

- Nicolson RII, Fawcett AJJ. 1990. Automaticity: A new framework for dyslexia research? *Cognition* 35: 159–182.
- Nopola-Hemmi J, Taipale M, Haltia T, Lehesjoki AE, Voutilainen A, Kere J. 2000. Two translocations of chromosome 15q associated with dyslexia. *J. Med. Genet.* 37: 771–5.
- Oksenberg N, Stevison L, Wall JD, Ahituv N. 2013. Function and regulation of AUTS2, a gene implicated in autism and human evolution. *PLoS Genet.* 9: e1003221.
- Onai T, Irie N, Kuratani S. 2014. The Evolutionary Origin of the Vertebrate Body Plan: The Problem of Head Segmentation. *Annu. Rev. Genomics Hum. Genet.* 15: 443–459.
- Onuma Y, Takahashi S, Haramoto Y, Tanegashima K, Yokota C, Whitman M, Asashima M. 2005. Xnr2 and Xnr5 unprocessed proteins inhibit Wnt signaling upstream of dishevelled. *Dev. Dyn.* 234: 900–910.
- Paracchini S. 2011. Dissection of genetic associations with language-related traits in population-based cohorts. *J. Neurodev. Disord.* 3: 365–73.
- Paracchini S, Diaz R, Stein J. 2016a. *Advances in Dyslexia Genetics???New Insights Into the Role of Brain Asymmetries.* Elsevier Ltd. 53-97 p.
- Paracchini S, Diaz R, Stein J. 2016b. Chapter Two – *Advances in Dyslexia Genetics—New Insights Into the Role of Brain Asymmetries.* *Adv. Genet.* 96: 53–97.
- Paracchini S, Scerri T, Monaco AP. 2007. The genetic lexicon of dyslexia. *Annu. Rev. Genomics Hum. Genet.* 8: 57–79.
- Paracchini S, Steer CD, Buckingham L-L, Morris AP, Ring S, Scerri T, Stein J, Pembrey ME, Ragoussis J, Golding J, Monaco AP. 2008. Association of the KIAA0319 dyslexia susceptibility gene with reading skills in the general population. *Am. J. Psychiatry* 165: 1576–84.
- Paracchini S, Thomas A, Castro S, Lai C, Paramasivam M, Wang Y, Keating BJ, Taylor JM, Hacking DF, Scerri T, Francks C, Richardson AJ, Wade-Martins R,

- Stein JF, Knight JC, Copp AJ, Loturco J, Monaco AP. 2006a. The chromosome 6p22 haplotype associated with dyslexia reduces the expression of KIAA0319, a novel gene involved in neuronal migration. *Hum. Mol. Genet.* 15: 1659–66.
- Paracchini S, Thomas A, Castro S, Lai C, Paramasivam M, Wang Y, Keating BJ, Taylor JM, Hacking DF, Scerri T, Francks C, Richardson AJ, Wade-Martins R, Stein JF, Knight JC, Copp AJ, Loturco J, Monaco AP. 2006b. The chromosome 6p22 haplotype associated with dyslexia reduces the expression of KIAA0319, a novel gene involved in neuronal migration. *Hum Mol Genet* 15: 1659–1666.
- Parker MO, Brock AJ, Millington ME, Brennan CH. 2013a. Behavioral Phenotyping of Casper Mutant and 1-Pheny-2-Thiourea Treated Adult Zebrafish. *2Zebrafish* 10: 466–471.
- Parker MO, Gaviria J, Haigh A, Millington ME, Brown VJ, Combe FJ, Brennan CH. 2012a. Discrimination reversal and attentional sets in zebrafish (*Danio rerio*). *Behav. Brain Res.* 232: 264–268.
- Parker MO, Ife D, Ma J, Pancholi M, Smeraldi F, Straw C, Brennan CH. 2013b. Development and automation of a test of impulse control in zebrafish. *Front. Syst. Neurosci.* 7: 65.
- Parker MO, Millington ME, Combe FJ, Brennan CH. 2012b. Development and implementation of a three-choice serial reaction time task for zebrafish (*Danio rerio*). *Behav. Brain Res.* 227: 73–80.
- Paulesu E, Danelli L, Berlingeri M, Zoccolotti P, Pernet CR, Klaver P. 2014. Reading the dyslexic brain: multiple dysfunctional routes revealed by a new meta-analysis of PET and fMRI activation studies.
- Paulesu E, Démonet J-F, Fazio F, McCrory E, Chanoine V, Brunswick N, Cappa SF, Cossu G, Habib M, Frith CD, Frith U. 2001. Dyslexia: Cultural Diversity and Biological Unity. *Science* (80-.). 291.
- Pennacchio LA, Ahituv N, Moses AM, Prabhakar S, Nobrega MA, Shoukry M, Minovitsky S, Dubchak I, Holt A, Lewis KD, Plajzer-Frick I, Akiyama J, De Val S,

- Afzal V, Black BL, Couronne O, Eisen MB, Visel A, Rubin EM. 2006. In vivo enhancer analysis of human conserved non-coding sequences. *Nature* 444: 499–502.
- Pennington BF, Bishop DVM. 2009. Relations among speech, language, and reading disorders. *Annu. Rev. Psychol.* 60: 283–306.
- Peschansky VJ, Burbridge TJ, Volz AJ, Fiondella C, Wissner-Gross Z, Galaburda AM, Turco JJ Lo, Rosen GD. 2010. The Effect of Variation in Expression of the Candidate Dyslexia Susceptibility Gene Homolog *Kiaa0319* on Neuronal Migration and Dendritic Morphology in the Rat. *Cereb. Cortex* April 20: 884–897.
- Peterson RL, Pennington BF. 2015. Developmental dyslexia. *Annu Rev Clin Psychol* 11: 283–307.
- Phan ML, Vicario DS. 2010. Hemispheric differences in processing of vocalizations depend on early experience. *Proc. Natl. Acad. Sci.* 107: 2301–2306.
- Pinel P, Fauchereau F, Moreno A, Barbot A, Lathrop M, Zelenika D, Le Bihan D, Poline J-B, Bourgeron T, Dehaene S. 2012. Genetic Variants of *FOXP2* and *KIAA0319/TTRAP/THEM2* Locus Are Associated with Altered Brain Activation in Distinct Language-Related Regions. *J. Neurosci.* 32: 817–825.
- Pini A. 1993. Chemorepulsion of axons in the developing mammalian central nervous system. *Science* 261: 95–8.
- Pitrone PG, Schindelin J, Stuyvenberg L, Preibisch S, Weber M, Eliceiri KW, Huisken J, Tomancak P. 2013a. OpenSPIM: an open-access light-sheet microscopy platform. *Nat. Methods* 10: 598–599.
- Pitrone PG, Schindelin J, Stuyvenberg L, Preibisch S, Weber M, Eliceiri KW, Huisken J, Tomancak P. 2013b. OpenSPIM: an open-access light-sheet microscopy platform. *Nat. Methods* 10: 598–599.
- Platt MP, Adler WT, Mehlhorn a J, Johnson GC, Wright K a, Choi RT, Tsang WH, Poon MW, Yeung SY, Wayne MMY, Galaburda a M, Rosen GD. 2013. Embryonic disruption of the candidate dyslexia susceptibility gene homolog *Kiaa0319*-like

results in neuronal migration disorders. *Neuroscience* 248C: 585–593.

Poon M-W, Tsang W-H, Waye MM-Y, Chan S-O. 2011a. Distribution of Kiaa0319-like immunoreactivity in the adult mouse brain--a novel protein encoded by the putative dyslexia susceptibility gene KIAA0319-like. *Histol. Histopathol.* 26: 953–63.

Poon MW, Tsang WH, Chan SO, Li HM, Ng HK, Waye MMY. 2011b. Dyslexia-associated Kiaa0319-Like protein interacts with axon guidance Receptor Nogo Receptor 1. *Cell. Mol. Neurobiol.* 31: 27–35.

des Portes V, Francis F, Pinard JM, Desguerre I, Moutard ML, Snoeck I, Meiners LC, Capron F, Cusmai R, Ricci S, Motte J, Echenne B, Ponsot G, Dulac O, Chelly J, Beldjord C. 1998. doublecortin is the major gene causing X-linked subcortical laminar heterotopia (SCLH). *Hum. Mol. Genet.* 7: 1063–70.

Praetorius C, Grill C, Stacey SN, Metcalf AM, Gorkin DU, Robinson KC, Van Otterloo E, Kim RSQ, Bergsteinsdottir K, Ogmundsdottir MH, Magnusdottir E, Mishra PJ, Davis SR, Guo T, Zaidi MR, Helgason AS, Sigurdsson MI, Meltzer PS, Merlino G, Petit V, Larue L, Loftus SK, Adams DR, Sobhiafshar U, Emre NCT, Pavan WJ, Cornell R, Smith AG, McCallion AS, Fisher DE, Stefansson K, Sturm R a, Steingrimsson E. 2013. A polymorphism in IRF4 affects human pigmentation through a tyrosinase-dependent MITF/TFAP2A pathway. *Cell* 155: 1022–33.

Price CJ, Devlin JT. 2011. The Interactive Account of ventral occipitotemporal contributions to reading. *Trends Cogn. Sci.* 15: 246–253.

Price CJ, Mechelli A. 2005. Reading and reading disturbance. *Curr. Opin. Neurobiol.* 15: 231–238.

Prince VE, Joly L, Ekker M, Ho RK. 1998. Zebrafish hox genes: genomic organization and modified colinear expression patterns in the trunk. *Development* 125: 407–20.

Rabin M, Wen XL, Hepburn M, Lubs HA, Feldman E, Duara R. 1993. Suggestive linkage of developmental dyslexia to chromosome 1p34-p36. *Lancet (London,*

England) 342: 178.

- Ramus F, Ahissar M. 2012. Developmental dyslexia: The difficulties of interpreting poor performance, and the importance of normal performance. *Cogn. Neuropsychol.* 29: 104–122.
- Ramus F, Rosen S, Dakin SC, Day BL, Castellote JM, White S, Frith U. 2003. Theories of developmental dyslexia: insights from a multiple case study of dyslexic adults. *Brain* 126: 841–865.
- Rana AA, Collart C, Gilchrist MJ, Smith JC. 2006. Defining synphenotype groups in *Xenopus tropicalis* by use of antisense morpholino oligonucleotides. *PLoS Genet.* 2: 1751–1772.
- Ray NJ, Fowler S, Stein JF. 2005. Yellow filters can improve magnocellular function: Motion sensitivity, convergence, accommodation, and reading. *Ann. N. Y. Acad. Sci.* 1039: 283–293.
- Raymond M, Pontier D, Dufour A-B, Moller AP. 1996. Frequency-Dependent Maintenance of Left Handedness in Humans. *Proc. R. Soc. B Biol. Sci.* 263: 1627–1633.
- Rendall AR, Tarkar A, Contreras-Mora HM, LoTurco JJ, Fitch RH. 2017. Deficits in learning and memory in mice with a mutation of the candidate dyslexia susceptibility gene *Dyx1c1*. *Brain Lang.* 172: 30–38.
- Richlan F. 2012. Developmental dyslexia: dysfunction of a left hemisphere reading network. *Front. Hum. Neurosci.* 6: 120.
- Richlan F, Kronbichler M, Wimmer H. 2011. Meta-analyzing brain dysfunctions in dyslexic children and adults.
- Roh T-Y, Cuddapah S, Zhao K. 2005. Active chromatin domains are defined by acetylation islands revealed by genome-wide mapping. *Genes Dev.* 19: 542–552.
- Roh T, Wei G, Farrell CM, Zhao K. 2007. Genome-wide prediction of conserved and nonconserved enhancers by histone acetylation patterns. *Genome Res.* 17: 74–

81.

- Rosen GD, Bai J, Wang Y, Fiondella CG, Threlkeld SW, LoTurco JJ, Galaburda AM. 2007. Disruption of neuronal migration by RNAi of *Dyx1c1* results in neocortical and hippocampal malformations. *Cereb. Cortex* 17: 2562–72.
- Rumsey JM, Andreason P, Zametkin AJ, Aquino T, King AC, Hamburger SD, Pikus A, Rapoport JL, Cohen RM. 1992. Failure to activate the left temporoparietal cortex in dyslexia. An oxygen 15 positron emission tomographic study. *Arch. Neurol.* 49: 527–34.
- Rumsey JM, Nace K, Donohue B, Wise D, Maisog JM, Andreason P. 1997. A Positron Emission Tomographic Study of Impaired Word Recognition and Phonological Processing in Dyslexic Men. *Arch. Neurol.* 54: 562–573.
- Salmelin R, Kiesilä P, Uutela K, Service E, Salonen O. 1996. Impaired visual word processing in dyslexia revealed with magnetoencephalography. *Ann. Neurol.* 40: 157–162.
- Sandelin A, Bailey P, Bruce S, Engström PG, Klos JM, Wasserman WW, Ericson J, Lenhard B. 2004. Arrays of ultraconserved non-coding regions span the loci of key developmental genes in vertebrate genomes. *BMC Genomics* 5: 99.
- Sander JD, Joung JK. 2014. CRISPR-Cas systems for editing, regulating and targeting genomes. *Nat. Biotechnol.* 32: 347–355.
- Scerri TS, Brandler WM, Paracchini S, Morris AP, Ring SM, Richardson AJ, Talcott JB, Stein J, Monaco AP. 2011a. PCSK6 is associated with handedness in individuals with dyslexia. *Hum. Mol. Genet.* 20: 608–14.
- Scerri TS, Fisher SE, Francks C, MacPhie IL, Paracchini S, Richardson a J, Stein JF, Monaco a P. 2004. Putative functional alleles of *DYX1C1* are not associated with dyslexia susceptibility in a large sample of sibling pairs from the UK. *J. Med. Genet.* 41: 853–857.
- Scerri TS, Morris AP, Buckingham LL, Newbury DF, Miller LL, Monaco AP, Bishop DVM, Paracchini S. 2011b. *DCDC2*, *KIAA0319* and *CMIP* are associated with

- reading-related traits. *Biol. Psychiatry* 70: 237–245.
- Schier AF. 2003. Nodal signaling in vertebrate development. *Annu. Rev. Cell Dev. Biol.* 19: 589–621.
- Schilling TF, Concordet J-P, Ingham PW. 1999. Regulation of Left–Right Asymmetries in the Zebrafish by Shh and BMP4. *Dev. Biol.* 210: 277–287.
- Schindelin J, Arganda-Carreras I, Frise E, Kaynig V, Longair M, Pietzsch T, Preibisch S, Rueden C, Saalfeld S, Schmid B, Tinevez J-Y, White DJ, Hartenstein V, Eliceiri K, Tomancak P, Cardona A. 2012. Fiji: an open-source platform for biological-image analysis. *Nat. Methods* 9: 676–682.
- Schroeder W, Martin K, Lorensen B. 2006a. *The Visualization Toolkit* (4th ed.).
- Schroeder W, Martin K, Lorensen B, Kitware I. 2006b. *The visualization toolkit: an object-oriented approach to 3D graphics*. Kitware. 512 p.
- Schueler M, Braun DA, Chandrasekar G, Gee HY, Klasson TD, Halbritter J, Bieder A, Porath JD, Airik R, Zhou W, LoTurco JJ, Che A, Otto EA, Bockenbauer D, Sebire NJ, Honzik T, Harris PC, Koon SJ, Gunay-Aygun M, Saunier S, Zerres K, Bruechle NO, Drenth JP, Pelletier L, Tapia-Paez I, Lifton RP, Giles RH, Kere J, Hildebrandt F. 2015a. DCDC2 Mutations Cause a Renal-Hepatic Ciliopathy by Disrupting Wnt Signaling. *Am J Hum Genet* 96: 81–92.
- Schueler M, Braun DA, Chandrasekar G, Gee HY, Klasson TD, Halbritter J, Bieder A, Porath JD, Airik R, Zhou W, LoTurco JJ, Che A, Otto EA, Böckenbauer D, Sebire NJ, Honzik T, Harris PC, Koon SJ, Gunay-Aygun M, Saunier S, Zerres K, Bruechle NO, Drenth JPH, Pelletier L, Tapia-Páez I, Lifton RP, Giles RH, Kere J, Hildebrandt F, Bockenbauer D, Sebire NJ, Honzik T, Harris PC, Koon SJ, Gunay-Aygun M, Saunier S, Zerres K, Bruechle NO, Drenth JPH, Pelletier L, Tapia-Paez I, Lifton RP, Giles RH, Kere J, Hildebrandt F. 2015b. DCDC2 Mutations Cause a Renal-Hepatic Ciliopathy by Disrupting Wnt Signaling. *Am. J. Hum. Genet.* 96: 1–12.
- Schulte-Körne G, Bruder J. 2010. Clinical neurophysiology of visual and auditory

processing in dyslexia: A review. *Clin. Neurophysiol.* 121: 1794–1809.

Schumacher J, Anthoni H, Dahdouh F, König IR, Hillmer AM, Kluck N, Manthey M, Plume E, Warnke A, Remschmidt H, Hülsmann J, Cichon S, Lindgren CM, Propping P, Zucchelli M, Ziegler A, Peyrard-Janvid M, Schulte-Körne G, Nöthen MM, Kere J. 2006. Strong genetic evidence of DCDC2 as a susceptibility gene for dyslexia. *Am. J. Hum. Genet.* 78: 52–62.

Schumacher J, Hoffmann P, Schmä C, Schulte-Körne G, Nöthen MM. 2007. Genetics of dyslexia: the evolving landscape. *J. Med. Genet.* 44: 289–97.

Seeger M, Tear G, Ferres-Marco D, Goodman CS, Jan LY, Jan YN, Goodman CS, Carretto R, Uemara T, Grell EH, Jan LY, Jan YN. 1993. Mutations affecting growth cone guidance in *Drosophila*: genes necessary for guidance toward or away from the midline. *Neuron* 10: 409–26.

Shah AN, Davey CF, Whitebirch AC, Miller AC, Moens CB. 2015. Rapid reverse genetic screening using CRISPR in zebrafish. *Nat Methods* 12: 535–540.

Shaywitz BA, Shaywitz SE, Pugh KR, Mencl WE, Fulbright RK, Skudlarski P, Constable RT, Marchione KE, Fletcher JM, Lyon GR, Gore JC. 2002. Disruption of Posterior Brain Systems for Reading in Children with Developmental Dyslexia. *Biol Psychiatry* 52: 101–110.

Shaywitz SAES. 1998. Dyslexia. *N. Engl. J. Med.*: 307–312.

Shaywitz SE. 2003. *Overcoming dyslexia: a new and complete science-based program for reading problems at any level.* A.A. Knopf. 416 p.

Shaywitz SE, Fletcher JM, Holahan JM, Shneider AE, Marchione KE, Stuebing KK, Francis DJ, Pugh KR, Shaywitz BA. 1999. Persistence of Dyslexia: The Connecticut Longitudinal Study at Adolescence. *Pediatrics* 104.

Shaywitz SE, Shaywitz BA. 2005. Dyslexia (Specific Reading Disability). *Biol. Psychiatry* 57: 1301–1309.

Shaywitz SE, Shaywitz BA. 2004. Reading Disability and The Brain. *What Res. Says*

about Read. 61: 630–633.

Shaywitz SE, Shaywitz BA, Fulbright RK, Skudlarski P, Mencl WE, Constable RT, Pugh KR, Holahan JM, Marchione KE, Fletcher JM, Lyon GR, Gore JC. 2003. Neural systems for compensation and persistence: young adult outcome of childhood reading disability. *Biol. Psychiatry* 54: 25–33.

Shen MM. 2007. Nodal signaling: developmental roles and regulation. *Development* 134: 1023–1034.

Shin J, Park H-C, Topczewska JM, Mawdsley DJ, Appel B. 2003. Neural cell fate analysis in zebrafish using olig2 BAC transgenics. *Neural cell fate analysis in zebrafish using olig2 BAC transgenics. Methods Cell Sci.:* 7–14.

Shore R. 2015. A functional characterisation of the PCSK6 locus associated with handedness Robert Shore at the University of St Andrews Date of Submission : November 30 2015.

Shore R, Covill L, Pettigrew KA, Brandler WM, Diaz R, Xu Y, Tello JA, Talcott JB, Newbury DF, Stein J, Monaco AP, Paracchini S. 2016. The handedness-associated PCSK6 locus spans an intronic promoter regulating novel transcripts. *Hum. Mol. Genet.* 25: 1771–1779.

Simos PG, Breier JI, Fletcher JM, Bergman E, Papanicolaou AC. 2000. Cerebral Mechanisms Involved in Word Reading in Dyslexic Children: a Magnetic Source Imaging Approach. *Cereb. Cortex* 10: 809–816.

Skaper SD. 2012. Neuronal Growth-Promoting and Inhibitory Cues in Neuroprotection and Neuroregeneration. In: *Methods in molecular biology* (Clifton, N.J.), p 13–22.

Smith SD, Kimberling WJ, Pennington BF, Lubs HA. 1983. Specific reading disability: identification of an inherited form through linkage analysis. *Science* 219: 1345–7.

Sommer IEC, Ramsey NF, Mandl RCW, Kahn RS. 2002. Language lateralization in monozygotic twin pairs concordant and discordant for handedness. 2710–2718.

Spence R, Gerlach G, Lawrence C, Smith C. 2007. The behaviour and ecology of the

- zebrafish, *Danio rerio*. *Biol. Rev.* 83: 13–34.
- Stein J. 2001a. The magnocellular theory of developmental dyslexia. *Dyslexia* 7: 12–36.
- Stein J. 2001b. The Sensory Basis of Reading Problems. *Dev. Neuropsychol.* 20: 509–534.
- Stemple DL. 2005. Structure and function of the notochord: an essential organ for chordate development. *Development* 132: 2503–2512.
- Stoodley CJ, Stein JF. 2011. The cerebellum and dyslexia. *Cortex* 47: 101–116.
- Stooke-Vaughan GA, Huang P, Hammond KL, Schier AF, Whitfield TT. 2012. The role of hair cells, cilia and ciliary motility in otolith formation in the zebrafish otic vesicle. *Development* 139: 1777–1787.
- Summerton J. 1999. Morpholino antisense oligomers: The case for an RNase H-independent structural type. *Biochim. Biophys. Acta - Gene Struct. Expr.* 1489: 141–158.
- Summerton J, Weller D. 1997. Morpholino antisense oligomers: design, preparation, and properties. *Antisense Nucleic Acid Drug Dev.* 7: 187–195.
- Sun Y-F, Lee J-S, Kirby R. 2010. Brain Imaging Findings in Dyslexia. *Pediatr. Neonatol.* 51: 89–96.
- Suster ML, Abe G, Schouw A, Kawakami K. 2011. Transposon-mediated BAC transgenesis in zebrafish. *Nat. Protoc.* 6: 1998–2021.
- Suster ML, Kikuta H, Urasaki A, Asakawa K, Kawakami K. 2009. Transgenesis in zebrafish with the tol2 transposon system. 561.
- Szalkowski CE, Booker AB, Truong DT, Threlkeld SW, Rosen GD, Fitch RH. 2013. Knockdown of the candidate dyslexia susceptibility gene homolog *dyx1c1* in rodents: effects on auditory processing, visual attention, and cortical and thalamic anatomy. *Dev. Neurosci.* 35: 50–68.

- Szalkowski CE, Fiondella CG, Galaburda AM, Rosen GD, Loturco JJ, Fitch RH. 2012a. Neocortical disruption and behavioral impairments in rats following in utero RNAi of candidate dyslexia risk gene Kiaa0319. *30*: 293–302.
- Szalkowski CE, Fiondella CG, Galaburda AM, Rosen GD, Loturco JJ, Fitch RH. 2012b. Neocortical disruption and behavioral impairments in rats following in utero RNAi of candidate dyslexia risk gene Kiaa0319. *Int J Dev Neurosci* *30*: 293–302.
- Taipale M, Kaminen N, Nopola-Hemmi J, Haltia T, Myllyluoma B, Lyytinen H, Muller K, Kaaranen M, Lindsberg PJ, Hannula-Jouppi K, Kere J. 2003. A candidate gene for developmental dyslexia encodes a nuclear tetratricopeptide repeat domain protein dynamically regulated in brain. *Proc. Natl. Acad. Sci. U. S. A.* *100*: 11553–8.
- Tamplin OJ, Cox BJ, Rossant J. 2011. Integrated microarray and ChIP analysis identifies multiple Foxa2 dependent target genes in the notochord. *Dev. Biol.* *360*: 415–425.
- Tarkar A, Loges NT, Slagle CE, Francis R, Dougherty GW, Tamayo J V, Shook B, Cantino M, Schwartz D, Jahnke C, Olbrich H, Werner C, Raidt J, Pennekamp P, Abouhamed M, Hjeij R, Kohler G, Griese M, Li Y, Lemke K, Klana N, Liu X, Gabriel G, Tobita K, Jaspers M, Morgan LC, Shapiro AJ, Letteboer SJ, Mans DA, Carson JL, Leigh MW, Wolf WE, Chen S, Lucas JS, Onoufriadis A, Plagnol V, Schmidts M, Boldt K, Roepman R, Zariwala MA, Lo CW, Mitchison HM, Knowles MR, Burdine RD, Loturco JJ, Omran H. 2013a. DYX1C1 is required for axonemal dynein assembly and ciliary motility. *Nat Genet* *45*: 995–1003.
- Tarkar A, Loges NT, Slagle CE, Francis R, Dougherty GW, Tamayo J V, Shook B, Cantino M, Schwartz D, Jahnke C, Olbrich H, Werner C, Raidt J, Pennekamp P, Abouhamed M, Hjeij R, Köhler G, Griese M, Li Y, Lemke K, Klana N, Liu X, Gabriel G, Tobita K, Jaspers M, Morgan LC, Shapiro AJ, Letteboer SJF, Mans D a, Carson JL, Leigh MW, Wolf WE, Chen S, Lucas JS, Onoufriadis A, Plagnol V, Schmidts M, Boldt K, Roepman R, Zariwala M a, Lo CW, Mitchison HM, Knowles MR, Burdine RD, Loturco JJ, Omran H, Kohler G, Griese M, Li Y, Lemke K, Klana N, Liu X, Gabriel G, Tobita K, Jaspers M, Morgan LC, Shapiro AJ, Letteboer SJF,

- Mans D a, Carson JL, Leigh MW, Wolf WE, Chen S, Lucas JS, Onoufriadis A, Plagnol V, Schmidts M, Boldt K, Roepman R, Zariwala M a, Lo CW, Mitchison HM, Knowles MR, Burdine RD, Loturco JJ, Omran H. 2013b. DYX1C1 is required for axonemal dynein assembly and ciliary motility. *Nat. Genet.* 45: 995–1003.
- Thisse C, Thisse B. 2008. High-resolution in situ hybridization to whole-mount zebrafish embryos. *Nat. Protoc.* 3: 59–69.
- Thompson PM, Cannon TD, Narr KL, van Erp T, Poutanen V-P, Huttunen M, Lönngqvist J, Standertskjöld-Nordenstam C-G, Kaprio J, Khaledy M, Dail R, Zoumalan CI, Toga AW. 2001. Genetic influences on brain structure. *Nat. Neurosci.* 4: 1253–1258.
- Threlkeld SW, McClure MM, Bai J, Wang Y, LoTurco JJ, Rosen GD, Fitch RH. 2007. Developmental Disruptions and Behavioral Impairments in Rats Following In Utero RNAi of *Dyx1c1*. *Brain Res Bull* 71: 508–514.
- Toga AW, Thompson PM. 2003. Mapping brain asymmetry. *Nat. Rev. Neurosci.* 4: 37–48.
- Truong DT, Che A, Rendall AR, Szalkowski CE, LoTurco JJ, Galaburda AM, Holly Fitch R. 2014. Mutation of *Dcdc2* in mice leads to impairments in auditory processing and memory ability. *Genes Brain Behav* 13: 802–811.
- Urasaki A, Morvan G, Kawakami K. 2006. Functional dissection of the *Tol2* transposable element identified the minimal cis-sequence and a highly repetitive sequence in the subterminal region essential for transposition. *Genetics* 174: 639–49.
- Varshney GK, Pei W, LaFave MC, Idol J, Xu L, Gallardo V, Carrington B, Bishop K, Jones M, Li M, Harper U, Huang SC, Prakash A, Chen W, Sood R, Ledin J, Bruggess SM. 2015. High-throughput gene targeting and phenotyping in zebrafish using CRISPR / Cas9. *Genome Res.*: 1030–1042.
- Velayos-Baeza A, Toma C, Paracchini S, Monaco AP. 2008. The dyslexia-associated gene *KIAA0319* encodes highly N- and O-glycosylated plasma membrane and

- secreted isoforms. *Hum. Mol. Genet.* 17: 859–871.
- Velayos-Baeza A, Toma C, da Roza S, Paracchini S, Monaco AP. 2007. Alternative splicing in the dyslexia-associated gene KIAA0319. *Mamm Genome* 18: 627–634.
- Villefranc JA, Amigo J, Lawson ND. 2015. Gateway Compatible Vectors for Analysis of Gene Function in the Zebrafish. 73: 389–400.
- Vinckier F, Dehaene S, Jobert A, Dubus JP, Sigman M, Cohen L. 2007. Hierarchical Coding of Letter Strings in the Ventral Stream: Dissecting the Inner Organization of the Visual Word-Form System. *Neuron* 55: 143–156.
- Visel A, Blow MJ, Li Z, Zhang T, Akiyama JA, Holt A, Plajzer-Frick I, Shoukry M, Wright C, Chen F, Afzal V, Ren B, Rubin EM, Pennacchio LA. 2009. ChIP-seq accurately predicts tissue-specific activity of enhancers. *Nature* 457: 854–858.
- Walhout a J, Temple GF, Brasch M a, Hartley JL, Lorson M a, van den Heuvel S, Vidal M. 2000. GATEWAY recombinational cloning: application to the cloning of large numbers of open reading frames or ORFeomes. *Methods Enzymol.* 328: 575–592.
- Wang Y, Paramasivam M, Thomas A, Bai J, Kaminen-Ahola N, Kere J, Voskuil J, Rosen GD, Galaburda AM, Loturco JJ. 2006. DYX1C1 functions in neuronal migration in developing neocortex. *Neuroscience* 143: 515–22.
- Weinberg ES, Allende ML, Kelly CS, Abdelhamid A, Murakami T, Andermann P, Doerre OG, Grunwald DJ, Riggleman B. 1996. Developmental regulation of zebrafish MyoD in wild-type, no tail and spadetail embryos. *Development* 122: 271–80.
- Wernicke C. 1874. *Der aphasische Symptomencomplex eine psychologische Studie auf anatomischer Basis.* Breslau: Cohn & Weigert.
- Wigg KG, Couto JM, Feng Y, Anderson B, Cate-Carter TD, Macciardi F, Tannock R, Lovett MW, Humphries TW, Barr CL. 2004. Support for EKN1 as the susceptibility locus for dyslexia on 15q21. *Mol. Psychiatry* 9: 1111–1121.

- Wong K, Park HT, Wu JY, Rao Y. 2002. Slit proteins: molecular guidance cues for cells ranging from neurons to leukocytes. *Curr. Opin. Genet. Dev.* 12: 583–91.
- Woolfe A, Goodson M, Goode DK, Snell P, McEwen GK, Vavouri T, Smith SF, North P, Callaway H, Kelly K, Walter K, Abnizova I, Gilks W, Edwards YJK, Cooke JE, Elgar G. 2004. Highly Conserved Non-Coding Sequences Are Associated with Vertebrate Development. *PLoS Biol.* 3: e7.
- Wu JY, Rao Y, Wu W, Wong K, Chen J, Jiang Z, Dupuis S. 1999. Directional guidance of neuronal migration in the olfactory system by the protein Slit. *Nature* 400: 331–336.
- Yamamoto M, Morita R, Mizoguchi T, Matsuo H, Isoda M, Ishitani T, Chitnis AB, Matsumoto K, Crump JG, Hozumi K, Yonemura S, Kawakami K, Itoh M. 2010. Mib-Jag1-Notch signalling regulates patterning and structural roles of the notochord by controlling cell-fate decisions. *Development* 137: 2527–2537.
- Zhang Z, Liu S, Lin X, Teng G, Yu T, Fang F, Zang F. 2011. Development of fetal brain of 20 weeks gestational age: Assessment with post-mortem Magnetic Resonance Imaging. *Eur. J. Radiol.* 80: e432–e439.
- Zhu Y, Li H, Zhou L, Wu JY, Rao Y. 1999. Cellular and molecular guidance of GABAergic neuronal migration from an extracortical origin to the neocortex. *Neuron* 23: 473–85.

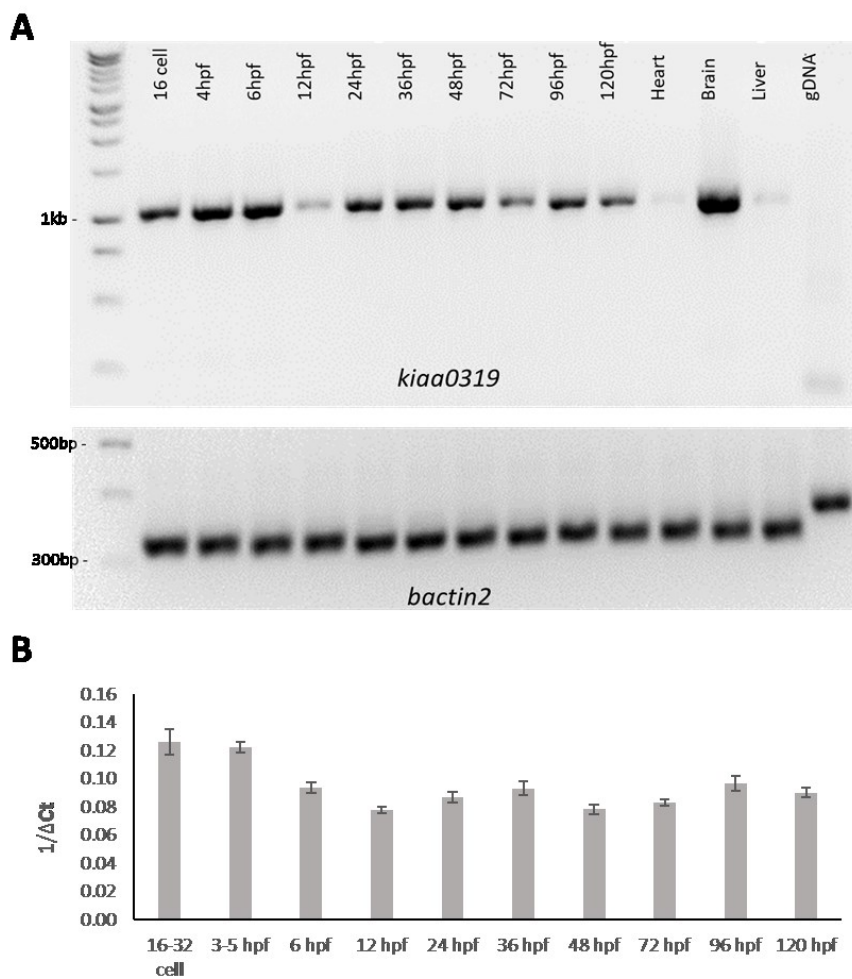


Figure 1. *kiao0319* is expressed during different stages of development. A) The top panel shows RT-PCR amplicons generated with primers targeting different *kiao0319* exons using cDNA prepared at different zebrafish developmental stages (hours post-fertilisation, hpf) and in selected adult tissues. The amplicons have the expected size of 1024 bp. The lower panel shows fragments (322 bp) for *bacin2* used as a control for cDNA quality at the corresponding stages and tissues. Genomic DNA (gDNA) in the last lane demonstrate the specificity of the assay with no band for the *kiao0319* reaction and a fragment of 407 bp for the *bacin2* as expected. *kiao0319* is expressed throughout the different development stages and in the adult brain but with only weak signal in the hearth and liver. The adult data are consistent with the expression profiles observed in human adult tissue (Supplementary Figure S1). The top and lower panel are images from two separate gels where samples were loaded in the same order. **B)** Quantification of the expression of *kiao0319* by qPCR measured during the first five days of development. Expression is measured against the *eef1a1/2* gene, used as reference. Mean values are derived from biological triplicates and error bars indicate standard deviations.

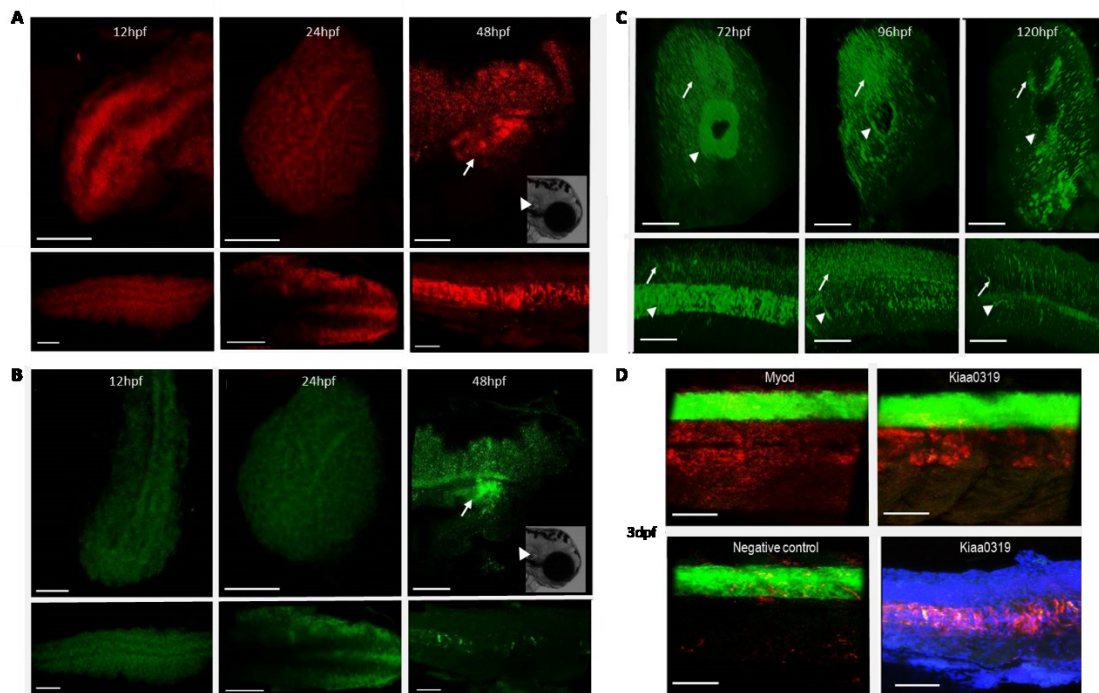


Figure 2. *kiao0319* is specifically expressed in the notochord. The expression of *kiao0319* (A) and *kiao0319l* (B) was examined at three embryonic stages (12, 24 and 48 hpf; WT zebrafish) using the RNAScope Fluorescent Multiplex Assay with results shown for the head (top panels) and the body (lower panels). *kiao0319* (red) is expressed throughout the three stages. High expression is detected in the developing brain and body midline. At 48 hpf, *kiao0319* is still highly expressed in the brain and strong signal is detected in the otic vesicles (top panel; white arrows and white triangle in reference image) and in the notochord (lower panel). *kiao0319l* shows a similar pattern of expression, including a strong signal in the otic vesicles, but the expression in the notochord at 48hpf is very weak. Black area in the brain at 48 hpf correspond to the pigmentation of the embryo. C) Transverse (top panels) and lateral (lower panels) 3D reconstructions from light-sheet microscopy images at three developmental stages (72, 96 and 120 hpf; WT zebrafish) on samples labelled with the *kiao0319* probe. *kiao0319* expression is localised to the notochord (white triangle). The signal diminishes as development progresses and this transient structure regresses. A well-defined signal in the spinal cord (white arrow) is also detected but it weakens at the later stages of development. D) *kiao0319* expression in the notochord was confirmed with the Tg(gfap:GFP);Tg(Oligo2:dsRed) transgenic line, which present GFP (green) in the spinal cord. Images were collected at 42 hpf by confocal microscopy. *myoD1* (myogenic differentiation 1, a universal target for myogenic cells [Weinberg et al., 1996]) was used as positive control and demonstrates the specificity of the assay. For reference, the bottom right image shows a wild type embryo treated with the *kiao0319* RNAScope probe (red) together with DAPI staining (blue). The white arrow indicates the spinal cord where only isolated dots are visible while a strong signal is detected throughout the notochord. The scale bar indicates 50 μ m in all panels. For the positive and negative controls see Supplementary Figure S3.

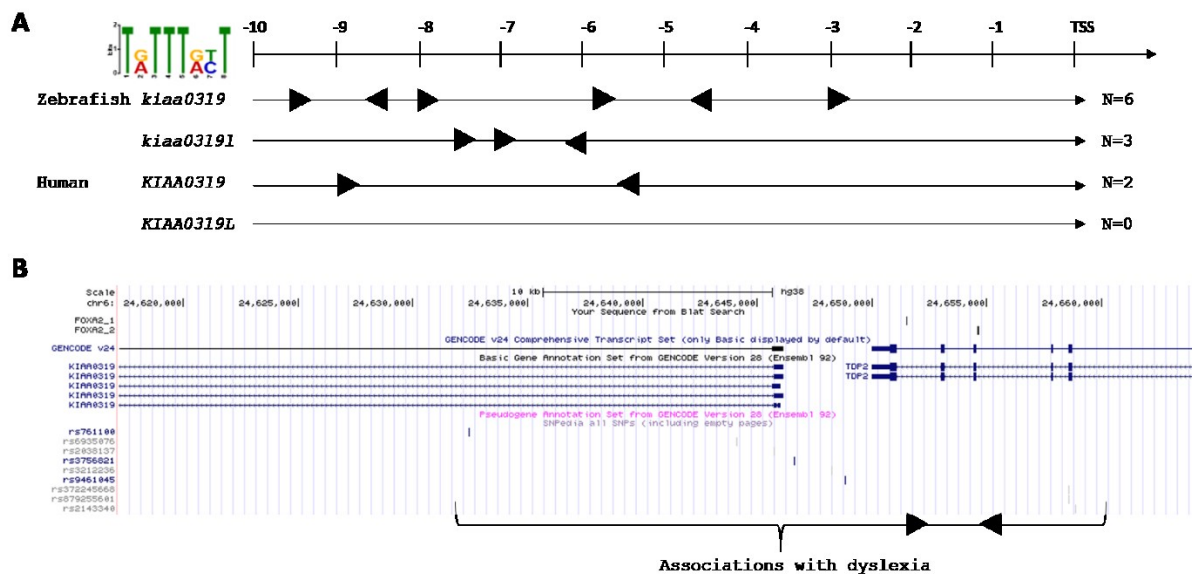


Figure 3. FOXA2 consensus sequences at the KIAA0319 and KIAA0319-LIKE regulatory regions. A) The 10 kb regions upstream of the transcription start sites (TSS) of KIAA0319 and KIAA0319L in the zebrafish and human genomes were scanned for the presence of FOXA2 consensus sequences (Indicated in the top left corner). The results are visualised as black triangles with right and left orientation in reference to the positive and negative strand where the consensus sequence was found. The number of motifs is indicated at the right side of the figure. The exact position of the consensus sequences is shown in Supplementary Table S3. **B)** A snapshot from the UCSC Genome Browser shows the genomic location of the human FOXA2 consensus sequences (top track). The two sequences are located in introns of TDP2, within the KIAA0319 dyslexia-associated region, indicated by the SNPs in the bottom track. The brace at the bottom provides a visualization of where the FOXA2 sequences map within the dyslexia associations.

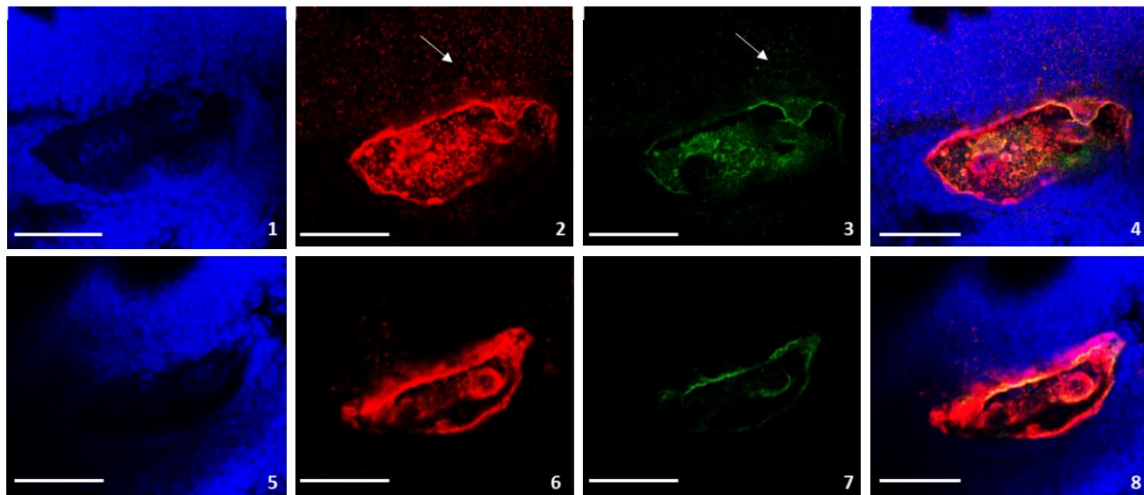


Figure 4 RNAscope analysis at the otic vesicles. *kiao0319*, labelled in red (panel 2), and *kiao0319-like*, labelled in green (panel 3) are compared against the negative controls (panels 6 and 7). The signal for both *kiao0319* and *kiao0319-like* is characterised by the presence of speckles which can be detected also in the brain (white arrows; panels 2 and 3), which are both signs suggestive of genuine expression. In contrast, expression is not detected in the negative control in the brain, suggesting that the signal observed could be due to probe trapping at the contour of the otic vesicles. DAPI (panels 1 and 5) shows nuclear staining and panels 4 and 8 show the merged signal for all channels. All images show the left side of WT zebrafish at 48 hpf oriented with brain on the left and tail on the right. The scale bar is 50 μm in all panels.

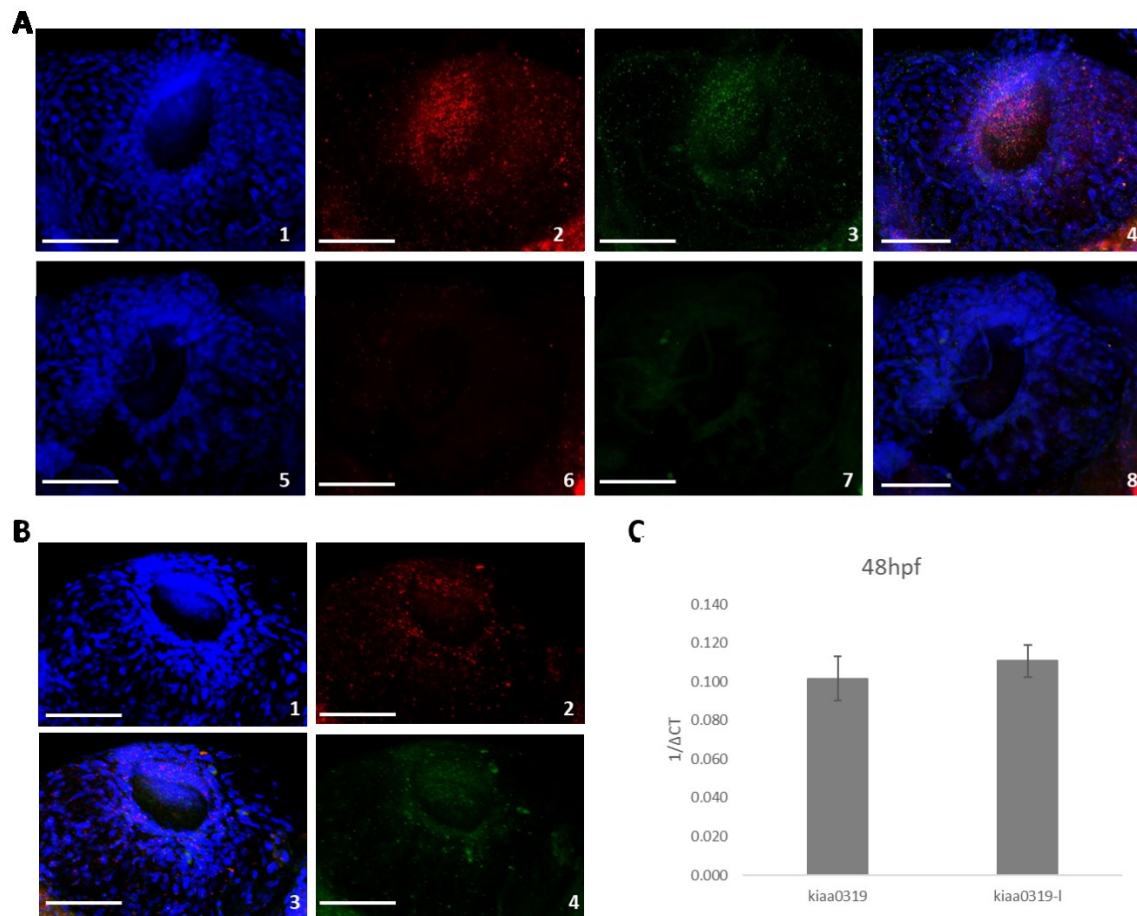


Figure 5. *kiaz0319* and *kiaz0319-like* are expressed in the eyes. A) and B) show two different views of RNAscope analysis in the eyes for *kiaz0319* (labelled in red; panels A2 and B2) and *kiaz0319-like* (labelled in green; panel A3 and B4). The triple negative control shows no signal (A6 and A7). DAPI (A1, A5, and B1) shows nuclear staining and panels A4, A8 and B3 shows the merged signal for all channels. All images show the left side of animals oriented with brain on the left and tail on the right at 48 hpf (WT zebrafish). The scale bar is 50 μm in all panels. **C)** Quantification of expression by qPCR of *kiaz0319* and *kiaz0319-like*. Expression is measured as $1/\Delta\text{Ct}$ referenced against the *eef1a1/2* gene. The measurement is derived after pooling a total of forty eyes collected at 48 hpf. The mean values were derived from three technical replicates. The error bars indicate standard deviations.

Supplementary Methods

Quantitative PCR. Gene expression was assessed by quantitative PCR (qPCR) conducted with the Luna Universal RT-qPCR Kit (NEB) and using a Vii7 instrument (Life Technologies, Paisley, UK). Cycling conditions were as follows: 95°C for 1' followed by 40 cycles of denaturing (95°C) for 10" and annealing for 30" (60°C). The primer pairs were designed to span across *kiaa0319* and *kiaa0319-like* exons. Reaction efficiency was calculated using a 5-point standard curve generated by 2 fold dilutions starting from 50 ng. A no-template sample was included as negative control. Melt curve analysis showed a single clear peak for each assay. Gene expression was plotted as $1/\Delta Ct$ referenced against the *eef1a1/2* gene with each gene expression value derived from at least three technical replicates. All primers used are listed in Supplementary Table S1 and were designed from the annotations of the University of California, Santa Cruz (UCSC) and ENSEMBL genome browsers.

Light-sheet microscopy. We used an in-house built light-sheet microscope based on the OpenSPIM design [Pitrone et al., 2013b]. The original setup was modified to achieve an inverted configuration to accommodate larger varieties of samples. The microscope fits on a 450 mm × 300 mm breadboard (MB3045/M, Thorlabs), as in the original OpenSPIM design. A 488 nm wavelength laser (Solstis with frequency doubler, M Squared) provides the illumination through a single mode fibre. A beam expander is followed by an adjustable slit (VA100/M, Thorlabs) to control the width of the beam and a cylindrical lens (LJ1695RM-A, FL 50mm, Thorlabs) to focus the beam into a sheet of light. A steering mirror directs the beam to the illumination objective (UMPLFLN 10XW, water dipping, NA=0.3, Olympus) through a relay lens. The two objectives are mounted on a customized holder which not only simplifies the system but also minimizes adjustment required. This holder also allows a change of objective lens if needed. The fluorescence signal is first collected by a detection objective (LUMPLFLN 20XW NA=0.5, water dipping, Olympus) coupled with an achromatic lens (as tube lens, LA1708-A-ML, FL 200 mm, Thorlabs) and is then projected onto a sCMOS camera (ORCA-Flash4.0 sCMOS camera, Hamamatsu).

The imaging was performed by scanning the sample through the light sheet with a manual scanning stage. The 3D images were reconstructed by choosing an arbitrary z step using ImageJ [Schindelin et al., 2012] or through the VTK library Visualization Tool Kit [Schroeder et al., 2006b] in the open source software Icy [de Chaumont et al., 2012].

Supplementary Table S1. List of primers

Gene	Zebrafish gene name	ENSEMBL gene ID	Sequences	Fragment size (bp)	Experiment
<i>kiaa0319</i>			AGGGTCAGTACACGTTTCAGC CACAGAGGGTCACAGGAACAG	1024	RT-PCR
<i>kiaa0319</i>	si:ch73-215d9.1	ENSDARG00000103001	AACCATCGCTGTGAAAAGGC CTTTCAGAGTAGGTTGCGGC	121	qPCR
<i>kiaa0319</i>			AGGGTCAGTACACGTTTCAGC CGCAATTAACCCTCACTAAAGGGACACAGAGGGTCACAGGAACAG	1066	WISH probe
<i>kiaa0319-like</i>	si:ch211-193k19.1	ENSDARG00000035660	CGCAGCCACATGTAGAGTCT AGAAGACATGTCCTGCTCCG	119	qPCR
<i>β-actin2</i>	actb2	ENSDARG00000037870	GCAGAAGGAGATCACATCCCTGGC CATTGCCGTCACCTTCACCGTTC	322 (407, genomic)	RT-PCR
<i>eef1a1l2</i>	eef1a1l2	ENSDARG00000020850	TTGAGAAGAAAATCGGTGGTGCTG GGAACGGTGTGATTGAGGGAAATTC	91	qPCR

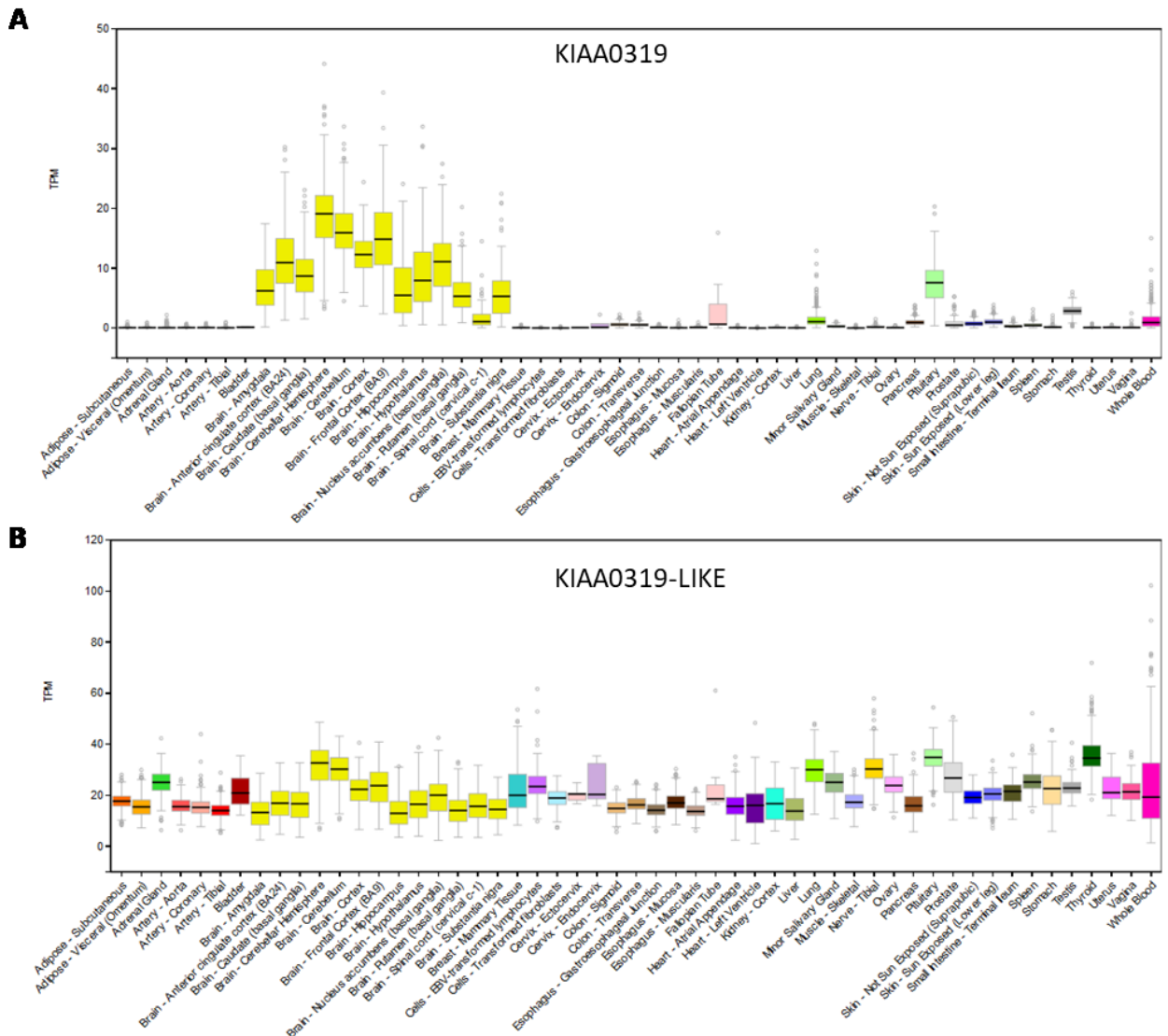
Supplementary Table S2. PFA treatment duration for the RNAscope protocol

Stage	Pre-treatment (min)	PFA treatment (h)
>12hpf		4 (with chorion)
12hpf	1.5	1 (with chorion)
24hpf	3	0.5 (without chorion)
36hpf	5	0.5
48hpf	7	0.5
72hpf	10	0.5
96hpf	12	0.5
120hpf	15	0.5

Supplementary Table S3. Location of FOXA2 consensus sequences

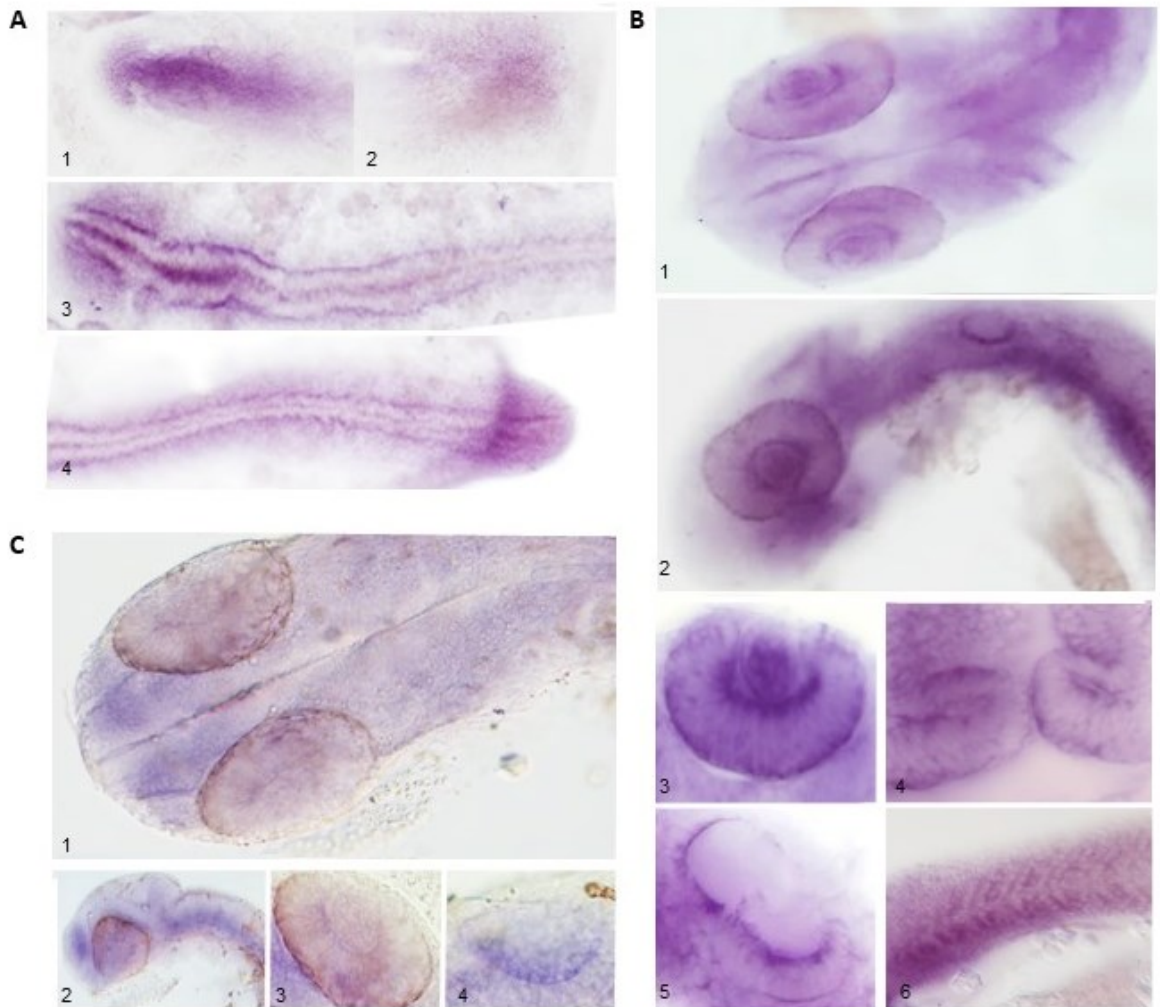
Gene	Genome	Start	End	p-value	Strand	Matched Sequence
kiaa0319-like	danRer10	-7558	-7551	8.32E-05	+	tgtttact
kiaa0319-like	danRer10	-6948	-6941	8.32E-05	+	tgtttact
kiaa0319-like	danRer10	-6030	-6023	8.32E-05	-	TGTTTGTT
kiaa0319	danRer10	-9449	-9442	8.32E-05	+	tgtttggt
kiaa0319	danRer10	-8439	-8432	8.32E-05	-	TGTTTGTT
kiaa0319	danRer10	-7999	-7992	8.32E-05	+	tgtttact
kiaa0319	danRer10	-5770	-5763	1.79E-05	+	tgtttgct
kiaa0319	danRer10	-4354	-4347	8.32E-05	-	TGTTTGTT
kiaa0319	danRer10	-2746	-2739	8.32E-05	+	tatttgct
KIAA0319	hg38	-8603	-8596	1.79E-05	+	tgtttgct
KIAA0319	hg38	-5499	-5492	1.79E-05	-	TGTTTGCT

The target motif was TRTTTRYT; The Start and End position refers to the transcription start site of the gene



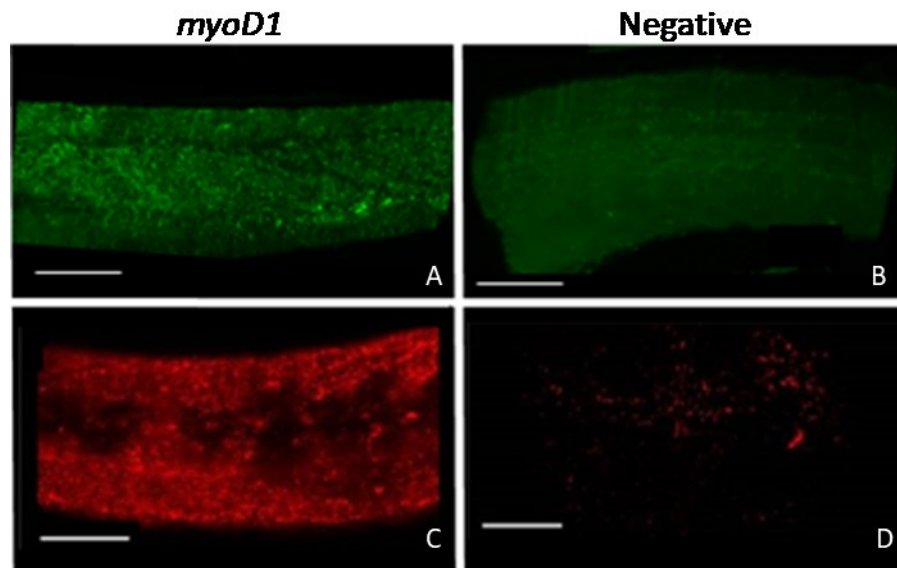
Supplementary Figure S1. KIAA0319 is specifically expressed in the human brain.

Expression profiles across human adult tissues are shown for the *KIAA0319* (A) and the *KIAA0319-LIKE* (B) genes. *KIAA0319* is specifically expressed in the adult brain. In comparison, *KIAA0319-LIKE* expression is higher, including in the brain, and widespread across tissues. The images are screenshots following queries to the GTEx database using the default settings [Consortium, 2013]. TPM = transcript per million.



Supplementary Figure S2. *In situ* hybridization suggests a specific spatiotemporal expression pattern for *kiasa0319*. **A)** At the 3 somite stage, *kiasa0319* is expressed throughout the embryo with the strongest signal in the head (A1) and to a lesser extent, in the tail bud (A2). At the 14 the somite stage, high expression continues in the head (A3) and is visible along the developing body midline and in the tail (A3 and A4). All images are dorsal views with the head on the left side. **B)** At 30 hpf *kiasa0319* is still expressed throughout the embryo but strong expression emerges in specific structures observed from dorsal (B1) and lateral (B2) views. Details of expression are shown for the eyes (B3; dorsolateral view), the midbrain-hindbrain boundary (B4; dorsal view), the otic vesicles (B5; dorsolateral view) and the notochord (B6; lateral view). **C)** In a dorsal view at 48 hpf,

kiaa0319 expression in the eyes is diminished, while signal in the telencephalon emerges (C1). The signal in the telencephalon is particularly visible in a lateral view (C2) along with expression in the eyes and the region around the notochord. Detailed dorsolateral views of the eye (C3) and otic vesicle (C4) show weaker intensity at these structures when compared to the pattern observed at 30 hpf.



Supplementary Figure S3. Controls for the RNAScope Fluorescent Multiplex Assay.

For all experiments a probe for *myoD1* (myogenic differentiation 1) was used as a positive control (panels A and C) and three unspecific probes for each of the three channels were used as a triple negative control (panel B and D). The picture shows representative lateral views along the body of animals (120 hpf) taken with a confocal microscope to test the settings of the channels used for the detection of the *kiaa0319* and *kiaa0319l* probes. The scale bar indicates 50 μ m in all panels.